

**Faculdade de Engenharia da Universidade do Porto**



**Interaction of Chitosan Microspheres with Human  
Gastrointestinal Microbiota**

Francisca Alexandra Morais Marques

Dissertation carried out under Master's Degree in Biomedical Engineering

Supervisor: Inês Gonçalves; INEB/i3S  
Co-supervisor: Cristina Martins; INEB/i3S

Porto, September 2018





A Dissertação intitulada

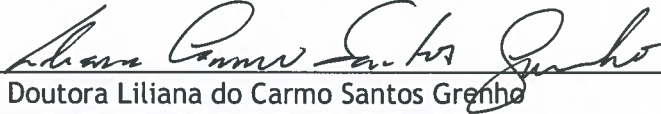
“Interaction of Chitosan Microspheres with Human Gastrointestinal Microbiota”

foi aprovada em provas realizadas em 20-09-2018

o júri

  
Presidente Prof. Doutor Fernando Jorge Mendes Monteiro  
Professor Catedrático do Departamento de Engenharia Metalúrgica e de Materiais da FEUP - U.Porto

  
Doutora Inês de Castro Gonçalves de Almada Lobo  
Investigadora Auxiliar do Departamento de Engenharia Metalúrgica e de Materiais - FEUP - U. Porto

  
Prof.ª Doutora Liliana do Carmo Santos Grenho  
Professora Auxiliar Convidada da Faculdade de Medicina Dentária da U. Porto

O autor declara que a presente dissertação (ou relatório de projeto) é da sua exclusiva autoria e foi escrita sem qualquer apoio externo não explicitamente autorizado. Os resultados, ideias, parágrafos, ou outros extratos tomados de ou inspirados em trabalhos de outros autores, e demais referências bibliográficas usadas, são corretamente citados.

  
Autor - Francisca Alexandra Morais Marques

# Abstract

The gastrointestinal microbiota plays an important role in maintaining a state of health, since any changes in its composition and diversity can cause problems. The infections caused, for example, by pathogenic bacteria, as well as the acquisition of resistance to the treatments used to combat those infections, contribute into reducing success rates in the treatment of infectious diseases and to the triggering and/or persistence of some diseases.

The composition of the microbial community of the healthy GI tract it has been the subject of analysis by many studies and an ecosystem has been identified predominantly dominated by five phyla: Bacteroidetes, Firmicutes, Fusobacteria, Actinobacteria, and Proteobacteria.

Some studies have been published that focus on the consequences of existing therapies (mainly antibiotherapies) applied for the eradication of *H. pylori* pathogenic bacteria from the human stomach in relation to commensal bacteria of the gastrointestinal microbiota. There are evidences that antibiotics can significantly alter the community of microorganisms that colonize the gastrointestinal tract in all stages of human life.

In order to overcome the problems resulting from the existing therapies used to treat bacterial infections of the human gastrointestinal tract, alternative therapies have emerged to the administration of antibiotics, with special interest in biomaterials with antimicrobial properties, such as some polymers, as chitosan biomaterials.

Although chitosan is considered a non-cytotoxic biomaterial for mammalian cells, it presents a toxic behaviour for several microorganisms, which allows its use as an agent capable of eliminating/inhibiting the activity of pathogenic microorganisms. Particles obtained from chitosan, as in the case of chitosan microspheres, may also be used as binding agents to bacteria, in particular described for *H. pylori*. These biomaterials have the ability to eliminate this bacterium from the human organism, thus constituting a complement to the therapies used, or even as an alternative to these.

Given the scarcity of information regarding the interaction of chitosan microspheres with pathogenic bacteria and also commensal bacteria of the human gastrointestinal microbiota, the present research intends to contribute with new data, to understand if the promising chitosan microparticles may represent an alternative therapy to the currently used treatments for bacterial infections, associated with gastrointestinal diseases, so that the human commensal microbiota is kept under normal conditions.

The main objective of the proposed research project was to evaluate the behaviour of these microspheres in terms of adhesion to bacteria from gastrointestinal microbiota at different pHs

that mimic the environment of stomach and intestine in man. For that, bacteria representative of the phyla Firmicutes and Proteobacteria were selected.

Adhesion assays of chitosan microspheres to bacteria from the human gastrointestinal microbiota were established for evaluation on ImageStream<sup>X</sup> and demonstrated that chitosan microspheres adhere to all the bacteria tested, namely *Helicobacter pylori*, *Campylobacter jejuni*, *Escherichia coli*, *Lactobacillus casei*, *Enterococcus faecalis* and *Bacillus cereus*, in citrate-phosphate buffer at pH 4.0, 6.0 and 7.5. The species *H. pylori*, *C. jejuni*, *L. casei* and *B. cereus* showed preferential adherence to the microspheres at pH 6.0, while *E. coli* and *E. faecalis* had a higher adhesion to pH 7.5, which is within the pH values observed in the lower portions of the gastrointestinal tract (stomach and intestine), where these bacteria are mostly found.

In order to better understand the results obtained regarding the adhesion of bacteria to the chitosan microspheres, the zeta potential at pH 2.6, 4.0, 6.0 and 7.5 was determined in the Zetasizer Nano ZS and ElectroKinetic Analyzer equipments, respectively. The higher bacterial adhesion observed at pH 6.0 and 7.5 does not seem to be justified by the surface charge of the bacteria and microspheres, since at these pHs both presented negative zeta potential. Chitosan microspheres were characterized regarding size and shape under the same incubation and reading conditions on ImageStream<sup>X</sup>, presenting an average size of about  $9 \pm 3 \mu\text{m}$  in diameter and  $18 \pm 8 \mu\text{m}$  in length and a rounded shape with Aspect Ratio values close to 1.

This study showed that chitosan microspheres adhere to bacteria over a wide range of pHs, revealing that these microparticles are not specific for pathogenic bacteria, also adhering to commensal bacteria of the human gastrointestinal tract.

**Keywords:** Gastrointestinal tract; Gastrointestinal microbiota; Chitosan microspheres; Bacterial adhesion.

## Resumo

A microbiota gastrointestinal humana desempenha um papel importante na manutenção de um estado de saúde, já que quaisquer alterações na sua composição e diversidade podem causar problemas. As infecções provocadas, por exemplo, por bactérias patogênicas, bem como a aquisição de resistência aos tratamentos usados no seu combate, contribuem para a redução das taxas de sucesso e para o despoletar e/ou para a persistência de algumas doenças.

A composição da comunidade microbiana do trato gastrointestinal saudável tem sido objeto de análise por parte de muitos estudos e tem sido identificado um ecossistema dominado maioritariamente por cinco filos: Bacteroides, Firmicutes, Actinobacteria, Fusobacteria and Proteobacteria.

Foram publicados alguns estudos centrados nas consequências das terapias (maioritariamente antibióticas) aplicadas para a erradicação da bactéria patogénica *Helicobacter pylori* do estômago humano em relação a bactérias comensais da microbiota gastrointestinal. Há evidências de que os antibióticos podem alterar significativamente a comunidade de microorganismos que colonizam o trato gastrointestinal, em todas as etapas da vida humana.

A fim de superar os problemas resultantes das terapias utilizadas para tratar infecções bacterianas do trato gastrointestinal humano, surgiram terapias alternativas à aplicação de antibióticos, nomeadamente biomateriais com propriedades antimicrobianas, como alguns polímeros, de que são exemplo os biomateriais de quitosano.

Apesar do quitosano ser considerado um biomaterial não citotóxico para células de mamíferos, apresenta um comportamento tóxico para vários microorganismos, o que possibilita a sua utilização como agente capaz de eliminar/inibir a atividade de microorganismos patogénicos. Partículas obtidas a partir do quitosano, como as microesferas de quitosano, podem também ser usadas como agentes de ligação às bactérias, como já descrito para a *H. pylori*. Estes biomateriais possuem a capacidade de eliminar esta bactéria do organismo humano, constituindo assim um complemento às terapêuticas em uso, ou até mesmo como uma sua alternativa.

Dada a escassez de informações relativas ao comportamento das microesferas de quitosano em relação a bactérias patogénicas, bem como a bactérias comensais da microbiota gastrointestinal humana, a presente investigação pretendeu dar um contributo para compreender se as promissoras microesferas de quitosano poderiam representar uma terapia alternativa aos tratamentos de infecções bacterianas, associadas a doenças gastrointestinais, de modo que a microbiota comensal humana seja mantida em condições normais.

O projeto de investigação proposto teve como principal objetivo avaliar o comportamento dessas microesferas em termos de adesão a bactérias da microbiota gastrointestinal a diferentes pHs que mimetizem o ambiente do estômago e do intestino no Homem. Para isso, foram selecionadas bactérias representativas dos filos Firmicutes e Proteobacteria.

Os ensaios de adesão das microesferas de quitosano a bactérias da microbiota gastrointestinal humana foram estabelecidos para avaliação no ImageStream<sup>x</sup> e demonstraram que ocorre, de um modo geral, adesão das microesferas de quitosano às bactérias *Helicobacter pylori*, *Campilobacter jejuni*, *Escherichia coli*, *Lactobacillus casei*, *Enterococcus faecalis* e *Bacillus cereus*, em tampão citrato-fosfato a pH 4.0, 6.0 e 7.5, com maiores valores de intensidade no canal 2, e portanto, de maior adesão bacteriana a pH 6.0 e 7.5. As espécies *H. pylori*, *C. jejuni*, *L. casei* e *B. cereus* demonstraram aderir preferencialmente às microesferas a pH 6.0, enquanto que as espécies *E. coli* e *E. faecalis* apresentaram maior adesão a pH 7.5, o que se encontra dentro dos valores de pH observados nas porções inferiores do trato gastrointestinal (estômago e intestino), onde estas bactérias maioritariamente se encontram.

Com o intuito de melhor compreender os resultados obtidos relativos à adesão das bactérias às microesferas de quitosano, determinou-se o potencial zeta a pH 2.6, 4.0, 6.0 e 7.5 nos equipamentos Zetasizer Nano ZS e ElectroKinetic Analyzer, respetivamente. A maior adesão bacteriana observada a pH 6.0 e 7.5 não parece ser justificada pela carga superficial das bactérias e das microesferas, já que a estes pHs ambas apresentaram potencial zeta negativo. Relativamente à caracterização das microesferas de quitosano em estudo quanto ao tamanho e forma, nas mesmas condições de incubação e leitura no ImageStream<sup>x</sup>, apresentaram um tamanho médio de cerca  $12 \pm 3 \mu\text{m}$  de diâmetro e  $18 \pm 8 \mu\text{m}$  de comprimento e uma forma mais arredondada com valores de *Aspect Ratio* perto de 1.

Este estudo, ao provar a adesão das microesferas de quitosano a bactérias num amplo intervalo de pHs revela que estas micropartículas não são específicas para bactérias patogénicas, aderindo também a bactérias comensais do trato gastrointestinal humano.

*Palavras-chave:* Tracto gastrointestinal; Microbiota gastrointestinal; Microesferas de quitosano; Adesão bacteriana.

**The research work described in this thesis was conducted at:**

Instituto de Investigação e Inovação em Saúde - i3S  
Universidade do Porto, Portugal



Instituto de Engenharia Biomédica - INEB  
Universidade do Porto, Portugal



**The research work described in this thesis was financially supported by:**

Project POCI-01-0145-FEDER-007274 (Institute for Research and Innovation in Health Sciences); Project NORTE-01-0145-FEDER-000012, funded by FEDER funds through COMPETE2020 – Programa Operacional Competitividade e Internalização (POCI) and Programa Operacional Regional do Norte, and by national funds through FCT - Fundação para a Ciência e para a Tecnologia; Project PYLORIBINDERS - *Helicobacter pylori* specific biomaterials for antibiotic-free treatment/diagnostic of gastric infection, funded by FCT - (PTDC/CTM-BIO/4043/2014) Fundação para a Ciência e para a Tecnologia and the research position of Inês C. Gonçalves (IF/01479/2015).







# Acknowledgements

À Doutora *Inês Gonçalves*, pelo conhecimento transmitido, pela orientação e por me ter ajudado a levar a bom porto este projeto de investigação.

Também à Doutora *Cristina Martins*, pela pertinência das suas observações e sugestões, elementos impulsionadores e decisivos na consecução desta Dissertação, que me fizeram pensar mais além.

De uma forma particular, a todas as minhas colegas do grupo de investigação *BioEngineered Surfaces* que sempre se prontificaram a ajudar, e por todos os conselhos e ombros amigos que disponibilizaram nos momentos mais difíceis, contribuindo muito para que este caminho fosse trilhado com sucesso.

À *Maria Lázaro* e ao *Ricardo Vidal*, pela formação e apoio nos aparelhos ImageStream<sup>X</sup>, ZetaSize e EKA, essenciais para o desenvolvimento deste projeto.

De uma forma muito especial à minha família, nomeadamente aos meus pais, *Luísa e Paulo*. Jamais irei esquecer as noites que passaram sem dormir para estar ao meu lado, e os abraços fortes em silêncio, que me impeliram a continuar, que me 'obrigaram' a ver o que parecia não existir. Foi aí, quando precisei, que eles acreditaram que sou capaz de ultrapassar quaisquer obstáculos, porque tenho vontade e empenho, e uma força imensa que advém da minha fé.

Ainda mais especialmente à minha mana, *Maria Eduarda*, pelas palavras sempre certas no momento exato, pela força que me transmitias pelo teu olhar e, claro, por todas as correções a este documento. Obrigada pelo teu interesse e inteligência.

Ao meu namorado, *Tiago Gil*, por todos os incentivos e por tentar, sempre, que eu seja mais positiva, confiando nas minhas qualidades pessoais e profissionais. Obrigada por acreditares sempre em mim e na minha capacidade de concretização.

Por último e não menos importante, à 'minha miúda' (a minha cadela *Ruca*), que só com o seu olhar meigo me fazia sorrir. Por todas as torrinhas de mimalhice máxima e por todas as recusas de mimo. Porque és o meu maior tesouro e serás sempre, mas sempre, a minha 'bebe'.



“Failure will never overtake me if my determination to succeed is strong enough.”  
Og Mandino



# Table of contents

<b>Abstract</b> .....	<b>iii</b>
<b>Resumo</b> .....	<b>v</b>
<b>Table of contents</b> .....	<b>xiii</b>
<b>Figures List</b> .....	<b>xvii</b>
<b>Tables List</b> .....	<b>xxi</b>
<b>Abbreviations, Acronyms and Symbols</b> .....	<b>xxiii</b>
<b>Chapter 1</b> .....	<b>27</b>
<b>Introduction</b> .....	<b>27</b>
<b>1.1 - Anatomical and physiological considerations of the lower gastrointestinal tract</b> .....	<b>27</b>
1.1.1 - Stomach .....	27
1.1.2 - Intestine .....	29
<b>1.2 - Human gastrointestinal microbiota</b> .....	<b>32</b>
1.2.1 - Interactions between the commensal gastrointestinal microbiota, pathogenic bacteria and host .....	41
<b>1.3 - <i>Helicobacter pylori</i> gastric infection</b> .....	<b>44</b>
1.3.1 - <i>Helicobacter pylori</i> : general considerations .....	44
1.3.2 - Colonization of gastric mucosa by <i>Helicobacter pylori</i> .....	46
1.3.3 - Existing therapies for <i>Helicobacter pylori</i> infection .....	48
1.3.4 - Effect of therapies for <i>Helicobacter pylori</i> infections under the human gastrointestinal microbiota .....	50
1.3.5 - Alternative therapies for <i>Helicobacter pylori</i> infection .....	53
<b>1.4 - Chitosan</b> .....	<b>56</b>
1.4.1 - Chitosan: general considerations and applications .....	56
1.4.2 - Interactions between chitosan biomaterials and bacteria .....	59
1.4.2.1 - Chitosan biomaterials as alternative therapy to <i>Helicobacter pylori</i> infection .....	63
1.4.3 - Chitosan microspheres .....	65
<b>Chapter 2</b> .....	<b>69</b>
<b>Motivation and Aim</b> .....	<b>69</b>
<b>Chapter 3</b> .....	<b>71</b>
<b>Materials and Methods</b> .....	<b>71</b>
<b>3.1 - Preperation of buffer solutions</b> .....	<b>71</b>

<b>3.2 - Preparation of bacteria culture media</b>	<b>71</b>
<b>3.3 - Bacteria culture conditions</b>	<b>72</b>
3.3.1 - <i>Helicobacter pylori</i> culture conditions	72
3.3.2 - <i>Campilobacter jejuni</i> culture conditions and growth curve	72
3.3.3 - <i>Escherichia coli</i> culture conditions	73
3.3.4 - <i>Lactobacillus casei</i> culture conditions	73
3.3.5 - <i>Enterococcus faecalis</i> culture conditions	73
3.3.6 - <i>Bacillus cereus</i> culture conditions and growth curve	74
<b>3.4 - Bacteria Zeta Potential</b>	<b>74</b>
<b>3.5 - Chitosan microspheres</b>	<b>75</b>
3.5.1 - Chitosan microspheres preparation	76
3.5.2 - Chitosan microspheres Zeta Potential	76
<b>3.6 - Chitosan microspheres adhesion to bacteria from human gastrointestinal microbiota</b>	<b>77</b>
3.6.1 - Adhesion assay	77
3.6.2 - ImageStream <sup>X</sup> Flow Cytometer	80
3.6.2.1 - Acquisition	81
3.6.2.2 - Analysis	81
3.6.2.2.1 - Bacterial adhesion to chitosan microspheres	82
3.6.2.2.2 - Characterization of chitosan microspheres	83
<b>Chapter 4</b>	<b>87</b>
<b>Results and Discussion</b>	<b>87</b>
<b>4.1 - Bacterial growth curves</b>	<b>87</b>
4.1.1 - <i>Campilobacter jejuni</i> growth curve	87
4.1.2 - <i>Bacillus cereus</i> growth curve	88
<b>4.2 - Bacteria zeta potential</b>	<b>89</b>
<b>4.3 - Characterization of chitosan microspheres</b>	<b>90</b>
4.3.1 - Evaluation of chitosan microspheres size and shape features by ImageStream <sup>X</sup>	90
4.3.2 - Chitosan microspheres Zeta Potential	95
<b>4.4 - Chitosan microspheres adhesion to bacteria from human gastrointestinal microbiota</b>	<b>96</b>
4.4.1 - Adhesion assay	96
4.4.1.1 - Chitosan microspheres adhesion to <i>Helicobacter pylori</i>	98
4.4.1.2 - Chitosan microspheres adhesion to <i>Campilobacter jejuni</i>	101
4.4.1.3 - Chitosan microspheres adhesion to <i>Escherichia coli</i>	105
4.4.1.4 - Chitosan microspheres adhesion to <i>Lactobacillus casei</i>	108
4.4.1.5 - Chitosan microspheres adhesion to <i>Enterococcus faecalis</i>	112
4.4.1.6 - Chitosan microspheres adhesion to <i>Bacillus cereus</i>	115
4.4.1.7 - General discussion	118
<b>Chapter 5</b>	<b>127</b>
<b>Conclusions and Future perspectives</b>	<b>127</b>
<b>5.1 - Conclusions</b>	<b>127</b>
<b>5.2 - Future perspectives</b>	<b>128</b>
<b>Annex</b>	<b>131</b>
<b>A.1 - Evaluation of the antibacterial effect of chitosan microspheres</b>	<b>131</b>

A.1.1 - Live/Dead fluorescent staining-----	131
A.1.2 - Colony-forming units counting -----	140
<b>References</b> -----	<b>145</b>





## Figures List

Figure 1.1 - Representative scheme of the different parts that make up the stomach [3]. -----	28
Figure 1.2 - Structural scheme of intestinal villi [3]. -----	30
Figure 1.3 - Representative scheme of the location of dominant bacterial groups in different portions of the intestine. Given the nutrient richness in the small intestine, both used by the host organism, and by the microorganism symbionts for its growth, in this portion of the intestine we find a greater amount of <i>Proteobacteria spp.</i> . In the large intestine the amount of nutrients is reduced, but in contrast the amount of fibers that do not undergo digestion is high, so that in this portion of the intestine is enriched with Bacteroidetes and Clostridia, able to use these fibers as an energy source (Adapted from [8]).-----	38
Figure 1.4 - Distribution of human gastrointestinal flora from the esophagus to the large intestine and amount of bacteria present in each portion per gram of contents (Adapted from [39]–[44]).-----	40
Figure 1.5 - Graphical representation of the phyla found by pirosequencing of 16S rRNA gene in control subjects (A, B and C) and in patients treated with dual therapy containing clarithromycin and metronidazole (D, E and F) on days 0, 8-13 and 1 and 4 years (Adapted from [16]).-----	51
Figure 1.6 - Mundial prevalence of <i>Helicobacter pylori</i> (Adpted from [112]). -----	54
Figure 1.7 - Chemical structure of chitin and chitosan from the alkaline deacetylation of chitin (Adapted from [130]). -----	56
Figure 1.8 - Representative scheme of chitosan solubility at different pHs. At pH below 6.3 the chitosan amine groups are protonated, imparting a polyatonic behaviour to this polymer and thus soluble while at pH above 6.3 the chitosan amines are deprotonated and reactive, thereby reducing the charge of this polymer rendering it insoluble (Adapted from [131]). -	58
Figure 1.9 - Spectral Confocal Microscope images of different strains of <i>Helicobacter pylori</i> (green) adhesion to chitosan microspheres (red) after incubation at pH 2.6 or 6.0 (Adapted from [140]). -----	64
Figure 1.10 - Spectral Confocal Microscope image of <i>Helicobacter pylori</i> adhesion (green) to a chitosan microspheres (red) modified with Le <sup>p</sup> surface glycans (Adapted from [84]). -----	65
Figure 3.1 - Scheme of the production of chitosan microspheres with a DA of 6 % by the ionotropic gelation method, in particular by aerodynamically driven system. -----	76
Figure 3.2 - Protocol of the adhesion assay of chitosan microspheres to bacteria from the human gastrointestinal microbiota. -----	79
Figure 3.3 - Principles of operation layout of ImageStream <sup>®</sup> X (Adapted from Amnis Corporation). -----	80

Figure 3.4 - ImageStream <sup>®</sup> INSPIRE <sup>®</sup> Software interface. -----	81
Figure 3.5 - ImageStream <sup>®</sup> IDEAS <sup>®</sup> 6.2 image analysis software user interface for bacterial adhesion assays. -----	82
Figure 3.6 - ImageStream <sup>®</sup> IDEAS <sup>®</sup> 6.2 image analysis software interface for bacterial adhesion assays with an example created for the adhesion assay of the chitosan microspheres to <i>Helicobacter pylori</i> . -----	83
Figure 3.7 - ImageStream <sup>®</sup> IDEAS <sup>®</sup> 6.2 image analysis software interface for chitosan microspheres size and shape features. -----	84
Figure 4.1 - Growth curve of <i>Campilobacter jejuni</i> , cultured in Tryptic Soy Broth during 48 h, at 37 °C and 150 rpm under microaerophilic conditions. -----	88
Figure 4.2 - Growth curve of <i>Bacillus cereus</i> , cultured in Brain Heart Infusion during 48 h, at 37 °C and 150rpm, under aerobic conditions. -----	89
Figure 4.3 <i>Helicobacter pylori</i> , <i>Campilobacter jejuni</i> , <i>Escherichia coli</i> , <i>Lactobacillus casei</i> , <i>Enterococcus faecalis</i> and <i>Bacillus cereus</i> zeta potential under citrate-phosphate buffer at pH 2.6, 4.0, 6.0 and 7.5, determined using Zetasizer Nano ZS (n = 3). The zeta potential values presented are approximate to tenths. -----	90
Figure 4.4 - IDEAS <sup>®</sup> 6.2 histograms and BoxPlots obtained in SPSS for the size features, in particular Area, Diameter, Perimeter, Length, Major Axis and Minor Axis. For better observation of the results, the IDEAS <sup>®</sup> 6.2 graphs obtained have a maximum Histogram Smoothing. In the BoxPlots the outliers (●) and extremes (*) are present, as well as the statistically significant differences between the samples when p < 0.05 (▼). -----	92
Figure 4.5 - IDEAS <sup>®</sup> 6.2 histogram for the feature Aspect Ratio and examples of chitosan microspheres images for different shape values. For a better analysis of the obtained results, the right histogram has a maximum Histogram Smoothing. -----	94
Figure 4.6 - Chitosan microspheres zeta potential under citrate-phosphate buffer at pH 2.6, 4.0, 6.0 and 7.5 with the correspondent standard deviation, determined using EKA (n = 6). The zeta potential values presented are approximate to tenths. -----	95
Figure 4.7 - Example of ImageStream <sup>®</sup> images of <i>Helicobacter pylori</i> J99 adhesion assay to chitosan microspheres at pH 6.0 (MICs_ <i>H. pylori</i> ) and the corresponding controls, only with microspheres (MICs_) or bacteria ( <i>H. pylori</i> _), with and without compensation matrix (Comp, noComp). All the samples were labelled with SYTO9 0.015 μM. Scale bar corresponds to 10 μm. -----	97
Figure 4.8 - ImageStream <sup>®</sup> images of <i>Helicobacter pylori</i> adhesion assay to chitosan microspheres (MICs_ <i>H. pylori</i> ) at pH 2.6, 4.0, 6.0 and 7.5, and the correspondent controls (MICs_ and <i>H. pylori</i> ). All samples were labelled with 0.015 μM of SYTO9. Scale bar corresponds to 10 μm. -----	99
Figure 4.9 - IDEAS <sup>®</sup> 6.2 histograms for the intensity in channel 2 for the samples MICs_ <i>H. pylori</i> and MICs_ at pH 2.6, 4.0, 6.0 and 7.5. For a better analyse of the obtained results, the histograms obtained has a maximum Histogram Smoothing. -----	100
Figure 4.10 - BoxPlot of the intensity on channel 2 for the samples MICs_ <i>H. pylori</i> . Statistically significant differences between samples when p < 0.05 (▼). The graph on the right is a zoom-in excluding outliers (●) and extremes (*), in order to better understand the main behaviour between the different samples. -----	101
Figure 4.11 - ImageStream <sup>®</sup> images of <i>Campilobacter jejuni</i> adhesion assay to chitosan microspheres (MICs_ <i>C. jejuni</i> ) at pH 2.6, 4.0, 6.0 and 7.5, and the correspondent controls	

- (MICs\_ and *C. jejuni*). All samples were labelled with 0.015  $\mu$ M of SYTO9. Scale bar corresponds to 10  $\mu$ m.----- 103
- Figure 4.12 - IDEAS® 6.2 histograms for the intensity in channel 2 for the samples MICs\_*C. jejuni* and MICs\_ at pH 2.6, 4.0, 6.0 and 7.5. For a better analyse of the obtained results, the histograms obtained has a maximum Histogram Smoothing.----- 104
- Figure 4.13 - BoxPlot of the intensity on channel 2 for the samples MICs\_*C. jejuni*. Statistically significant differences between samples when  $p < 0.05$  ( $\blacktriangledown$ ). The graph on the right is a zoom-in excluding outliers ( $\bullet$ ) and extremes (\*), in order to better understand the behaviour between the different samples. ----- 105
- Figure 4.14 - ImageStream®<sup>x</sup> images of *Escherichia coli* adhesion assay to chitosan microspheres (MICs\_*E. coli*) at pH 2.6, 4.0, 6.0 and 7.5, and the correspondent controls (MICs\_ and *E. coli*). All samples were labelled with 0.015  $\mu$ M of SYTO9. Scale bar corresponds to 10  $\mu$ m.----- 106
- Figure 4.15 - IDEAS® 6.2 histograms for the intensity in channel 2 for the samples MICs\_*E. coli* and MICs\_ at pH 2.6, 4.0, 6.0 and 7.5. For a better analyse of the obtained results, the histograms obtained has a maximum Histogram Smoothing.----- 107
- Figure 4.16 - BoxPlot of the intensity on channel 2 for the samples MICs\_*E. coli*. Statistically significant differences between samples when  $p < 0.05$  ( $\blacktriangledown$ ). The graph on the right is a zoom-in excluding outliers ( $\bullet$ ) and extremes (\*), in order to better understand the behaviour between the different samples. ----- 108
- Figure 4.17 - ImageStream®<sup>x</sup> images of *Lactobacillus casei* adhesion assay to chitosan microspheres (MICs\_*L. casei*) at pH 2.6, 4.0, 6.0 and 7.5, and the correspondent controls (MICs\_ and *L. casei*). All samples were labelled with 0.015  $\mu$ M of SYTO9. Scale bar corresponds to 10  $\mu$ m.----- 110
- Figure 4.18 - IDEAS® 6.2 histograms for the intensity in channel 2 for the samples MICs\_*L. casei* and MICs\_ at pH 2.6, 4.0, 6.0 and 7.5. For a better analyse of the obtained results, the histograms obtained has a maximum Histogram Smoothing.----- 111
- Figure 4.19 - BoxPlot of the intensity on channel 2 for the samples MICs\_*L. casei*. Statistically significant differences between samples when  $p < 0.05$  ( $\blacktriangledown$ ). The graph on the right is a zoom-in excluding outliers ( $\bullet$ ) and extremes (\*), in order to better understand the behaviour between the different samples. ----- 112
- Figure 4.20 - ImageStream®<sup>x</sup> images of *Enterococcus faecalis* adhesion assay to chitosan microspheres (MICs\_*E. faecalis*) at pH 2.6, 4.0, 6.0 and 7.5, and the correspondent controls (MICs\_ and *E. faecalis*). All samples were labelled with 0.015  $\mu$ M of SYTO9. Scale bar corresponds to 10  $\mu$ m.----- 113
- Figure 4.21 - IDEAS® 6.2 histograms for the intensity in channel 2 for the samples MICs\_*E. faecalis* and MICs\_ at pH 2.6, 4.0, 6.0 and 7.5. For a better analyse of the obtained results, the histograms obtained has a maximum Histogram Smoothing.----- 114
- Figure 4.22 - BoxPlot of the intensity on channel 2 for the samples MICs\_*E. faecalis*. Statistically significant differences between samples when  $p < 0.05$  ( $\blacktriangledown$ ). c. ----- 115
- Figure 4.23 - ImageStream®<sup>x</sup> images of *Bacillus cereus* adhesion assay to chitosan microspheres (MICs\_*B. cereus*) at pH 2.6, 4.0, 6.0 and 7.5, and the correspondent controls (MICs\_ and *B. cereus*). All the samples were labelled with 0.015  $\mu$ M of SYTO9 and the scale bar chosen was 10  $\mu$ m.----- 116

- Figure 4.24 - IDEAS® 6.2 histograms for the intensity in channel 2 for the samples MICs\_ *B. cereus* and MICs\_ at pH 2.6, 4.0, 6.0 and 7.5. For a better analyse of the obtained results, the histograms obtained has a maximum Histogram Smoothing.----- 117
- Figure 4.25 - BoxPlot for the intensity on channel 2 for the samples MICs\_ *B. cereus*. Statistically significant differences between samples when  $p < 0.05$  (▼). The graph on the right is a zoom-in excluding outliers (●) and extremes (\*), in order to better understand the behaviour between the different samples. ----- 118
- Figure 4.26 - *Helicobacter pylori*, *Campilobacter jejuni*, *Escherichia coli*, *Lactobacillus casei*, *Enterococcus faecalis*, *Bacillus cereus* and chitosan microspheres zeta potential under citrate-phosphate buffer at pH 2.6, 4.0, 6.0 and 7.5, determined using Zetasizer Nano ZS (n = 3) and EKA (n = 6), respectively. ----- 123
- Figure 4.27 - Scheme of the hypothetical adhesion of chitosan microspheres to the bacterial species *Helicobacter pylori*, *Campilobacter jejuni*, *Escherichia coli*, *Lactobacillus casei*, *Enterococcus faecalis* and *Bacillus cereus* along the lower portions of the human gastrointestinal tract (Adapted from [39]–[44]). ----- 126
- Figure A.1 - Protocol for the adhesion tests of chitosan microspheres to *Escherichia. coli* in ImageStream®<sup>x</sup> and Spectral Confocal Microscope for the optimization of bacteria labelling with different fluorescent dyes for Live/Dead studies. Filled arrows indicate the pathways performed for the adhesion assay in ImageStream®<sup>x</sup> and in the Spectral Confocal Microscope, with live and dead bacteria. In the case of dashed arrows correspond to the pathways performed for the adhesion assay in Spectral Confocal Microscope, with killing bacteria afterwards to the incubation.----- 136
- Figure A.2 - ImageStream®<sup>x</sup> images of *Escherichia coli* Live/Dead assay with chitosan microspheres. All samples were labelled with 0.015 µM of SYTO9 and 0.3 µM of DRAQ7. Scale bar corresponds to 10 µm. ----- 137
- Figure A.3 - Spectral Confocal Microscope images of dead *Escherichia coli* adhesion assay to chitosan microspheres with an HCX PL 40.0x1.30 OIL UV objective and a laser power of 2 % for 561 nm laser and 8 % for 405 nm laser. The samples were labelled with 0.075 µM of PI and 1.5 µM of DRAQ7, respectively. Scale bar corresponds to 20 µm. ----- 138
- Figure A.4 - Spectral Confocal Microscope images of fixed *Escherichia coli* adhesion assay to chitosan microspheres with an HCX PL 40.0x1.30 OIL UV objective and a laser power of 19 % for 561 nm laser and 8 % for 405 nm laser. The samples were labelled with 0.075 µM of PI and 1.5 µM of DRAQ7, respectively. Scale bar corresponds to 20 µm. ----- 139
- Figure A.5 - Protocol for the evaluation of antibacterial activity of chitosan microspheres. ---- 142
- Figure A.6 - Effect of chitosan microparticles on the growth of *Escherichia coli* at pH 2.6, 4.0 and 6.0, at different time-points (T2 and T2+24\_Cent). ----- 142
- Figure A.7 - Effect of chitosan microparticles on the growth of *Lactobacillus casei* at pH 2.6, 4.0 and 6.0, at different time-points (T2 T2+48\_noCent and T2+48\_Cent) and the control for bacterial growth without chitosan microspheres at the time-point T2. ----- 143

## Tables List

Table 1.2 - Schematic representation of the five main bacterial phyla of the human gastrointestinal microbiota and some of the bacterial species that can be observed at this level. -----	33
Table 1.2 - Virulence factors of <i>Helicobacter pylori</i> bacteria and their effects (Adapted from [51], [62]). -----	46
Table 3.1 - Optical density at 600 nm corresponding, approximately, to $1.0 \times 10^7$ CFU/ml for each bacteria under study. -----	78
Table 3.2 - Visual scheme for chitosan microspheres size features measure from the mask in the brightfield channel. -----	85
Table 3.3 - Visual scheme for chitosan microspheres shape feature measure from the mask in the brightfield channel. -----	86
Table 4.1 - Table with the mean and standard deviation values obtained for the size features used in the characterization of the chitosan microspheres in citrate-phosphate buffer at pH 2.6, 4.0, 6.0 and 7.5. The average values presented are approximated to units. -----	93
Table 4.2 - Table with the mean values obtained for the shape feature used in the characterization of the chitosan microspheres for the samples at pH 2.6, 4.0, 6.0 and 7.5. The average values presented are approximated to tenths. -----	955
Table 4.3 - Table with the mean and standard deviation values, of the fluorescence intensity in channel 2, obtained on SPSS® for each of the samples containing chitosan microspheres and <i>Helicobacter pylori</i> labelled with SYTO9. The average values presented are approximate to the unit. -----	101
Table 4.4 - Table with the mean and standard deviation values, of the fluorescence intensity in channel 2, obtained on SPSS® for each of the samples containing chitosan microspheres and <i>Campilobacter jejuni</i> labelled with SYTO9. The average values presented are approximate to the unit. -----	105
Table 4.5 - Table with the mean and standard deviation values, of the fluorescence intensity in channel 2, obtained on SPSS® for each of the samples containing chitosan microspheres and <i>Escherichia coli</i> labelled with SYTO9. The average values presented are approximate to the unit. -----	108
Table 4.6 - Table with the mean and standard deviation values, of the fluorescence intensity in channel 2, obtained on SPSS® for each of the samples containing chitosan microspheres and <i>Lactobacillus casei</i> labelled with SYTO9. The average values presented are approximate to the unit. -----	112

Table 4.7 - Table with the mean and standard deviation values, of the fluorescence intensity in channel 2, obtained on SPSS® for each of the samples containing chitosan microspheres and *Enterococcus faecalis* labelled with SYTO9. The average values presented are approximate to the unit. ----- 115

Table 4.8 - Table with the mean and standard deviation values, of the fluorescence intensity in channel 2, obtained on SPSS® for each of the samples containing chitosan microspheres and *Bacillus cereus* labelled with SYTO9. The average values presented are approximate to the unit. ----- 118

## Abbreviations, Acronyms and Symbols

### Abbreviations and Acronyms List

A	Area
AR	Aspect Ratio
ATCC	American Type Culture Collection
BA	Blood agar base N. 2
<i>B. cereus</i>	<i>Bacillus cereus</i>
BHI	Brain Heart Infusion
BB	Brucella Broth
CagA	Cytotoxin associated protein
<i>cagA</i>	CagA gene
<i>C. jejuni</i>	<i>Campilobacter jejuni</i>
CCD	Coupled charging device
CFAs	Cyclopropane fatty acids
CFUs	Colony-forming units
Ch	Chitosan
Ch01	Brightfield channel
Ch02	Channel 2
Ch05	Channel 5
Ch06	Channel 6
CLSI	Clinical and Laboratory Standards Institute
cm	centimeter
CO <sub>2</sub>	Carbon dioxide
cP	Centipoise
d	Diameter
DA	Degree of Acetylation
DD	Degree of Deacetylation
DHA	Docosahexaenoic acid
DMSO	Dimethyl sulfoxide
DNA	Deoxyribonucleic acid



EDAX	Energy dispersive X-ray analysis
ELS	Electrophoretic light scattering
EPM	ElectroPhoretic Mobility
<i>E. coli</i>	<i>Escherichia coli</i>
<i>E. faecalis</i>	<i>Enterococcus faecalis</i>
EKA	ElectroKinetic Analyzer
FBS	Fetal Bovine Serum
FDA	Food and Drug Administration
FITC	Fluorescein isothiocyanate
FTIR	Fourier-transform infrared spectroscopy
g	G-force
GI	Gastrointestinal
h	Hour
HCl	Hydrochloric acid
HpaA	<i>Helicobacter pylori</i> specific lipoprotein
<i>H. pylori</i>	<i>Helicobacter pylori</i>
IARC	International Agency for Research on Cancer
I3S	Institute for Research and Innovation in Health from University of Porto
KatA	Catalase
KCl	Potassium chloride
LAS AF	Leica Application Suite Advanced Fluorescence
LAS X	Leica Application Suite X
<i>L. casei</i>	<i>Lactobacillus casei</i>
l	Liter
LPSs	Lipopolysaccharides
m	Meter
mbar	Millibar
MICs	Microspheres
Milli-Q water	Ultrapure water of Type 1
min	Minutes
ml	Milliliter
mm	millimeter
mm <sup>3</sup>	Cubic millimeters
MRS	De Man-Rogosa and Sharpe
MW	Molecular Weight
NaOH	Sodium hydroxide
NapA	Neutrophil activating protein
nm	Nanometer
N <sub>2</sub>	Nitrogen
O <sub>2</sub>	Oxygen

OD <sub>600</sub>	Optical density at 600nm
PBS	Phosphate-buffered saline
PPI	Proton Pump Inhibitor
PUFAs	Polyunsaturated fatty acids
rDNA	Ribosomal deoxyribonucleic acid
rpm	Rotations per minute of rotor
rRNA	Ribosomal ribonucleic acid
RT	Room temperature
s	Second
SabA	Sialic acid binding adhesion
SCM	Spectral Confocal Microscope
TDI	Time-delayed integration
TNF- $\alpha$	Tumor necrosis factor alpha
TPP	Sodium Tripolyphosphate
TSA	Tryptic Soy Agar
TSB	Tryptic Soy Broth
UFAs	Unsaturated fatty acids
VacA	Vacuolating cytotoxin A
<i>vacA</i>	Vacuolating cytotoxin gene A
ZP	Zeta potential
$\mu$ l	Microliter
$\mu$ m	Micrometer
$\mu$ m <sup>2</sup>	Square micrometers

#### Symbols List

$\beta$	Beta
$^{\circ}$ C	Degrees Celsius
%	Percent
$\xi$	Zeta
dU	Streaming potential
dp	Pressure differential
$\eta$	Viscosity
$\epsilon$	Relative dielectric constant
$\epsilon_0$	Vacuum permittivity
K	Electrical conductivity
$\lambda_{em}$	Emission wavelength
$\lambda_{ex}$	Excitation wavelength
$\sqrt{\quad}$	Square root
$\pi$	Pi



# Chapter 1

## Introduction

### 1.1 - Anatomical and physiological considerations of the lower gastrointestinal tract

The digestive system is formed by the digestive tube, which is composed by a set of organs of the digestive tract or gastrointestinal (GI) tract from the mouth to the anus, with important functions for the digestion and absorption process, mainly the supply of nutrients and electrolytes to the cells, essential for their survival, maintenance of water homeostasis and exclusion of pathogenic microorganisms. It is also constituted by the annexed digestive glands, which secrete substances that aid the digestive process that occurs in the organs of the GI tract [1].

In general, the morphology of the GI tract of mammals may vary greatly between species and it is, among other aspects, greatly influenced by the body size and shape of the individuals, frequency of food intake, need for nutrient storage and nature of the ingested food [2]. The digestive tract is formed by the oral cavity, pharynx, esophagus, stomach, small intestine, large intestine and anus, with an average length of approximately 5 m in adult man [1].

In this study, some of the anatomical and physiological characteristics of the stomach and intestine will be summarized, since these portions of the GI tract are of particular interest for the present research work [1].

#### 1.1.1 - Stomach

The stomach is a kind of expandable muscular sac, about 20 cm long and 15 cm in diameter, which can be macroscopically divided into different regions: a) cardia, with a distal location relative to the gastroesophageal junction, where the contents from the esophagus are deposited; b) fundus, where there is accumulation of gases produced during digestion; c) body, the largest portion of the stomach where the digestive process occurs; d) pyloric antrum, the most distal portion of this organ and e) pylorus, formed by the pyloric sphincter (Figure 1.1). The three main portions of the stomach, that is, the fundus, the body and the pyloric antrum differ morphologically among themselves in the inner portion [3].

This is the most dilated organ of the digestive tract and it is located between the esophagus and the duodenum [1], [3], [4] The separation between the esophagus and the stomach is done

through the esophageal sphincter, preventing reflux of the contents of the stomach into the esophagus, whereas the passage of chyme to the duodenum is mediated by the pyloric sphincter located in the terminal region of the pyloric antrum, which retreat the chyme back to the stomach [3]. The division of the stomach into these portions is based not only on anatomical differences, but also on significant structural and functional differences of the cells that constitute them [4].

The stomach plays an essential role in the digestive process, through its various secretory, motor and humoral functions important to the body, among which: 1) formation of chyme through the grinding and emulsion of the food bolus into smaller portions; 2) temporary storage of nutrients absorbed from food; 3) chemical digestion of proteins; 4) secretion of intestinal hormones important for the digestion process, as well as the release of acid that aids this process; 5) secretion of the intrinsic factor for absorption of vitamin B12; 6) regulation of the passage of chyme to the initial portion of the small intestine, the duodenum; 7) protection against pathogens through the release of proteolytic enzymes [3], [4].

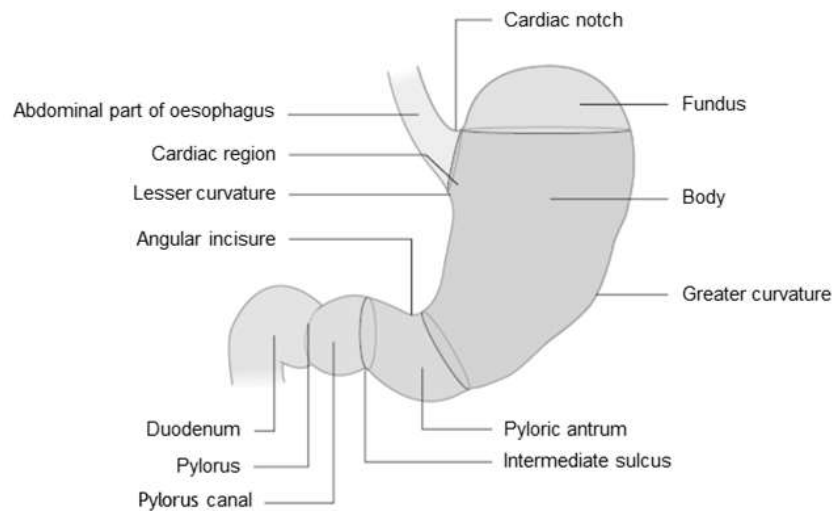


**Figure 1.1** - Representative scheme of the different parts that make up the stomach [3].

In general, the gastric wall, when analysed microscopically, has a similar structure to the other organs of the digestive system and it is formed by four layers: mucosa, submucosa, muscularis externa and serosa, whose microstructure reflects the functions performed by this organ [3], [4].

The mucosa membrane layer known as gastric mucosa divides into epithelium, lamina propria and muscularis mucosa and presents a soft and smooth surface, composed by numerous pleats mostly longitudinal, resulting from folds from the connective tissue of the underlying submucosa layer and not as a result of variations in its thickness. Gastric folds cover the inner surface of the stomach, forming a sort of small and irregular gastric crypts, pits or foveolae, where gastric glands are housed with exocrine cells producing mucus, digestive enzymes and hydrochloric acid [3]–[6].

The cells of the gastric glands produce gastric juice (about 2 l per day), which contains a variety of substances, such as water, electrolytes, hydrochloric acid (HCl), pepsin, mucus, and intrinsic factor. The stomach also secretes bicarbonate and mucus that help to protect the inner surface from possible injuries. The mucosal layer consists essentially of mucins, phospholipids,

electrolytes and water, which give it protection against hydrochloric acid, ethanol, bile salts and produced pepsins. The mucins of this layer are very important in the lubrication of the surface of gastric mucosa, giving it mechanical protection, which aims to minimize the abrasive effect of some foods that reach the stomach [3], [4], [6].

The stomach epithelium is composed of several cell types, in particular parietal cells responsible for the release of acid and intrinsic factor (essential for absorption of vitamin B12), pepsinogen-secreting main cells, later converted to pepsin (when luminal pH is less than 3.0) to initiate protein digestion, and at the level of gastric glands there are also mucus secreting cells, neuroendocrine cells, producing biogenic amines and important polypeptides in the control of stomach motility and glandular secretion, and stem cells responsible for the renewal of all the cells that constitute the epithelium [3], [4].

Gastric mucus is secreted by various types of mucus-producing cells and serves as a protective coating of the acid produced in stomach. The mucus and bicarbonate ions retained within the mucosal layer maintain a neutral pH in this region and contribute to the so-called barrier of the physiological gastric mucosa. In addition, mucus serves as a physical barrier between the cells of the gastric mucosa and the ingested material into the lumen of stomach [6].

The submucosal layer is formed by loose connective tissue surrounding the mucosa layer, containing extensive bundles of collagen and elastin, blood vessels and nerve plexuses, including the Meissner plexus, which innervates the vessels of the submucosa and smooth muscle of the muscularis mucosa [3], [6].

The muscularis externa layer is formed by a thick layer of smooth muscle with variable arrangement and of difficult differentiation in different regions of the stomach, with the main function of producing intense peristaltic movements that allow the emulsion of the foods with the gastric secretions for the formation of chyme and passage of this into the duodenum, as well as the reduction of solid food particles [3], [4], [6]. Lastly, the serosa layer is part of the visceral peritoneum of the abdominal cavity that covers the main external layer of the majority of viscera from abdominal region [3], [6].

### 1.1.2 - Intestine

The human and other mammal's intestines are divided into small intestine and large intestine. The small intestine is an organ of the digestive system with an average length of 5 m in the adult man and it is anatomically divided into 3 portions: duodenum, jejunum and ileum [1], [3], [6], [7].

The duodenum is the shortest and widest portion of the small intestine, extending from the pylorus region of the stomach to the jejunum with approximately 25 cm long and 5 cm in diameter in an adult man [1], [3], [6], [7].

Although there is no clear boundary separating jejunum from ileum, a gradual morphological transition occurs along the small intestine, thus considering that the initial 2/5 corresponds to the jejunum and the final 3/5 to the portion of the ileum [3], [6], [7].

The main functions of this organ are the digestion, absorption of nutrients into the internal environment of the organism, through the extensive network of blood vessels present in the circular folds and intestinal villi, maintenance of hemostasis of fluids and electrolytes, as well as immune regulation of certain hormones secretion. The high intestinal nutrient absorption capacity is mainly due to the high number of round folds composed of villi (Figure 1.2), which in turn consist of innumerable intestinal microvilli which considerably increase the contact area [3], [6], [7].

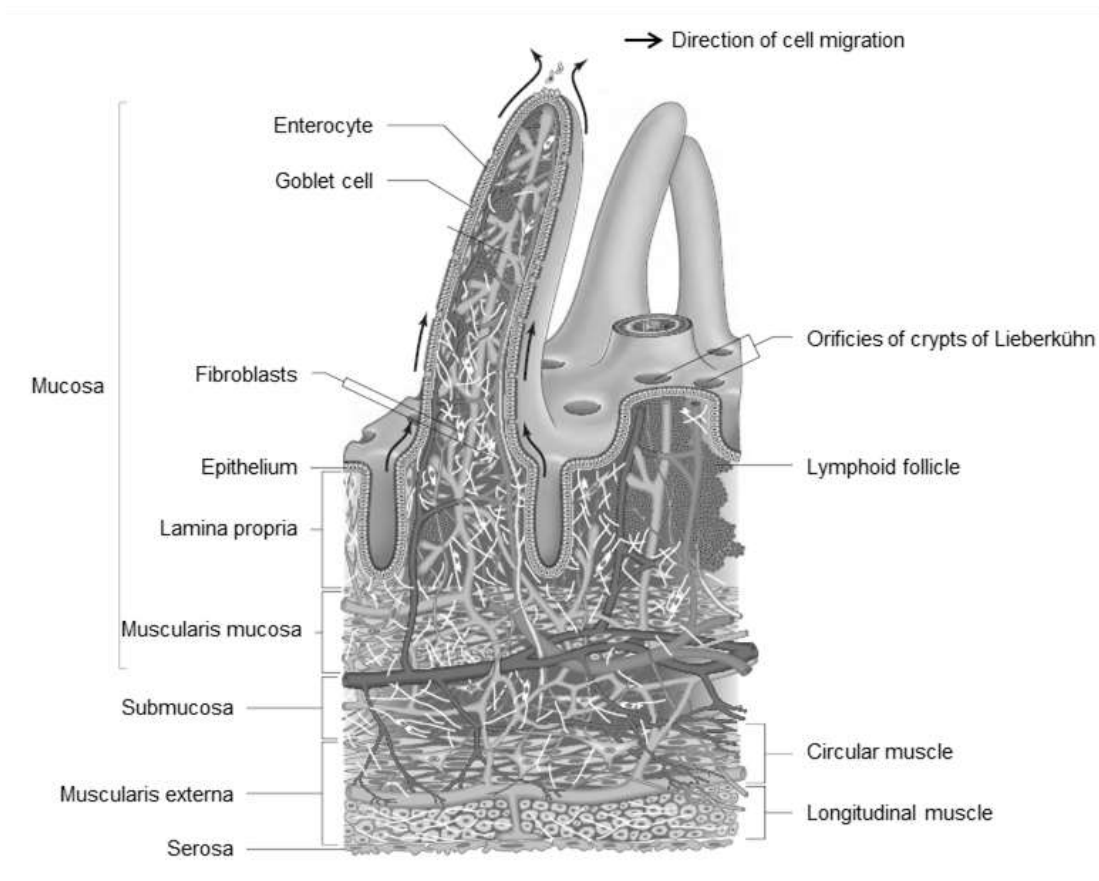


**Figure 1.2** - Structural scheme of intestinal villi [3].

In general, the processes inherent to digestion and absorption of the different nutrients are highly efficient; for example, with 95 % absorption of ingested lipids in the adult intestine. Although the digestive process begins in the mouth, the great majority occurs at the level of the small intestine, by enzymes produced by specialized epithelial cells and pancreatic enzymes [5], allowing the food conversion into forms that can be absorbed into the internal environment and its distribution to all cells of the body through the bloodstream [4].

With the exception of the initial portion of the duodenum, the small intestine is composed throughout its extension, by circular folds, called *plicae circulares* or *connivent valves*, with a transverse orientation or slightly oblique to the main axis, projecting towards the lumen of this organ. In opposition to the gastric folds, the intestinal folds do not disappear during the physiological distension of the intestine and, as such, are easily distinguished. These connivent valves decrease in number and size along the small intestine, disappearing almost completely in the portion of the terminal ileum [6], [7]. The inner wall of the small intestine, in addition to being composed of intestinal folds, is also lined throughout its extension with villi, highly vascularized on the surface of the mucosal layer, which increase in about seven times the surface area of the lumen. As in the case of intestinal folds, villus size and density also decrease gradually along the small intestine [3], [6], [7].

Together with the *plicae circulares*, intestinal villi causes an increase not only in surface contact area with the internal environment, but also an increase in mechanical segmentation, optimizing the process of nutrient absorption, with the passage of these from the lumen of the small intestine to the bloodstream. Invaginations of intestinal villi form the so-called Lieberkühn crypts at the base of the villi, which are generally more prominent in the proximal small intestine.

In turn, the wall of the small intestine is composed of 4 layers: mucosa, submucosa, muscularis externa and serosa or adventitia [3], [6].

The mucosa membrane layer is formed by the epithelium with a single layer of epithelial cells with microvilli in the apical region, covering the entire surface of the intestinal villi, including the Lieberkühn crypts, by the lamina propria, composed mainly of connective tissue, giving mechanical support to the epithelium and by the muscularis mucosa layer composed of circular and longitudinal bands of smooth muscle, which follows the profile of the intestinal folds. This layer is thicker and formed by a greater number of blood vessels in the proximal small intestine and thinner and less vascularized in more distal regions [3], [6].

The intestinal epithelium is composed of a large number of cell types, among which: 1) enterocytes, which are the cells present in greater quantity in the small intestine and are responsible for the absorption of nutrients; 2) Goblet cells, important mucin producers, not only for the protection and combat against toxins and pathogenic microorganisms, but also for the purpose of lubricating and giving mechanical protection to the intestine; 3) lymphocytes, which constitute an important means of defense of the immune system against pathogens and other environmental aggressions; 4) mucosal cells similar to Goblet cells; 5) Paneth cells, also important for the coordination of physiological functions such as defense, through the production and secretion of lysozyme, defensin and TNF- $\alpha$ ; 6) stem cells, essential for the renewal of the intestinal epithelium, once that they are able to produce all the different kinds of cells that form it; 7) neuroendocrine cells producing bioactive peptides, such as gastrin, cholecystokinin and secretin [3], [6].

As for the submucosa, this layer is essentially constituted of loose connective tissue, with collagen and elastin fibers in all directions, facilitating the development of peristaltic movements, without neglecting the mechanical support and the elasticity that confers to the tissue. This layer in the duodenum portion is also formed by Brunner glands, that secrete alkaline mucus (pH between 8.1 and 9.3), which allows the neutralization of the gastric juice that reaches this portion of the small intestine. The outer muscle layer is composed of fibers of smooth muscle cells with a thinner, longitudinally disposed outer layer and a thicker inner layer of circular shape. Finally, the serous layer formed by loose connective tissue is part of the so-called visceral peritoneum, which covers the great majority of the external muscular layer of the small intestine, except for the retroperitoneal portion of the duodenum and the region immediately adjacent to the mesentery [3], [6].

The large intestine is an organ approximately 1-1.5 m long in the adult individual, with a wall formed by haustrations or sacculations. The haustrations are nothing less than invaginations of mucous and submucosal layers of the wall of the large intestine, and may form a kind of an incomplete ring in the lumen of the intestine. The muscularis externa layer of the large intestine is formed by 3 longitudinal bands designated as taeniae coli (taenia libera, taenia omentalis and taenia mesocolica) and by appendices epiploicae that are small pockets of fat from peritoneum distributed throughout the surface [3], [6].

The large intestine is divided into 8 major regions: vermiform appendix, cecum, ascending colon, transverse colon, descending colon, sigmoid colon, rectum and anal canal [3], [6], [7].

The wall of the large intestine is formed by the same layers as the small intestine. The epithelium of the mucosa layer consists mainly of columnar or absorptive cells, with shorter apical microvilli and less regular than in the case of enterocytes of the epithelium of the small intestine, and mucous or Goblet cells (present in high numbers in crypts), structurally similar to those found in the small intestine [3], [6].



The crypts of the large intestine are narrow and formed by tubular glands distributed perpendicularly, more numerous, longer and closer to each other, than in the small intestine [3], [6].

Generally it takes 18 to 25 h for material from the small intestine to pass through the large intestine and it is in this organ, particularly in the region of the colon, that the formation of feces begins, with absorption of water and salts, such as  $\text{Na}^+$ , mucus secretion and intensive action of commensal microorganisms. Some proteins and carbohydrates can not be digested in the small intestine, suffering at the level of the large intestine alterations by bacterial enzymes, which allows their absorption in the colon region [2], [4], [7].

## 1.2 - Human gastrointestinal microbiota

Vertebrates harbor in their organism, in particular in mucus-producing organs, such as the oral cavity and intestine, a densely populated microbial community, called microbiota [8]. The human microbiota consists of 10 to 100 trillion commensal microbial cells housed in each individual, ten times the number of human cells, consisting mainly of bacteria present in the gut, whereas the human microbiome is described as the set of genes of all the microorganisms housed in the human organism. Thus, the term microbiota is defined as the rate of microorganisms that live in the human body, whereas the term microbiome refers to the set of all genes of all microorganisms in a microbial community [9]–[11].

Although some studies consider the human microbiota as a community of symbiont microorganisms, the truth is that pathogenic and pathobiont organisms are part of this microbiota community, which does not necessarily mean that these organisms will act negatively in the human body. These may simply establish relations of commensalism, without ever harming the normal functioning of the human organism.

It is not difficult to understand that both factors intrinsic to humans and external factors will influence the relations established between the human organism and the community of microorganisms that inhabit it, so that in this study it was decided to consider as microbiota all microorganisms described as capable of inhabiting the human organism.

The human GI microbiota represents the largest human microbial community and is defined as a complex ecosystem, mostly of an anaerobic nature [1], [12], consisting essentially of bacteria [represented by a great diversity of phyla (Table 1.1)], archaea (mainly methanogens) and eukaryotes (in particularly yeasts and filamentous fungi) and some virus. Contrarily to bacteria, archaea and eukaryotic domains are represented in the GI tract by microorganisms belonging to a small number of phyla [8], [13]. Currently and although a significant part of microorganisms capable of inhabiting the human GI tract has not yet been cultured, more than 1000 microorganisms species have been identified, based on the phylogenetic structuring of the small subunit sequences of the rRNA gene of these microorganisms. These species are described in *Rajilić-Stojanović M. and de Vos W.M.*, [14]. The human being harbors more than  $10^{14}$  microorganisms in the intestine, with density and diversity of the GI microbiota increasing from the stomach to the colon [1].

**Table 1.1** - Schematic representation of the five main bacterial phyla of the human gastrointestinal microbiota and some of the bacterial species that can be observed at this level.

Phylum	Genus	Species	Species localization in the GI tract	References
Bacteroidetes	<i>Prevotella</i>	<i>Prevotella pallens</i>	Stomach	[15]
		<i>Prevotella intermedia</i>	Stomach	[15]
		<i>Prevotella nigrescens</i>	Stomach	[15]
		<i>Prevotella melaninogenica</i>	Stomach	[15]
		<i>Prevotella denticola</i>	Stomach	[15]
		<i>Prevotella oulora</i>	Stomach	[15]
		<i>Prevotella oris</i>	Stomach	[15]
		<i>Prevotella oralis</i>	Stomach	[15]
	<i>Prevotella spp.</i>	Oral cavity, throat, stomach	[15]–[18]	
	<i>Capnocytophaga</i>	<i>Capnocytophaga granulosa</i>	Stomach	[15]
		<i>Capnocytophaga ochracea</i>	Stomach	[15]
	<i>Porphyromonas</i>	<i>Porphyromonas gingivalis</i>	Stomach	[15]
	<i>Tannerella</i>	<i>Tannerella forsythensis</i>	Stomach	[15]
	<i>Bergeyella</i>	<i>Bergeyella spp.</i>	Stomach	[15]
<i>Chryseobacterium</i>	<i>Chryseobacterium spp.</i>	Stomach	[15]	
<i>Bacteroides</i>	<i>Bacteroides thetaiotamicron</i>	Colon	[16], [19]	
	<i>Bacteroides fragilis</i>	Stomach, intestine	[20]–[23]	
	<i>Bacteroides melaninogenicus</i>	Intestine	[20]	
	<i>Bacteroides distasonis</i>			
	<i>Bacteroides plebeius</i>	GI tract	[24]	
	<i>Bacteroides caccae</i>		[25]	
	<i>Bacteroides spp.</i>	Lower intestine	[16], [18], [20], [24]	
Fusobacteria	<i>Leptotrichia</i>	<i>Leptotrichia amnionii</i>	Stomach	[15]
	<i>Fusobacterium</i>	<i>Fusobacterium nucleatum</i>	Stomach	[15]

		<i>Fusobacterium spp.</i>	Stomach, intestine	[15], [20]
Actinobacteria	<i>Cryptobacterium</i>	<i>Cryptobacterium curtum</i>	Stomach	[15]
	<i>Atopobium</i>	<i>Atopobium parvulum</i>	Stomach	[15]
		<i>Rothia mucilaginoso</i>	Stomach	[15]
	<i>Rothia</i>	<i>Rothia dentocariosa</i>	Stomach	[15]
		<i>Rothia spp.</i>	Oral cavity, stomach	[15], [17], [18]
		<i>Actinomyces odontolyticus</i>	Stomach	[15]
	<i>Actinomyces</i>	<i>Actinomyces viscosus</i>	Stomach	[15]
		<i>Actinomyces spp.</i>	Oral cavity, throat, stomach, intestine	[15]–[18], [20]
		<i>Corynebacterium glaucum</i>	Stomach	[15]
	<i>Corynebacterium</i>	<i>Corynebacterium mucifaciens</i>	Stomach	[15]
		<i>Corynebacterium spp.</i>	Oral cavity, stomach	[15], [17]
		<i>Bifidobacterium bifidum</i>	Large intestine	[11], [16], [23]
<i>Bifidobacterium</i>	<i>Bifidobacterium spp.</i>	Stomach, intestine	[16]–[18], [20], [21], [24]	
Firmicutes		<i>Streptococcus cristatus</i>	Stomach	[15]
		<i>Streptococcus infantis</i>	Stomach	[15]
		<i>Streptococcus mitis</i>	Oral cavity, stomach	[15], [17], [26]
		<i>Streptococcus gordonii</i>	Stomach	[15]
	<i>Streptococcus</i>	<i>Streptococcus parasanguinis</i>	Stomach	[15], [17]
		<i>Streptococcus sanguinis</i>	Stomach	[15]
		<i>Streptococcus salivarius</i>	Stomach	[15], [17]
		<i>Streptococcus constellatus</i>	Stomach	[15]
		<i>Streptococcus thermophilus</i>	Stomach, intestine	[22]
		<i>Streptococcus spp.</i>	Throat, stomach	[11], [15], [16], [18], [21]
	<i>Granulicatella</i>	<i>Granulicatella elegans</i>	Stomach	[15]
		<i>Granulicatella</i>	Oral cavity, throat, stomach	[15], [17], [18]
	<i>Abiotrophia</i>	<i>Abiotrophia para-adiacens</i>	Stomach	[15]
<i>Enterococcus</i>	<i>Enterococcus hirae</i>	Stomach	[15]	

	<i>Enterococcus faecalis</i>	Intestine	[16], [20], [23], [27], [28]
	<i>Enterococcus rectale</i>		[21]
	<i>Enterococcus spp.</i>	Stomach	[15], [16], [20], [21]
	<i>Lactobacillus fermentum</i>	Stomach	[15], [17]
	<i>Lactobacillus delbrueckii</i>	Stomach	[15]
	<i>Lactobacillus acidophilus</i>	Intestine	[16], [20], [29]
<i>Lactobacillus</i>	<i>Lactobacillus rhamnosus</i>	Stomach	[16, 24]
	<i>Lactobacillus gasseri</i>	Stomach	[17]
	<i>Lactobacillus casei</i>	Intestine	[22], [29]–[32]
	<i>Lactobacillus gastricus</i>		[26]
	<i>Lactobacillus spp.</i>	GI tract	[11], [15]–[17], [20], [21], [24]
<i>Weissella</i>	<i>Weissella confusa</i>	Stomach	[15]
	<i>Gemella haemolysans</i>	Stomach	[15]
<i>Gemella</i>	<i>Gemella adiacens</i>	Oral cavity	[17]
	<i>Gemella spp.</i>	Throat, stomach	[15], [18]
<i>Veillonela</i>	<i>Veillonela atypica</i>	Stomach	[15]
	<i>Veillonela spp.</i>	Oral cavity, throat, stomach	[15], [17], [18], [20]
<i>Eubacterium</i>	<i>Eubacterium saphenum</i>	Stomach	[11], [15]
	<i>Eubacterium spp.</i>	Stomach, lower intestine	[15], [18], [20]
<i>Mogibacterium</i>	<i>Mogibacterium neglectum</i>	Stomach	[15]
<i>Filifactor</i>	<i>Filifactor alocis</i>	Stomach	[15]
<i>Lachnospiraceae</i>	<i>Lachnospiraceae</i> genomospecies	Stomach	[15]
<i>Megasphaera</i>	<i>Megasphaera spp.</i>	Stomach	[15]
<i>Selenomonas</i>	<i>Selenomonas spp.</i>	Stomach	[15]
<i>Firmicutes</i>	<i>Firmicutes spp.</i>	Stomach	[15]
	<i>Clostridium difficile</i>	Intestine	[20], [21], [25], [33]
	<i>Clostridium innocuum</i>	Intestine	[20]
<i>Clostridium</i>	<i>Clostridium perfringens</i>	Intestine	[20]
	<i>Clostridium histolyticum</i>		[21]
	<i>Clostridium coccooides</i>		[21]

	<i>Clostridium spp.</i>	Lower intestine	[16], [18], [20], [21]
<i>Bacillus</i>	<i>Bacillus subtilis</i>	-	[11]
<i>Neisseria</i>	<i>Neisseria subflava</i>	Stomach	[15]
	<i>Neisseria flava</i>	Stomach	[15]
	<i>Neisseria elongata</i>	Stomach	[15]
	<i>Neisseria spp.</i>	Oral cavity, throat, stomach	[15]–[17]
<i>Delftia</i>	<i>Delftia acidovorans</i>	Stomach	[15]
<i>Comamonas</i>	<i>Comamonas testosteroni</i>	Stomach	[15]
<i>Lautropia</i>	<i>Lautropia mirabilis</i>	Stomach	[15]
<i>Moraxella</i>	<i>Moraxella osloensis</i>	Stomach	[15]
<i>Acinetobacter</i>	<i>Acinetobacter junii</i>	Stomach	[15]
<i>Escherichia</i>	<i>Escherichia coli</i>	Stomach, intestine	[11], [15], [19]–[23], [25], [29], [34]
<i>Haemophilus</i>	<i>Haemophilus paraphrophilus</i>	Stomach	[15]
	<i>Haemophilus influenzae</i>	Stomach	[15]
	<i>Haemophilus spp.</i>	Oral cavity, throat, stomach	[15]–[18]
<i>Actinobacillus</i>	<i>Actinobacillus pleuropneumoniae</i>	Stomach	[15]
<i>Brevundimonas</i>	<i>Brevundimonas vesicularis</i>	Stomach	[15]
<i>Caulobacter</i>	<i>Caulobacter bacteroides</i>	Stomach	[15]
<i>Blastobacter</i>	<i>Blastobacter denitrificans</i>	Stomach	[15]
<i>Pedomicrobium</i>	<i>Pedomicrobium ferrugineum</i>	Stomach	[15]
<i>Campylobacter</i>	<i>Campylobacter showae</i>	Stomach	[15]
	<i>Campylobacter concisus</i>	Stomach	[15]
<i>Helicobacter</i>	<i>Helicobacter pylori</i>	GI tract	[15], [18], [22], [24], [26], [27], [35]
	<i>Helicobacter hepaticus</i>		[33]
	<i>Helicobacter spp.</i>	GI tract	[15], [17], [18], [24]
<i>Flexistipes</i>	<i>Flexistipes spp.</i>	Stomach	[15]
<i>Acidovorax</i>	<i>Acidovorax spp.</i>	Stomach	[15]
<i>Alcaligenes</i>	<i>Alcaligenes spp.</i>	Stomach	[15]
<i>Ralstonia</i>	<i>Ralstonia spp.</i>	Stomach	[15]

Proteobacteria

<i>Sphingomonas</i>	<i>Sphingomonas spp.</i>	Stomach	[15]
<i>Klebsiella</i>	<i>Klebsiella spp.</i>	-	[16], [20]

The bacterial community among different habitats of the human adult organism is greatly differentiated, unlike the bacterial communities present in newborns which, to a large extent, are undifferentiated among themselves. The birth of placental mammals and, in the case of man, occurs through the vaginal canal, a site highly colonized by microorganisms, which naturally supplies the primary microbial inoculum to these newborn living beings. After birth, newborns are exposed to a wide variety of microorganisms capable of colonizing different habitats in humans [24]. Members of the same human family tend to have a more similar microbiota and with bacterial strains shared among them when compared to unrelated individuals [24].

The composition of the human microbiota is closely related to the intimate co-evolution of man with the microorganisms that inhabit our body. These microorganisms are capable, among other things, to create complex ecological ecosystems with other bacteria to acquire nutrients, with high capacity of habitat adaptation and the environment in force at any given time, and perfectly adapted to the physiology of the host, sometimes oscillatory [13], [17], [36]. In response to these same environmental changes, whose variability depends on aspects intrinsic to the GI tract itself such as the presence of certain enzymes, adhesive capacity, metabolic activity, among others [1], alter the composition and gene expression. For example, the bacteria *Eubacterium dolichum* and *Lactobacillus spp.* can not synthesize certain amino acids and as such acquire essential molecules from their habitats in the intestine, whereas the methanogenic archaea obtains energy from residual hydrogen molecules of other anaerobic organisms required. Thus, it can be said that the individual nutritional requirements of commensal microorganisms, and the interactions established between microorganisms of the microbiota and between the host and the surrounding environment, determine the composition and distribution of the commensal microorganisms along the GI tract [8].

The commensal flora of the GI tract plays important roles in many physiological processes of the human organism, including: 1) protection against lesions on epithelial cells lining the organs, as well as against pathogen colonization and overgrowth of native pathogens, which may arise when changes in the equilibrium state of the microbial community occur; 2) stimulation of angiogenesis with renewal of the intestinal epithelium; 3) induction of response of the immune system, directing its maturation; 4) regulation of the stored fat of the host; 5) modulation of host metabolism; and 6) ability to facilitate absorption/acquisition of nutrients into the internal environment [1], [8], [19], [37]. There is then a beneficial relationship between the GI microbial community and the cells of the human host organism which assists in the control of temperature and the maintenance of an adequate pH, important for the maintenance of the essential metabolic activities verified at this level, so that changes in the steady state of the GI microbiota can lead to serious health problems [1], [16].

Man's small intestine is rich in mono and disaccharides, as well as amino acids, essential for the growth of some bacteria, especially Proteobacteria and Lactobacillus. In the distal portion of the small intestine, of which the terminal ileum is part, the absorption of simple sugars by the cells of the host is verified, reason why from this region occur modifications in the bacterial composition, as a result of the alteration of the sources of energy available for bacterial growth [38].

On the other hand, besides the ileocecal valve, the vast majority of available sugars are derived from diet based on plant foods and polysaccharides (complex carbohydrates) from host cells, such as cell debris, mucins (rich in fucose, galactose, sialic acid, N-acetylgalactosamine, N-acetylglucosamine and mannose), etc., indigestible by the host organism. Mucin sugars are used by Bacteroidales (saccharolytic members) in the large intestine, which provide these nutrients to species of the microbiota that do not have the ability to break down sugars as a source of energy in metabolism. However, pathogenic bacteria that colonize the GI tract are also able to utilize available carbohydrate availability, promoting their growth and enlargement in the intestine [38].

Proteobacteria do not use complex carbohydrates as a source of energy because they can not digest polysaccharides and as such are not normally found in this portion of the intestine. In contrast, Bacteroides and Clostridiales (bacteria class belonging to the phylum Firmicutes, which includes *Clostridium spp.*) have enzymes capable of breaking host complex carbohydrates, such as mucins and indigestible fibers, using them as the main source of energy and, consequently, these microorganisms are in greater quantity in this portion of the intestine [38]. As a consequence, the abundance of Proteobacteria and Lactobacillus (bacteria genus belonging to the phylum Firmicutes) is much larger in the small intestine, with a marked dominance of Bacteroides and Clostridiales in the large intestine (Figure 1.3), which indicates that the distribution of nutrients in the intestine is one of the main instigators of the structure and composition of the microbial community that occurs in it. Nevertheless, there is a high diversity in the ability of bacteria of the same phylum to use polysaccharides as energy source, so that the polysaccharide content of a given diet can considerably affect the relative abundance of bacterial species [8].

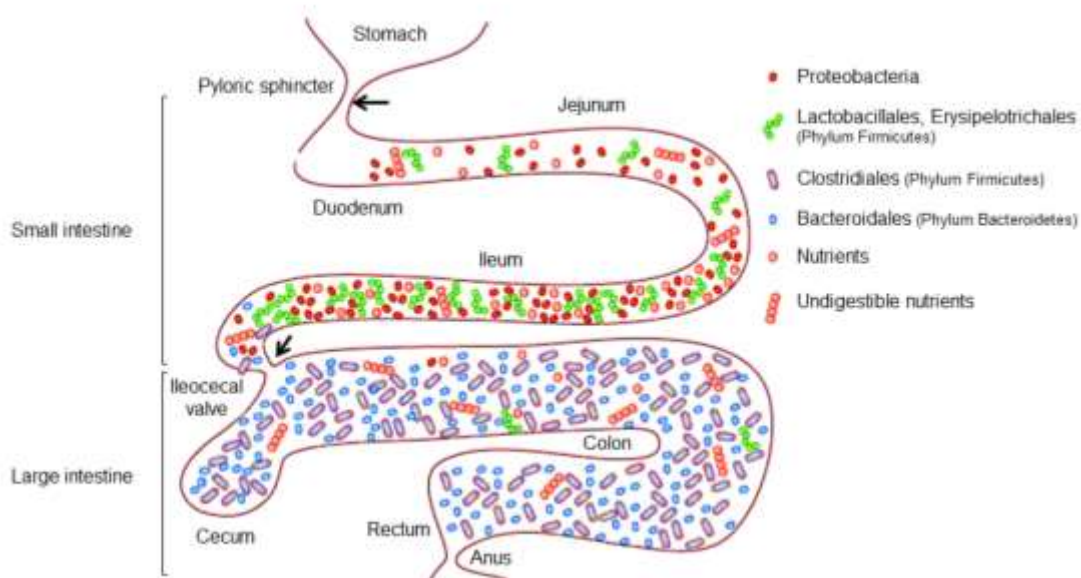


**Figure 1.3** - Representative scheme of the location of dominant bacterial groups in different portions of the intestine. Given the nutrient richness in the small intestine, both used by the host organism, and by the microorganism symbionts for its growth, in this portion of the intestine we find a greater amount of *Proteobacteria spp.*. In the large intestine the amount of nutrients is reduced, but in contrast the amount of fibers that do not undergo digestion is high, so that in this portion of the intestine is enriched with Bacteroidetes and Clostridia, able to use these fibers as an energy source (Adapted from [8]).

The composition of the microbiota that colonizes the human organism is influenced, among other factors, not only by the genetic constitution/disposition of the host, but also by the microbial habitat of the host, adapted to the colonization by certain groups of microorganism and whose niches are formed as result of diet, host genetics and the physical, chemical and immunological properties of the GI tract. In the case of newborns, the GI microbial community is composed of a relatively low number of species and lineages [24].

However, the diversity of microorganisms rapidly increases unstable in the first years of life (1-3 years), differentially for each individual, perhaps as a result of increased exposure to the environment surrounding individuals and/or as a result of growth of the GI tract, which may lead to the development of more microbial niches, a greater habitat for these microorganism to colonize or due to the increase of the taxonomic complexity of the microorganisms, associated to an increase in functional complexity by the host. Once established, this microbial community can be altered in response to alterations in the diet of individuals and/or pathological situations, among other aspects, providing adaptations to the various changes that man is subject to throughout his life. The bacterial populations present may still have influence on the physiological behaviour of the host organism [24].

The diet is a determinant factor in the establishment of the community of microorganisms that restrain the GI tract of man, intensifying the variability of species present among individuals and whose adaptation to changes in the diet of the host can occur through genomic alterations in this microbial community, in particular from the incorporation of bacterial genes from the environment. In its turn the GI microbiota varies between different geographic regions, due, in part, to the adaptation of these microorganisms to local diets [24].

The composition of the microbial community of the healthy GI tract and the number of species capable of inhabiting it (Figure 1.4) has been the subject of analysis by many studies. The major phyla of eubacteria present in the gut of healthy individuals are Proteobacteria (Gram-negative), Bacteroidetes and Firmicutes (Gram-positive, such as Clostridia and Lactobacilli) [8]. However, as a result of differences in the diversity of bacterial flora found between individuals and the small number of individuals undergoing analysis, the total number of microorganisms capable of colonizing the GI tract remains incomplete, due in part to the limitations of traditional methods (only a small fraction of bacteria colonizing the GI tract are amenable to be cultured; detection of a limited number of certain genomic sequences, etc.) [13].

From the use of molecular techniques it was possible to discover a much more complex number of bacteria that inhabit the GI flora and the understanding that the same microbiota dominated by phylotype, some of which have not yet been characterized, is specific for each individual, thus counteracting the hypothesis of a limited number of bacterial species inhabiting the GI tract [13].

The human oral cavity is composed of a high abundance of microorganisms in the order of  $10^9$  bacteria per ml of saliva. This region of the upper GI tract consists mainly of bacterial species of the following families and genera: *Prevotella*, *Rothia*, *Streptococcus*, *Actinomyces*, *Corynebacterium*, *Granulicatella*, *Veillonellaceae*, *Neisseria* and *Heamophilus*. Similar results were obtained for esophageal samples, with *Prevotella*, *Rothia*, *Streptococcus*, *Granulicatella* and *Veillonellaceae* as the most abundant genera in this region, despite presenting a much smaller amount of microorganisms than in the oral cavity [17].



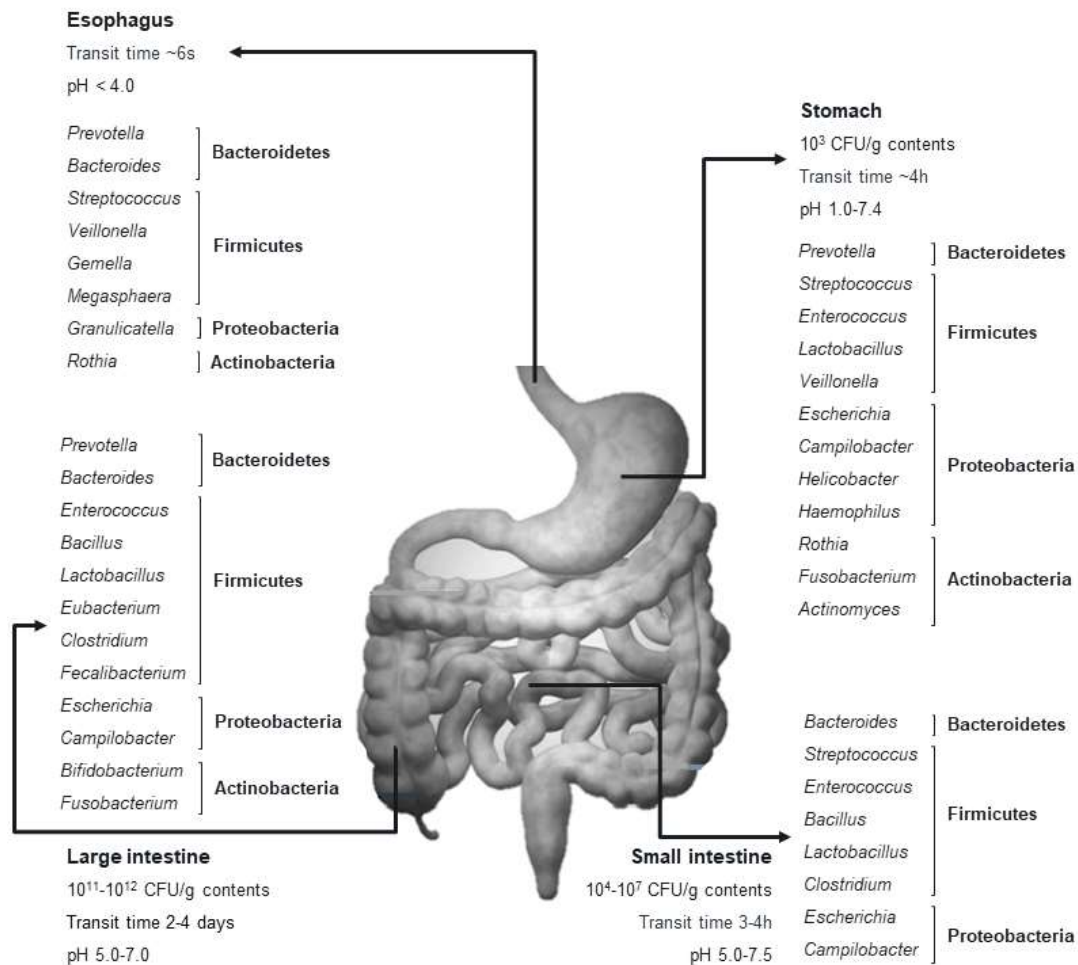


**Figure 1.4** - Distribution of human gastrointestinal flora from the esophagus to the large intestine and amount of bacteria present in each portion per gram of contents (Adapted from [39]–[44]).

The study of the microbiome began more than a century ago, through the sequencing of the 16S rRNA gene of the microorganisms, providing the first insights about the taxonomic composition of these communities. The main genera found in the human stomach are *Prevotella*, *Streptococcus*, *Veillonella* and *Rothia*, with the exception of the genus *Helicobacter* [16, 36]. Thus, technological advances related to the development of independent culture techniques allowed the identification and characterization of a wide variety of bacteria present throughout the GI tract, through the nucleotide sequencing of 16S rDNA or rRNA genes of bacteria [26]. Later, sequencing of the complete metagenome of the microbial communities allowed the acquisition of more detailed information about the total genetic capacity of the same community [38].

In 2006, *Bik, et al.* identified a microbial ecosystem of 128 gastric phylotypes, predominantly dominated by five phyla: Firmicutes, Bacteroides, Proteobacteria, Actinobacteria and Fusobacteria, through the analysis of the 16S rDNA of bacteria from gastric endoscopic biopsies of 23 patients, different from the microbial community of the oral and esophageal cavity analysed in some previous studies [15], [17], [26].

In 2010, *Qin Junjie, et al.*, established a microbial genomic catalog of the human gut by the method of metagenomic sequencing from fecal samples of 124 adult individuals of European origin (Nordic and Mediterranean), which at the time represented a considerable increase of the volume of sequenced genes, compared to the studies published so far. The majority of the genes

in the catalog obtained are of bacterial origin (99.1 %), the remainder being mostly archaea and only 0.1 % corresponding to eukaryotic microorganisms and virus [11], [36].

In this study [36], it was found that the phylotypes Firmicutes and Bacteroidetes represent the groups of bacteria present in greater abundance in the human gut, followed by Proteobacteria and Actinobacteria [38], and that, although the bacterial constitution was similar between different individuals in the analysis, it was possible to establish differences between healthy individuals and patients with inflammatory diseases. The results obtained, with respect to the high overlap of bacterial genetic sequences and, therefore, of a high number of intestinal bacterial species shared by the individuals, suggest the existence of a human GI microbiota constituted by a finite number of species with approximate value to that obtained by *Qin Junjie, et al.* [11].

These results make it difficult to identify a relatively constant set of microorganisms, understood as a normal human microbiota present universally in healthy individuals, as well as the detection of imbalances associated with disease states or reflecting pathological development.

Thus, it is important to understand, in addition to the diversity and richness of the healthy GI microbiota, the intrinsic metabolic and molecular properties and mechanisms of the microbial community of this specific habitat, whose composition may vary between individuals, allowing us to identify and produce changes in the associated configurations to the emergence of diseases of the GI tract [36], [45].

It has not yet been possible to achieve a faithful representation of the diversity of the human GI microbiota because a limited number of individuals have been subjected to analysis on the one hand and also due to the high complexity of the unique microbial community present in the individual household, thus making it impossible to describe the total richness of the species present [13].

As discussed previously, and despite the existence of an interpersonal variation in the human intestinal microbiota, it is known that there is a conserved set of coded functions of the intestinal microbiota, obtained from the analysis of specific genes of the fundamental microbiome, that allow to determine the functionality of the microbiota of the GI tract, rather than its composition. The set of genes constituting the microbiome, in particular the genes responsible for functions essential to the survival of the host organism, are not integrated into the human genome and as such are not encoded by the mechanisms associated to this. These functions and pathways encoded by the fundamental microbiome are important for the proper functioning of the intestine, thus providing benefits to the individual host [1].

### 1.2.1 - Interactions between the commensal gastrointestinal microbiota, pathogenic bacteria and host

The commensal GI microbiota plays an important role in maintaining a state of health, since any changes in its composition and diversity can promote infections caused by, for example, pathogenic bacteria, as well as the acquisition of resistance to the treatments used to combat those infections, thus reducing success rates in the treatment of infectious diseases [38].

Factors such as the genetic constitution of the host individual, diet and environmental conditions to which he is subject or antibiotherapies, can lead to physiological and immune changes, triggering a variable susceptibility to infectious diseases. The exacerbated use of antibiotics, in particular non-selective conventional antibiotics, in the fight against bacterial infections has induced a great functional, genomic and taxonomic impact, with effects sometimes *ad aeternum*, in the GI microbiota [38].

As mentioned in 1.2 and although the composition of the microbiota and the host diet have a strong influence on the availability and distribution of nutrients throughout the intestine, characteristics intrinsic to the host itself, such as the inflammatory response in infections caused by pathogenic microorganisms, also plays an important role [38].

The occurrence of dysbiosis in the composition of the human intestinal microbiota has been associated with the emergence of certain pathologies and the evolution to chronicity, such as obesity, type 1 and type 2 diabetes, inflammatory bowel disease, and gastric and colorectal cancer [36], [46]. The human healthy/commensal microbiota seems to be of great importance for host development, and therefore changes in the composition of these symbiotic microorganisms of the human organism appear to be factors that contribute to the triggering and/or persistence of some diseases, some of which have been previously mentioned [47]. Many studies have shown differences in the composition of the GI microbiota between patients with intestinal diseases and healthy individuals, which may reflect the occurrence of changes in factors and nutrients in a disease state and/or be secondary to the inflammatory response initiated by the immune system of the patients. However, additional ecological analysis regarding the interactions between these bacteria and the environment in which they are found, as well as the mechanisms involved in the individual metabolic activities of each bacterium, should be better studied for a better understanding of all the factors involved in diversity of the microbiota along the GI tract [8].

Dysbiosis can be understood as a change in the composition of the microbiota, in relation to the community of these microorganisms observed in healthy individuals [47] of the same community, that is, the removal of the ecological balance, although some studies have shown differences in microbiota, among healthy individuals, and that factors such as geographic location, type of feeding, and others, influence the diversity of the same microbiota [24], [36], [38]. Thus, a key factor in maintaining a healthy state in humans is the control and preservation of the normal balance of the GI microbiota.

*H. pylori* is a pathogenic bacterium of the human stomach, capable of causing infections in the gastric mucosa wall, thus initiating a cascade of inflammatory responses that may evolve into gastritis, a pathological condition associated with a reduction in the capacity of gastric cells to produce gastric acid and, consequently, the possibility of developing gastric cancer. This reduction of the acid production/secretion capacity of acidic substances in the stomach enables the proliferation and survival of microorganisms which in a normal situation would be killed by the acid environment, with an increase in the number of bacteria in this organ, especially *Streptococcus mitis* within the *Streptococcus spp.* [17].

Intestinal inflammation in humans is associated with an imbalance of the microbiota, with changes in the availability of nutrients in the large intestine, such as the complex carbohydrate composition, characterized by a reduced diversity of microorganisms, a decrease in the abundance of obligate anaerobic bacteria and by an increase of facultative anaerobic bacteria of the phylum Proteobacteria, especially species of the family Enterobacteriaceae, such as *Escherichia coli* and *Klebsiella spp.* [38].

The decrease in the diversity of the intestinal microbiota, with a change in the nutritional distribution of the intestine, may lead to a growth of populations of pathogenic microorganisms, as a consequence of the compromised resistance to colonization by pathogenic bacteria, which may lead to the development of serious pathological conditions as, for example, potentially fatal colitis as a result of the growth of *Clostridium difficile*. In a study on intestinal microbiota resistance to infection caused by *Campylobacter* bacteria [48], it was shown that individuals with a greater diversity of the intestinal microbiota and with a greater abundance of the bacterial genera *Dorea*

and Coprococcus presented high resistance to infection by *Campylobacter jejuni*, contrary to individuals with low microbial diversity and low abundance of Dorea and Coprococcus, thus demonstrating the ability of the microbiota to promote resistance to colonization by pathogen species [38].

The interaction between the commensal microbiota, the human host and pathogenic and/or pathobionts microorganisms is an essential process of controlling the infections and diseases caused by these microorganisms. Therefore, the understanding of the mechanisms inherent in these interactions may contribute to the emergence of new therapeutic approaches capable of manipulating the microbiota against infectious diseases [8], [38]. These interaction mechanisms, capable of regulating the behaviour of the microbiota in the restriction of the growth of pathogens, are complex systems that involve induction of response by the host immune system, location in specific intestinal niches and competitive metabolic interactions between the intestinal commensal microbiota and pathogenic microorganisms. On the other hand, pathogens have developed strategies capable of overcoming resistance to colonization, mediated by the commensal microbiota, and use carbon and nitrogen sources derived from the microbiota, such as nutrients and regulatory signals that promote their growth and virulence [8], [38]. Changes in the human GI microbiota have been associated with the onset of GI tract symptoms and diseases, such as gastric cancer, colorectal cancer and Bowel's inflammatory disease [1].

In a study on human gastric microbiota, *Bik, et al.* sought not only to evaluate whether the composition of the gastric microbiota is different from the oroesophageal microbial community and whether it varies between the various anatomical portions of the stomach (fundus, body, antrum and pylorus), but also to determine if the bacterium *H. pylori*, when present in the stomach, has influence on the composition of the commensal gastric microbiota [15]. Samples of the gastric biopsy were divided into three groups: Group I (n = 4) - Samples of negative individuals for the presence of *H. pylori* (determination from conventional laboratory methods) and for the presence of sequences of this bacterium; Group II (n = 7) - Samples of individuals negative for the presence of *H. pylori* and positive for the presence of sequences of this bacterium; Group III (n = 12) - Samples of individuals positive for the presence of *H. pylori* and for the presence of sequences of this bacterium. These investigators demonstrated the presence of a broad range of bacteria, in addition to *H. pylori*, the dominant bacteria in the human stomach and, therefore, a greater microbial diversity than previously described. Also, the presence of the *H. pylori* bacterium does not seem to affect the composition of the gastric microbiota [15], [24].

Some studies have demonstrated the crucial role of bacteria in the GI microbiota for the optimal functioning of the GI tract, thus corroborating the hypothesis that these bacteria may influence morphophysiology and contribute in some way to combating infections caused by *H. pylori* [49], [50]. The study by *Rolig A.S., et al.* allowed the *in vivo* observation of a change in the microbial community, following antibiotic treatment *a priori* of *H. pylori* infection, leading to a decrease in the inflammatory response of the immune system after an infection caused by this bacterium. This decrease in inflammatory response appears to be associated with a change in recruitment of CD4<sup>+</sup> T cells, which are produced and released in the stomach in response to infection caused by *H. pylori*. The most abundant phylotypes found in the mouse stomach were Firmicutes, Bacteroidetes, Proteobacteria and Actinobacteria, a composition similar to that found in humans. The great majority of the isolated bacteria belonged to the Firmicutes phylum, mainly of the class *Clostridia*, followed by the phyla Bacteroidetes and Verrucomicrobia (another phylum that can be found in the GI tract, but only with two species detected in the human GI tract), the second and third most abundant phyla [14], [49].

In this study, it was demonstrated that the composition of the general stomach microbiota of the animal model used was not significantly affected by *H. pylori* infections, but rather affects some members of this community, in particular an increase of Firmicutes from class *Clostridia*, Proteobacteria (genus *Helicobacter*), and Verrucomicrobia and also a decrease of Firmicutes from class *Bacilli*, Bacteroidetes, and Proteobacteria. Thus, manipulation of the GI microbiota may be used to prevent the onset of diseases associated with *H. pylori* infection and to use the composition of this microbial community as a marker to anticipate the onset of GI diseases [49].

On the other hand, *Khosravi Y., et al.* observed *in vitro* that the species *Sreptococcus mitis* induces the conversion of *H. pylori* to its coccoid form and causes inhibition of its growth, but did not record significant modifications of the gastric microbiota by *H. pylori*. This study suggests the existence of factors produced by members of the GI microbiota, such as a Tenovin-6-like compound, capable of inducing the conversion of the *H. pylori* bacterium into its cocoide form, suggesting the influence, even indirectly, of these bacteria, not only in the pathogenicity, but also in the severity of the disease in individuals infected by this pathogenic bacterium [50].

However, the studies developed until then, from the analysis of the genome of the human gastric microbiota, have some limitations that may have contributed to the occurrence of differences in the results obtained by the different research studies. In particular the lack of histomorphological correlation and gastric acidity, methodological limitations regardless to the semi-open GI tract and also the relatively low number of clusters used for analysis [26].

## 1.3 - *Helicobacter pylori* gastric infection

### 1.3.1 - *Helicobacter pylori*: general considerations

The *Helicobacter pylori* bacterium is a Gram-negative pathogenic bacterium that commonly infects the stomach of the human being, colonizing mainly the gastric mucosa of this organ. It has a generally bacillary/spiral shape with a length of between about 2 to 5  $\mu\text{m}$  and about 0.5 to 1  $\mu\text{m}$  in width, although it has also been observed *in vitro* in the coccoid form after prolonged culturing or as a result of treatment by antibiotics. The coccoid forms of *H. pylori* can exist in three different forms: cultivable viable form, viable but not cultivable form and still a degenerative dead form. These forms appear to have biochemical and genetic properties similar to spiral forms [51].

Changes in the conformation of the bacterium from its spiral form to the coccoid form are associated with an aging bacterium (prolonged culture which may lead to a non-cultured bacterial state and adhesion to the gastric epithelium but also as a result of exposure to unfavorable conditions, such as antibiotics, aerobic conditions and alteration of the pH and temperature of the medium. The presence of coccoid forms may allow the identification of dead and/or inactive bacteria and, in the case of the application of treatments containing materials with bacteriostatic effect to eradicate the bacterium, only its inactivation is achieved, leading to its recovery after ceasing the effect of the applied treatment. The *H. pylori* bacterium only provokes infection being in its bacillary form, it is thought that when *H. pylori* is in a coccoid form it is in a dormant/inactive state. This bacterium may still present between 4 and 6 unipolar flagella, in one of the poles of the cell, of approximately 3  $\mu\text{m}$  each [51]–[54].

Its cytoplasmic membrane is characteristic of Gram-negative bacteria. The internal cytoplasmic membrane is composed mainly of peptidoglycans; the outer cytoplasmic membrane is formed by phospholipids, containing single cholesterol glucosides (which is very rare in other

bacteria), LPSs and, still, periplasmic liquid present between these two portions of the cell membrane [55].

*H. pylori* is a microaerophilic bacterium with high survival capacity to the conditions in the human stomach, in particular the extremely acidic pH of this organ, with very specific characteristics essential to its development, namely an atmosphere rich in CO<sub>2</sub> (5-10 %), and low O<sub>2</sub> (2-5 %) and an ideal growth temperature of 37 °C [51], [53], [56], [57].

Said bacterium is a neutrophil microorganism with optimum growth at neutral pH, although it may exhibit growth over a broad pH range of 5.5 to 8 and therefore compatible with the region of the gastric mucosa where it is preferentially grown. The enzyme urease secreted in high quantities by *H. pylori* is the main route that catalyzes the hydrolysis of urea in ammonia (NH<sub>3</sub>) and CO<sub>2</sub>, thus allowing the neutralization of the immediate surrounding environment by the bacterium, as well as the dissolution of the mucins present in the gastric mucus. This effect, together with the helical shape of the bacterium and the flagellar motions, make it possible for the bacterium to penetrate the region of the gastric mucosa, which is generally less acid than the other regions of the human stomach, presenting better conditions for its growth and development [51], [56], [58]–[62].

Despite this, it is also found in other regions of the stomach, such as adhered to the epithelial cells, in addition to the gastric mucus layer, as a result of having the means to resist the oxidative stress to which it is subjected in the lumen stomach, through the reaction mediated by the enzyme superoxide dismutase (SODb) that catalyzes the dismutation of superoxide in oxygen and hydrogen peroxide, and the defense against hydrogen peroxide through the intracellular catalase enzyme (KatA) and the alkyl hydroperoxide reductase enzyme (AhpC) [60], [63]–[65].

*H. pylori* is a pathogenic bacterium that exhibits unique genetic heterogeneity, leading to a high number of strains with different genetic characteristics and, consequently, with different potential to cause pathogenicity in the host organism, through, for example, the release of toxins and factors of adhesion to the cells lining the gastric mucosa, which may be closely associated to the various mechanisms of adaptation of this bacterium to the conditions of the gastric environment and the high evasion capacity against the host immune system.

This bacterium has a series of virulence factors (Table 1.2) that facilitate colonization of the host, allow the pathogenic microorganism to avoid the defense mechanisms, and can cause damage to host tissues. Thus, strains isolated from *H. pylori* were divided into two types: highly virulent Type I strains expressing more pathogenic forms of CagA and VacA (associated with an increased risk of developing a variety of gastric diseases), intermediate strains and Type II strains of reduced virulence, which do not express any marker [51], [56], [66]–[70].

**Table 1.2** - Virulence factors of *Helicobacter pylori* bacteria and their effects (Adapted from [51], [62]).

Characteristics of bacteria	Virulence Factors	Effects
<b>Survival</b>	Intracellular surveillance	Prevents death in phagocytes
	Superoxide dismutation	Prevents phagocytosis and death, by detoxification of radicals of O <sub>2</sub> (H <sub>2</sub> O <sub>2</sub> )
	Catalase	
	Coccoide shape	Stable inactive form
	Heat shock proteins (coating antigens such as urease)	Prevents phagocytosis
<b>Colonization</b>	Flagella and Flagellins	Active movements of penetration through mucins of gastric mucus
	Adhesins	Adhesion to the epithelium
	Urease	Acid neutralization and nutrient acquisition
<b>Tissue damage</b>	Proteolytic enzymes	Degradation of mucins by glucosulfatase
	CagA	Causes severe ulcers and gastritis
	VacA	Epithelial damage
	Urease	Toxic effect on epithelial cells, disrupting the tight junctions of cells
	Phospholipase A	Diges the phospholipids of cell membranes
	Alcohol dehydrogenase	Lesion of gastric mucosa
	Neutrophil activating protein	It leads to neutrophil-mediated gastric mucosal damage
<b>Others</b>	Lipopolysaccharides	Low biological activity
	Homology of the Lewis x/y blood group	Autoimmunity

### 1.3.2 - Colonization of gastric mucosa by *Helicobacter pylori*

*H. pylori* is a pathogenic bacterium with a high capacity for adhesion to gastric epithelial cells, which preferentially colonizes the gastric mucosa of more than 50 % of the world's human population [46], [59] with the ability to survive the high acidic pH of the gastric environment. Although it is found in greater quantity free-swimming in the region of the mucus layer, it is also, although in smaller quantity, adhered to the mucus layer and to the surface of gastric epithelial cells in the stomach. It has documented the internalization of this bacteria in epithelial cells as well as in cells of the immune system [39], [65], [71]. According to *Schreiber et al.*, in Mongolian

gerbils model, 88 % of *H. pylori* bacteria is 15µm above the epithelial cells (10-15 µm – 26 %, 5-10 µm – 32 % and 0-5 µm – 30 %) lining the surface of the stomach, 12 % colonize the region immediately adjacent to or are adhered to epithelial cells [65].

According to the literature [72]–[75] and although most of the infected individuals do not present clinical symptoms (ie less than 20 % of individuals infected with *H. pylori* have symptoms [76]), chronic diseases caused by *H. pylori* are associated with an increased risk of gastric complications such as gastritis and peptic ulcers, sometimes associated with the onset of gastric adenocarcinomas and lymphoma of lymphatic tissue associated with gastric mucosa (mostly MALT) [21], [57], [72]. In 1994 this bacterium was classified by the IARC as being a carcinogen class I [77], possessing a series of virulence factors [51], [78] capable of leading to the onset of gastric cancer.

The risk of clinical complications or disease situations is determined in part by host genetic factors and genetic heterogeneity of the various *H. pylori* strains with different levels of pathogenicity that encode interaction factors between the host organism (including the environment) and the bacterium [74], [75], [79].

In general, man possesses a series of mechanisms capable of eliminating harmful bacteria of the organism, in this case in particular through the acidity of the stomach, of peristaltic movements and the mucus produced by specialized epithelial cells, thus preventing the adhesion and colonization of the gastric mucosa by these pathogenic organisms [62]. In addition, infection caused by the colonization of *H. pylori* in the stomach triggers a serious inflammatory response by the host's immune system in an attempt to eliminate the bacterium from the GI tract. However, once established in the gastric environment, it can persist throughout the entire life of the host and is the dominant microorganism [15], [80].

*H. pylori* has a number of virulence factors, some of which are mentioned in Table 1.2, which enable it to survive conditions found in the gastric environment. As stated in 1.3.1, *H. pylori* through the enzyme urease, actively produced by this bacterium, enables the conversion of urea to ammonia and carbon dioxide, thus leading to an increase in the pH in the vicinity of the bacterium to more neutral values and the dissolution of mucins from the gastric mucus, thus increasing the inflammatory process, which may evolve into gastric diseases [51]. This event, together with the flagellar movements of the bacterium, allows its passage to the region of the gastric mucosa (pH ~ 7.4), which covers and protects epithelial cells from external aggression and extremely acidic pH of the stomach lumen (pH 1.2 to 2.5) [39].

In order to avoid peristaltic movements and the acidic pH of the stomach lumen (*H. pylori* loses its mobility at acidic pH) and, for a better obtaining of nutrients, *H. pylori* has a mechanism of binding through specific proteins from the outer portion of the cytoplasmic membrane, adhesins, receptors or epitopes, i.e., proteins or glycoconjugates on the surface of epithelial cells and the gastric mucosal layer, which facilitates, among other aspects, initial colonization and persistence of infection [81]–[85].

The binding of *H. pylori* adhesins to the gastric mucosa is made from carbohydrate structures, ie Lewis blood group antigens Lewis b (Le<sup>b</sup>), found mostly on the epithelial surface, and Lewis x (Le<sup>x</sup>), localized in deeper regions. Lewis blood group antigen-binding adhesin (BabA) mediates binding to the gastric mucosa via binding to the Le<sup>b</sup> antigen, for example, whereas sialic acid binding adhesion (SabA) mediates adhesion to mucosal cells through the formation of sialized carbohydrate structures, such as sialyl-Le<sup>x</sup> (or directly binds to the Le<sup>x</sup> antigen) or sialyl-Le<sup>a</sup> [58], [62], [71], [81], [84]–[86]. Individuals infected with *H. pylori* strains that actively express the BabA gene are more likely to develop gastric diseases than individuals infected with *H. pylori* strains



that do not express this gene, particularly if they also have the *cagA* and *vacA* genes [69], [87], [88].

In addition, *H. pylori* has innumerable systems of resistance to oxidative stress caused by cells of the host immune system, mechanisms that facilitate the production of nutrients through the induction of tissue inflammation in the stomach and the production of antibacterial peptides to eliminate the competition from other bacteria, to which *H. pylori* is resistant [60], [63], [89].

Potentially pathogenic bacteria, such as most *H. pylori* strains, are able to deposit their membrane LPS into cells of the immune system and thus trigger a pro-inflammatory response. LPSs are normally formed by a lipid moiety 'A' and a side 'O' chain, and the 'O' side chain, when undergoing fucosylation, may be associated with molecular mimicry, adhesion, colonization and immune response modulation of the host, mimicking the Lewis blood group antigens (such as Le<sup>x</sup> and Le<sup>y</sup>), thereby aiding in the camouflage of the *H. pylori* bacterium of the host organism's immune system. In man, Lewis antigens are present in several cells, such as monocytes/macrophages and granulocytes. This bacterium is still able to deposit its LPSs into cells of the innate immune system, triggering proinflammatory responses [55], [57], [81], [90]–[93].

The antigens produced by *H. pylori* increase the capacity of internalization of bacteria in epithelial cells, thus suggesting their potential effect under innate immune system responses. However, it is not clear whether the ability to mimic Lewis blood group antigens promotes the elicitation of immune responses or attenuates the immunostimulatory effects of LPSs. This mechanism may be associated with an induction of the production of antibodies by the immune system of the host, with the intention of, for example, acting against PPIs during the antibiotic treatments applied to patients with infections caused by this pathogenic bacterium [57], [91].

Patients infected with *H. pylori* have been shown to produce antibodies against the LPSs of this bacterium, indicating that LPSs also act as an immunogenic agent capable of inducing cross-reactive antibody responses, thus increasing the local inflammatory process [91].

### 1.3.3 - Existing therapies for *Helicobacter pylori* infection

As previously mentioned, infection caused by the *H. pylori* bacterium in the stomach affects more than half of the human population worldwide, with geographically variable infection rates, and may lead to GI pathologies with a high socioeconomic impact [59], [94], [95]. Portugal is one of the European countries with the highest prevalence of infection, although in recent decades the rate of infection in developed countries has decreased considerably (less than 50 % in some European countries), possibly due to improved hygiene conditions domestic and sanitation. It is estimated that more than 70 % of individuals of the same age group in developing countries may be infected with *H. pylori* and less than 40 % in developed countries [95].

According to the Maastricht Consensus Report V, the recommended first line therapy for the treatment of *H. pylori* infection remains the triple therapy, based on the joint application of two antibiotics, such as amoxicillin and clarithromycin (in areas of low resistance to this antibiotic) or metronidazole, in order to eliminate the bacterium and a proton pump inhibitor, in particular omeprazole, rabeprazole or lansoprazole, which facilitates the action and stability of the antibiotics in the stomach by reducing the production of gastric acid, which increases the pH in the lumen of this organ, being the quadruple therapies based on bismuth compounds alternatives to the treatment as first line [96].

However, available treatments for patients with symptoms, ie about 20 % of infected persons [76], in particular first-line treatments based on the joint application of antibiotics and an IPP [96],

fail at a certain percentage of the cases, due, among other things, to the capacity of *H. pylori* strains in acquiring resistance to antibiotics used, high gastric acidity, high bacterial load, type of strains, recurrent possibility of infection, high costs, side effects and non-compliance of the treatment by patients [97]–[99]. More recent data reveal a decrease in the efficacy of this therapy for lower than expected values for infectious diseases, with success rates of only 70 % in some cases and with failure rates above 40 % in some European countries [95], [98], creating the need to apply second and third-line therapies with better success rates against antibiotic resistant *H. pylori* strains [96].

The growing increase in resistance to antibiotics by strains of this bacterium, coupled with a possible degradation of antibiotics in the human stomach due to the high gastric acidity; the lack of penetration to the region of the gastric mucosa, where this bacterium is found in greater quantity, as well as the recurrent possibility of infection (rare in developed countries, with 2.67%, but approximately 13.00% in developing countries) and non-compliance of the treatment by the patients due to other aspects of the side effects of the treatments, such as nausea, vomiting and diarrhea, are some of the problems inherent to the inefficiency of the treatments applied today [20], [39], [95], [100], [101].

Recently there has been worldwide evidence of *H. pylori* resistance to antibiotics, albeit with some variability between geographical areas, which confirm an increase in antibiotic resistance rates and a decrease in eradication rates of *H. pylori* [96]. Therefore, in order to prescribe a given treatment, it is important to make an early evaluation of the clinical history of antibiotic taking by patients in previous therapies, not necessarily for the treatment of infections caused by this bacterium, and also to collect information on the rate of antibiotic resistance in the population, allowing the structuring of a treatment using appropriate therapies, thus maximizing the rate of success in the eradication of *H. pylori* [74]. On the other hand, the instability of the antibiotics in the gastric environment, with pH values between 1.2 and 2.5 on the lumen, even in the presence of PPIs, decreases their bioavailability to act against *H. pylori* [39], [62], [101]–[103].

When the pH of the gastric environment is less than 6 and above 3, the action of antibiotics dependent on microbial replication (such as clarithromycin and amoxicillin) is compromised, since for these pH values it seems that *H. pylori* is in a non-replicative viable state. Increasing the pH to 6 or 7 promotes a greater susceptibility of the microbial response to the antibiotic or group of antibiotics in question [95]. The mucosal protector of the gastric mucosa, a region of greater colonization by the *H. pylori* bacterium, acts as a barrier that hinders the penetration/diffusion of antibiotics to this region, reducing the amount of antibiotic that effectively can act in the area of greatest colonization by this bacterium [62], [95].

Under adverse environmental conditions, such as the application of antibiotic and PPI treatments, *H. pylori* may acquire a coccoid form, remaining in a quiescent, non-receptive state to the action of antibiotics, until environmental conditions are favorable. After treatment, it can be reactivated by acquiring its more virulent spiral form. Some factors intrinsic to the host itself may also contribute to the failure of existing therapies, such as diseases such as obesity and diabetes, genetic polymorphisms, smoking, acid secretion, diet, etc. These factors contribute to the inconstancy of the success rate of the currently applied treatments for the eradication of *H. pylori* between geographic regions, for the increasing decrease in the success of current therapies and for the absence of a common treatment applied to all patients [95].

Regarding the virulence factors of *H. pylori*, it is thought that negative CagA strains are associated with higher levels of therapeutic failure, contrary to CagA-positive strains, which may be related to the fact that, the presence of CagA at inducing response of the immune system,

increases local inflammation, which may aid in the diffusion process of the applied antibiotics. On the other hand, the fact that CagA positive strains have a higher proliferation rate, coupled with a higher activity of antibiotics in growing bacteria, CagA positive strains are more susceptible to the action of antibiotics, which can lead to better rates of therapeutic success. The presence of VacA also increases bacterial receptivity to antibiotics, again being associated with higher levels of therapeutic success [95].

Despite the effort and attempt to develop new therapies for the eradication of *H. pylori* bacteria from the GI tract in order to prevent the onset of gastric cancer as a result of infections caused by this pathogenic bacterium and despite increasing knowledge about the intrinsic characteristics of gastric neoplasms, there is still no ideal, ie effective, inexpensive, easy to use and well tolerated treatment for patients, as well as vaccination against this infectious microorganism. Gastric cancer continues to be the world's second-leading cause of cancer death, with an estimated 650 thousand deaths and 880 thousand new cancers per year, two thirds of which occur in developing countries, with Portugal as the country of the European Union with a higher death rate from gastric cancer and the sixth country in the world [95], [104].

Thus, there is an urgent need to develop alternative therapies in order to definitively eradicate *H. pylori* bacteria from the human organism. In the preventive sense, avoiding the appearance of complications or diseases of the GI tract, but also to treat the problem when it exists, without damaging the healthy GI microbiota.

#### 1.3.4 - Effect of therapies for *Helicobacter pylori* infections under the human gastrointestinal microbiota

The effect of antimicrobial therapies on the level of homeostasis of the human GI microbiota depends on various factors such as pharmacokinetics, concentration of the antimicrobial agent on the lumen of the acting organ, route of administration of the administered agent and the extent of the spectrum of action of the antimicrobial agent. These therapies, in particular antibiotherapies, may however cause ecological alterations in the GI microbiota, disrupting the action of this native microbial community against the colonization of possible pathogenic microorganisms and the selection of species and strains that present long-term resistance to antibiotics and, to an overgrowth of infectious bacteria [21].

Some studies have been published that focus on the consequences of existing therapies applied for the eradication of *H. pylori* bacteria from the human stomach in relation to the human GI microbiota.

*Buhling A. et al.* did not observe prolonged negative effects (four weeks) of triple therapy with omeprazole, metronidazole and clarithromycin in patients *H. pylori* positive, on the intestinal microflora. At the same time, they found that the infection seems to induce a recovery of the normal microbial composition. During and immediately after treatment of the individuals *H. pylori* positives (n = 51), a transient reduction in quantitative (number of bacteria from gut microbiota) and qualitative (diversity of gut microbiota) terms of microorganisms was observed in the gut, mainly anaerobes, but also enterobacteria [20].

On the other hand, *Myllyluoma E. et al.*, observed long-term disturbances in the intestinal microbiota, and verified quantitative alterations of the dominant bacterial groups of intestinal microbiota, up to nine weeks after the antimicrobial treatment for *H. pylori*, which consisted of the application of three antibiotics (clarithromycin, amoxicillin and lansoprazole) [21]. These investigators observed a significant reduction in the total amount of bacteria, namely bifidobacteria, lactobacillus/enterococcus group, *Clostridium histolyticum* group, *Eubacterium*

rectale-*Clostridium coccoides* group, *Bacteroides spp.*, and *Faecalibacterium prausnitzii*, during and after anti-*H. pylori* treatment. Despite the number of bifidobacteria, lactobacilli/enterococci, *Bacteroides spp.* and *F. prausnitzii* increased after cessation of triple therapy action, these bacteria failed to reach normal levels (said similar to those verified *a priori* antibiotherapy [21]).

The discrepancies between the results obtained by *Buhling A., et al.* and *Myllyluoma E., et al.* may be due in part to the methodology applied in determining the composition and diversity of the human GI microbiota. While *Buhling A., et al.* used the traditional method of fecal culture, *Myllyluoma E., et al.* used, in addition to the culture method, molecular techniques [Fluorescence In Situ Hybridisation (FISH)] capable of rapidly determining quantitative and qualitative information about the composition of the microbial community of the human GI tract. Traditional culture methods sometimes fail to identify microorganisms present in the samples, due, for example, to poor selectivity of culture media, non-growth of microorganisms on artificial agar, the fact that some microbes prevent the growth of others or incorrect identification of microorganisms [21].

In the study “Short-Term Antibiotic Treatment Has Differential Long-Term Impacts on the Human Throat and Gut Microbiome”, *Jakobsson et al.*, by monitoring disorders in the human microbiome in subjects treated with clarithromycin and metronidazole (antibiotics commonly used to treat *H. pylori* infections), have found that these antibiotics have immediately short-term impact on the microbiota diversity, with reduced diversity found in the throat and fecal samples immediately after treatment (Figure 1.5).

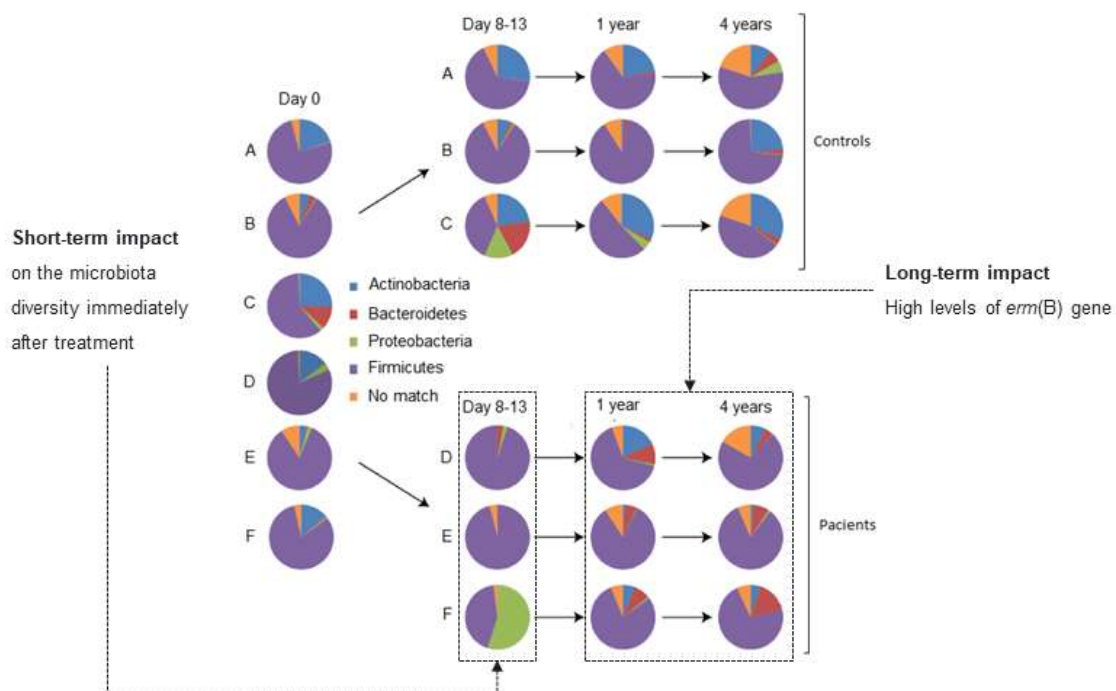


**Figure 1.5** - Graphical representation of the phyla found by pyrosequencing of 16S rRNA gene in control subjects (A, B and C) and in patients treated with dual therapy containing clarithromycin and metronidazole (D, E and F) on days 0, 8-13 and 1 and 4 years (Adapted from [16]).

They also found long-term impact on the intestinal microbiota, with disturbances four years after treatment, in some cases, despite a partial recovery of the diversity of the bacterial community one and four years after treatment with a bacterial diversity more similar to that found

*a priori* of the antibiotic treatment. The mean fecal microbiota of the six individuals analysed (three controls and three patients) during the study was dominated by four bacterial phyla: 78 % Firmicutes, 14 %, Actinobacteria, 3 % Bacteroidetes and 2 % Proteobacteria. Shortly after antibiotic treatment there was a decrease of the diversity in the bacterial microbiota, with a dominance of the phyla Firmicutes (78 %) and Proteobacteria (19 %). However, this study was performed with a small number of patients ( $n = 3$ ), and it was not possible to determine, with a high degree of confidence, whether the results observed were significant or not [16], [26].

These investigators also observed 4 years after treatment high levels of the macrolide resistant *erm(B)* gene, indicating that once established resistance to antibiotic treatments may persist for long periods of time. The *erm(B)* is a gene from the *erm* gene group, with the longest residence or expression time in the host, which by methylating the 23S rRNA prevents binding of the antibiotic to the bacterium and consequently hinders the antimicrobial action of these compounds [16].

The effects of the antibiotic treatment on the patients analysed may be due to the individual action of clarithromycin and metronidazole or as a result of the conjugated effect of these two antibiotics tested. It is important to note that these two antibiotics have different bacterial targets, insofar as the reduction of bacteria of the phylum Actinobacteria is possibly due to the action of the antibiotic clarithromycin, since it has bacteria susceptible to this antibiotic and presents natural resistance to metronidazole, while that metronidazole is active against anaerobic bacteria. On the other hand, together these antibiotics are capable of acting against bacteria of the genus *Streptococcus*, so in some cases the antibacterial activity is due to the individual action of clarithromycin or metronidazole and in other cases due to the joint action of these two antibiotics [16].

Thus, *Jakobsson et al.* found that double antibiotic treatment resulted in ecological changes in the GI microbiota with possible long-term impacts that could result in a long-term negative impact on the human GI microbiota [16].

On the other hand, treatments applied for the eradication of *H. pylori* containing PPIs, to patients positive for this bacterium, have been shown to cause alterations in the gastric microbiota, leading to an increase of the pH in this organ and, consequently, an excessive growth of bacteria, mainly of oral bacterial flora. These bacteria, once the pH of the gastric environment becomes higher by the action of PPIs, can survive, rather than the normal acidic environmental conditions verified in the stomach [17].

Possibly, the application of PPIs, leading to an abnormal growth of bacteria, which under normal conditions would not survive the acidic environment of the stomach, could more easily induce carcinogenic alterations in the gastric cells, leading to the onset of gastric cancer. These changes may occur as a result of increased production of cancerous nitrosamines by bacteria with exaggerated growth in the stomach. Increased gastric pH also leads to a migration of *H. pylori* to deeper regions of the gastric pits, further increasing local inflammation, with a more rapid progression of atrophy of this organ [17].

Since this abnormal development in the stomach only occurs in *H. pylori* positive patients, after treatment with PPIs, the microbiota itself does not alone cause this atrophy in the stomach, but in combination with the presence of *H. pylori* is able to induce the occurrence of cellular changes and the development of gastric adenocarcinomas [17].

Antibiotics radically alter the community of microorganisms that colonize the human GI tract in all stages of human life and may be eliminating an important set of microorganisms with which

we have evolved and which can be a source of information for us to better understand some processes inherent to human development [24].

These studies emphasize the importance of the dosage and the correct application of antibiotic treatments in order to prevent long-term ecological effects on the human GI microbiota and consequently the normal and correct functioning of the human organism [16]. In this sense, it is important to carry out further studies related to the effects on the intestinal microbiota of antibiotic-based therapies and/or with PPIs for the eradication of *H. pylori* from the human GI tract in order to better understand the mechanisms of action intrinsic to the antibiotics applied, as well as the role of the microbiota in the health/pathological state of man.

### 1.3.5 - Alternative therapies for *Helicobacter pylori* infection

In order to overcome the problems resulting from the existing therapies used to eradicate *H. pylori* from the human stomach, alternative therapies have emerged to the antibiotic application, with special interest in biomaterials and compounds with antimicrobial properties, such as vaccines, polyphenols, polyunsaturated fatty acids, some biodegradable polymers, among others [39], [105]–[111].

The search for vaccination seems to be especially urgent in countries with high resistance to antibiotics used in therapies for the treatment of infections caused by *H. pylori*, with a high prevalence of infection and with high morbidity and mortality rates caused by pathologies associated with this becoming a more economical alternative to existing therapies. The main objective is to develop a vaccine effective in preventing and/or curing or otherwise altering the interactions established between the host organism, in this case man, and the infectious microorganism, thus preventing a possible evolution of the disease [108].

Given the worldwide prevalence of *H. pylori* infection (Figure 1.6), estimated, in 2015 approximately 4.4 billion positive individuals for this bacterium [112]; efforts to develop *H. pylori* vaccination have focused on the search for antigens and adjuvants (substances that increase the specific or acquired immune response against coinoculated antigens [105]), as well as routes suitable for the performance and delivery of the vaccine, capable of inducing a response of the acquired immune system upon new contact with the bacterium [106].

Antigens such as urease (UreA and UreB), NapA, katA, CagA and VacA have been shown to be effective in inducing immune response, as they are recognized by antibodies from the host organism and as such appear to be the best candidates to integrate the vaccination in question. Urease is produced in high amounts by all strains of *H. pylori*, making it the best candidate for formulation of a vaccine from the present candidates. Studies performed in humans with the introduction of live attenuated salmonella, producing UreA (from *H. pylori*) and B subunits, did not obtain satisfactory results [106]. However, the combination of urease with other antigens such as HpaA induced strong immune responses to both antigens tested, with a strong synergistic effect on the protection of the host organism [107].

In a study in healthy, non-infected humans (*H. pylori* negative), in which intramuscular vaccination with recombinant CagA (cytotoxin-associated antigen), VacA (vacuolating cytotoxin) and NAP (neutrophil activator protein) with the aluminum hydroxide adjuvant, satisfactory safety and immunogenicity results were obtained [108]. Aluminum hydroxyl is an adjuvant approved by the FDA, which makes it a good alternative for studies conducted in humans. Despite the promising results obtained in animal models, denoting viability for the development of a safe and effective vaccine for human use, further clinical trials are still necessary so that one can say, with

a high degree of confidence, that the results obtained in animal models can be reproducible in man [106].

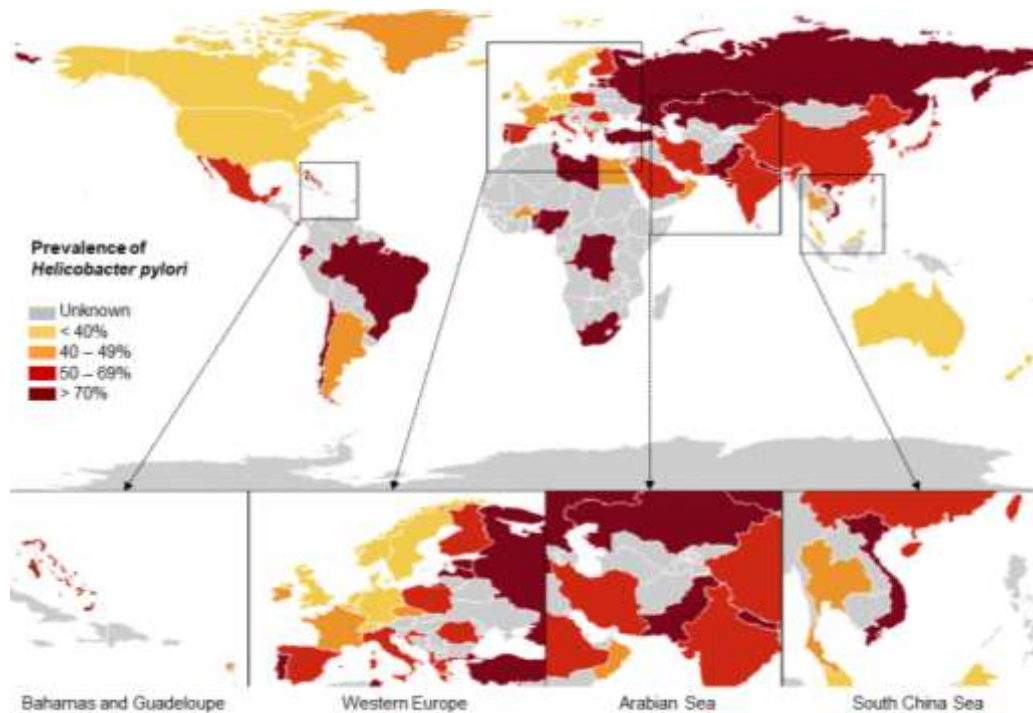


**Figure 1.6** - Mundial prevalence of *Helicobacter pylori* (Adpted from [112]).

In recent years, phenolic compounds have received special attention because of their beneficial properties to human health [109]. In this sense, new strategies capable of combining the synergic antimicrobial effects of phenolic compounds with their natural biological properties have been developed [111].

Phenolic compounds represent one of the most diverse groups of secondary metabolites in the human diet, which can be found in edible plants such as vegetables, stems, flowers, seeds, nuts and some fruits, as well as wine, tea, honey and propolis. In nature, these compounds are involved in several phenomena essential to plants, including growth and reproduction, resistance against pathogenic organisms and against the attack of predators and also protection of the early germination of preharvest cultures. Phenolic compounds are divided into 3 major classes, flavonoids, tannins and lignins, with several important characteristics for human health in general, especially their antimicrobial behaviour [111].

Several studies have demonstrated the antimicrobial capabilities of phenolic compounds, in particular against microorganisms pathogenic to man [111]. Although the mechanism by which phenolic compounds affect *H. pylori* growth is unknown, it may be associated with an inhibition of urease enzyme activity, disintegration of the outer membrane of microorganisms, inhibition of VacA activity, and adhesion of these compounds to human gastric mucus [109].

Romero C., *et al.* evaluated *in vitro* the activity of polyphenols from olive oil against *H. pylori* bacterium, since in an earlier study high antimicrobial activity of these compounds had been observed against a broad spectrum of pathogenic microorganisms transmitted by food, and a strong activity against *H. pylori*, and even detected, some strains resistant to antibiotics. These investigators demonstrated that, in fact, the microbial behaviour against *H. pylori* was due to

phenolic compounds diffused from olive oil to gastric juice. Olive oil, although it has to be used in higher concentrations than the antibiotics used to kill this bacterium, and further *in vivo* studies are needed to assess its bioactivity, it is a natural food rather than a remedy, so its use may be considered not only for the treatment of gastric lesions as peptic ulcers in infected patients but also as a chemopreventive agent in order to avoid infection by this and other pathogenic microorganisms and the development of peptic ulcers or even gastric cancer [109].

Studies of PUFAs, found naturally in many marine organisms in high quantities, have been considered due to their antibacterial behaviour, with an inhibitory effect on bacterial growth or causing the death of these microorganisms, in particular linolenic acid and docosa-hexaenoic acid [110].

DHA is an essentially omega-3 fatty acid present in fish oil, capable of inducing both *in vitro* and *in vivo* studies inhibition of *H. pylori* growth in a dose-dependent manner by means of the alteration of cell membrane integrity, inducing a stress condition and altering bacterial metabolism, which may lead to the release of important cellular metabolites or even bacterial lysis, with an evident reduction of colonization of the gastric mucosa by this microorganism [110], [113].

Seabra C., *et al.* have developed nanoparticles of DHA-loaded nanostructured lipid carriers (NCL) which improved the bactericidal behaviour of DHA against *H. pylori* (dose-dependent); uncharged NCL exhibited antimicrobial activity against *H. pylori* strains tested as a result of a change in cell membrane integrity with leakage of cytoplasmic content. NCL is a promising system for the delivery of lipophilic drugs, suitable for transport and protection of biotin compounds. The results obtained in this study indicate the incorporation of DHA into a NLC nanoparticle (non-cytotoxic below 50 mM), as a promising alternative to current treatment for *H. pylori* [110].

On the other hand, the joint application of DHA with standard antibiotic treatments (omeprazole, metronidazole and clarithromycin) has been shown to decrease *in vivo* (in a mouse model) the recurrence of *H. pylori* infection [113]. In this study, free DHA treatment led to a 50% reduction in gastric colonization by *H. pylori*, whose results may be related to the low penetration capacity of DHA in the gastric mucus, its degradation in the gastric environment due to oxidation, carboxylic protonation, esterification or lipid-protein complexation and its low residence time in the stomach [113], [114].

An alternative approach to existing therapies relates to an increased efficacy of the antibiotics used, from their encapsulation in stable systems and controlled release at the site of infection caused by this infectious microorganism. To that extent, previous studies have shown a greater efficacy in *H. pylori* eradication when antibiotics were applied locally at the site of infection rather than being constantly available [102], [115]–[119]. These systems are able to protect drugs from rapid degradation by increasing the time of antibiotic action through their retention (better solubility of drugs in the serum, prolonging their useful life in the systemic circulation), and their concentration, directly at the sites where it is necessary [115], [118], [120]–[122].

Most of the systems of antibiotic sustained-release available on the market are of hydrophilic matrix, owing, among other factors, to their high ease of production, excellent uniformity, biodegradability and low toxicity, among which natural biodegradable polymers such as chitosan and collagen or obtained synthetically, as is the case of polyurethane polymers, PHBV [Poly(3-hydroxybutyrate-co-3-hydroxyvalerate)] and pHEMA [Poly(2-hydroxyethyl methacrylate)]. Currently, only a few nanoparticles based on materials with antimicrobial properties have been approved for clinical use, despite their advantageous properties in the controlled release of drugs into human organisms, in particular its long circulation time and super small size. The main



limitations to its application are related to the high cost of production, the difficulty of obtaining some materials that constitute them and the unsatisfactory results regarding their loading with medicines, which could be surpassed by the production of amphipathic polymers and porous inorganic materials [115], [123], [124].

## 1.4 - Chitosan

### 1.4.1 - Chitosan: general considerations and applications

Chitosan is a naturally occurring polymer from the alkaline deacetylation of chitin (poly- $\beta$ -N-acetyl-D-glucosamine), the second most abundant polysaccharide in nature, found as the main constituent in the exoskeleton of arthropods. This polymer is a linear, semi-crystalline polysaccharide composed of repeating units of D-glucosamine and N-acetyl-D-glucosamine linked by  $\beta(1\rightarrow4)$  glycosidic bonds (Figure 1.7) [39], [125]–[129].

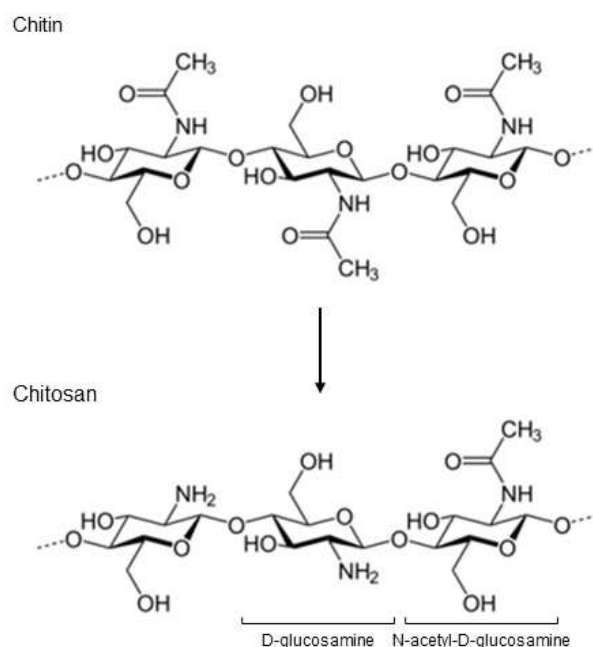


**Figure 1.7** - Chemical structure of chitin and chitosan from the alkaline deacetylation of chitin (Adapted from [130]).

Ch consists of 3 functional groups, with an amine group (at the C-6 position) and two primary and secondary hydroxyl groups (at positions C-6 and C-3 respectively). Deacetylation corresponds to the removal of acetyl functional groups from a chemical compound to form amine groups, and the degree of deacetylation of Ch is indicative of the number of free amine groups present in the chain of this polymer, insofar as an increase of DD Ch corresponds to an increase in the number of amine groups, with an increase in the number of positive charges, and consequently the greater the solubility under acidic conditions. The alkaline DD conditions of chitin determine MW and DD of Ch, influencing the physicochemical and biological properties of this polysaccharide [39], [127], [131]–[134].

Ch has been widely used in the pharmaceutical field not only by the encapsulation and release of drugs into the stomach, but also as a transfection system for gene therapy, being commercially available in various stable forms, such as films, fibers, scaffolds, micro and nanoparticles, among others, being able to be carried out in this polymer with numerous chemical modifications [125], [126], [135].

Ch presents as main characteristics intrinsic to its composition and structure, which give it a high potential to be used as biomaterial in the removal of pathogenic microorganisms from the GI tract, its biocompatibility, biodegradability, non-immunogenicity, non-carcinogenic character, antimicrobial behaviour and high mucoadhesive capacities [39], [126], [131], [136], [137]. These intrinsic properties of Ch seem to have high importance in applications not only in the field of Health Sciences but also in Biomedical Engineering.

The biodegradability of Ch is a very important aspect, especially when it is used for the incorporation and release of substances. If the size of the Ch biomaterial used is of a size that does not allow its filtration in the kidneys and elimination through the urine, or its elimination through the GI tract, it is important that, although non-toxic, it can be degraded enzymatically or chemically. Depending on the DD, Ch may undergo enzymatic degradation as a result of the action of enzymes such as lysozyme and other bacterial enzymes of the colon region in the case of vertebrates, with the hydrolysis of the D-glucosamine-D-glucosamine, D-glucosamine-N-acetyl-D-glucosamine and N-acetyl-D-glucosamine-N-acetyl-D-glucosamine, as well as chemical degradation at stomach level by the acid produced in this organ. An increase in DD of Ch was associated with an increase in the extent and rate of enzymatic degradation [138].

The compatibility of Ch with the physiological medium depends on the method and the conditions/parameters used in its preparation. For example, increasing the DD of Ch leads to a greater number of amines and therefore a higher positive charge, increasing the interaction of this biomaterial with the cells and leading to a better biocompatibility [126]. However, some chemical modifications implemented in the Ch structure may make it more or less toxic, so all parameters should be evaluated and any residual reagents at the time of production must be carefully removed [131].

Although Ch is normally insoluble in water and in organic solvents, as a result of the hydrogen bonds giving it a stable crystalline structure, this polymer is soluble in acidic solutions having a pH of less than 6.3, values for which the amine groups are converted into its soluble proton form ( $R-NH_3$ ). On the other hand, for pH values above 6.3, Ch becomes insoluble as a result of deprotonation of the amines (Figure 1.8) and consequent Ch load loss. Thus, a higher DD of Ch generally corresponds to a higher rate of acidic degradation of this polymer and, therefore, a higher solubility of this in acid medium [39], [131], [134], [138].

The main objective of the research in this field is the development of biomaterials capable of generating a beneficial cellular and tissue response appropriate to the circumstances of its application without causing undesired local or systemic side effects in the individual receiving a given therapy. To this extent, it is extremely important to take into account all the factors and characteristics of the production of Ch biomaterials, in order to optimize the clinical performance of the therapy in question [139].

In fact, Ch is considered a non-toxic and biologically compatible polymer approved for dietary applications in Finland, Japan and Italy and for use in FDA wound dressing material [131]. Biocompatibility is a different concept of toxicity. Biocompatibility refers to the beneficial or detrimental effect of the physiological environment on the behaviour or activity of the material,

while the toxicity points to the potential damage that a given material may cause on a given medium [139].

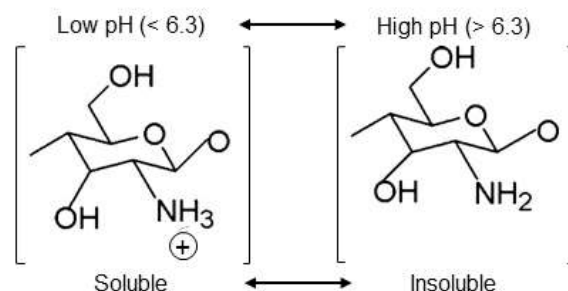


**Figure 1.8** - Representative scheme of chitosan solubility at different pHs. At pH below 6.3 the chitosan amine groups are protonated, imparting a polycationic behaviour to this polymer and thus soluble while at pH above 6.3 the chitosan amines are deprotonated and reactive, thereby reducing the charge of this polymer rendering it insoluble (Adapted from [131]).

Although Ch is considered a non-cytotoxic biomaterial for mammalian cells, it presents a toxic behaviour for several bacteria, fungi and parasites, as a result of the electrostatic interactions between the positively charged amine groups of the Ch and the anionic groups of the bacterial wall, which allows its use as an agent capable of eliminating or inhibiting the activity/proliferation of pathogenic microorganisms capable of causing infectious diseases in the human body [138], [140], [141].

The mucoadhesive capacities of Ch occur as a result of the establishment of electrostatic bonds between the D-glucosamine residues of positively charged amines with sialic acid residues of negatively charged mucins or gastric mucosal glycoproteins at gastric pH [142]. Other factors such as flexibility of the Ch molecule chain, the presence of strong hydrogen bonding groups such as hydroxyl (-OH) and carboxyl (-COOH), high MW, energetic properties of the surface of this polymer that promote its diffusion into the mucus gastric lining that covers the mucosal layer of the stomach, low or no toxicity and no absorbability are some of the characteristics of mucoadhesive polymers [122].

In 2004, *Dhawan S., et al.* evaluated the mucoadhesive properties of Ch microspheres from the analysis of the interaction between Ch MICs and mucins in aqueous solution. A high adsorption of mucins to positively charged Ch MICs, contrary to the low adsorption of these glycoproteins to negatively charged MICs, was then observed in the pH range used (pH 1.5, 3.5 and 5.5) [122].

The electrostatic attraction between positively charged Ch MICs and negatively charged mucosal surface glycoproteins also appears to play an important role in the bioadhesive behaviour of this polymer, improving the stability, bioavailability and retention time of the drugs incorporated in these particles, through of its penetration into the gastric mucosa, with controlled release of the drug immediately at the site of action [143], [144].

The antimicrobial activity of Ch depends on many factors, such as concentration, pH, MW, DD, type of microorganism, among others, which must be considered before its application, performing for such tests and optimizations necessary to obtain maximum efficiency in the antimicrobial behaviour of this polymer [134]. With respect to the MW factor of Ch, there is no common correlation between the bactericidal activity of Ch and its MW in the literature, since equivocal results are demonstrated in different studies. Some studies have shown that higher

MW was associated with higher bactericidal activity, while others observed the exact opposite, or even similar bactericidal behaviour of low and high MW Ch polymers for some bacteria [141].

Although the mechanism that gives Ch its antimicrobial behaviour is unknown, it is thought that at pH less than 6.3, the  $\text{NH}_3^+$  group of the glucosamine monomer (due to ionization of the amine groups at pH less than 6.0) interacts with the negatively charged cell membranes of microorganisms, leading to cell lysis. Thus, the antimicrobial activity of Ch appears to be higher at lower pH (pH < 6.0) as a result of increased surface charges, more readily associated with negative surface bacterial cells, and *vice versa*, due to the deprotonation of the groups amine (at pH > 6.0) [134].

Many studies have evaluated the correlation between the bactericidal activity of Ch and its MW. However, there does not seem to be a linear correlation to all microorganisms since, depending on the type of organism and sometimes exclusive characteristics, different molecular weights present different results. In some cases better results were obtained when high MW Ch was applied, while in others medium and low MW Ch was more effective in its bactericidal activity. High MW Ch (> 5000 kDa), as it can not cross the microbial cell membrane, accumulates on its surface and can not only alter membrane permeability but also lead to a blockage of nutrient transport, causing cellular lysis. On the other hand, low MW (< 5000 kDa) Ch particles can cross the cell membrane and be integrated into the cell, being able to associate with the DNA molecule and inhibit mRNA synthesis [134].

#### 1.4.2 - Interactions between chitosan biomaterials and bacteria

Infections caused by bacteria are a common cause of everyday pathological disorders, usually treated through systemic, local or intravenous injection of low MW antibiotics, such as ciprofloxacin, doxycycline and ceftazidime, unable to damage the integrity of the wall and membrane of bacterial cells and, consequently, leading to a greater ability to acquire resistance to antibiotics [145].

The ideal polymer with antimicrobial properties should have the following characteristics: long-term storage stability and storage at the temperature to be applied, easy and inexpensive production process, non-toxicity, biocidal activity to a broad spectrum of pathogenic microorganisms in a short time, non-degradability, non-water solubility in the case of application for the disinfection/treatment of water and can also be able to be regenerated after loss of activity [141].

Materials developed from natural polymers such as Ch have demonstrated a high ability to interact with different microorganisms, in particular because they possess many of the attributes mentioned above, such as their antimicrobial activity against a broad spectrum of pathogenic microorganisms, a high bactericidal rate against Gram-negative and Gram-positive bacteria, low cytotoxicity against mammalian cells [141] and also adhesive capacities to some bacteria, demonstrated by some studies [39], [84], [146], [147]. These materials have shown special interest in the field of Biomedical Engineering to be used as an alternative to antibiotics currently administered to combat bacterial infections.

Ch ultrathin films produced by spin-coating technique and crosslinked with genipin, with a homogeneous thickness of  $11.7 \pm 0.6$  nm, demonstrated the ability of Ch to bind and kill *H. pylori* in a range of pHs (2.6, 4.0 and 6.0) independent of the presence of urea in the environment [147]. *Nogueira F., et al.* also found that from the pH range tested, the adhesion of *H. pylori* to the Ch films is higher at pH 2.6 and that most of the adhered bacteria in all tested pHs were dead, with mortality rates always greater than 50 %. The bacteria adhered to the Ch films, even at pH 6.0,

were mostly dead, demonstrating that the viability of these microorganisms was not only affected by the acidic pH of the medium, but also as a result of the bactericidal behaviour of Ch. In the assays performed without urea and pepsin, Ch films at pH 2.6 presented 93 % of bacterial death and more than 75 % in the case of the assays performed at pH 6.0 [147].

On the other hand, these researchers also verified that the presence of pepsin, a protein produced by the stomach cells, able to unfold the proteins in simpler peptides, affects the adhesion of *H. pylori* to Ch, mainly at pH 2.6, which may be related to its negative charge at low pH and consequent high affinity for Ch binding. Pepsin adhered, by coating the surface of Ch films, reducing the amount of protonated amines and consequently decreasing the amount of bacteria adhered to this biomaterial. This protein seems to increase the viability of the bacteria adhered through induction in its coccoid form, functioning as a sealant of the bactericidal effect of Ch [147].

*Gonçalves I.C., et al.*, demonstrated that Ch MICs can adhere to different strains of *H. pylori*, regardless of pH and the presence of pepsin, thus contradicting the results presented by *Nogueira F., et al.* [140], [147]. However, these results may be indicative that Ch materials with different structure present a different behaviour, regarding to bacterial adhesion capacity [140].

In relation to the antimicrobial activity of Ch solutions, three possible mechanisms of action have been proposed in the literature: 1) The electrostatic attraction between the positive surface charge of Ch and the negative surface charge of the bacterial cell wall can lead to a change in membrane integrity cell, causing the release of important intracellular constituents, as well as cellular lysis and consequent death of the bacterium; 2) High MW Ch materials may involve the surface of the bacteria, making it difficult or even impossible to exchange cellular compounds with the exterior, as well as the absorption of nutrients, which can lead to the death of the bacteria; and 3) The chelating ability of Ch to capture metal residues and trace elements essential to bacterial development is involved in its antimicrobial behaviour, by unbalancing bacterial homeostasis [148].

*Liu. H., et al.*, found that the  $\text{NH}_3^+$  groups of the Ch solution interact with the phosphoryl groups of the cell membrane phospholipids of *Escherichia coli* and *Staphylococcus aureus* bacteria, causing a rapid increase in membrane permeability external and internal (observed by the increase of  $\beta$ -galactosidase release from the cytoplasm of bacteria), leading to the disintegration of the cell membrane and consequent release of the cytoplasmic content. The Ch solution thus presented bactericidal activity against the bacteria tested, causing its death, as a result of the electrostatic interaction between the Ch solution and the phospholipids of the bacterial membranes [149].

The determination of the Gram-negative and Gram-positive bacteria affinity for the action of Ch and the distinction of the sensitivity of this polymer between Gram-negative and Gram-positive bacteria is the subject of considerable controversy on the part of the scientific community. As such, it was established that the most likely cause of the different susceptibility to Ch between Gram-negative bacteria and Gram-positive bacteria is due to the structural differences of the cellular membrane of these bacteria. However, information regarding the relationship between the greater or lesser affinity of the bacteria to Ch and the hydrophilicity/hydrophobicity of the bacterial surface, density of the bacterial surface load, as well as pathogenicity are scarce and should be deepened in order to better understand some mechanisms inherent in the antimicrobial ability of Ch to act against bacteria [148].

*Chung Y., et al.* attempted to establish a relationship between the antibacterial activity of Ch and bacterial cell wall surface characteristics, in particular for five waterborne pathogenic bacteria,

including 3 species of Gram-negative bacteria (*Escherichia coli*, *Pseudomonas aeruginosa* and *Salmonella typhimurium*) and 2 species of Gram-positive bacteria (*Staphylococcus aureus* and *Streptococcus faecalis*). In order to establish this relationship, the authors evaluated the hydrophilic properties, negative charge and amount of Ch adsorbed on the bacterial cell surface. They found that in a medium containing water and hexane, the amount of Gram-positive bacteria decreased in the aqueous phase as the amount of hydrophobic hexane increased, whereas the Gram-negative bacteria did not appear to change their behaviour with the alteration of the medium. As for the cell surface charge, Gram-negative bacteria have a higher negative charge than Gram-positive bacteria. Lastly, the ability of Gram-negative bacteria to absorb Ch was higher than Gram-positive bacteria [150].

The surface characteristics of the bacterial cell sample tested thus appear to explain the relationship between surface charge and the success of antibacterial activity over Gram-negative bacteria, although the relationship of hydrophilicity with antimicrobial activity in relation to these bacteria is not evident, insofar as a greater negative charge on the surface of the cell wall, seems to facilitate the attraction between this type of bacteria and the positively charged amines of Ch. On the other hand, and although the hydrophobicity does not favor the interactions between the Ch and the surface of the Gram-positive bacteria, it was observed a decrease in the number of bacteria, which seems to be indicative of the bactericidal effect of this polymer [141], [150].

On the other hand, factors intrinsic to the microorganism itself, such as membrane and cell wall organization and age, may influence the interaction between these microorganisms and polymers with antimicrobial activity, dictating, among other things, the efficiency of this interaction. Some studies suggest changes in the electronic charge at the surface of the cell, depending on the stage of growth in which the bacteria are found, which can induce different susceptibility of cells in the interaction with Ch. The differences verified for several studies were associated to the different microorganisms tested, since differences in the surface load were also observed [141].

In order to evaluate the antibacterial behaviour of Ch in solid form, *Takahashi T. et al.* evaluated the behaviour of Ch membranes in the growth inhibitory effect on bacteria of the strains *Escherichia coli* 745 and *Staphylococcus aureus* 9779, which are representative of bacterial species important in food hygiene and public sanitation. In this study, Ch membranes were found to inhibit more strongly the growth of *S. aureus* (Gram-positive) than *E. coli* (Gram-negative), presenting a bactericidal behaviour against these strains [151].

The determination of the DD influence of Ch membranes on antibacterial activity was only determined for *S. aureus*, for which there was observed a decrease in the number of colonies for high DD values, especially between 83.9 % and 92.2 % of DD. The effect of surface area and particle shape also appear to influence the antibacterial activity of this material, so when studying with Ch particles it will be important to correlate these factors quantitatively in order to optimize the antimicrobial activity of these biopolymers [151].

In another research study for the determination of antibacterial mechanisms of action, were tested Ch nanofibers, produced by the electrospinning method, against bacteria frequently involved in contamination and food spoilage, in particular *Escherichia coli*, *Listeri innocua*, *Staphylococcus aureus* and *Salmonella enterica* serotype Typhimurium. *Arkoun M. et al.* demonstrated that this same mechanism of action was of bactericidal type and was related to the protonation of the amine groups of the nanofibers, regardless of the bacterial strain tested. On the other hand, the sensibility to the action of nanofibers was not Gram-dependent, contrary to the results obtained by *Chung Y., et al.*, for Ch solutions and *Takahashi T. et al.* for Ch

membranes, but rather dependent on the bacterial strain. Non-virulent strains (*E. coli* and *L. innocua*) showed greater sensitivity to the antibacterial action of this material [148].

In this study, for which all assays were conducted under the same experimental conditions according to *Chung Y., et al.*, Gram-negative bacteria were expected to exhibit a higher sensitivity to Ch nanofibers. However, this did not occur and the susceptibility of the strains tested (*E. coli* > *L. innocua* > *S. aureus* > *S. Typhimurium*) did not coincide with the order of hydrophilicity obtained (*E. coli* > *S. Typhimurium* > *L. innocua* > *S. aureus*) and in agreement with the results obtained by *Chung Y. et al.*. Thus, these investigators suggest that pathogenicity is a factor that may be involved in bacterial behaviour in relation to Ch, since innocuous bacteria such as *E. coli* demonstrated a high sensitivity to Ch nanofibers, contrary to *S. Typhimurium* that presented high resistance to this material [148].

*Luo D., et al.* evaluated *in vitro* and *in vivo* the anti-*H. pylori* effect of Ch nanoparticles (70-120 nm) produced by the polymer dispersion method and analysed the relationship between the DD or the pH of Ch nanoparticle solution and the antimicrobial activity. These investigators observed a bacteriostatic behaviour of Ch nanoparticles in relation with the two strains of *H. pylori* tested (NCTC 11637 and NCTC 11639), without significant differences between them. They further verified that the bacteriostatic effect of these nanoparticles decreased with increasing pH, at pH values between 4.0 and 6.0, and obtained an optimum pH of antimicrobial action equal to 4.0. As previously described, at lower pH, and therefore more acidic conditions, the amount of protonated amines formed on the surface of the Ch nanoparticles is higher and, consequently, the antimicrobial efficacy is improved [129].

On the other hand, Ch nanoparticles produced with a higher DD had a higher anti-*H. pylori* action, which is in agreement with the fact that a higher DD corresponds to a larger amount of  $\text{NH}_3^+$  group, which are an important component of the antimicrobial properties of these polymer particles. This research group also demonstrated that Ch nanoparticles have a higher bacteriostatic efficacy against *H. pylori* than Ch powders (with larger sizes and a lower amount of  $\text{NH}_3^+$  groups). The nanoparticles produced may interact electrostatically with the outer membrane of *H. pylori* and cause structural damage, as well as changes in permeability and consequent release of intracytoplasmic contents, or may enter into the bacterium (due to its small size) and compromise the normal metabolism of this microorganism [129].

Low and high MW (LMW and HMW, respectively) sodium phytate Ch nanospheres with high positive charge (20-80 nm/+58.5 mV and 80-100 nm/+52.5 mV, respectively), stable under high temperature and acidic conditions and without evident cytotoxicity were developed by *Yanga J., et al.*, with the objective of evaluating the antibacterial behaviour of these particles in relation to the bacterial species *Escherichia coli*, *Salmonella typhus*, *Pseudomonas aeruginosa*, *Bacillus subtilis* and *Staphylococcus aureus*. *Yanga J. et al.*, found that the Ch nanospheres showed good antibacterial activity, with better bacteriostatic results of LMW nanospheres compared to HMW nanospheres, which may be related to the smaller size and higher load of LMW nanospheres (20-80 nm and +58.5 mV) [138].

The bacteriostatic effect of LMW nanospheres was also higher against Gram-negative bacteria (*Escherichia coli*, *Salmonella typhus* and *Pseudomonas aeruginosa*) when compared to Gram-positive bacteria (*Bacillus subtilis* and *Staphylococcus aureus*). This study demonstrated the high potential of Ch sodium phytate nanospheres to be used in the pharmaceutical and food industry, among others, as an alternative or system to support therapies containing drugs, nutraceuticals, etc., due to its antibacterial activity in the fight against infections caused by bacteria [145].

The main difference between Gram-negative and Gram-positive bacteria is the structure and composition of the bacterial wall. Gram-positive bacteria are formed by a thick wall of peptidoglycans, consisting of chains of linear polysaccharides interconnected by small peptides, which impart robustness and high structural rigidity to these bacteria, thus hindering the action of Ch nanospheres. On the other hand, the three-dimensional structure of Gram-negative bacteria seems to be weaker and more flexible, formed by a thin layer of peptidoglycans containing lipopolysaccharides, thus facilitating the disintegration of the cell wall of these bacteria by the Ch nanospheres better results obtained regarding the bacteriostatic activity of these nanospheres [145].

#### 1.4.2.1 - Chitosan biomaterials as alternative therapy to *Helicobacter pylori* infection

The development of nano and microparticles of degradable biomaterials, such as Ch, used for the encapsulation and local controlled release of drugs for the treatment of patients infected with *H. pylori*, is increasingly being used as an innovative approach in biomedical engineering and the pharmaceutical sciences due to the properties of these biomaterials. These materials are able to overcome the limitations of the conventional application of drugs (tablets and capsules) such as low bioavailability, limited efficacy and still non-selectivity [62], [152], [153].

This encapsulation of the antibiotics provides protection against enzymatic degradation and acidic environment of the stomach, allowing better therapeutic efficacy, with a controlled release of the antibiotics at the *H. pylori* infection site, as well as an increase of the contact surface, which allows the decrease of the frequency of dosing and the increase of the retention time, as well as the absorption of the drug, decrease in the diffusion distance and increase of the penetration of the antibiotic through the layer of gastric mucus, contributing to the adhesion on the part of the patients proposed to the treatment and minimizing the problems associated with the acquisition of resistance, as a result of the systemic application of antibiotics [39], [62], [99], [120], [143].

These particles may also be used as binding agents to bacteria, in particular negatively charged bacteria, such as *H. pylori* [154]. These materials have the ability to eliminate this bacterium from the human organism, through the GI tract, as a result of its mucoadhesive properties, but also with antimicrobial (bacteriostatic or bactericidal) characteristics, thus constituting a complement to the therapies used, or even as a therapy alternative to these [39], [84], [131], [146], [147].

In a study on the binding capacity of Ch MICs, it was demonstrated the ability of Ch MICs of approximately 170µm with 84 % DD to adhere non-specifically to different strains of *H. pylori* (J99, 17875/Leb, 17875 isogenic mutant babA1A2 and 097UK) (Figure 1.9), decreasing bacterial adhesion to gastric epithelial cells by approximately 50 %, regardless of pH and bacterial strain. The results also demonstrated that Ch MICs are non-cytotoxic and no significant differences were observed in bacterial adhesion to gastric cells when the addition of Ch MICs occurred before or after *H. pylori* inoculation, whereby these microparticles have been shown to be able to reduce and prevent the adhesion of this bacterium by at least 50%. According to ISO International Standard 10993-5 these Ch MICs were not considered to be cytotoxic particles, although they reduced the metabolic activity of gastric cells in about 20 % [140].



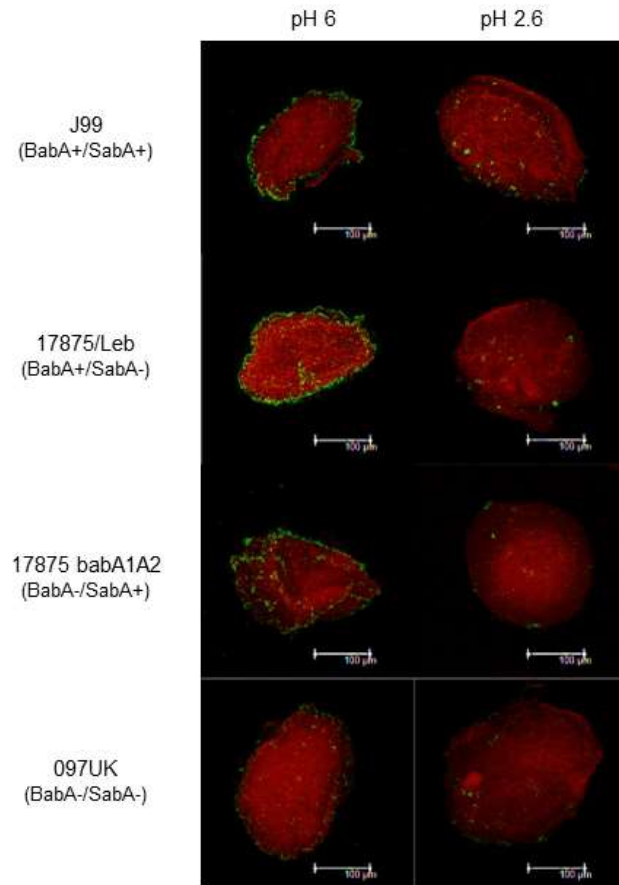


**Figure 1.9** - Spectral Confocal Microscope images of different strains of *Helicobacter pylori* (green) adhesion to chitosan microspheres (red) after incubation at pH 2.6 or 6.0 (Adapted from [140]).

In order to evaluate the ability of Ch MICs to reach deeper regions of the gastric mucosa, the so-called gastric pits, which are regions of difficult access also colonized by *H. pylori*, and thus increase the efficacy of this system, were developed Ch MICs of approximately 50µm. These MICs, when analysed on fresh mouse stomach samples, had the ability to penetrate the gastric mucosa and bind to the *H. pylori* J99 strain, whereas in the results with human gastric mucosa samples, only a few MICs were visualized in planes suggesting the difficulty of these microparticles to penetrate the gastric mucus [5].

Recently, *Gonçalves I.C., et al.* developed Ch microparticles chemically modified with Lewis b and sialyl-Lewis x glycans at the surface, for which they evaluated *in vitro*, through Leb positive portions of human and mouse gastric mucosa and *ex vivo*, from fresh samples of the mouse stomach, the specificity of the BabA glycan-adhesin interaction and the ability of these MICs to remove adhered bacteria in mice. The results showed that Leb immobilization enhances the attraction/affinity of *H. pylori* to the Ch microparticle, since it competes directly with the gastric mucin glycan receptors to bind *H. pylori* adhesins (Figure 1.10) [84].

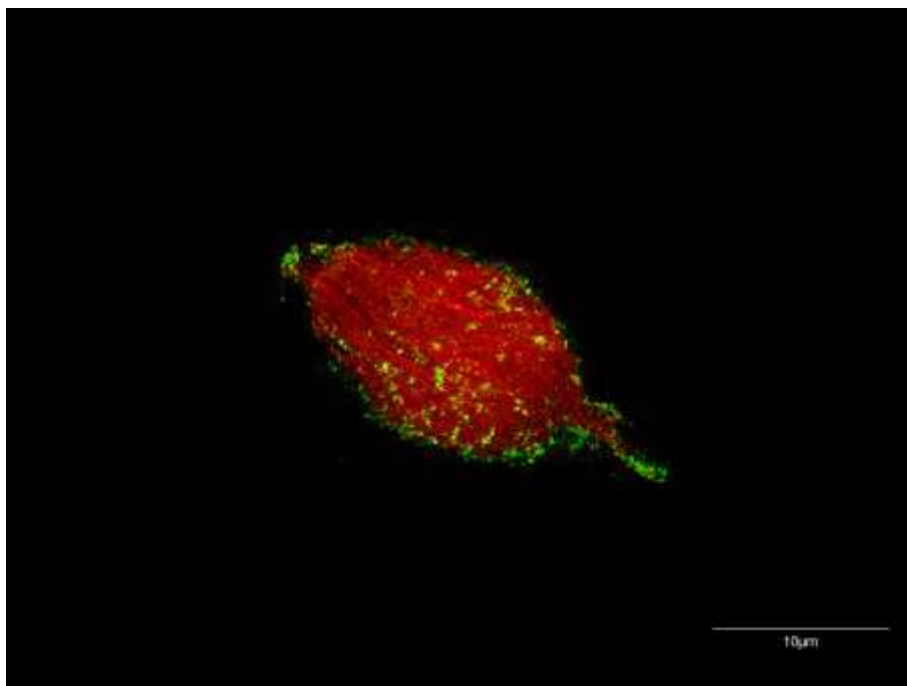


**Figure 1.10** - Spectral Confocal Microscope image of *Helicobacter pylori* adhesion (green) to a chitosan microspheres (red) modified with Le<sup>b</sup> surface glycans (Adapted from [84]).

### 1.4.3 - Chitosan microspheres

The methods and conditions used in the production of nano and microparticles developed with the intention of being used for therapeutic purposes are very important aspects that must be carefully considered and evaluated so that the performance of these materials is optimized, with maximum effectiveness of performance and low or no cytotoxicity according to the purposes of its application. The selection of the method depends on factors such as the required particle size, nature of the drug molecule to be incorporated (in case the production of these materials is desired as a drug delivery system), solubility, chemical and thermal stability of the active drug molecule, cytotoxicity, reproducibility of the drug release kinetic profile, stability of the final product and, not least, the type of delivery device intended to be obtained [155].

Focusing on the production of Ch nano/microparticles there are several methods that can be used in the development of these materials and depending on the objectives of the research and according to the prerequisites required to achieve them, it is possible to combine different strategies, such as 1) emulsion crosslinking; 2) ionotropic gelation, 3) coacervation/precipitation; 4) emulsion-droplet coalescence; 5) spray drying; 6) reverse micellar method; 7) suppression; 8) solvent evaporation and 9) supercritical solvent precipitation [39], [155].

It is important to note that the method used will determine the physico-chemical characteristics (DD, MW, particle size, particle pore size, crystallinity, surface area, water content, antimicrobial activity, etc.) of the particle and thus the behaviour of this polymer, whereby the evaluation of all the factors is essential so that the particles produced are stable, reproducible and exhibit the desired behaviour [39], [155], [156].

For example, in the case of the development of nano/microparticles for application in the GI tract, it is important to note the high solubility of this biomaterial under acidic pH conditions, as well as the chemical and enzymatic activity observed in the human stomach. At acid pH the Ch

MICs increase in size as a result of the ionization of the D-glucosamine residues of Ch, which in the case of their use for the encapsulation of medicines results in a faster release of these. *Hejazi R. and Amiji M.* have observed that the release of tetracycline from Ch MICs, produced by ionic crosslinking, is strongly affected by the pH of the medium [102].

As such, approaches capable of preserving the chemical and physical stability as well as the three-dimensional structure of the Ch nano/microparticles under acidic conditions, allowing, for example, a controlled local release and for a longer time of antibiotics, should be considered and evaluated, in the case of its application for adhesion to pathogenic microorganisms, and its consequent elimination outside the host organism [39].

When applying Ch biomaterials in acidic environments, such as gastric juice, it is important to avoid the chemical or enzymatic degradation of this biomaterial so that it can act at this level. One way of overcoming the normal behaviour of Ch under acidic conditions is through the crosslinking of the Ch particles by physical/ionic crosslinking using sodium tripolyphosphate (TPP) as a crosslinking agent or by chemical/covalent crosslinking using glutaraldehyde or genipine [39].

TPP is a non-cytotoxic polyanion that interacts by establishing electrostatic forces with the positively charged amines of Ch, forming a crosslinked ionic structure, which results in the precipitation of Ch as more or less spherical particles. This crosslinking method is based on the complexation of Ch chains, induced by the interaction of  $\text{OH}^-$  and  $\text{P}_3\text{O}_{10}^{5-}$  [from sodium tripolyphosphate solution ( $\text{Na}_5\text{P}_3\text{O}_{10}$ )] with  $\text{Ch NH}_3^+$  and its deprotonation and ionic crosslinking [146].

Although TPP has a rapid gelling ability, a greater stability in gastric fluids than Ch alone and good mucoadhesive properties, the obtained particles present a wide variety of sizes, dissolution/degradation in the gastric environment, as well as dilation of the particles and, furthermore, their application results in a rapid release of hydrophilic drugs [39], [131], [136], [157]–[159].

In the method of chemical crosslinking, chemical binding agents, such as formaldehyde, glutaraldehyde, polyepoxy compounds, tannic acid, dimethyl suberimidate, carbodiimides and acyl azide are used to link functional amino acid groups. However, these synthetic crosslinking agents have demonstrated cytotoxic behaviour in some applications [160].

Genipin ( $\text{C}_{11}\text{H}_{14}\text{O}_5$ ) is a naturally occurring chemical which functions as a crosslinking agent capable of attaching biological tissues and biopolymers (particularly effective on amine group containing polymers) through covalent bonds with the primary amines of the glucosamine subunits, forming amines secondary and amino-heterocyclic bonds, leading to Ch crosslinking [131], [136], [146], [160], [161]. Genipin is the most commonly used crosslinking agent because it has slower degradation and lower cytotoxicity levels than the above compounds, in particular about 5000 to 10000 times lower than glutaraldehyde, a synthetic crosslinking agent [39], [128], [131], [133], [160], [161].

Unlike physical crosslinking, the chemical one exhibits lower levels of mucosal adhesion of Ch particles, as a result of the decrease in the number of primary amines available in the Ch molecule, but more controlled release of encapsulated drugs in these systems [39]. This crosslinking process must be controlled in order to achieve a balance between the different properties of the polymer, taking into account the purpose of its application [146].

Crosslinking is a process occurring through the amine groups of the Ch, leading to a decrease in the number of free primary amines capable of being protonated, so that an increase in the degree of crosslinking results in a reduction of the mucoadhesive properties and the size of the

particles of Ch, as well as an increase in the stiffness of the particles, with consequences to the level of the release of drugs encapsulated in these systems [39].

Some studies related to the evaluation of the mucoadhesive properties of Ch MICs report the combination of crosslinking methods, in particular TPP and genipine [133], [146], in order to obtain more stable MICs under acidic conditions, since ionic crosslinking with TPP alone, does not appear to be sufficient to prevent rapid dissolution of MICs under these environmental conditions [146].

*Mi, et al.*, produced gel granules based on Ch by ionic (TPP) and chemical (genipine) co-crosslinking, and verified by UV, FTIR and EDAX analysis that this co-crosslinking mechanism is pH dependent, with effect on the degradation and dilation of this polymer. For pH values between 1.0 and 5.0 the ionic crosslinking by TPP is dominant, with higher affinity of Ch to establish bonds with the TPP ions, due to a possible inhibition of the chemical crosslinking as a result of the presence of H<sup>+</sup> in the co-crosslinking process, whereas for pH values higher than 7.0 the chemical crosslinking by genipine is the dominant crosslinking method. At a lower pH, rapid electrostatic interactions occur between P<sub>3</sub>O<sub>10</sub><sup>5-</sup> of TPP and the NH<sub>3</sub><sup>+</sup> group of Ch, unlike genipine that can not readily react with protonated Ch amines. On the other hand at a higher pH as occurs instantaneous deprotonation of most NH<sub>3</sub><sup>+</sup> groups of Ch by OH<sup>-</sup>, coupled with partial ionic crosslinking, Ch free amines (NH<sub>2</sub>) suffer more easily chemical crosslink with genipine [133].

Ch MICs produced by ionotropic gelation with TPP and subsequent covalent crosslinking with 10mM of genipine for 1h demonstrated a suitable balance between the free amines required for the stability of Ch under acidic conditions with a gastric retention time *in vivo* of about two hours, and with high mucoadhesive capacities [146], in particular the capacity of adhesion to *H. pylori* and their consequent elimination along the GI tract [140].



## Chapter 2

### Motivation and Aim

Previous studies from our group have demonstrated the high ability of Ch MICs to adhere to different strains of *H. pylori*, leading to its removal from the human stomach and, consequently, reducing the colonization of this organ by this pathogenic bacterium [84].

Taking into account the work developed so far regarding the development of alternative therapies to eradicate *H. pylori* from the human stomach using Ch MICs and the lack of information regarding the possible interactions of this biomaterial with the human GI microbiota, the main objective of the proposed research project was to evaluate the behaviour of these MICs in terms of binding to bacteria from human GI microbiota at different pHs that mimic the environment of stomach and intestine in humans.

With a view to a future clinical application of Ch MICs, it would be interesting that these microparticles have the ability to adhere and eliminate from the GI tract pathogenic bacteria or potential pathobionts capable of causing pathological reactions in the human body and not significantly altering the diversity and quantity of commensal bacteria that contribute to the normal functioning of the organism and that are commonly present in the human GI tract.

In order to evaluate the capacity of Ch MICs to adhere bacteria of the human GI microbiota, adhesion tests were carried out with the bacteria *Helicobacter pylori*, *Campilobacter jejuni*, *Escherichia coli*, *Lactobacillus casei*, *Enterococcus faecalis* and *Bacillus cereus*. These bacteria were selected because they belong to two of the most abundant bacterial phyla represented in the human GI tract, namely the Proteobacteria and Firmicutes phyla, covering both commensal and pathogenic species.

Bacterial adhesion to MICs prepared using Ch with a DA of 6 %, was evaluated using ImageStream<sup>x</sup>, after incubation of the Ch MICs with the different bacteria in a range of pHs, namely 2.6, 4.0, 6.0 and 7.5, simulating the different pHs verified throughout the lower GI tract.

For visualization of bacteria adhered to Ch MIC by ImageStream<sup>x</sup>, the bacteria were stained with the fluorescent label SYTO9, since they do not have autofluorescence like Ch MICs.

ImageStream<sup>x</sup> was chosen as the technique to evaluate the bacterial adhesion to Ch MICs, since in addition to making it possible to obtain a high number of images in a very short time, it allows, through a software of image analysis (IDEAS® 6.2) to perform semi-quantitative and qualitative analysis of the collected images.



## Chapter 3

# Materials and Methods

In this chapter, are described the materials and techniques developed during the realization of the experimental work.

### 3.1 - Preparation of buffer solutions

Citrate-phosphate buffer solutions were composed of 0.1 M citric acid monohydrate and 0.2 M disodium hydrogen phosphate dehydrate solutions (Merck).

Different proportions of these two solutions were mixed in order to obtain different citrate-phosphate buffers at pH 2.6, 4.0, 6.0, and 7.5. All buffers were sterilized using a 0.22  $\mu\text{m}$  filter (Frilabo).

### 3.2 - Preparation of bacteria culture media

Brucella broth (BB, Fluka) medium was prepared by dissolving 28.1 g/l of BB in deionized water ( $\text{dH}_2\text{O}$ ) to the desired final volume, autoclaved at 121 °C for 15 min and stored at 4 °C, until use. Blood agar base N. 2 (BA, Liofilchem) plates with 5 % horse blood were supplemented with an antibiotic/antifungal cocktail containing Polimixin B (0.115 g/l; Sigma-Aldrich), Amphotericin B (1.25 g/l, Sigma-Aldrich), Trimethoprim (3.125 g/l, Sigma-Aldrich) and DMSO (2.5 % v/v, Sigma-Aldrich). For this, it was dissolved 42.5 g/l of BA in  $\text{dH}_2\text{O}$  to the desired volume, and then autoclaved at 121 °C for 15 min. After autoclaving, 5 % defibrinated horse blood was added when the BA reached 55 °C along with the antibiotic/antifungal cocktail previously prepared and the medium transferred to sterile petri dishes. About 2 h after preparation of the BA plates these were stored at 4 °C, until use.

Tryptic Soy Broth (TSB, Biomérieux) medium was prepared by dissolving 30.0 g/l of TSB (Sigma-Aldrich) in  $\text{dH}_2\text{O}$  to the desired final volume, autoclaved at 121 °C for 15 min and stored at 4 °C, until use. Tryptic Soy Agar (TSA, Sigma-Aldrich) medium was prepared by dissolving 40.0g/l of TSA in  $\text{dH}_2\text{O}$  to the desired final volume, autoclaved at 121 °C for 15 min and then transferred to sterile petri dishes. About 2h after culture plates preparation these were stored at 4 °C, until use.



De Man-Rogosa and Shape (MRS) broth (Biokar) medium was prepared by dissolving 55.3 g/l of this medium powder in dH<sub>2</sub>O to the desired final volume, autoclaved at 121 °C for 15 min and then stored at 4 °C, until use. MRS agar (Biokar) plates were produced by dissolving 70.3 g/l of MRS agar in dH<sub>2</sub>O to the desired final volume, autoclaved at 121 °C for 15 min and then transferred to a sterile petri dishes. About 2 h after culture plates preparation this were stored at 4 °C, until use.

Brain Heart Infusion (BHI) broth (Liofilchem) medium was prepared by dissolving 37.0 g/l of BHI broth in dH<sub>2</sub>O to the desired final volume, autoclaved at 121 °C for 15 min and stored at 4 °C, until use. BHI agar (Liofilchem) plates were also produced by dissolving 52.0 g/l of BHI agar in dH<sub>2</sub>O to the desired final volume, autoclaved at 121 °C for 15 min and then transferred to sterile petri dishes. About 2 h after preparation of the BHI agar plates these were stored at 4 °C, until use.

### 3.3 - Bacteria culture conditions

#### 3.3.1 - *Helicobacter pylori* culture conditions

*H. pylori* J99 was supplied by Department of Medical Biochemistry and Biophysics, Umeå University, Sweden, and stored in a criotube (CryoTube™ Vials, Thermo Scientific) at -80 °C in a solution of BB with 20 % of glycerol. About 4 to 5 drops of 20 µl of frozen bacteria suspension were placed on BA medium containing 5 % defibrinated horse blood supplemented with an antibiotic/antifungal cocktail at 37 °C for 32 to 48 h under microaerophilic conditions (Genbox Microaer Ref. 96125, Biomérieux) (85 % N<sub>2</sub>, 10 % CO<sub>2</sub>, and 5 % O<sub>2</sub>), in a drying oven (Binder). After this time, a spot was withdrawn and the spread performed on BA at 37 °C for another 48 h under identical conditions, in a drying oven (Binder).

After this incubation period, 1000 µl of BB with 10 % inactivated Fetal Bovine Serum (FBS, Sigma-Aldrich) was added to the culture plate and, with the aid of a spreader, all the bacteria grown in the solid culture medium were removed to an eppendorf. Bacteria inoculum was adjusted to an optical density at 600 nm (OD<sub>600</sub>) of 0.1 on a spectrometer (PerkinElmer Lambda 35 UV/VIS Spectrometer), followed by incubation of the *H. pylori* in 20 ml of BB with 10 % FBS in a T25 flask at 37 °C, overnight (around 16 hours) and 150 rpm under microaerophilic conditions, on an orbital agitation oven (IKA® KS 4000 ic control).

#### 3.3.2 - *Campilobacter jejuni* culture conditions and growth curve

*C. jejuni* (NCTC 11168, ATCC® 700819™) was kindly provided by Céu Figueiredo from the i3S Group Epithelial Interactions in Cancer and stored in a criotube (CryoTube™ Vials, Thermo Scientific) at -80 °C in a solution of BB with 10 % of glycerol.

Incubation of *C. jejuni* in solid medium was done in TSA with 5 % defibrinated sheep blood at 37 °C for 48 h under microaerophilic conditions (Genbox Microaer Ref. 96125) (85 % N<sub>2</sub>, 10 % CO<sub>2</sub> and 5 % O<sub>2</sub>).

After this incubation period, 1000 µl of TSB was added directly to the culture plate and with the aid of a spreader, the bacterium grown in the culture medium was removed to an eppendorf. The OD<sub>600</sub> was adjusted to 0.1, followed by incubation of the bacterium in 20 ml of TSB in a T25 flask at 37 °C, overnight (arund 16 hours) and 150 rpm under microaerophilic conditions, on an orbital agitation oven (IKA® KS 4000 ic control).

A growth curve of *C. jejuni* was performed by cultivating this bacterium in TSB during 48 h culture at 37 °C and 150 rpm, measuring at different time-points (0, 6, 12, 24 and 48 h) the OD<sub>600</sub>. The initial optical density was adjusted to 0.1 in TSB medium. To correlate the OD<sub>600</sub> values obtained when performing the culture in liquid medium versus solid medium, colony-forming units per milliliter (CFU/ml) were counted in TSA with 5 % defibrinated horse blood at different time-points, namely 0, 6, 12, 24 and 48 h. The CFU/ml at different time-points were performed by doing several serial dilutions and 10 µl of each dilution were plated in TSA with 5 % defibrinated horse blood and count after 48 h.

### 3.3.3 - *Escherichia coli* culture conditions

*E. coli* (ATCC® 25922™) was acquired at ATCC (American Type Culture Collection) and stored in a criotube (CryoTube™ Vials, Thermo Scientific) at -80 °C in a solution of TSB with 10 % glycerol.

To spread the bacterium in a solid medium, a little of the contents of the vial was removed with a loop without thawing it completely and the TSA culture plate scratched with *E. coli*. Then the culture plate was incubated in a drying oven (Binder) during 24 h at 37 °C, under aerobic conditions.

After 24 h, with the aid of a loop, two bacteria colonies were transferred into 5 ml of TSB. The inoculum was homogenized to emulsify the bacteria with the liquid medium and then incubated on an orbital agitation oven (IKA® KS 4000 ic control) at 37 °C and 150 rpm, overnight (around 16 hours), under aerobic conditions.

### 3.3.4 - *Lactobacillus casei* culture conditions

*L. casei-01* was provided by Chr. Hansen, Hørsholm Denmark, and stored in a criotube (CryoTube™ Vials, Thermo Scientific) at -80 °C in a solution of MRS broth with 10 % of glycerol.

To spread this bacterium on MRS agar, 50 µl of the completely thawed criotube contents were pipetted and spread on the culture plate. Then the culture plate was incubated in a drying oven (Binder) during 48 h at 37 °C, under aerobic conditions.

After 48 h, fill a loop well with bacteria content and transfer into 5 ml of MRS broth. The inoculum was homogenized to emulsify the bacteria with the liquid medium and then incubate on an orbital agitation oven (IKA® KS 4000 ic control) at 37 °C and 150 rpm, overnight (around 16 hours), under aerobic conditions.

### 3.3.5 - *Enterococcus faecalis* culture conditions

*E. faecalis* is a clinical isolate from Hospital de São João in Porto, kindly provided by Benedita Sampaio Maia and stored in a criotube (CryoTube™ Vials, Thermo Scientific) at -80 °C in a solution of BHI broth with 10 % of glycerol.

To spread *E. faecalis* in BHI agar, a small amount of the content of the criotube was removed with a loop without thawing it completely and scratching the culture plate with this bacterium. *E. faecalis* was then incubated on a drying oven (Binder) at 37 °C for 24 h, under aerobic conditions.

After 24 h, fill a loop well with bacteria content and transfer into 5 ml of BHI broth. The inoculum was homogenized to emulsify the bacteria with the liquid medium and then incubated on an orbital agitation oven (IKA® KS 4000 ic control) at 37 °C and 150 rpm, overnight (around 16 hours), under aerobic conditions.

### 3.3.6 - *Bacillus cereus* culture conditions and growth curve

*B. cereus* is a clinical isolate from Hospital de São João in Porto, kindly provided by Benedita Sampaio Maia and stored in a criotube (CryoTube™ Vials, Thermo Scientific) at -80 °C in a solution of BHI broth with 10 % of glycerol.

To spread *B. cereus* in BHI agar, a small amount of the content of the criotube was removed with a loop without thawing it completely and scratching the culture plate with this bacterium. *B. cereus* was then incubated on a drying oven (Binder) at 37 °C for 24 h, under aerobic conditions.

After 24 h, with the aid of a loop, two bacteria colonies were transferred into 5 ml of BHI broth. The inoculum was homogenized to emulsify the bacteria with the liquid medium and then incubated on an orbital agitation oven (IKA® KS 4000 ic control) at 37 °C and 150 rpm, during 6 h, under aerobic conditions.

For *B. cereus*, a growth curve was performed cultivating this bacterium during 24 h in BHI agar and after this time during 48 h in BHI broth at 37 °C and 150 rpm, measuring at different time points (0, 6, 12, 24 and 48 h) the OD<sub>600</sub>. The initial OD<sub>600</sub> was adjusted to 0.03 in the referred medium. To correlate the OD<sub>600</sub> values obtained when performing the culture in liquid medium versus solid medium, CFU/ml were counted in BHI agar at different time-points, namely 0, 6, 12, 24 and 48 h. The CFU/ml at different time-points were performed by doing several serial dilutions and 10 µl of each dilution were plated in BHI agar and the number of colony-forming units (CFU) counted after 24 h.

## 3.4 - Bacteria Zeta Potential

The zeta potential (ZP) of the bacterial species *H. pylori*, *C. jejuni*, *E. coli*, *L. casei*, *E. faecalis* and *B. cereus* was evaluated using the instrument Zetasizer Nano ZS (Malvern Instruments, UK) with a 4 mW helium–neon laser beam with a wavelength of 633 nm performed at 25 °C with a backscattering angle of 13°.

Bacteria were cultured in the conditions previously described for each bacteria, and then were adjusted at a final concentration of approximately  $1.0 \times 10^7$  CFU/ml on citrate-phosphate buffer at pH 2.6, 4.0, 6.0 and 7.5. Bacteria samples were then incubated at 37 °C for 2 h and 120 rpm of stirring on an orbital shaker (IKA® KS 4000 ic control).

After incubation time, the samples were placed in polycarbonate folded capillary cells, incorporated with gold plated electrodes (DTS1070; Malvern Instruments, UK) and the ZP measurements were performed at 25 °C, using the electrophoretic light scattering (ELS), using the Software DTS Nano v.7.12 to estimate the viscosity (1.0558 cP), dielectric constant and refraction index (1.3376) of the measure solution.

The analysis was done using the “Automode” analysis model, with the applied voltage and the number of subruns automatically defined by the software. The ZP values are based on the average of three individual measurements for each condition and these values were automatically calculated by the software from the EPM (ElectroPhoretic Mobility) values using the Henry equation with the Smoluchowski approximation.

### 3.5 - Chitosan microspheres

The Ch MICs used in this research were previously produced by the research group BioEngineered Surfaces by ionotropic gelation using an aerodynamically driven system (Nisco Encapsulation Unit Var J30, NISCO) (see Figure 3.1).

The method of producing Ch particles by ionotropic gelation consists of the dissolution of Ch in aqueous acid solution to obtain cationic chitosan. Mild addition of chitosan solution (positively charged) under constant agitation in a polyanionic (negatively charged, usually TPP) solution. Complexation between oppositely charged species results in the precipitation of chitosan in the form of spherical particles. This technique is a simple process with production under mild conditions and free of organic solvents, which are toxic.

In this particular case, the chitosan solution of 0.5 % (w/v) in 0.1 M acetic acid with a DA of 6 % placed in the syringe was set in the syringe pump and connected to the 0.25 mm diameter syringe pump nozzle (PE-00515, NISCO). The nozzle is contained within a chamber of compressed air with controlled pressure (525 mbar) where the chitosan solution passes with a flow rate of 0.5 ml/min.

The structure and width of the exit port of the compressed air chamber leads to a jet-like aerodynamic effect through which the chitosan passes, leading to the formation of microspheres. The air is the driving force that leads the solution to fall into a TPP (Sigma-Aldrich) solution (5 % w/v in dH<sub>2</sub>O; pH 9.0) under stirring at 35 rpm, as a regulated compressed air beam that forces the solution to exit a pressurized chamber in a conical spray. Then the Ch MICs were rinsed in Milli-Q water.

Since these MICs were meant to assess the adhesive and antibacterial properties in the GI tract and, given the behaviour of Ch biomaterials under acidic conditions, such as those observed in the human stomach [39], [127], [129], [131], [132], [134], [136], the Ch MICs were then crosslinked with genipine (Wako Chemicals GmbH). The crosslinking was performed by incubating the Ch MICs with 10 mM of genipin, prepared in 0.01 M phosphate buffered saline solution (PBS) (pH 7.4; Sigma-Aldrich), at 25 °C for 45 min and 120 rpm, so that this material exhibits a more stable behaviour under these conditions.

Afterwards the Ch MICs were rinsed three times with Milli-Q water, frozen in liquid nitrogen and lyophilized at -80 °C and then stored until use at 4 °C in ethanol 70 % v/v.

Ch MICs prepared using Ch with a DA of 6 % were selected for the present study, as particles with lower DA should have more exposed amines to interact with the bacteria.

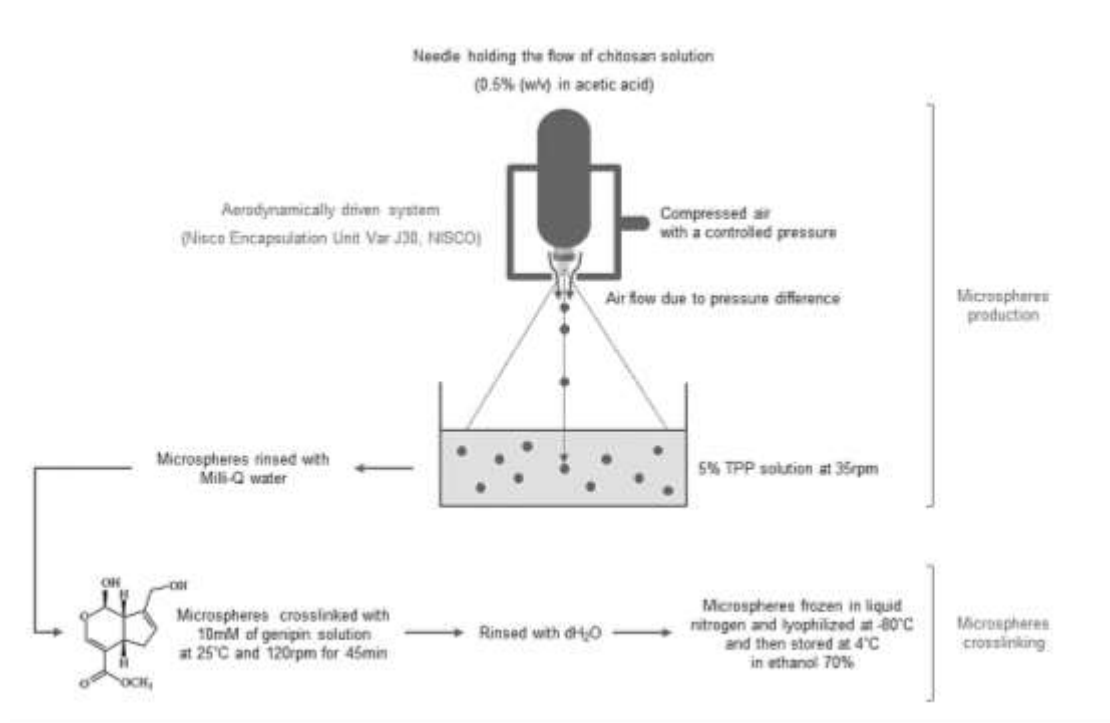


**Figure 3.1** - Scheme of the production of chitosan microspheres with a DA of 6 % by the ionotropic gelation method, in particular by aerodynamically driven system.

### 3.5.1 - Chitosan microspheres preparation

Chitosan microspheres prepared using Ch with a DA of 6 % are stored in ethanol 70 % at 4 °C and protected from light, until use.

About 2000 Ch MICs were pipetted from the initial suspension for each eppendorf corresponding to each condition, namely only Ch MICs (MICs\_) and Ch MICs with bacteria (MICs\_bacteria) at different citrate-phosphate buffer at different pHs, namely 2.6, 4.0, 6.0 and 7.5.

These microspheres were then rinsed three times for 8 min at 11200 g in the corresponding citrate-phosphate buffer (pH 2.6, 4.0, 6.0 and 7.5) to clean these particles from the ethanol 70 % and stored at 4 °C, until use.

### 3.5.2 - Chitosan microspheres Zeta Potential

The ZP of Ch MICs prepared using Ch with a DA of 6 % was determined using an ElectroKinetic Analyzer (EKA; Anton Paar GmbH, Austria) based on streaming potential measurements with a special powder cell adapted inside a cylindrical cell, used for particles.

Ch MICs were incubated in citrate-phosphate buffer at pH 2.6, 4.0, 6.0 and 7.5 at 37 °C for 2 h and 120 rpm on an orbital shaker (IKA® KS 4000 ic control).

After incubation, the samples were frozen at -80 °C and lyophilized at -80 °C overnight to obtain dry samples and then placed between two filter membranes to hold the sample within the measuring cell. The solid particles were mounted inside the powder cell occupying a volume of roughly 48.75 mm<sup>3</sup>, thus maintaining an overall constant height of sample for all the measurements.

Streaming potential was measured using Ag/AgCl electrodes installed at both ends of the streaming channel (the cylindrical cell) and the analysis was performed using 1 mM of KCl (Sigma-Aldrich) as the electrolyte flowing solution through the measuring cell.

The measurements were performed at RT at pH values around 2.6, 4.0, 6.0 and 7.5 for each condition, respectively, to maintain as best as possible the surface charge of chitosan microspheres acquired during the incubation time with citrate-phosphate buffer at different pHs. pH values were adjusted with 0.1 M of HCl and NaOH solutions.

For the evaluation of the ZP of Ch MICs the electrical conductivity of the electrolyte solution was measured during the analysis and the streaming potential determined by the application of an electrolyte flow in alternating directions using pressure ranges from 0 to 200 mbar. For each, six pressure ramps were performed (three in each flow direction), in order to cope with the asymmetric potential fluctuations. The ZP was calculated using the Helmholtz–Smoluchowsky equation (3.1):

$$\xi = \frac{dU}{dp} \times \frac{\eta}{\epsilon \epsilon_0} \times K, \quad (3.1)$$

where  $\xi$  is the zeta potential,  $dU$  is the streaming potential,  $dp$  is the pressure differential across the sample,  $\eta$  is the viscosity of the electrolyte solution,  $\epsilon$  is the relative dielectric constant of the electrolyte fluid,  $\epsilon_0$  is the vacuum permittivity and  $K$  is the specific electrical conductivity of the electrolyte solution.

## 3.6 - Chitosan microspheres adhesion to bacteria from human gastrointestinal microbiota

As previously mentioned, motivated by the lack of knowledge of the interaction of Ch MICs with bacteria of the human GI microbiota, the development of this investigation focused on the evaluation of the adhesion capacity of Ch MICs to bacteria of the human GI microbiota and the main steps to achieve this objective are described below.

### 3.6.1 - Adhesion assay

Adhesion of Ch MICs to different bacteria of the human GI microbiota was evaluated in the ImageStream<sup>®</sup> Mark II Imaging Flow Cytometer by labelling adherent bacteria with a dye for total bacteria (live and dead).

Figure 3.2 illustrates the protocol scheme of the adhesion tests. The bacterial inoculum content after incubation in liquid medium (overnight in the case of *H. pylori*, *C. jejuni*, *E. coli*, *L. casei* and *E. faecalis*, and 6 h for *B. cereus*), was centrifuged (Eppendorf Centrifuge 5810R) for 10 min at 816 g in NaCl 0.85 %. After the last centrifugation, supernatant was discarded and the remaining bacteria pellet resuspended in 10 ml of NaCl 0.85 % and its OD<sub>600</sub> measured on a spectrometer (PerkinElmer Lambda 35 UV/VIS Spectrometer) at a dilution of 1:10. The bacterial inoculum was then adjusted with citrate-phosphate buffer at pH 2.6, 4.0, 6.0 and 7.5 for an OD<sub>600</sub> specific for each bacteria, corresponding, approximately, to 1.0×10<sup>7</sup> CFU/ml calculated by CFU counting (Table 3.1).

**Table 3.1** - Optical density at 600 nm corresponding, approximately, to  $1.0 \times 10^7$  CFU/ml for each bacteria under study.

Bacterial species	Optical density 600 nm (OD <sub>600</sub> )
<i>Helicobacter pylori</i>	0.03
<i>Campilobacter jejuni</i>	0.0017
<i>Escherichia coli</i>	0.0017
<i>Lactobacillus casei</i>	0.1
<i>Enterococcus faecalis</i>	0.008
<i>Bacillus cereus</i>	0.24

After culturing the different bacterial species under analysis, 50 µl of Ch MICs (with approximately 2000 MICs) in citrate-phosphate buffer at pH 2.6, 4.0, 6.0 and 7.5 were incubated with 50 µl of bacteria (*H. pylori*, *C. jejuni* and *E. coli*, *L. casei*, *E. faecalis* or *B. cereus*) in the same respective buffers, at 37 °C for 2 h and 120 rpm of stirring on an orbital shaker (IKA® KS 4000 ic control). A final concentration of approximately  $0.5 \times 10^7$  CFU/ml was obtained for each bacteria. After incubation, the samples were rinsed three times in 100 µl of filtered dH<sub>2</sub>O after centrifugation for 6 min and 1792 g at RT, in order to remove non-adherent bacteria.

Bacteria were then labelled with the fluorescent marker SYTO9 (LIVE/DEAD™ Backlight™ Bacterial Viability Kit L13152, Invitrogen by Thermo Scientific) at a concentration of 0.015 µM and after 15 min of staining the samples were run in the ImageStream®<sup>X</sup> Mark II Imaging Flow Cytometer (ImageStream<sup>X</sup>, Merck) in filtered dH<sub>2</sub>O, using the 488 nm excitation laser, which allows the observation of both Ch MICs, due to their autofluorescence, and bacteria, since they were labelled with SYTO9. Before reading the samples on ImageStream<sup>X</sup> it is necessary to filter the samples through a Falcon™ Cell Strainer with a mesh size of 70 µm (Fisher Scientific).

The images obtained in ImageStream<sup>X</sup> were acquired by INSPIRE® software (INSPIRE) and analysed in IDEAS® 6.2 software (Image Data Exploration and Analysis Software, IDEAS 6.2; Merck), as described in the following section.

It is important to note that the samples were rinsed with filtered dH<sub>2</sub>O, since according to *L. Boulos, et al.*, [162], SYTO9 shows a different fluorescence intensity at different pHs and as one of the objectives of this investigation work is the evaluation of the behaviour of adhesion of Ch MICs to bacteria at different pHs, these buffers must be removed so that the intensity values measured on ImageStream<sup>X</sup> image analysis software (IDEAS 6.2) correspond to the amount of bacteria and not to the different intensity of SYTO9 at different pHs. In the LIVE/DEAD™ Backlight™ Bacterial Viability Kit L13152 (Invitrogen by Thermo Scientific) [163] it is advised the use of filtered dH<sub>2</sub>O, when samples are analysed in Flow Cytometry.

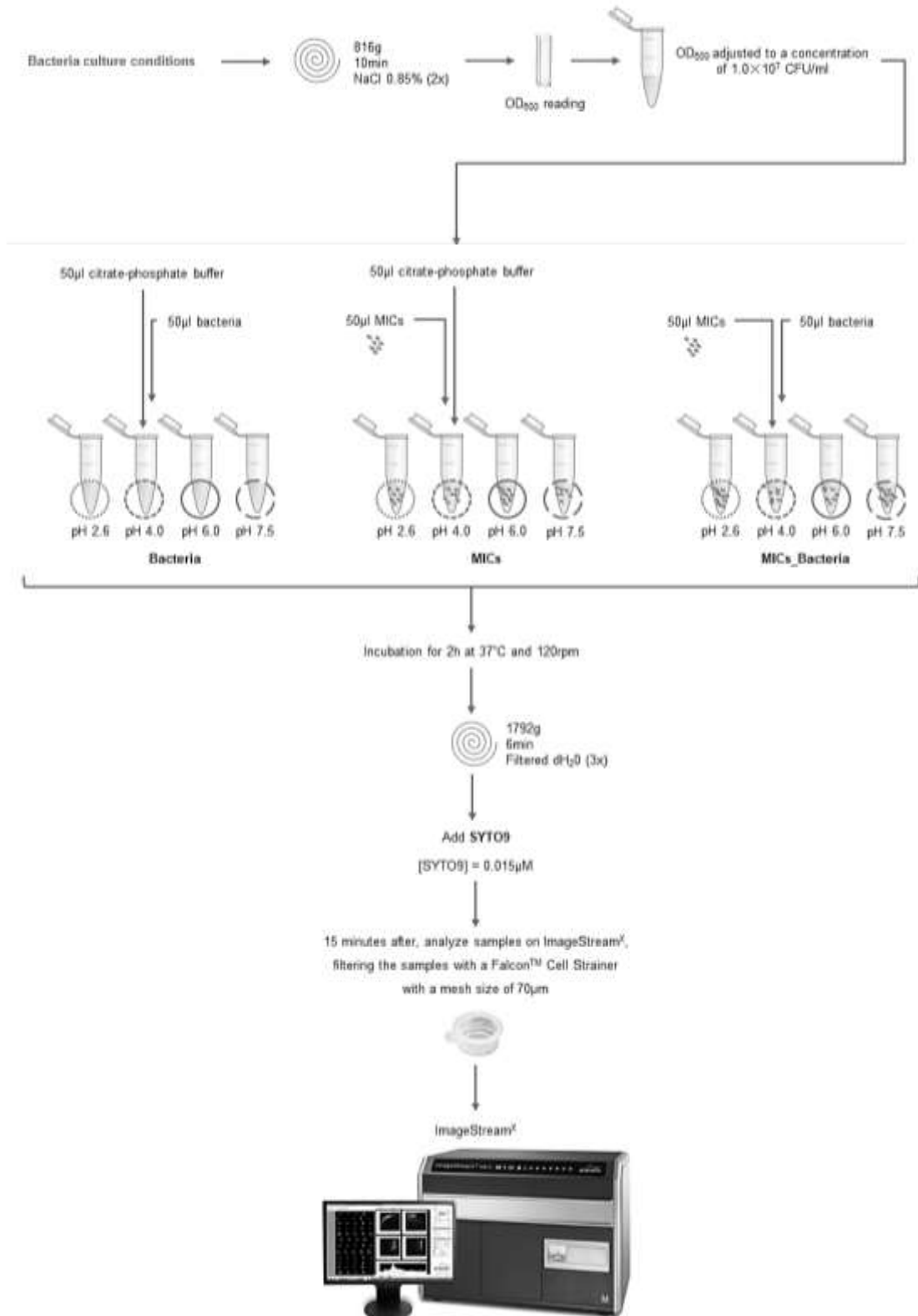


**Figure 3.2** - Protocol of the adhesion assay of chitosan microspheres to bacteria from the human gastrointestinal microbiota.



### 3.6.2 - ImageStream<sup>X</sup> Flow Cytometer

ImageStream<sup>X</sup> was both used to visualize adhesion of the Ch MICs to bacteria of the human GI microbiota, as well as for the characterization of the microspheres used in the adhesion assays. For this, a first step of image acquisition was performed and then a step of analysing the obtained images, which are described in 3.6.2.1 and 3.6.2.2.

ImageStream<sup>X</sup> is a Flow Cytometer that combines the analysis rate of Conventional Flow Cytometry with the sensitivity and resolution of the Microscopy, allowing the obtaining of images of the particles/cells under analysis. This device has the main advantages of obtaining images of a large number of cells in a short period, enabling a semi-quantitative and qualitative analysis of the results through IDEAS 6.2 software and the identification of individualized cells by the intensity of fluorescent markers applied. As main disadvantages, this device present in i3S only possesses a laser, the 488 nm and only allows the analysis of particles with a size smaller than 70  $\mu\text{m}$ .

As for the working principles of the ImageStream<sup>X</sup> (Figure 3.3), as in conventional Flow Cytometry, the particles pass in a flowing system and are illuminated by the brightfield and the 488 nm laser. First, light that is collected from the particles flowing through objective lenses and then is subsequently transmitted to the spectral decomposition element, which is nothing less than a set of long-pass filters in an angular matrix. The filters then direct different spectral bands to laterally distinct channels in the coupled charging device (CCD) detector.

Finally, the images of the particles are then collected from time-delayed integration (TDI) technology, allowing the optical decomposition of the images into a set of sub-images with different colours and spatially isolated from each other.

The combination of the CCD detector with TDI technology allows the detection of about 1000 times more signal than the more traditional approaches, so it seems to be a promising system even for the detection of bacteria adhered to microparticles. This system, in addition to considerably increasing the sensitivity of the photomultiplier tubes, allows the preservation of the quality of the images obtained from moving 'cells'.

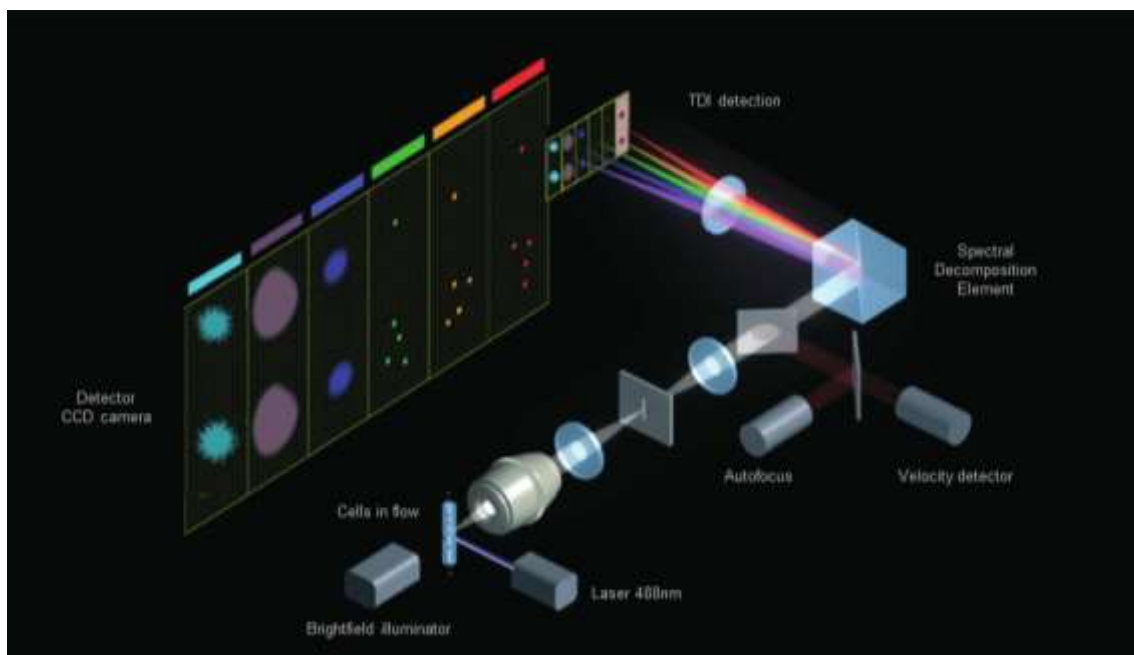


**Figure 3.3** - Principles of operation layout of ImageStream<sup>®</sup> (Adapted from Amnis Corporation).

### 3.6.2.1 - Acquisition

INSPIRE® software (INSPIRE) is integrated with ImageStream<sup>X</sup> and is used to run the instrument and to read the samples according to the parameters selected specifically for the samples.

In order for the system to be ready to run samples it is necessary that the flow velocity is stabilized close to 60 mm/s and that the focus of the beads is below 0.1-0.2 of deviation. The beads are small spheres with an average length of 1 µm, from which the system will focus the Ch MICs and the bacteria under analysis.

In INSPIRE it is still possible to configure the system, selecting parameters that allow to detect and select what is wanted to observe, such as laser power, number of events to collect, size of 'cells' to observe, among others, so that the best detection of bacteria and chitosan microspheres under study is optimized. In the image of Figure 3.4 the interface of the INSPIRE software is shown, with the system stabilized and ready to run samples on the device.

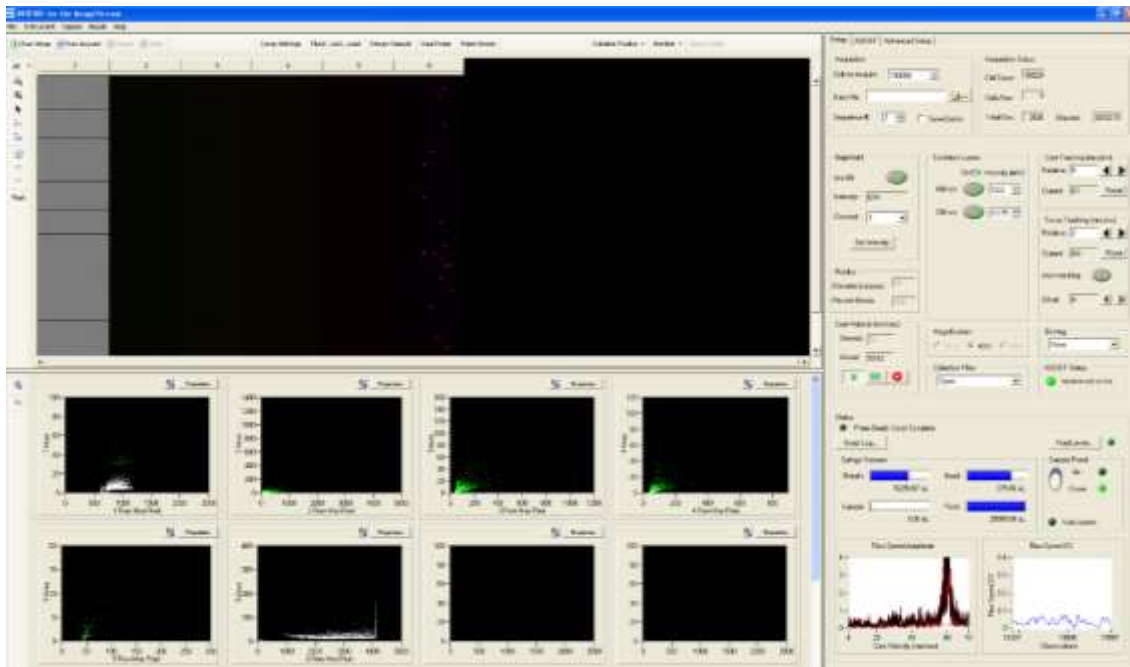


**Figure 3.4** - ImageStream<sup>X</sup> INSPIRE® Software interface.

### 3.6.2.2 - Analysis

Image Data Exploration and Analysis Software 6.2 is, as its name implies, an image analysis software of the images obtained in the ImageStream<sup>X</sup> multispectral imaging flow cytometer. The ImageStream<sup>X</sup> IDEAS® 6.2 image analysis software user interface for bacterial adhesion assays is represented in Figure 3.5. For the analysis of the results obtained when running the samples in the ImageStream<sup>X</sup>, it is necessary to create for each of the conditions under study, that is for each of the samples with citrate-phosphate buffers at pH 2.6, 4.0, 6.0 and 7.5, a compensation matrix. In this case, for the adhesion tests, the compensation matrix serves to remove the contribution of the autofluorescence of the Ch MICs in channel 2 (Ch02), so that the intensity of the fluorescence in this channel, corresponding to the bacteria adhered to the Ch MICs, can be determined more precisely.

Thus, despite the emission wavelength ( $\lambda_{em}$ ) of the Ch MICs when excited by the 488nm laser, encompassing all available channels in the ImageStream<sup>X</sup>, it is possible by applying a compensation matrix to reduce the amount of fluorescence in Ch02 from the Ch MICs.

For a better interpretation of the obtained results, a maximum histogram smoothing was applied to the graphs for the fluorescence intensity in Ch02.



**Figure 3.5** - ImageStream<sup>X</sup> IDEAS® 6.2 image analysis software user interface for bacterial adhesion assays.

### 3.6.2.2.1 - Bacterial adhesion to chitosan microspheres

In the image of Figure 3.6 the IDEAS 6.2 interface created for the adhesion assay of the Ch MICs with the bacterium *Helicobacter pylori* is shown by way of example.

Regarding the images observed in the IDEAS 6.2 software, although the colours represented in each channel are arbitrary, Ch02 has a band of  $\lambda_{em}$  in the green region ( $\lambda_{em}$  of 480-560 nm) and channel 5 (Ch05) a  $\lambda_{em}$  band in the red region ( $\lambda_{em}$  of 660-745 nm) of the visible light spectrum. Therefore, it was chosen to represent each channel, with the colours corresponding to the region of the spectrum in which they emit light.

Before analysing the results, it is necessary to select from all the data, the images to be considered for the study. First, through a Gradient RMS histogram, is selected the range of microparticles that are focused. Gradient RMS detects large changes in pixel values in the image thus measuring the sharpness of an image, which allows the selection of more focused images.

Then, from the focused images, on a scatterplot by the Aspect Ratio and the area, the images that are considered to be Ch MICs are selected and, finally, the positive images for Ch05 are selected, where it is intended to observe the Ch MICs, through a histogram of fluorescence intensity in Ch05.

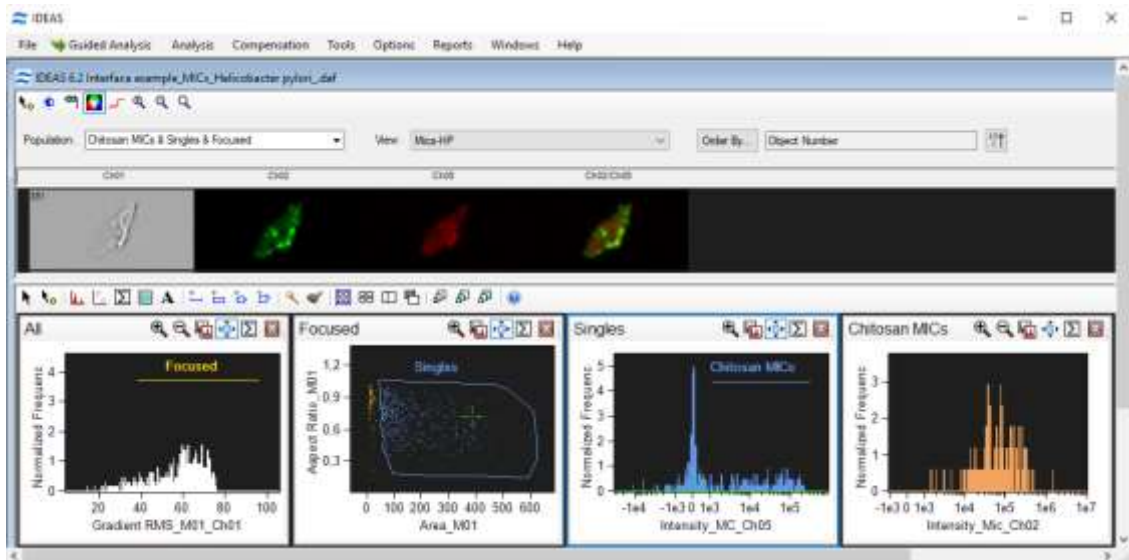


**Figure 3.6** - ImageStream<sup>X</sup> IDEAS<sup>®</sup> 6.2 image analysis software interface for bacterial adhesion assays with an example created for the adhesion assay of the chitosan microspheres to *Helicobacter pylori*.

The significant differences between the mean values for samples containing Ch MICs and bacteria at different pHs were evaluated in the IBM<sup>®</sup> SPSS<sup>®</sup> Statistics Base 25 statistical analysis software, using the One-Way ANOVA model, after unidirectional analysis of variances with homogeneity test of variances based on the mean, from the Levene's statistics. P-values less than 0.05 were considered statistically significant. Cases where the level of significance was less than 0.05 and therefore equal variances not-assumed, the significant difference between mean values for the different samples was determined using One-Way ANOVA with Post-Hoc Tamhane, Dunnett T3, Games-Howell and Dunnett C tests for multiple comparisons. Cases where the level of significance was greater than 0.05 and therefore equal variances assumed, the significant difference between mean values for the different samples was determined using One-Way ANOVA with Post-Hoc Tukey HSD and Bonferroni tests for multiple comparisons.

### 3.6.2.2.2 - Characterization of chitosan microspheres

Characterization of Ch MICs regarding different size and shape parameters, in particular Area, Diameter, Perimeter, Length, Major and Minor Axis, and Aspect Ratio was performed using ImageStream<sup>X</sup>.

For the characterization assay of the Ch MICs the adhesion test samples containing only Ch MICs (MICs positive control), incubated in different citrate-phosphate buffers at different pHs, namely at pH 2.6, 4.0, 6.0 and 7.5, were used after running the samples in filtered dH<sub>2</sub>O in the equipment, to evaluate in the software IDEAS 6.2 these parameters for its characterization, through the images obtained in the ImageStream<sup>X</sup> brightfield channel (Ch01).

The characterization of these Ch MICs according to the selected features was performed in the IDEAS 6.2 software after reading the samples in ImageStream<sup>X</sup> INSPIRE software. From the images obtained in the brightfield channel and through the selection of a mask adjusted as much as possible to the area of the different Ch MICs, it is possible to obtain histograms to evaluate the different features. In Figure 3.7 is shown the IDEAS 6.2 interface created for the Ch MICs characterization.

Before analysing the results, it is necessary to select from all the data, the images to be considered for the study. First, through a Gradient RMS histogram, is selected the range of

microparticles that are focused. Gradient RMS detects large changes in pixel values in the image thus measuring the sharpness of an image, which allows the selection of more focused images.

Then, from the focused images, on a scatterplot by the Aspect Ratio and the area, the images that are considered to be Ch MICs are selected and, finally, the positive images are selected for Ch05, where it is intended to observe the Ch MICs, through a histogram of fluorescence intensity in Ch05.

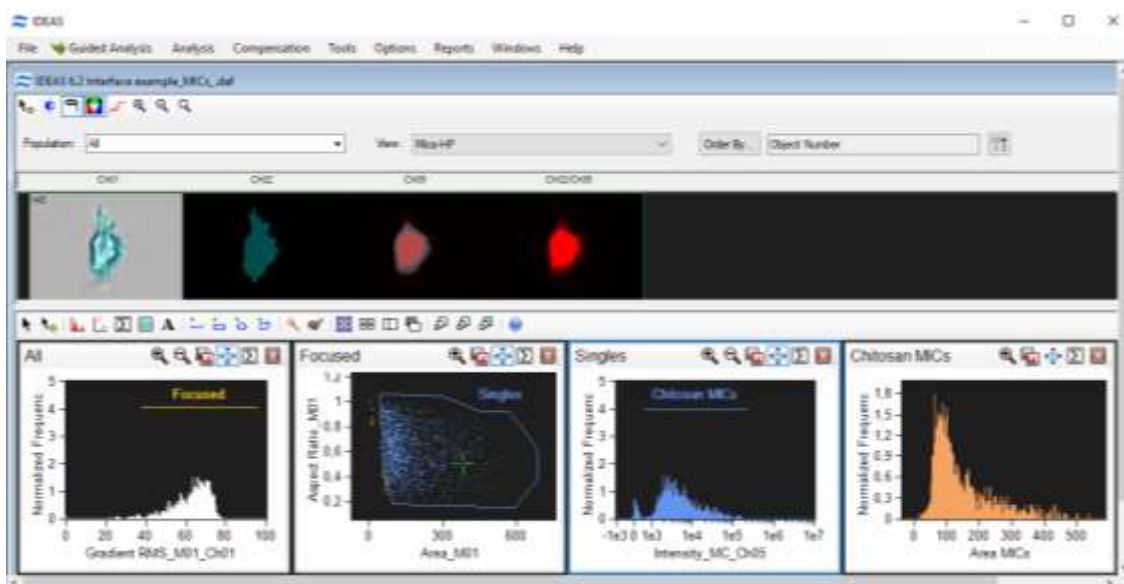


**Figure 3.7** - ImageStream<sup>X</sup> IDEAS® 6.2 image analysis software interface for chitosan microspheres size and shape features.

The significant differences between the mean values for samples containing Ch MICs at different pHs were evaluated in the SPSS software, using the One-Way ANOVA model, after unidirectional analysis of variances with homogeneity test of variances based on the mean, from the Levene's statistics. P-values less than 0.05 were considered statistically significant. In the cases where the level of significance was less than 0.05 and therefore equal variances non-assumed, the significant difference between mean values for the different samples was determined using One-Way ANOVA with Post-Hoc Tamhane, Dunnett T3, Games-Howell and Dunnett C tests for multiple comparisons. In the cases where the level of significance was greater than 0.05 and therefore equal variances assumed, the significant difference between mean values for the different samples was determined using One-Way ANOVA with Post-Hoc Tukey HSD and Bonferroni tests for multiple comparisons.

- **Size Features**

In Table 3.2 is represented a visual scheme for the measure of each size feature to characterize Ch MICs.

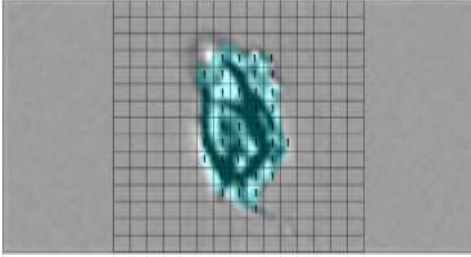
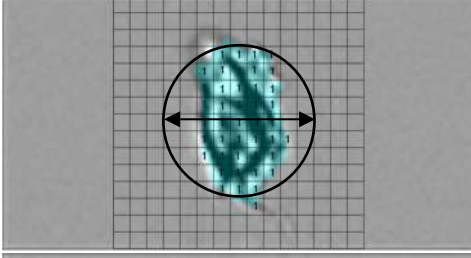
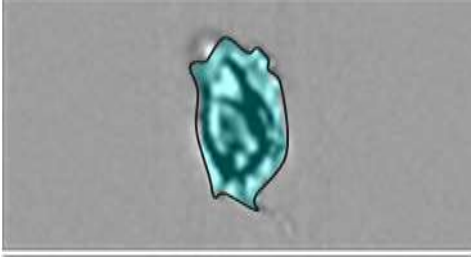
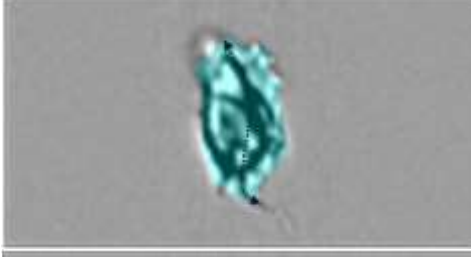
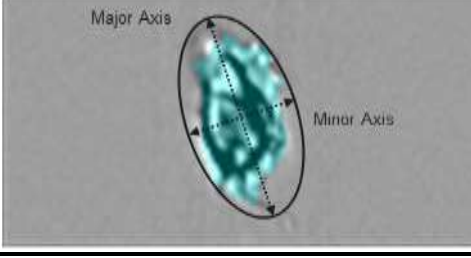
The Area parameter is defined as the mask size in Ch01 in square micrometers ( $\mu\text{m}^2$ ), that is, the number of  $\mu\text{m}^2$  in the brightfield mask. The number of pixels in the mask is converted to square micrometers, so that one pixel is equal to  $0.25 \mu\text{m}^2$ . The feature Diameter (d) gives the diameter of the object mask in  $\mu\text{m}$ , based on its area and is calculated by the following equation:  $d = 2 \times \sqrt{(A/\pi)}$ . In other words, this feature provides the diameter of a circle that has the same



area of the object, which is highly dependent of the mask and the circularity of the object. Consequently, objects with the same area but different circularity will present the same diameter.

The Perimeter parameter in turn measures the length of the outer mask border (in  $\mu\text{m}$ ) of the brightfield channel in  $\mu\text{m}$ . The Length as its name indicates, measures the longest part of the object under analysis (in  $\mu\text{m}$ ) and, unlike the Major Axis, it can measure the length of the object even if it does not form its axis in a straight line. The Major and Minor Axis allow to describe, respectively, the largest and smallest portion of an elliptical shape, adjusted to the shape of the object as best as possible (in  $\mu\text{m}$ ).

**Table 3.2** - Visual scheme for chitosan microspheres size features measure from the mask in the brightfield channel.

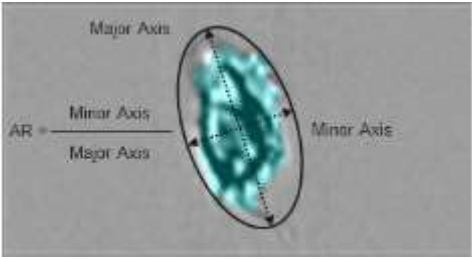
Type of feature	Feature name	Chitosan microspheres in brightfield channel
<b>Size</b>	Area	
	Diameter	
	Perimeter	
	Length	
	Major and Minor Axis	

- **Shape Feature**

In Table 3.3 is represented a visual scheme for the measure of Aspect Ratio (AR) feature to characterize the shape of Ch MICs.

Through the object's Major and Minor Axis, the AR determine how round a given object is. This feature is determined by the following equation:  $AR = \text{Minor Axis} / \text{Major Axis}$ .

**Table 3.3** - Visual scheme for chitosan microspheres shape feature measure from the mask in the brightfield channel.

Type of feature	Feature name	Chitosan microspheres in brightfield channel
Shape	Aspect Ratio	

# Chapter 4

## Results and Discussion

In this chapter the results obtained, based on the methodology applied are presented and analysed, in an attempt to respond to the objectives initially proposed for this research project.

### 4.1 - Bacterial growth curves

The growth curves of *H. pylori*, *E. coli*, *L. casei* and *E. faecalis* bacteria obtained by reading OD<sub>600</sub> at different time-points, when cultured in corresponding liquid medium, as well as the correspondence in CFU/ml, when cultured in solid medium, were available from the BioEngineered Surfaces i3S group unpublished data and therefore were not performed.

#### 4.1.1 - *Campilobacter jejuni* growth curve

The growth curve for *Campilobacter jejuni* was obtained and this bacterium showed exponential growth between 6 and 24h when cultured in liquid medium (TSB) during 48 h and 150rpm of agitation under microaerophilic conditions (Figure 4.1). For the time-points analysed, this bacterium presented a higher OD<sub>600</sub> and, consequently, a higher quantity of CFU/ml at the time-point 24 h and after 48 h *C. jejuni* is in the death phase.

During this assay, it was not possible to obtain a growth match in liquid medium for CFU/ml when grown on solid medium, as this medium prepared with TSA supplemented with 5 % defibrillated horse blood, caused a sort of scattering of the colonies in all dilutions tested and individualized colonies could not be observed.

*C. jejuni* was then cultured with the ATCC TSA with 5 % defibrinated Sheep Blood plates recommended for this bacterium and the formation of individualized colonies was observed. Comparing the composition of the two media, none were supplemented with antibiotics and the only difference between the two was the type of blood used. Although hemolysis of the blood in the culture plates has not been observed, there should be some component in horse blood that did not allow a normal growth of this bacterium and formation of individualized colonies that already could be observed in the plates supplemented with sheep blood.



The number of viable bacteria (CFU) of about  $1.0 \times 10^7$  CFU/ml corresponded to an OD<sub>600</sub> of 0.0017 and therefore for the adhesion tests were performed with an overnight bacterial inoculum, and then the OD<sub>600</sub> adjusted to 0.0017.

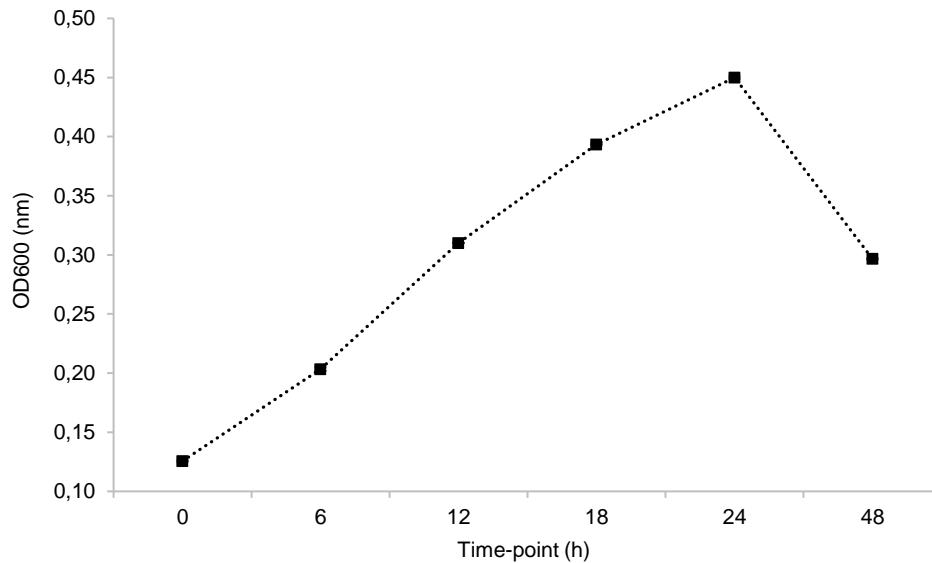


**Figure 4.1** - Growth curve of *Campilobacter jejuni*, cultured in Tryptic Soy Broth during 48 h, at 37 °C and 150 rpm under microaerophilic conditions.

#### 4.1.2 - *Bacillus cereus* growth curve

A growth curve for *Bacillus cereus* and the corresponding CFU/ml when cultured in solid medium (BHI agar) was obtained and this bacterium showed higher growth at the time-point 6h when cultured in liquid medium (BHI broth) during 48 h at 37 °C and 150 rpm (Figure 4.2).

This is a fast growing bacterium that should be in the exponential phase sometime before 6 h until sometime before 12 h. However, although lower time-points were not achieved, the growth curve obtained was sufficient to know where the exponential phase was. At 6 h it is certain that it is in the exponential phase, and for this reason it was chosen to put it to grow during 6 h in liquid medium.

The number of viable bacteria (CFU) of about  $1.0 \times 10^7$  CFU/ml corresponded to an OD<sub>600</sub> of 0.24 and therefore for the adhesion tests were performed a bacterial inoculum during no more than 6 h in liquid medium, and then the OD<sub>600</sub> adjusted to 0.24.

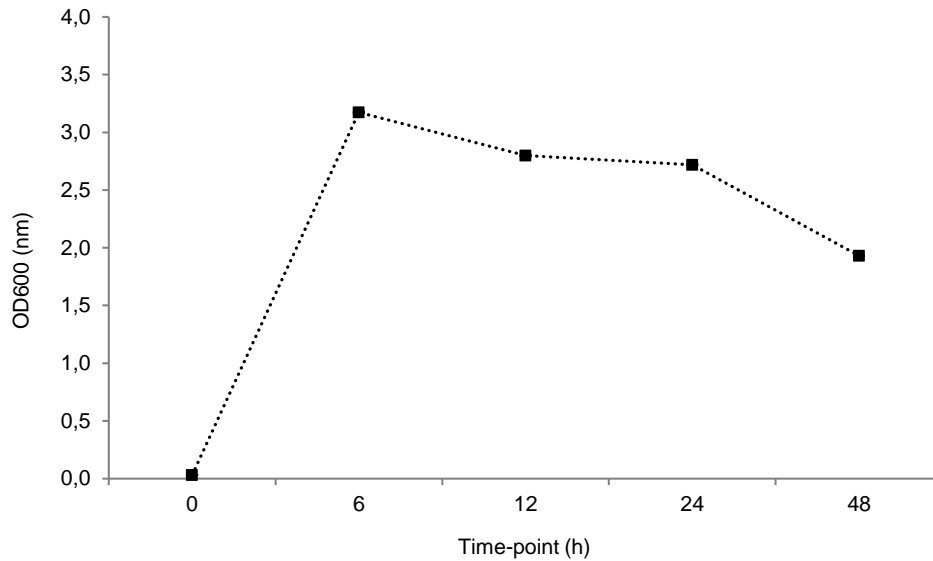


**Figure 4.2** - Growth curve of *Bacillus cereus*, cultured in Brain Heart Infusion during 48 h, at 37 °C and 150 rpm, under aerobic conditions.

## 4.2 - Bacteria zeta potential

The surface charge is particularly quantified by the zeta potential, a parameter which gives information about the net charge of particles or cells in this case in a liquid environment, whereby the value of this parameter is closely related to the surface coating of those particles or cells and the stability of the suspension in which they are [164].

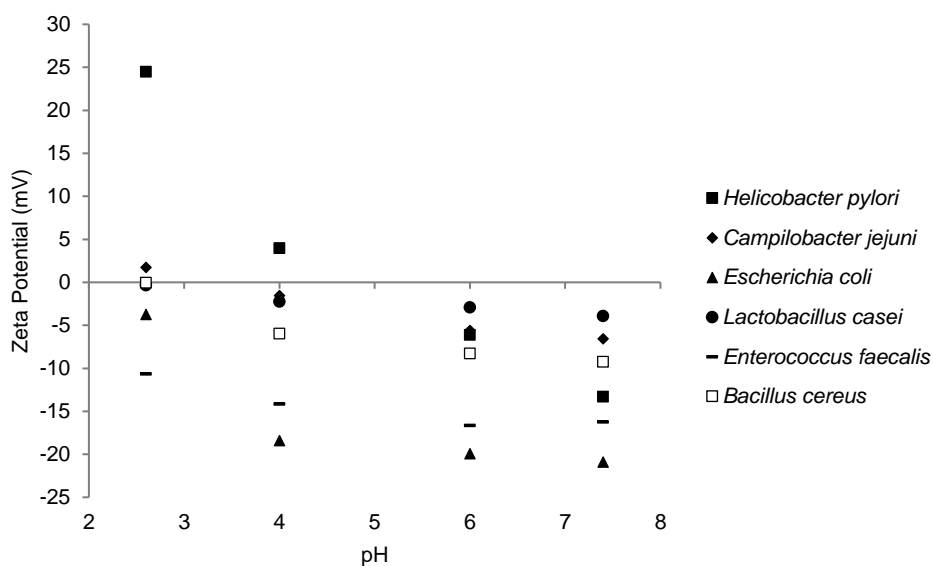
The effect of citrate-phosphate buffer at pH 2.6, 4.0, 6.0 and 7.5 on the surface charge of *H. pylori*, *C. jejuni*, *E. coli*, *L. casei*, *E. faecalis* and *B. cereus* is shown in Figure 4.3, observing a decrease in ZP values with the increase of the pH for all bacteria.

*H. pylori* ZP, after 2 h incubation at pH 2.6 and 4.0 was positive, with ZP values of  $24.5 \pm 1.7$  mV and  $4.0 \pm 0.5$  mV, respectively, while at pH 6.0 and 7.5 the ZP values were negative, with a surface charge of  $-6.1 \pm 0.6$  mV and  $-13.3 \pm 1.1$  mV, in their respective order. *Nogueira F., et al.*, demonstrated a similar behaviour of this bacterium at pH 2.6, 4.0 and 6.0, which seems to be in agreement with the ZP results obtained in the present research work for *H. pylori* [147].

In the case of *C. jejuni*, the ZP values were slightly positive at pH 2.6, with a surface charge of  $1.7 \pm 0.3$  mV and turned negative at pH 4.0, 6.0 and 7.5, with ZP values of  $-1.5 \pm 0.7$  mV,  $-5.6 \pm 0.5$  mV and  $-6.6 \pm 0.5$  mV, respectively.

Regarding *B. cereus*, the ZP was approximately neutral at pH 2.6, with a surface charge of  $0.0 \pm 0.4$  mV and negative at pH 4.0, 6.0 and 7.5, with ZP values of  $-6.0 \pm 1.2$  mV,  $-8.3 \pm 0.3$  mV and  $-9.2 \pm 1.2$  mV, in their respective order.

As for *E. coli*, *L. casei* and *E. faecalis* bacteria, the surface charge was always negative for all tested pHs.



pH	2.6	4.0	6.0	7.5
<i>Helicobacter pylori</i>	24.5 ± 1.7	4.0 ± 0.5	-6.1 ± 0.6	-13.3 ± 1.1
<i>Campilobacter jejuni</i>	1.7 ± 0.3	-1.5 ± 0.7	-5.6 ± 0.5	-6.6 ± 0.5
<i>Escherichia coli</i>	-3.7 ± 2.7	-18.4 ± 1.0	-19.9 ± 1.9	-20.9 ± 0.7
<i>Lactobacillus casei</i>	-0.3 ± 0.3	-2.2 ± 0.4	-2.9 ± 0.3	-3.9 ± 0.6
<i>Enterococcus faecalis</i>	-10.6 ± 0.1	-14.1 ± 0.4	-16.6 ± 0.6	-16.2 ± 1.4
<i>Bacillus cereus</i>	0.0 ± 0.4	-6.0 ± 1.2	-8.3 ± 0.3	-9.2 ± 1.2

**Figure 4.3** *Helicobacter pylori*, *Campilobacter jejuni*, *Escherichia coli*, *Lactobacillus casei*, *Enterococcus faecalis* and *Bacillus cereus* zeta potential under citrate-phosphate buffer at pH 2.6, 4.0, 6.0 and 7.5, determined using Zetasizer Nano ZS (n = 3). The zeta potential values presented are approximate to tenths.

## 4.3 - Characterization of chitosan microspheres

### 4.3.1 - Evaluation of chitosan microspheres size and shape features by ImageStream<sup>X</sup>

Ch MICs were evaluated regarding size and shape, in particular Area, Diameter, Perimeter, Length, Larger Axis, Minor Axis and Aspect Ratio, after 2 h incubation at pH 2.6, 4.0, 6.0 and 7.5 and upon ImageStream<sup>X</sup> analysis in filtered dH<sub>2</sub>O.

#### ▪ Size Features

Size Features as its name indicates allow to determine the size of the Ch MICs from a set of parameters, obtained from the mask applied in the Ch01. In Figure 4.4 the graphs obtained in the

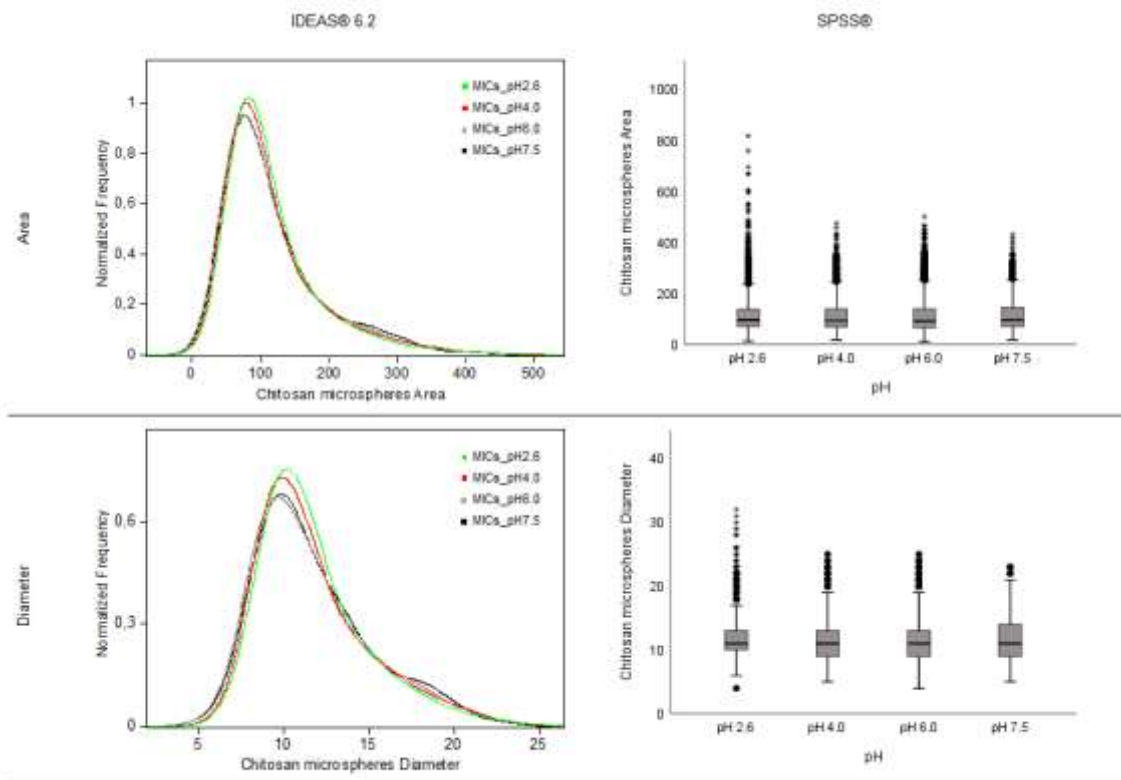
IDEAS 6.2 image analysis software, as well as SPSS, are presented for each size feature evaluated for the characterization of the Ch MICs.

In general, observing the graphs obtained in the IDEAS 6.2 for the different parameters under study, the behaviour of Ch MICs at pH 2.6, 4.0, 6.0 and 7.5 seems to be very similar between the different experimental conditions, although there is some dispersion of the values. This dispersion is not a limiting factor, since the adhesion of the Ch MICs to bacteria should not be influenced by the size differences observed for the evaluated features.

Regarding the statistical analysis of the results in SPSS, were considered statistically significant values for each features at pH 2.6, 4.0, 6.0 and 7.5 with  $p < 0.05$ . The results obtained for the characteristic length between the MICs\_pH4.0 and MICs\_pH6.0 samples in relation to the MICs\_pH7.5 sample were considered statistically significant, with a significant decrease in mean value for length.

Likewise, statistically significant results were also observed for the Minor Axis feature between the MICs\_pH6.0 and MICs\_pH7.5 samples, although the mean value was similar between the different samples. From the MICs\_pH6.0 sample for the MICs\_pH7.5 sample, there was a significant increase in the mean value for Minor Axis.

The outlier (●) and extreme (\*) values in the BoxPlot charts present in Figure 4.15 correspond to feature values between 1.5 and 3 times the interquartile range, where most of the feature values are found, and to feature values 3 times the interquartile range, respectively.



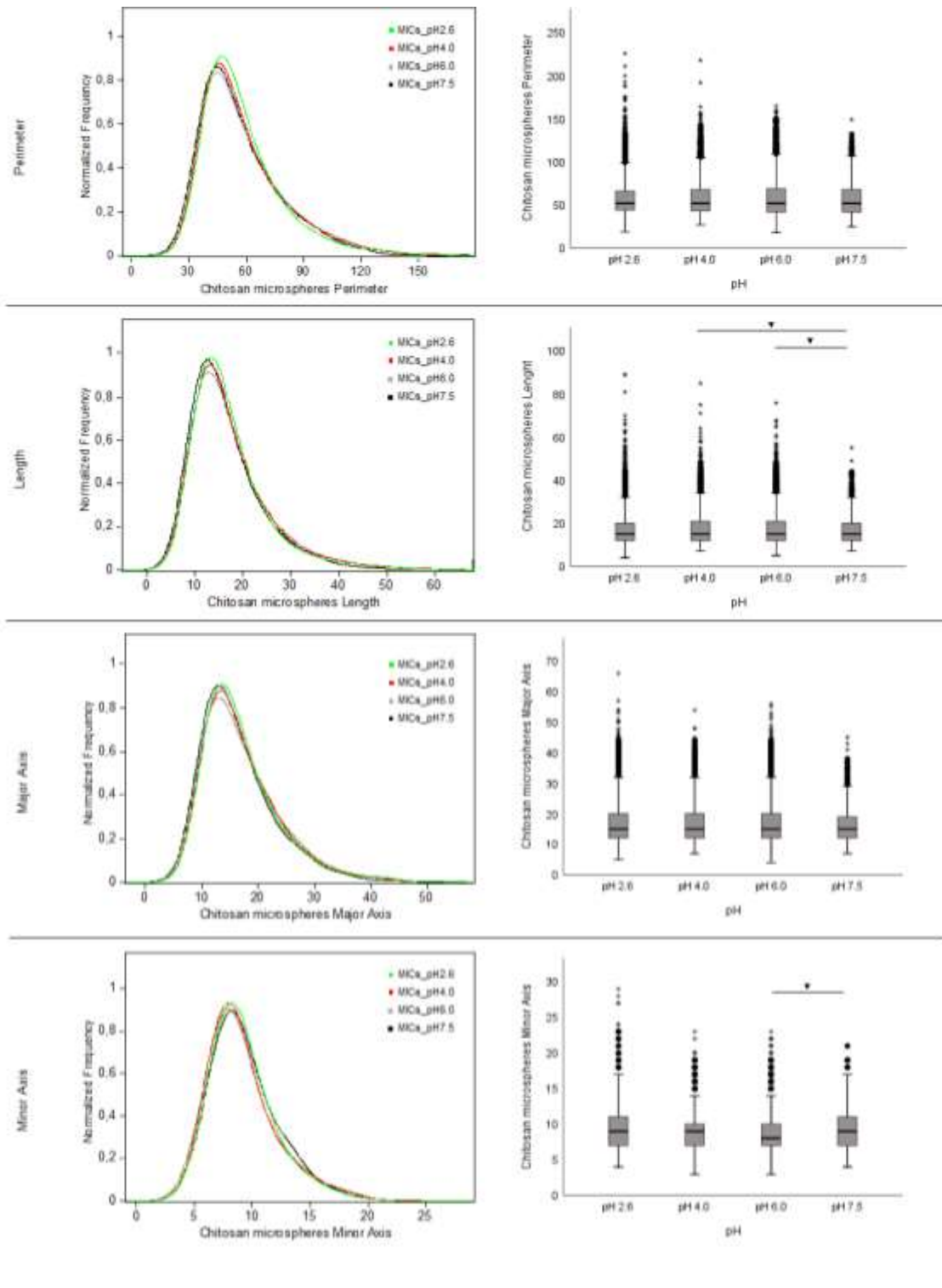


**Figure 4.4** - IDEAS® 6.2 histograms and BoxPlots obtained in SPSS® for the size features, in particular Area, Diameter, Perimeter, Length, Major Axis and Minor Axis. For better observation of the results, the IDEAS® 6.2 graphs obtained have a maximum Histogram Smoothing. In the BoxPlots the outliers (●) and extremes (\*) are present, as well as the statistically significant differences between the samples when  $p < 0.05$  (▼).

The mean and standard deviation values obtained in SPSS for the size features used in the characterization of Ch MICs in ImageStream<sup>x</sup> are represented in Table 4.1. The Ch MICs under analysis had an average diameter of about  $12 \pm 3 \mu\text{m}$ , and an average length of about  $18 \pm 8 \mu\text{m}$ .

**Table 4.1** - Table with the mean and standard deviation values obtained for the size features used in the characterization of the chitosan microspheres after 2 h incubation in citrate-phosphate buffer at pH 2.6, 4.0, 6.0 and 7.5 and upon ImageStream<sup>®</sup> analysis in dH<sub>2</sub>O. The average values presented are approximated to units.

pH		2.6	4.0	6.0	7.5
<b>Area (µm<sup>2</sup>)</b>	Mean	118	117	115	119
	Standard deviation	73	70	71	71
<b>Diameter (µm)</b>	Mean	12	12	12	12
	Standard deviation	3	3	3	3
<b>Perimeter (µm)</b>	Mean	58	59	59	57
	Standard deviation	21	22	22	20
<b>Length (µm)</b>	Mean	18	18	18	17
	Standard deviation	8	8	8	7
<b>Major Axis (µm)</b>	Mean	17	17	17	16
	Standard deviation	7	7	6	6
<b>Minor Axis (µm)</b>	Mean	9	9	9	9
	Standard deviation	3	3	3	3

According to *Gonçalves I.C., et al.*, Ch MICs with a diameter of ~170 µm prepared using Ch with a DA of 16 %, appear to maintain their average size at citrate-phosphate buffer at pH 4.0, 6.0 and 7.4 [140]. However, for more acidic pH values (at pH 2.6 and 1.2), these same microspheres presented higher diameters, practically doubling their size at pH 1.2. *Henriques P.C., et al.*, also demonstrated that Ch MICs produced using Ch with a DA of 6 %, increase in size at pH 1.2 [165].

Although the incubation conditions were the same as those previously described in *Gonçalves I.C., et al.*, in the herein presented research work Ch MICs were washed in filtered dH<sub>2</sub>O to follow the same experimental conditions as the samples containing chitosan microspheres and bacteria for the adhesion tests [140]. These results may be indicative that Ch MICs, after incubation in citrate-phosphate buffer at different pHs, are able to reacquire their normal average size, when transferred to filtered dH<sub>2</sub>O. However, it was possible to observe that the sample at more acidic pH (MICs\_pH2.6) reached higher values for the different size features tested, which seems to be in agreement with the data demonstrated in *Gonçalves I.C., et al.* and *Henriques P.C., et al.* [140], [165].

### ▪ Shape Feature

The shape feature Aspect Ratio allows the analysis of the shape of the Ch MICs from the shape of the mask used for these microparticles in the Ch01. In Figure 4.5, the graph obtained in the IDEAS 6.2 image analysis software, as well as in SPSS is shown for the characterization of the Ch MICs shape.

As discussed in 3.6.2.2.2, the Aspect Ratio feature from the values obtained for the major and minor axes of the chitosan microspheres allows us to evaluate whether a Ch MICs is more or less round. Values close to 1 correspond to a more circular shape of the microparticles, while Aspect Ratio values less than 1 correspond to a more oblong form of these ones (Figure 4.5).

By the interpretation of the graph obtained in IDEAS 6.2 for this parameter, the Aspect Ratio of the Ch MICs for the different samples under study seems to be similar among the different samples, with mean values for this feature around 0.6-0.7 (Table 4.2). These values are indicative of a more round shape of the Ch MICs, as can be seen from the image shown in Figure 4.5.

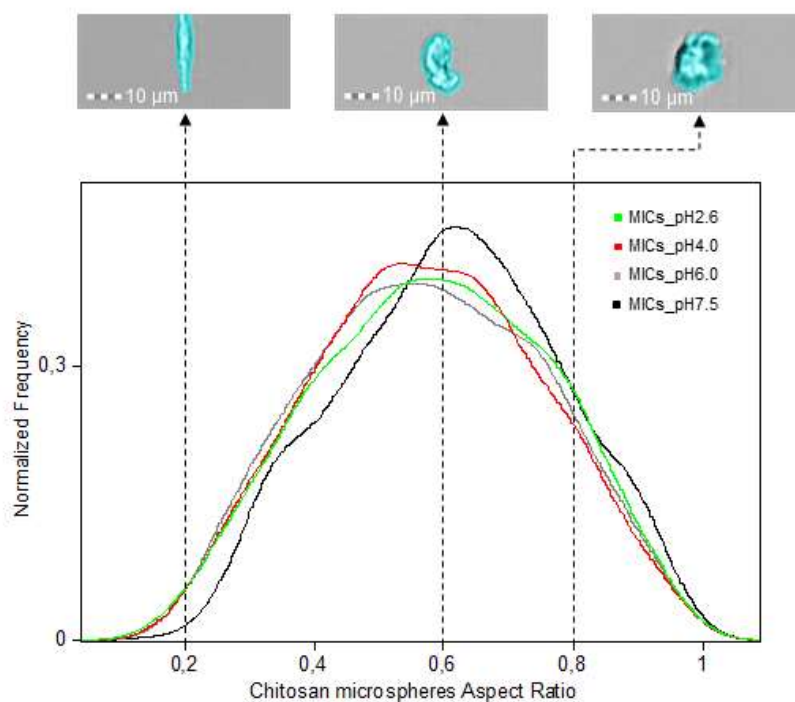


**Figure 4.5** - IDEAS® 6.2 histogram for the shape feature Aspect Ratio and examples of chitosan microspheres images for different shape values. For a better analysis of the obtained results, the histogram has a maximum Histogram Smoothing.

A statistically significant increase of the Aspect Ratio was verified for MICs\_pH7.5 sample comparing to all other samples, and for MICs\_pH2.6 sample comparing to MICs\_pH6.0 samples and.

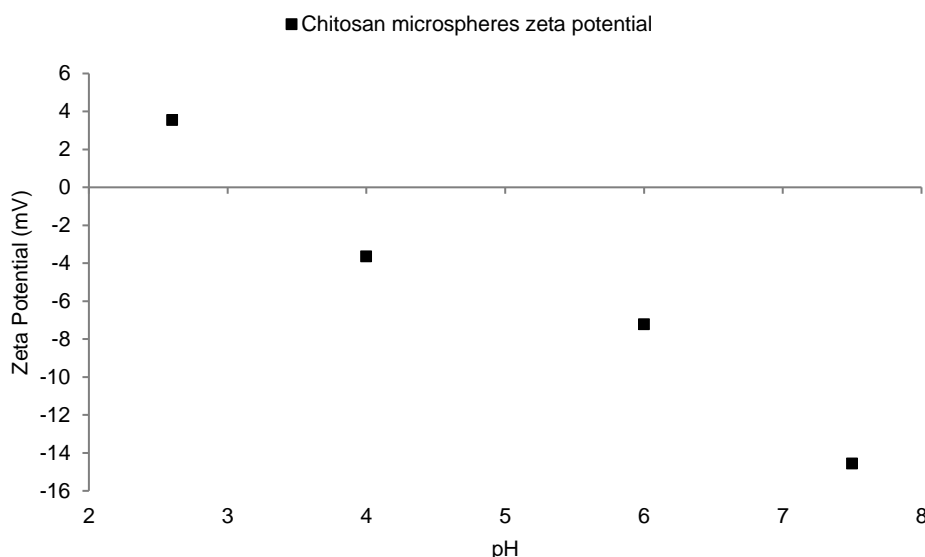
**Table 4.2** - Table with the mean and standard deviation values obtained for the shape feature used in the characterization of the chitosan microspheres for the samples at pH 2.6, 4.0, 6.0 and 7.5. The average values presented are approximated to tenths.

pH		2.6	4.0	6.0	7.5
<b>Aspect Ratio (Arbitrary units)</b>	Mean	0.7	0.7	0.6	0.7
	Standard deviation	0.5	0.5	0.5	0.4

In general, the Ch MICs used in the present research project showed an intermediate Aspect Ratio around 0.6-0.7, which means that these microparticles have a more round shape (Aspect Ratio close to 1).

#### 4.3.2 - Chitosan microspheres Zeta Potential

The ZP of these Ch MICs were evaluated after incubation with citrate-phosphate buffer at different pHs, under the same experimental conditions as the adhesion assays. In Figure 4.6 is represented the ZP variation for Ch MICs prepared using Ch with a DA of 6 %.



pH	2.6	4.0	6.0	7.5
<b>Zeta Potential (mV)</b>	3.5 ± 2.5	-3.6 ± 1.0	-7.2 ± 1.1	-14.6 ± 1.7

**Figure 4.6** - Chitosan microspheres zeta potential under citrate-phosphate buffer at pH 2.6, 4.0, 6.0 and 7.5 with the correspondent standard deviation, determined using EKA (n = 6). The zeta potential values presented are approximate to tenths.

At pH 2.6 and, therefore under acidic conditions, the Ch MICs are positively charged ( $3.5 \pm 2.5$  mV), as expected, due to the protonation of the remaining primary amines of Ch MICs.

Furthermore, a decrease in ZP values with the increase of the pH was also observed, from  $3.5 \pm 2.5$  mV at pH 2.6 to  $-14.6 \pm 1.7$  mV at pH 7.5. The ZP values for Ch MICs at pH 4.0, 6.0 and



7.5 were negative,  $-3.6 \pm 1.0$  mV,  $-7.2 \pm 1.1$  mV and  $-14.6 \pm 1.7$  mV, respectively, which means that at these pH values, the Ch MICs are negatively charged on its surface.

*Fernandes M., et al.*, demonstrated that the ZP of Ch MICs with a diameter of  $\sim 170$   $\mu\text{m}$  and prepared using Ch with a DA of 16 %, crosslinked for 0.5, 1 and 2 h with 10 mM of genipin, presented positive ZP values close to the neutral at pH 3.6 and negative values at pH 5.6 [146].

Although these Ch MICs were prepared using Ch with a different DA (6 %) from the microspheres described by *Fernandes M., et al.*, and a 45 min crosslinking time with genipin, they follow the same trend of ZP values.

## 4.4 - Chitosan microspheres adhesion to bacteria from human gastrointestinal microbiota

The main objective initially proposed for the present investigation focused on the evaluation of the interaction of Ch MICs with bacteria of the human GI microbiota at different pHs found in the different portions of the human stomach and intestine.

Thus, the interaction of these Ch MICs with the bacterial species *H. pylori*, *C. jejuni*, *E. coli*, *L. casei*, *E. faecalis* and *B. cereus*, in citrate-phosphate buffer at pH 2.6, 4.0, 6.0 and 7.5 was tested for 2 h at 37 °C and 120 rpm.

### 4.4.1 - Adhesion assay

Adhesion of the Ch MICs to bacteria of the GI microbiota was performed at 37 °C for 2 h and at 120 rpm of lateral stirring in citrate-phosphate buffer at pH 2.6, 4.0, 6.0 and 7.5, respectively, in order to mimic the pH conditions verified in human gastric and intestinal fluids.

The adhesion of the Ch MICs to different bacteria was observed in the INSPIRE software of the ImageStream<sup>x</sup>, through the laser 488 nm with a minimum laser power of 10.0 mW and with a magnification of 40x and evaluated later from the IDEAS 6.2 software associated to this flow cytometer.

In order to evaluate the number of bacteria adhered in each of the experimental conditions under study, the fluorescence intensity in Ch02 was used, where the bacteria labelled with the fluorescent dye SYTO9 were detected. The intensity in Ch02 in the IDEAS 6.2 corresponds to the sum of the intensities of each pixel, calculated in the area indicated as being a Ch MICs by the brightfield channel what are bacteria. Thus, a greater fluorescence intensity in Ch02 should correspond to a greater amount of bacteria adhered to the Ch MICs.

The labelling of the bacteria with SYTO9 has been optimized so that the intensity of this dye does not vary according to the pH of the buffer, so that a higher intensity in Ch02 should correspond to a larger amount of adhered bacteria.

By analysing the images obtained in samples containing only Ch MICs (MICs<sub>0</sub>), it was generally observed that these microparticles had a higher intensity of fluorescence in Ch05, so this channel was chosen for visualization of these microparticles from here on.

As mentioned in 3.6.2.2 to analyse the images it was applied to each one a corresponding compensation matrix in order to remove as much as possible the autofluorescence of Ch MICs in Ch02, which is the channel that it intended to detect only bacteria.

In Figure 4.7 examples of images obtained in IDEAS 6.2 for an assay of *H. pylori* adhesion to Ch MICs with and without compensation matrix, 'Comp' and 'noComp', respectively, in Ch02 are

shown samples containing Ch MICs and bacteria (MICs\_ *H. pylori*) and samples containing only Ch MICs (MICs\_).

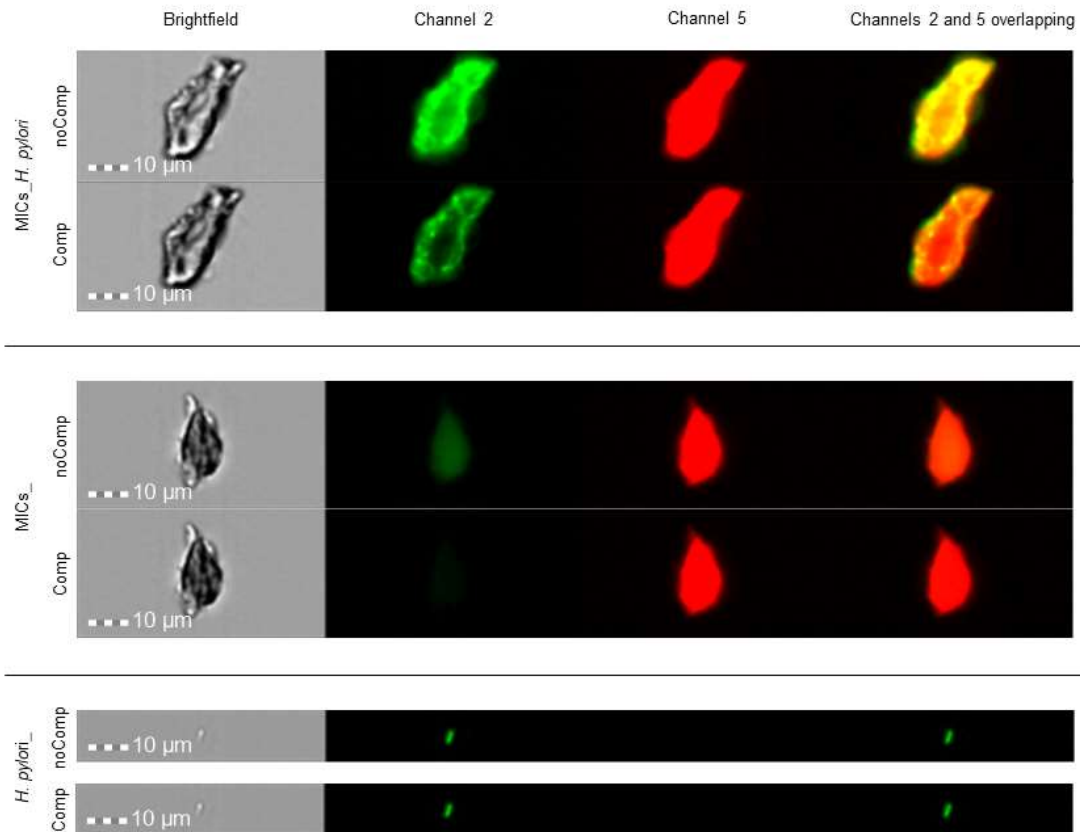


**Figure 4.7** - Example of ImageStream®X images of *Helicobacter pylori* J99 adhesion assay to chitosan microspheres at pH 6.0 (MICs\_ *H. pylori*) and the corresponding controls, only with microspheres (MICs\_) or bacteria (*H. pylori*\_), with and without compensation matrix ('Comp', 'noComp'). All the samples were labelled with SYTO9 0.015 µM. Scale bar corresponds to 10 µm.

Although the compensation matrix applied is not perfect and could leave some fluorescence from the Ch MICs to Ch02, the quantification of bacterial adhesion from the images for which compensation matrix was applied will be closer to the actual intensity value, only if bacteria were observed in this channel. The fact that the removal of as much fluorescence as possible from the microspheres in Ch02 will cause less intensity to be quantified in this channel corresponding to the microparticles and mostly corresponding to the adhered bacteria labelled with SYTO9.

The system does not allow to quantitatively determine the number of bacteria adhered to the Ch MICs at each citrate-phosphate buffer. For example, regions of high bacterial adhesion to microspheres, even with bacterial aggregates, especially bacteria overlapping with each other, the system does not have the ability to individualize them and, as such, the results may not correspond to the actual number of bacteria adhered to Ch MICs.

Thus, by analysing the fluorescence intensity in Ch02 for each sample, it should be possible to correlate a higher intensity to a larger number of bacteria adhered, but not to quantify the number itself.

Some preliminary studies described in Annex A.1.1 were also performed aiming to evaluate if the bacteria adhered to the Ch MIC were live or dead. However, among the fluorescent dyes capable of labelling dead bacteria, it was not possible in the experiments carried out in the

ImageStream<sup>X</sup> and Spectral Confocal Microscope TCS-SP5 AOBS (Acoust Optical Bream Splitter) to select a fluorochrome that had the required characteristics and presented an emission spectrum not overlaid with the emission spectrum of the Ch MICs.

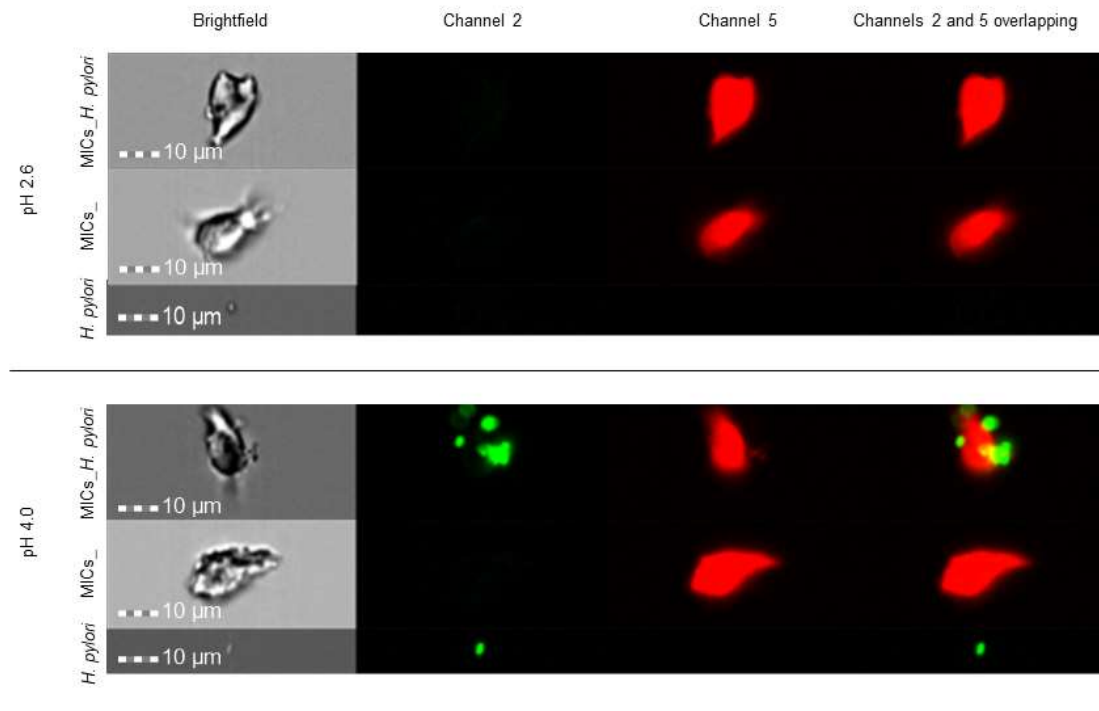
#### 4.4.1.1 - Chitosan microspheres adhesion to *Helicobacter pylori*

In Figure 4.8 are represented images of *H. pylori* adherent to Ch MICs (MICs\_*H. pylori*) at the different citrate-phosphate buffers tested (pH 2.6, 4.0, 6.0 e 7.5), in Ch02 and in the column corresponding to the overlay of channels 2 and 5 of the IDEAS 6.2 image analysis software, as well as the respective controls (MICs\_ and *H. pylori*) labelled with 0.015  $\mu$ M of SYTO9. In this image it is also visible only the Ch MICs in Ch05.

By observing the images obtained for MICs\_*H. pylori* samples it is apparent that these microparticles appear to adhere to this bacterium in citrate-phosphate buffers at pH 4.0, 6.0 and 7.5, since in Ch02 there is observed green fluorescent staining that is not visible in the controls containing only Ch MICs (MICs\_).

These data confirm what is described in the literature regarding the capacity of Ch MICs of  $\sim$ 170  $\mu$ m and prepared using Ch with a DA of 16 % adhering to *H. pylori* in citrate-phosphate buffer at pH 2.6, 4.0 and 6.0. In *Gonçalves I.C., et al.* the evaluation of Ch MICs adhesion to different strains of *H. pylori* was performed using bacteria previously fixed with fluorescein isothianate (FITC) [140].

Although in the present assay data there was not detected bacteria at pH 2.6, it may be related to the fact that at this pH the bacteria would eventually die, causing damage to the DNA molecule, which could hinder the binding of SYTO9 to the nucleic acids of the bacteria. Incorrect binding of SYTO9 to these molecules may not allow detection of the bacteria by the non-emission of fluorescence [166], [167].



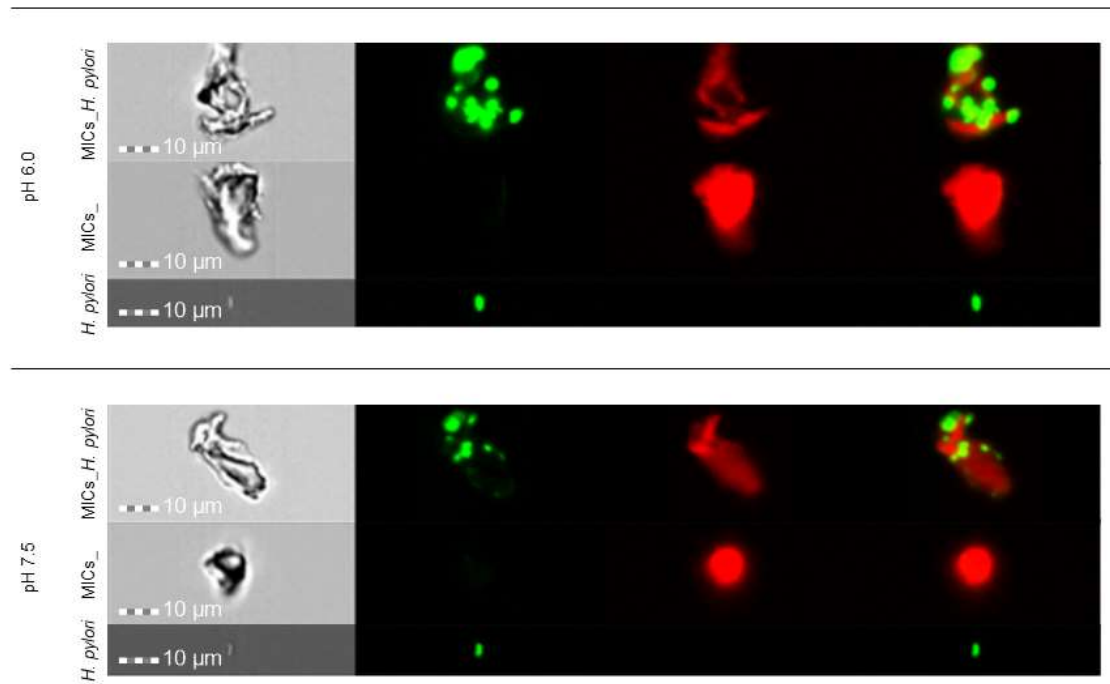


**Figure 4.8** - ImageStream®X images of *Helicobacter pylori* adhesion assay to chitosan microspheres (MICs\_ *H. pylori*) at pH 2.6, 4.0, 6.0 and 7.5, and the correspondent controls (MICs\_ and *H. pylori*). All samples were labelled with 0.015 µM of SYTO9. Scale bar corresponds to 10 µm.

The graphs in Figure 4.9 correspond to the fluorescence intensity in Ch02graphs obtained in the IDEAS 6.2 software for the MICs\_ *H. pylori* and MICs\_ samples.

Comparing the intensity graphs in Ch02 for MICs\_ *H. pylori* and MICs\_ samples, it is possible to observe that samples showing bacterial adhesion to Ch MICs have higher intensity values than samples containing only microspheres (MICs\_), confirming bacterial adhesion at pH 4.0, 6.0 and 7.5. In the case of the MICs\_ *H. pylori*\_pH2.6 sample, since no bacterial adhesion was observed at this pH, it presents intensity values similar to the intensity values for this channel in the MICs\_ samples. However, as in *H. pylori*\_pH2.6 control was not observed bacteria, no conclusions can be drawn about MICs\_ *H. pylori*\_pH2.6 sample.

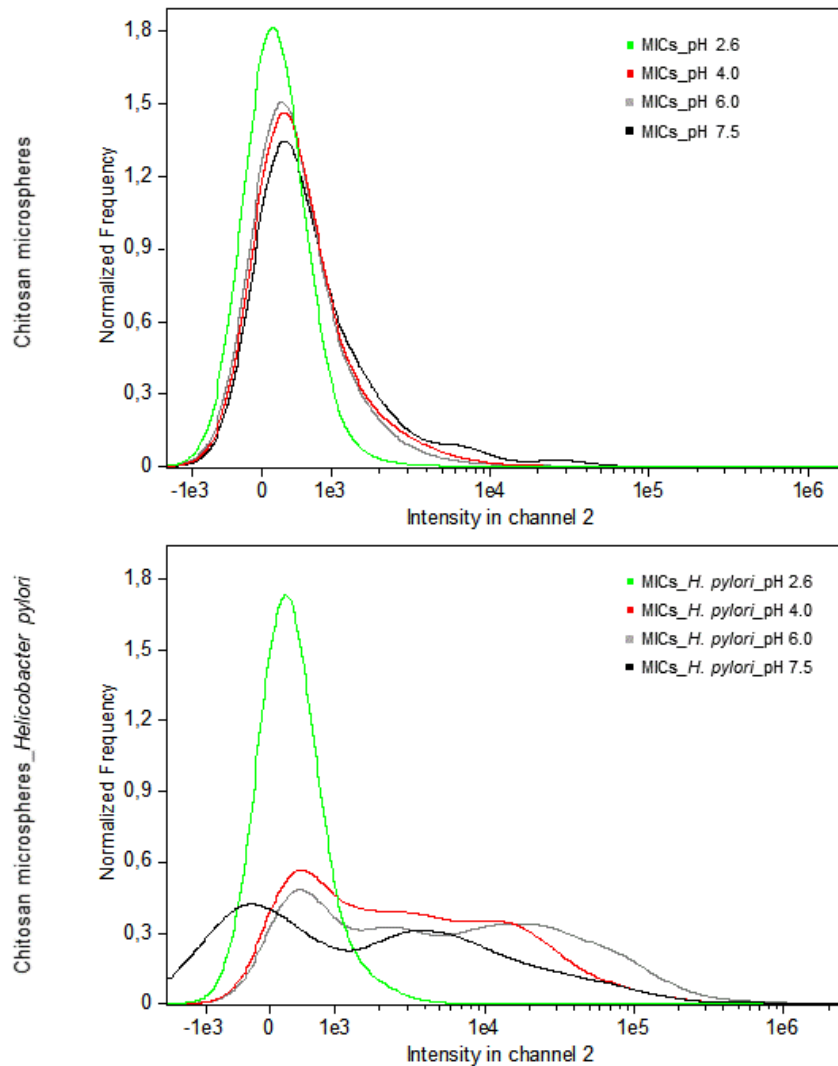


**Figure 4.9** - IDEAS® 6.2 histograms for the intensity in channel 2 for the samples MICs\_*H. pylori* and MICs\_ at pH 2.6, 4.0, 6.0 and 7.5. For a better analyse of the obtained results, the histograms obtained has a maximum Histogram Smoothing.

The fact that the samples showing bacterial adhesion (MICs\_*H. pylori*) at pH 4.0, 6.0 and 7.5, with higher values of fluorescence intensity in Ch02, had some intensity values close to the MICs\_ samples mean that *H. pylori* adhesion did not occur to all Ch MICs in the different samples. Therefore, it is important to note that these samples show a large dispersion of results, related to the fact that within the same sample MICs\_*H. pylori*, both Ch MICs with *H. pylori* adhesion to their surface and Ch MICs without bacterial adhesion were observed.

According to the mean values obtained in SPSS for the fluorescence intensity in Ch02 for MICs\_*H. pylori* samples, in each experimental conditions under study (citrate-phosphate buffer pH 2.6, 4.0, 6.0, and 7.5), this bacterium appears to preferentially adhere to the Ch MICs at pH 6.0 with an average intensity value of about 23100, followed by the samples at pH7.5 and 4.0, with average intensity values of about 11827 and 10325, respectively (Table 4.3).

**Table 4.3** - Table with the mean and standard deviation values, of the fluorescence intensity in channel 2, obtained on SPSS® for each of the samples containing chitosan microspheres and *Helicobacter pylori* labelled with SYTO9. The average values presented are approximate to the unit.

pH		2.6	4.0	6.0	7.5
Intensity in channel 2 (Arbitrary units)	Mean	327	10325	23100	11827
	Standard deviation	367	22832	53871	34148

By the analysis of the results obtained after statistical analysis in the SPSS, based on the significant differences between the mean values for the MICs\_ *H. pylori* samples (Figure 4.10), there were statistically significant differences between some samples, with adhesion at pH 6.0 having the highest fluorescence intensity in Ch02, followed by pH 7.5, 4.0 and 2.6.

The outlier (●) and extreme (\*) values in the BoxPlot charts present in Figure 4.10 correspond to intensity values between 1.5 and 3 times the interquartile range, where most of the intensity values are found, and to intensity values 3 times the interquartile range, respectively.

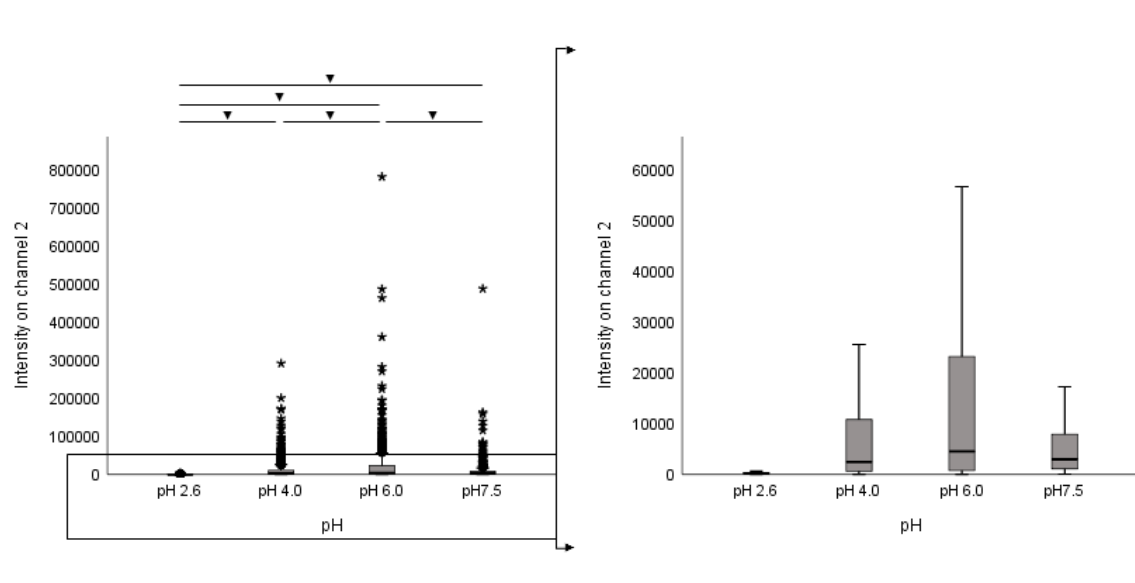


**Figure 4.10** - BoxPlot of the intensity on channel 2 for the samples MICs\_ *H. pylori*. Statistically significant differences between samples when  $p < 0.05$  (▼). The graph on the right is a zoom-in excluding outliers (●) and extremes (\*), in order to better understand the main behaviour between the different samples.

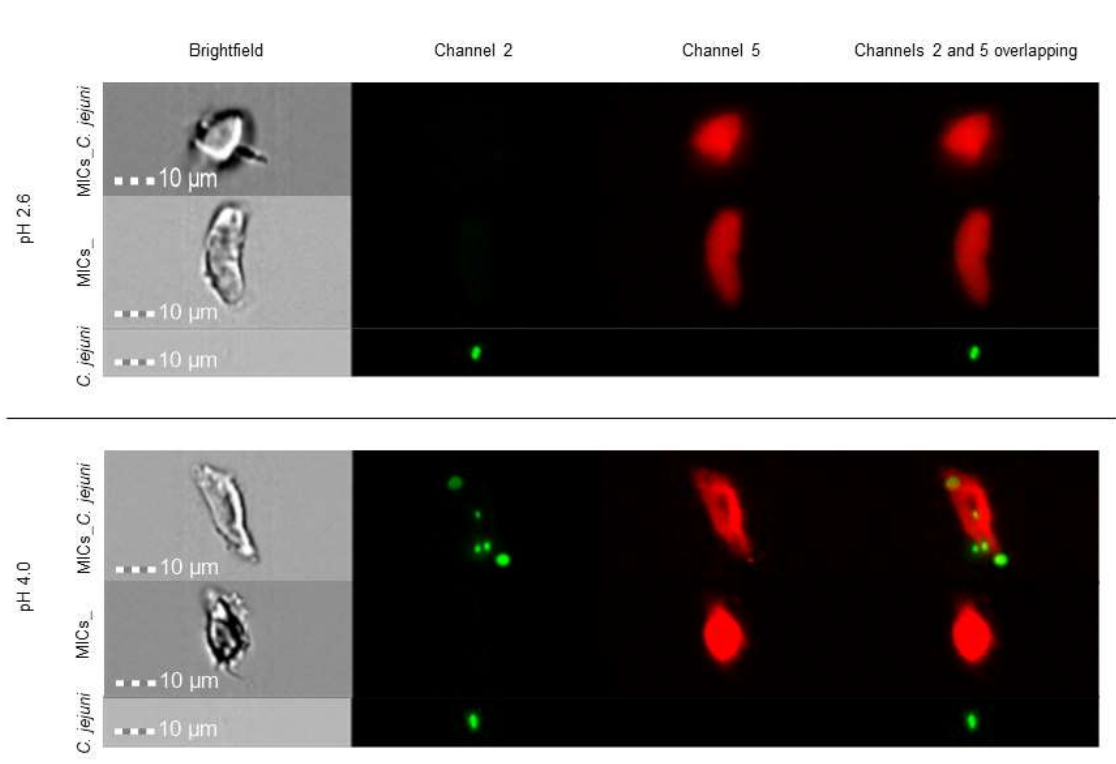
#### 4.4.1.2 - Chitosan microspheres adhesion to *Campilobacter jejuni*

In Figure 4.11 are represented images of *C. jejuni* adherent to the Ch MICs (MICs\_ *C. jejuni*) at the different citrate-phosphate buffers tested (pH 2.6, 4.0, 6.0 e 7.5), in Ch02 and in the column corresponding to the overlay of channels 2 and 5 of the IDEAS 6.2 image analysis software, as well as the respective controls (MICs\_ e *C. jejuni*) labelled with 0.015 $\mu$ M of SYTO9. In this image it is also visible only the Ch MICs in Ch05.

By observing the images obtained for MICs\_ *C. jejuni* samples it is apparent that these microspheres appear to adhere to this bacterium at pH 4.0, 6.0 and 7.5, since in Ch02 there is

observed green fluorescent staining that is not visible in the controls containing only Ch MICs (MICs<sub>-</sub>).

In the data from the present assay there was no bacterial adhesion at pH 2.6, although bacteria labelled with SYTO9 were observed in the control sample (*C. jejuni*), suggesting that at this pH this species does not appear to adhere to these Ch MICs.



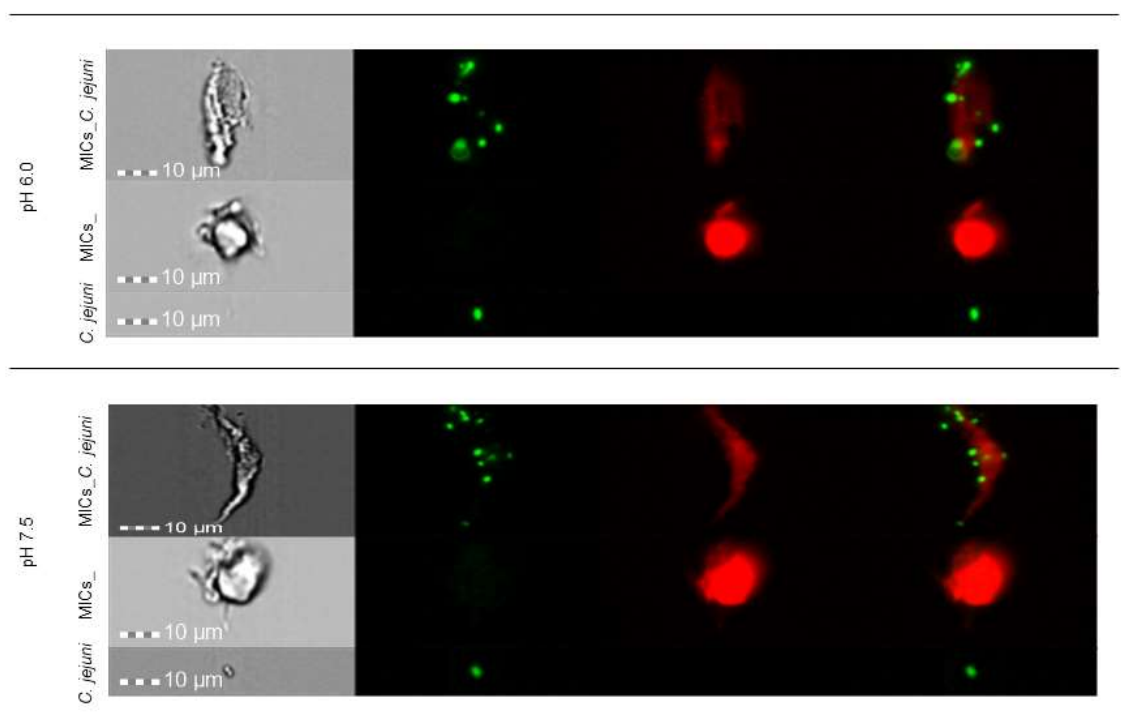


**Figure 4.11** - ImageStream®X images of *Campilobacter jejuni* adhesion assay to chitosan microspheres (MICs\_ *C. jejuni*) at pH 2.6, 4.0, 6.0 and 7.5, and the correspondent controls (MICs\_ and *C. jejuni*). All samples were labelled with 0.015 µM of SYTO9. Scale bar corresponds to 10 µm.

The graphs in Figure 4.12 correspond to the fluorescence intensity in Ch02 graphs obtained in the IDEAS 6.2 software for the MICs\_ *C. jejuni* and MICs\_ samples.

Comparing the intensity graphs in Ch02 for MICs\_ *C. jejuni* and MICs\_ samples, it is possible to observe that samples showing bacterial adhesion to Ch MICs have higher intensity values than samples containing only microspheres (MICs\_), confirming bacterial adhesion at pH 4.0, 6.0 and 7.5. In the case of the MICs\_ *C. jejuni*\_pH2.6 sample, since no bacterial adhesion was observed at this pH, it presents intensity values similar to the intensity values for this channel in the MICs\_ samples.

The fact that the samples showing bacterial adhesion (MICs\_ *C. jejuni*) at pH 4.0, 6.0 and 7.5, with higher values of fluorescence intensity in Ch02, had some intensity values close to the MICs\_ samples mean that *C. jejuni* adhesion did not occur to all Ch MICs in the different samples. Therefore, It is important to note that these samples show a large dispersion of results, related to the fact that within the same sample MICs\_ *C. jejuni*, both Ch MICs with *C. jejuni* adhesion to their surface and Ch MICs without bacterial adhesion were observed.



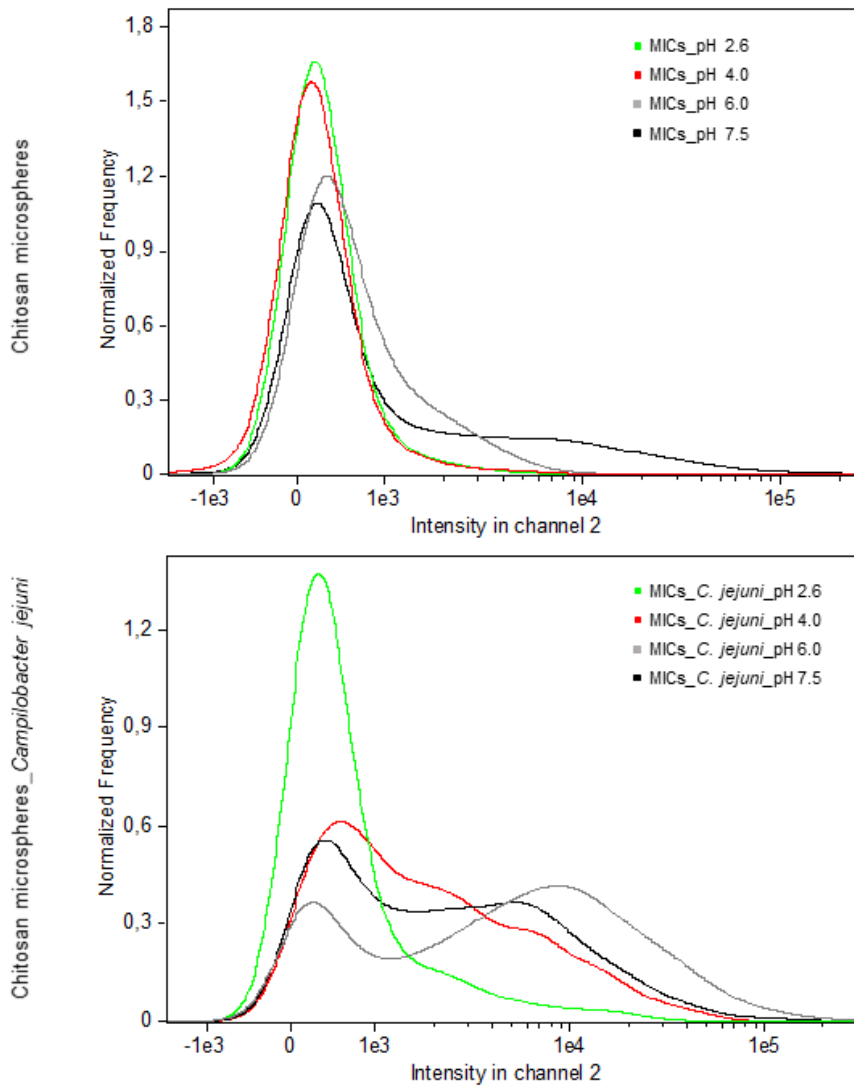


**Figure 4.12** - IDEAS® 6.2 histograms for the intensity in channel 2 for the samples MICs\_*C. jejuni* and MICs\_ at pH 2.6, 4.0, 6.0 and 7.5. For a better analyse of the obtained results, the histograms obtained has a maximum Histogram Smoothing.

According to the mean values obtained in SPSS for the intensity of fluorescence in Ch02 for MICs\_*C. jejuni* samples, in each experimental condition (citrate-phosphate buffer at pH 2.6, 4.0, 6.0, and 7.5), this bacterium appears to preferentially adhere to the Ch MICs at pH 6.0 with an average intensity value of about 11396, followed by pH7.5 and 4.0, with average intensity values of about 5416 and 3850, respectively (Table 4.4).

**Table 4.4** - Table with the mean and standard deviation maximum values, of the fluorescence intensity in channel 2, obtained on SPSS® for each of the samples containing chitosan microspheres and *Campilobacter jejuni* labelled with SYTO9. The average values presented are approximate to the unit.

pH		2.6	4.0	6.0	7.5
Intensity in channel 2 (Arbitrary units)	Mean	1116	3850	11396	5416
	Standard deviation	3111	6345	19567	10870

By the analysis of the results obtained after statistical analysis in the SPSS, based on the significant differences between the mean values for the MICs\_ *C. jejuni* samples (Figure 4.13), there were statistically significant differences between all samples, with adhesion at pH 6.0 having the highest fluorescence intensity in Ch02, followed by pH 7.5, 4.0 and 2.6.

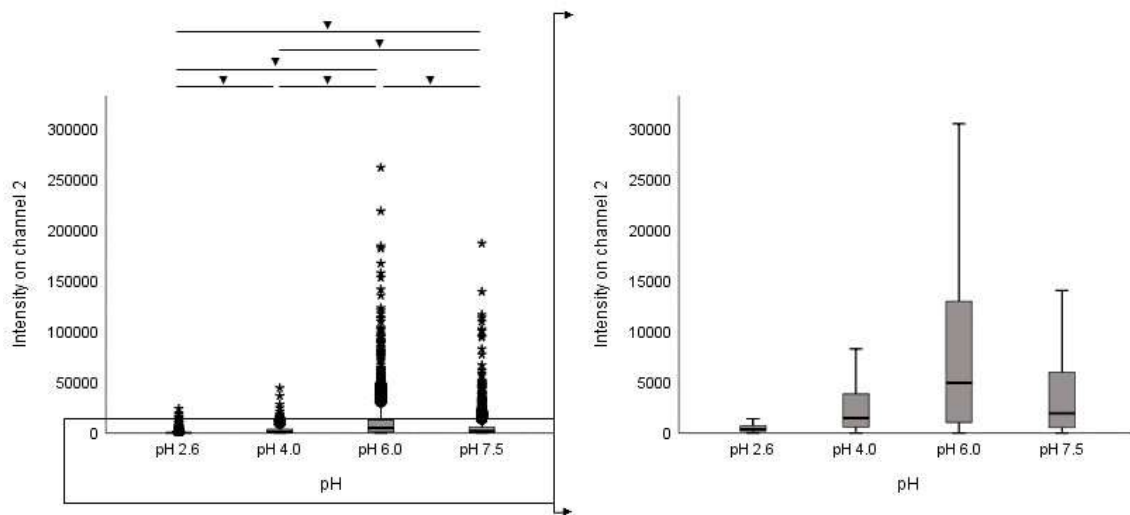


**Figure 4.13** - BoxPlot of the intensity on channel 2 for the samples MICs\_ *C. jejuni*. Statistically significant differences between samples when  $p < 0.05$  (▼). The graph on the right is a zoom-in excluding outliers (●) and extremes (\*), in order to better understand the behaviour between the different samples.

#### 4.4.1.3 - Chitosan microspheres adhesion to *Escherichia coli*

In Figure 4.14 are represented images of *E. coli* adherent to Ch MICs (MICs\_ *E. coli*) at the different citrate-phosphate buffers tested (pH 2.6, 4.0, 6.0 e 7.5), in Ch02 and in the column corresponding to the overlay of channels 2 and 5 of the IDEAS 6.2 image analysis software, as well as the respective controls (MICs\_ *e. coli*), labelled with 0.015 $\mu$ M of SYTO9. In this image it is also visible only the Ch MICs in Ch05.

By observing the images obtained for MICs\_ *E. coli* samples it is apparent that these microspheres appear to adhere to this bacterium in pH 4.0, 6.0 and 7.5, since in Ch02 there is observed green fluorescent staining that is not visible in the controls containing only Ch MICs (MICs\_).

In the data from the present assay there was no bacterial adhesion at pH 2.6, although bacteria labelled with SYTO9 were observed in the control sample (*E. coli*), suggesting that at this pH this species does not appear to adhere to these Ch MICs.

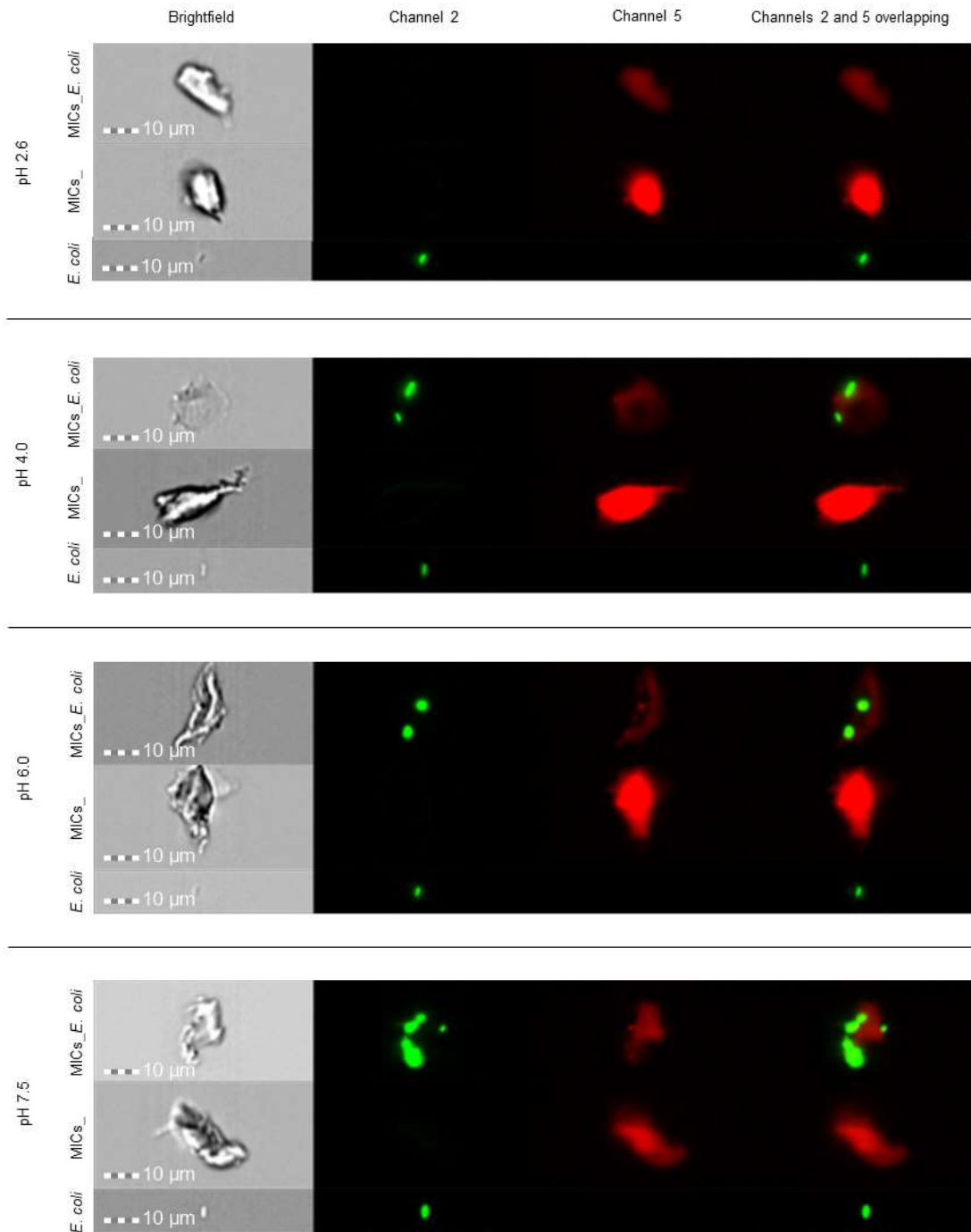


**Figure 4.14** - ImageStream®x images of *Escherichia coli* adhesion assay to chitosan microspheres (MICs\_ *E. coli*) at pH 2.6, 4.0, 6.0 and 7.5, and the correspondent controls (MICs\_ and *E. coli*). All samples were labelled with 0.015 µM of SYTO9. Scale bar corresponds to 10 µm.

The graphs in Figure 4.15 correspond to the fluorescence intensity in Ch02 graphs obtained in the IDEAS 6.2 software for the MICs\_ *E. coli* and MICs\_ samples.

Comparing the intensity graphs in Ch02 for MICs\_*E. coli* and MICs\_ samples, it is possible to observe that samples showing bacterial adhesion to Ch MICs have higher intensity values than samples containing only microspheres (MICs\_), confirming bacterial adhesion at pH 4.0, 6.0 and 7.5. In the case of the MICs\_*E. coli*\_pH2.6 sample, since no bacterial adhesion was observed at this pH, it presents intensity values similar to the intensity values for this channel in the MICs\_ samples.

The fact that the samples showing bacterial adhesion (MICs\_*E. coli*) at pH 4.0, 6.0 and 7.5, with higher values of fluorescence intensity in Ch02, had some intensity values close to the MICs\_ samples means that *E. coli* adhesion did not occur to all Ch MICs in the different samples. Therefore, it is important to note that these samples show a large dispersion of results, related to the fact that within the same sample MICs\_*E. coli*, both Ch MICs with *E. coli* adhesion to their surface and Ch MICs without bacterial adhesion were observed.

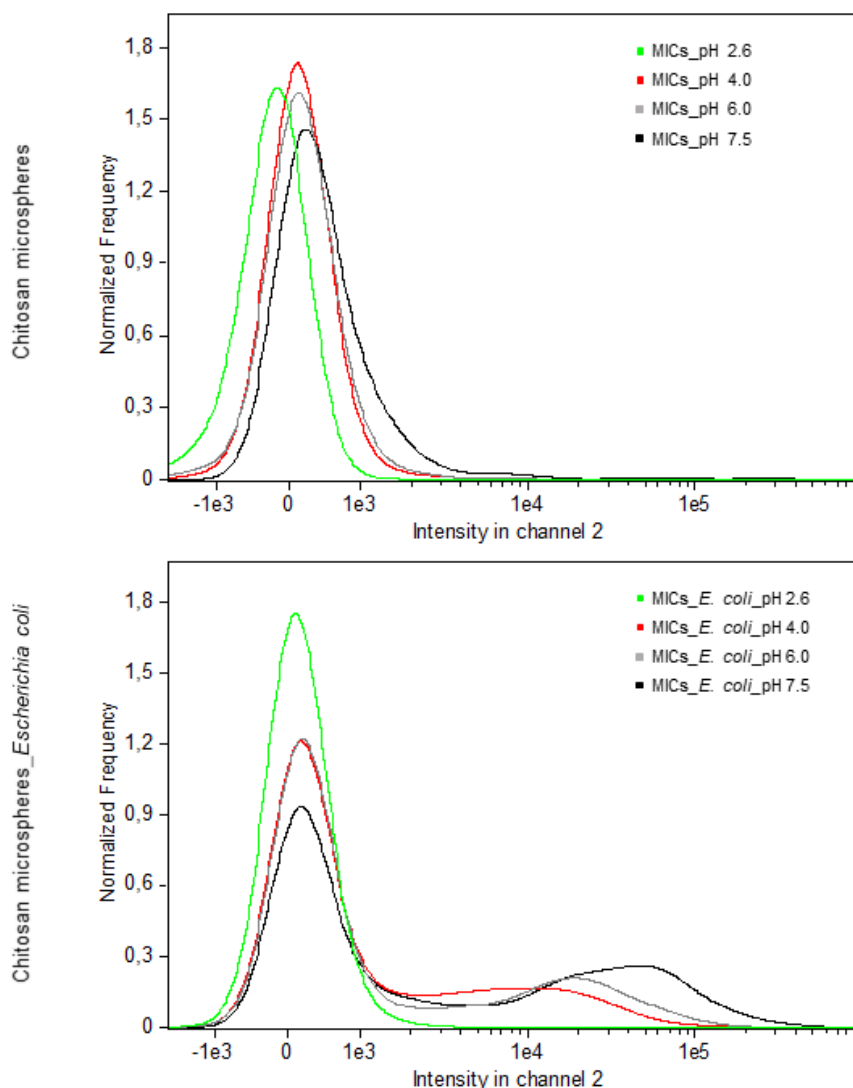


**Figure 4.15** - IDEAS® 6.2 histograms for the intensity in channel 2 for the samples MICs\_*E. coli* and MICs\_ at pH 2.6, 4.0, 6.0 and 7.5. For a better analyse of the obtained results, the histograms obtained has a maximum Histogram Smoothing.

According to the mean values obtained in SPSS for the intensity of fluorescence in Ch02 for MICs\_ *E. coli* samples, in each experimental condition (citrate-phosphate buffer at pH 2.6, 4.0, 6.0, and 7.5), this bacterium appears to preferentially adhere to the Ch MICs at pH 7.5, with an average intensity value of about 18722, followed by pH 6.0 and 4.0, with average intensity values of about 6310 and 3785, respectively (Table 4.5).

**Table 4.5** - Table with the mean and standard deviation values, of the fluorescence intensity in channel 2, obtained on SPSS® for each of the samples containing chitosan microspheres and *Escherichia coli* labelled with SYTO9. The average values presented are approximate to the unit.

pH		2.6	4.0	6.0	7.5
Intensity in channel 2 (Arbitrary units)	Mean	159	3785	6310	18722
	Standard deviation	417	10173	15150	39633

By the analysis of the results obtained after statistical analysis in the SPSS, based on the significant differences between the mean values for the MICs\_ *E. coli* samples (Figure 4.16), there were statistically significant differences between all samples, with adhesion at pH 7.5 having the highest fluorescence intensity in Ch02, followed by pH 6.0, 4.0 and 2.6.

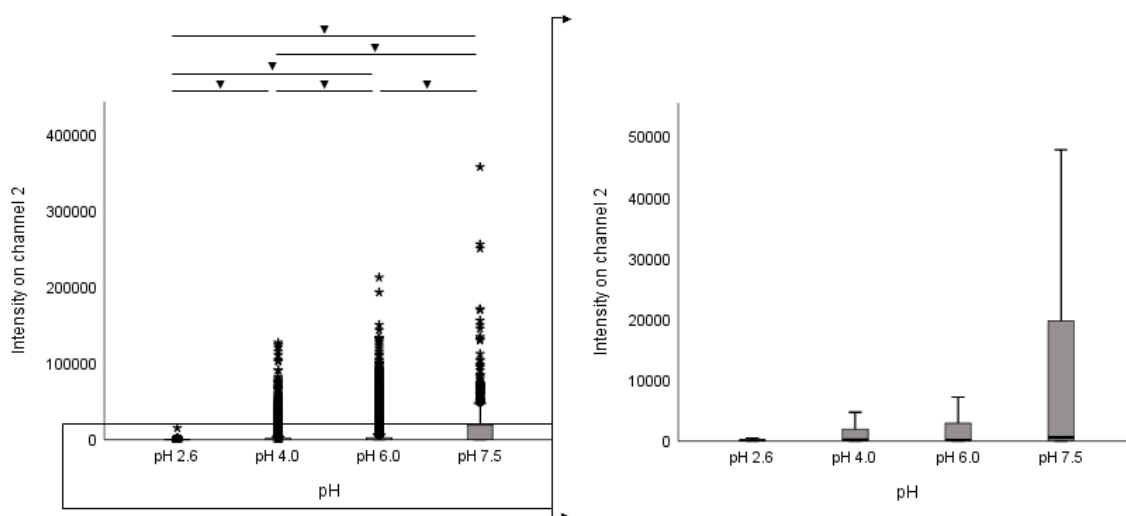


**Figure 4.16** - BoxPlot of the intensity on channel 2 for the samples MICs\_ *E. coli*. Statistically significant differences between samples when  $p < 0.05$  (▼). The graph on the right is a zoom-in excluding outliers (●) and extremes (\*), in order to better understand the behaviour between the different samples.

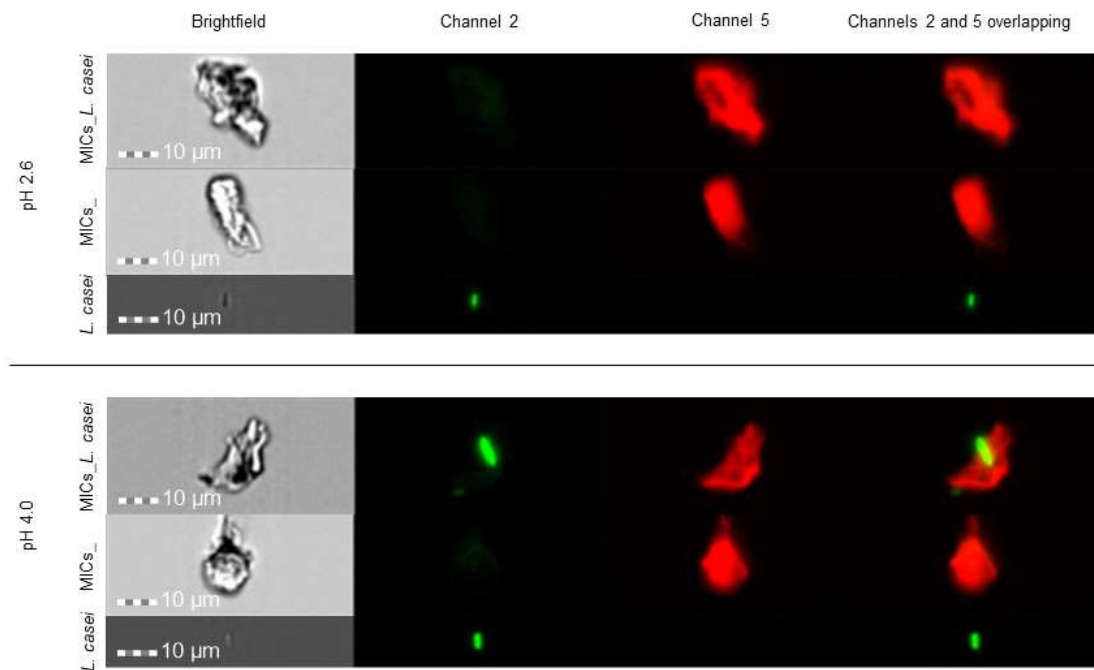
#### 4.4.1.4 - Chitosan microspheres adhesion to *Lactobacillus casei*

In Figure 4.17 are represented images of *L. casei* adherent to Ch MICs (MICs\_ *L. casei*) at the different citrate-phosphate buffers tested (pH 2.6, 4.0, 6.0 e 7.5), in Ch02 and in the column corresponding to the overlay of channels 2 and 5 of the IDEAS 6.2 image analysis software, as

well as the respective controls (MICs\_ e *L. casei*), labelled with 0.015  $\mu\text{M}$  of SYTO9. In this image it is also visible only the Ch MICs in Ch05.

By observing the images obtained for MICs\_*L. casei* samples it is apparent that these Ch MICs appear to adhere to this bacterium in citrate-phosphate buffers at pH 4.0, 6.0 and 7.5, since in Ch02 there is observed green fluorescent staining that is not visible in the controls containing only Ch MICs (MICs\_).

In the data from the present assay there was no bacterial adhesion at pH 2.6, although bacteria labelled with SYTO9 were observed in the control sample (*L. casei*), suggesting that at this pH this species does not appear to adhere to these Ch MICs.



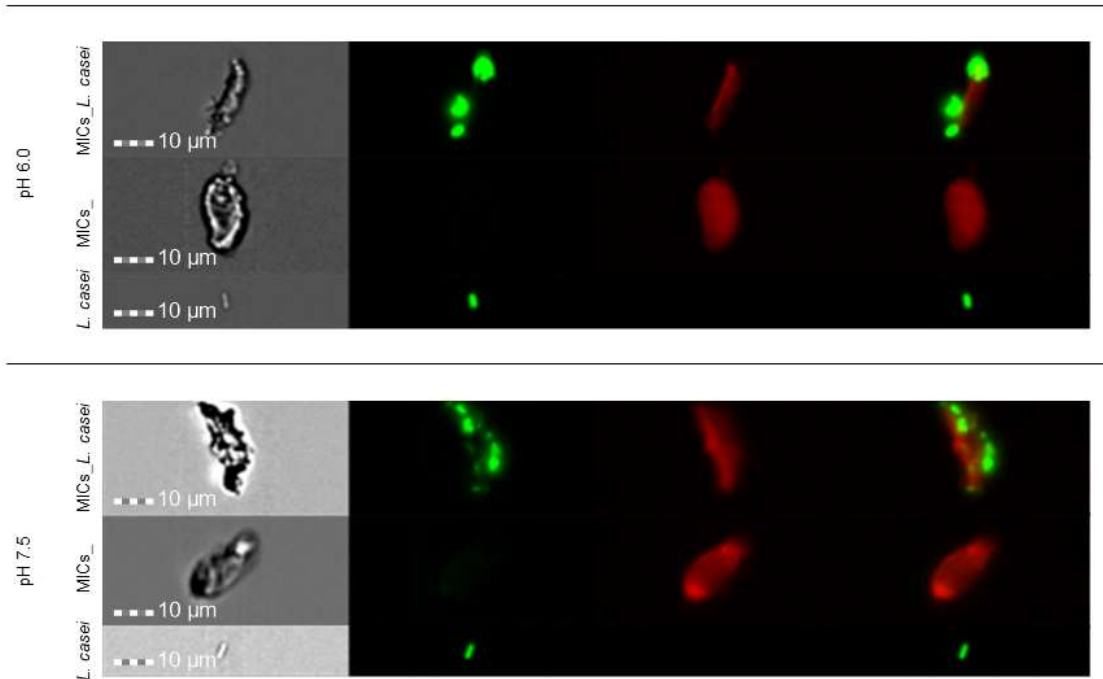


**Figure 4.17** - ImageStream®X images of *Lactobacillus casei* adhesion assay to chitosan microspheres (MICs\_ *L. casei*) at pH 2.6, 4.0, 6.0 and 7.5, and the correspondent controls (MICs\_ and *L. casei*). All samples were labelled with 0.015 µM of SYTO9. Scale bar corresponds to 10 µm.

The graphs in Figure 4.18 correspond to the fluorescence intensity in Ch02 graphs obtained in the IDEAS 6.2 software for the MICs\_ *L. casei* and MICs\_ samples.

Comparing the intensity graphs in Ch02 for MICs\_ *L. casei* and MICs\_ samples, it is possible to observe that samples showing bacterial adhesion to Ch MICs have higher intensity values than samples containing only microspheres (MICs\_), confirming bacterial adhesion at pH 4.0, 6.0 and 7.5. In the case of the MICs\_ *L. casei*\_pH2.6 sample, since no bacterial adhesion was observed at this pH, it presents intensity values similar to the intensity values for this channel in the MICs\_ samples.

In the case of the MICs\_ *L. casei*\_pH4.0 sample, the amount of microspheres with bacterial adhesion was restricted to a very small number of events, hence the values of fluorescence intensity in Ch02 for this sample were very similar to the values obtained for the sample control at pH 4.0 (MICs\_pH4.0).

Both the MICs\_ *L. casei*\_pH2.6 sample and the control samples MICs\_ at pH 2.6 and 4.0 showed higher intensity values than expected, as a result of the compensation matrix applied in these cases was not the best.

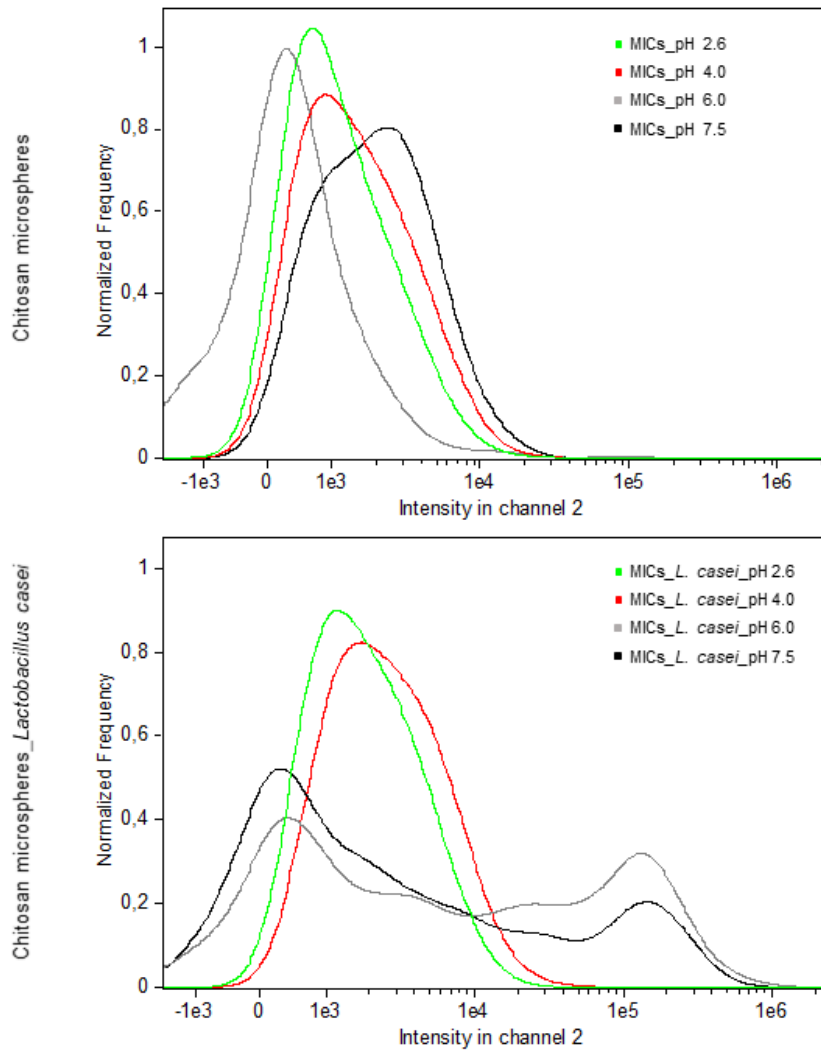


**Figure 4.18** - IDEAS® 6.2 histograms for the intensity in channel 2 for the samples MICs\_*L. casei* and MICs\_ at pH 2.6, 4.0, 6.0 and 7.5. For a better analyse of the obtained results, the histograms obtained has a maximum Histogram Smoothing.

The fact that the samples showing bacterial adhesion (MICs\_*L. casei*) at pH 4.0, 6.0 and 7.5, with higher values of fluorescence intensity in Ch02, had some intensity values close to the MICs\_ samples means that *L. casei* adhesion did not occur to all Ch MICs in the different samples. Therefore, it is important to note that these samples show a large dispersion of results, related to the fact that within the same sample MICs\_*L. casei*, both Ch MICs with *L. casei* adhesion to their surface and Ch MICs without bacterial adhesion were observed.

According to the mean values obtained in SPSS for the intensity of fluorescence in Ch02 for MICs\_*L. casei* samples, in each experimental condition (citrate-phosphate buffer at pH 2.6, 4.0, 6.0, and 7.5), this bacterium appears to preferentially adhere to the Ch MICs at pH 6.0, with an average intensity value of about 27275, followed by pH 7.5 and 4.0, with average intensity values of about 8172 and 3442, respectively (Table 4.6).



**Table 4.64** - Table with the mean and standard deviation, of the fluorescence intensity in channel 2, obtained on SPSS® for each of the samples containing chitosan microspheres and *Lactobacillus casei* labelled with SYTO9. The average values presented are approximate to the unit.

pH		2.6	4.0	6.0	7.5
Intensity in channel 2 (Arbitrary units)	Mean	1823	3442	27275	8172
	Standard deviation	5183	4979	69132	27612

By the analysis of the results obtained after statistical analysis in the SPSS, based on the significant differences between the mean values for the MICs\_ *L. casei* samples (Figure 4.19), there were statistically significant differences between all samples, with adhesion at pH 6.0 having the highest fluorescence intensity in Ch02, followed by pH 7.5, 4.0 and 2.6.

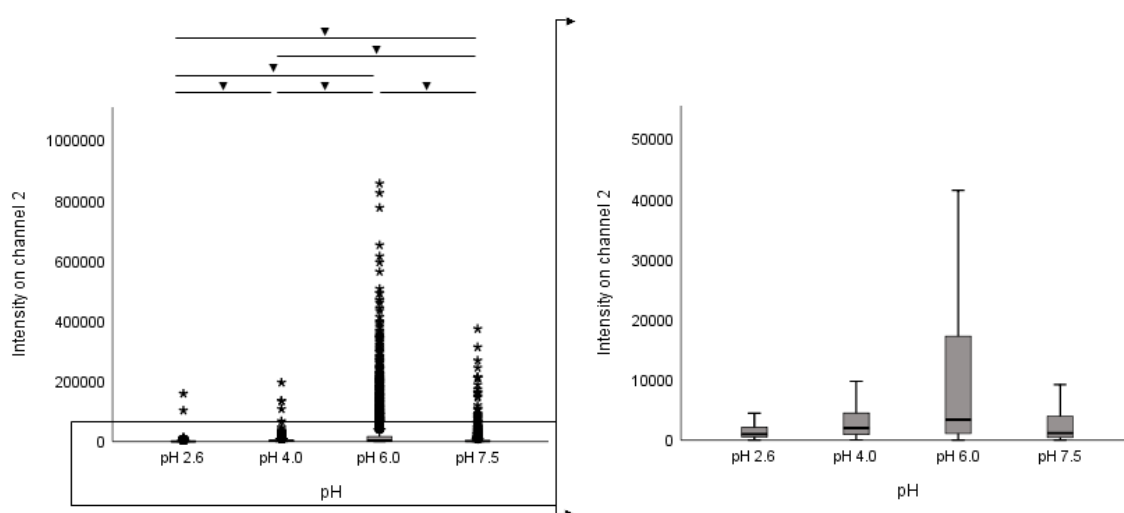


**Figure 4.19** - BoxPlot of the intensity on channel 2 for the samples MICs\_ *L. casei*. Statistically significant differences between samples when  $p < 0.05$  (▼). The graph on the right is a zoom-in excluding outliers (●) and extremes (\*), in order to better understand the behaviour between the different samples.

#### 4.4.1.5 - Chitosan microspheres adhesion to *Enterococcus faecalis*

In Figure 4.20 are represented images of *E. faecalis* adherent to Ch MICs (MICs\_ *E. faecalis*) at the different citrate-phosphate buffers tested (pH 2.6, 4.0, 6.0 e 7.5), in Ch02 and in the column corresponding to the overlay of channels 2 and 5 of the IDEAS 6.2 image analysis software, as well as the respective controls (MICs\_ e *E. faecalis*), labelled with 0.015µM of SYTO9. In this image it is also visible only the Ch MICs in Ch05.

By observing the images obtained for MICs\_ *E. faecalis* samples it is apparent that these microspheres appear to adhere to this bacterium in citrate-phosphate buffers at pH 2.6, 4.0, 6.0 and 7.5, since in Ch02 there is observed green fluorescent staining that is not visible in the controls containing only Ch MICs (MICs\_).

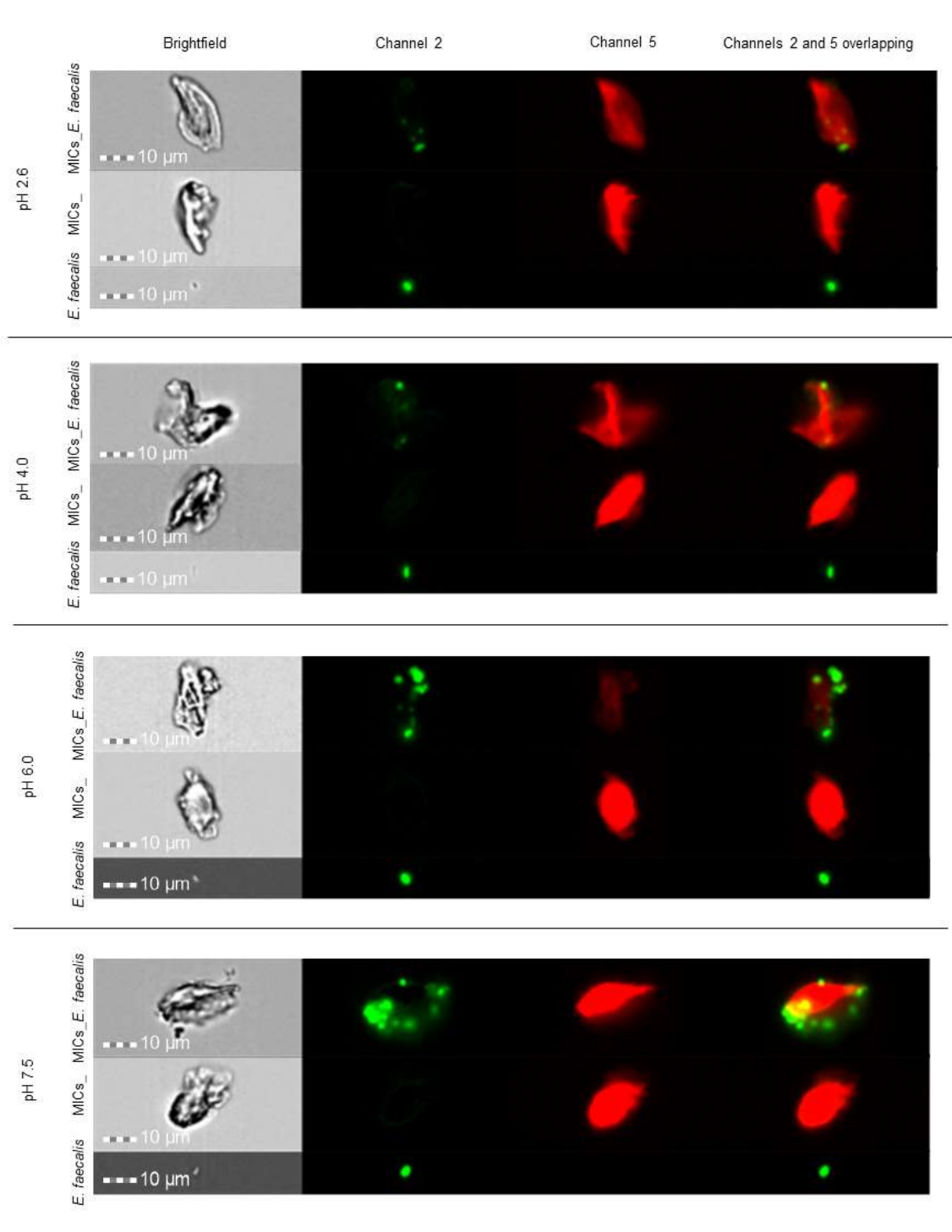


**Figure 4.20** - ImageStream®X images of *Enterococcus faecalis* adhesion assay to chitosan microspheres (MICs\_ *E. faecalis*) at pH 2.6, 4.0, 6.0 and 7.5, and the correspondent controls (MICs\_ and *E. faecalis*). All samples were labelled with 0.015 µM of SYTO9. Scale bar corresponds to 10 µm.

The graphs in Figure 4.21 correspond to the fluorescence intensity in Ch02 graphs obtained in the IDEAS 6.2 software for the MICs\_ *E. faecalis* and MICs\_ samples.

Comparing the intensity graphs in Ch02 for MICs\_ *E. faecalis* and MICs\_ samples, it is possible to observe that samples showing bacterial adhesion to Ch MICs have higher intensity values than samples containing only microspheres (MICs\_), confirming bacterial adhesion at pH 2.6, 4.0, 6.0 and 7.5.

In the case of the MICs\_ *E. faecalis*\_pH2.6 and MICs\_ *E. faecalis*\_pH4.0 samples, the amount of microspheres with bacterial adhesion was restricted to a very small number of events, hence the values of fluorescence intensity in Ch02 for this sample were very similar to the values obtained for the sample control at pH 2.6 and 4.0 (MICs\_pH2.6 and MICs\_pH4.0). MICs\_pH7.5 sample showed higher intensity values than expected, as a result of the compensation matrix applied in this case was not the best.

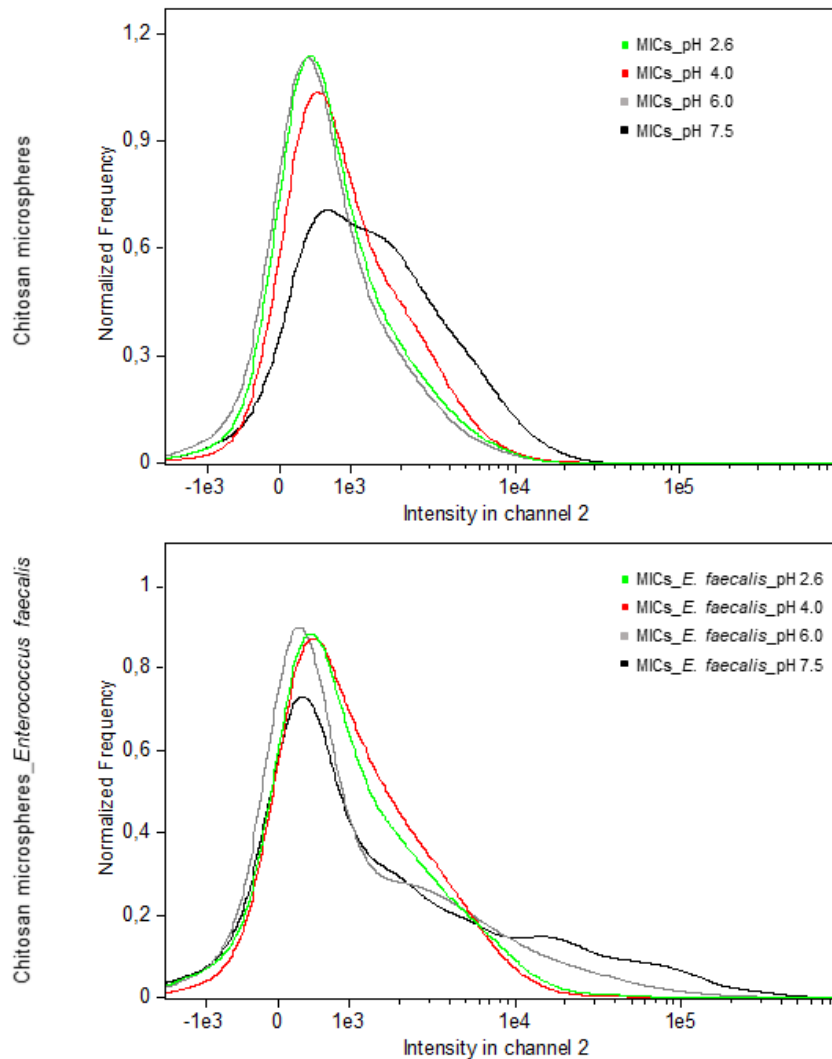


**Figure 4.21** - IDEAS® 6.2 histograms for the intensity in channel 2 for the samples MICs\_ *E. faecalis* and MICs\_ at pH 2.6, 4.0, 6.0 and 7.5. For a better analyse of the obtained results, the histograms obtained has a maximum Histogram Smoothing.

The fact that the samples showing bacterial adhesion (MICs\_ *E. faecalis*) at pH 2.6, 4.0, 6.0 and 7.5, with higher values of fluorescence intensity in Ch02, had some intensity values close to the MICs\_ samples means that *E. faecalis* adhesion did not occur to all Ch MICs in the different samples. Therefore, it is important to note that these samples show a large dispersion of results, related to the fact that within the same sample MICs\_ *E. faecalis*, both Ch MICs with *E. faecalis* adhesion to their surface and Ch MICs without bacterial adhesion were observed.

According to the mean values obtained in SPSS for the intensity of fluorescence in Ch02 for MICs\_ *E. faecalis* samples, in each experimental condition (citrate-phosphate buffer at pH 2.6, 4.0, 6.0, and 7.5), this bacterium appears to preferentially adhere to the Ch MICs at pH 7.5, with an average intensity value of about 9128, followed by pH 6.0, 2.6 and 4.0, with average intensity values of about 3588, 1532 and 1501, respectively (Table 4.7).

**Table 4.7** - Table with the mean and standard deviation values, of the fluorescence intensity in channel 2, obtained on SPSS® for each of the samples containing chitosan microspheres and *Enterococcus faecalis* labelled with SYTO9. The average values presented are approximate to the unit.

pH		2.6	4.0	6.0	7.5
Intensity in channel 2 (Arbitrary units)	Mean	1532	1501	3588	9128
	Standard deviation	3039	2485	12225	29053

By the analysis of the results obtained after statistical analysis in the SPSS, based on the significant differences between the mean values for the MICs\_ *E. faecalis* samples (Figure 4.22), there were statistically significant differences between some samples, with adhesion at pH 7.5 having the highest fluorescence intensity in Ch02, followed by pH 6.0, 2.6 and 4.0.

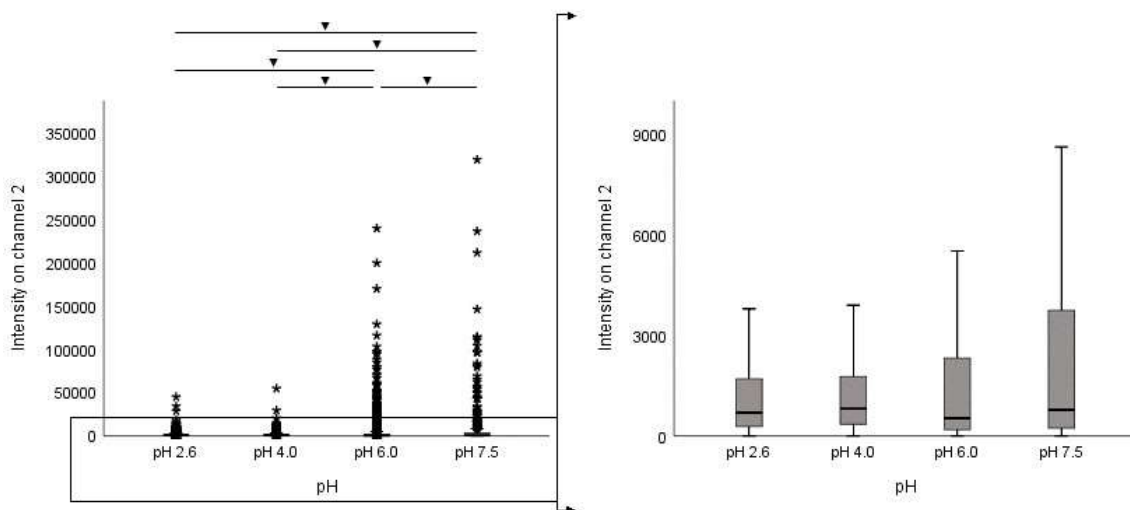


**Figure 4.22** - BoxPlot of the intensity on channel 2 for the samples MICs\_ *E. faecalis*. Statistically significant differences between samples when  $p < 0.05$  (▼). The graph on the right is a zoom-in excluding outliers (●) and extremes (\*), in order to better understand the behaviour between the different samples.

#### 4.4.1.6 - Chitosan microspheres adhesion to *Bacillus cereus*

In Figure 4.23 are represented images of *B. cereus* adherent to Ch MICs (MICs\_ *B. cereus*) at the different experimental conditions (citrate-phosphate buffers at pH 2.6, 4.0, 6.0 e 7.5), in Ch02 and in the column corresponding to the overlay of channels 2 and 5 of the IDEAS 6.2 image analysis software, as well as the respective controls (MICs\_ e *B. cereus*), labelled with 0.015µM of SYTO9. In this image it is also visible only the Ch MICs in Ch05.

By observing the images obtained for MICs\_ *B. cereus* samples it is apparent that these Ch MICs appear to adhere to this bacterium in citrate-phosphate buffers at pH 2.6, 4.0, 6.0 and 7.5, since in Ch02 there is observed green fluorescent staining that is not visible in the controls containing only Ch MICs (MICs\_).

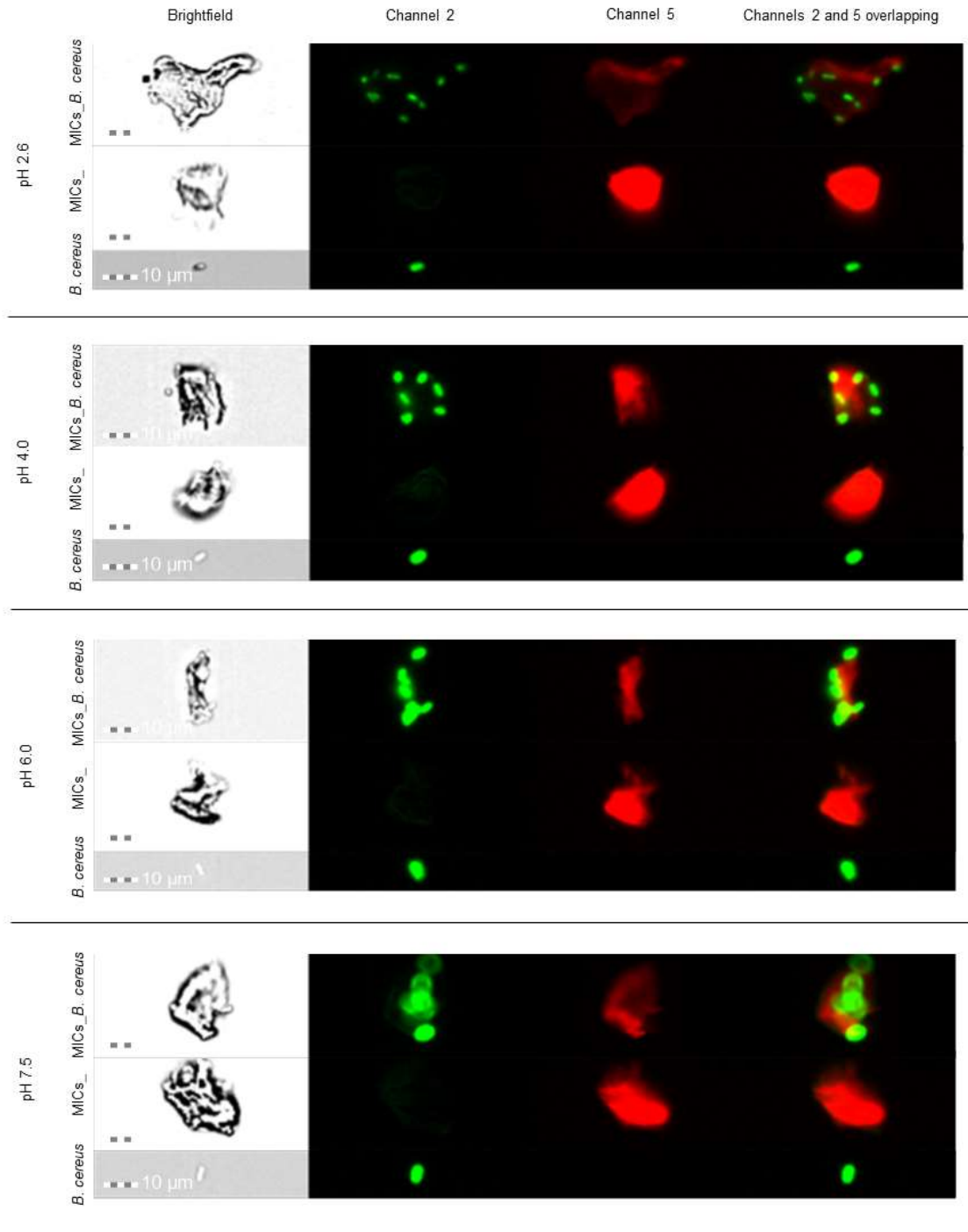


**Figure 4.23** - ImageStream®X images of *Bacillus cereus* adhesion assay to chitosan microspheres (MICs\_ *B. cereus*) at pH 2.6, 4.0, 6.0 and 7.5, and the correspondent controls (MICs\_ and *B. cereus*). All the samples were labelled with 0.015 μM of SYTO9 and the scale bar chosen was 10 μm.

The graphs in Figure 4.24 correspond to the fluorescence intensity in Ch02 graphs obtained in the IDEAS 6.2 software for the MICs\_ *B. cereus* and MICs\_ samples. Comparing the intensity graphs in Ch02 for MICs\_ *B. cereus* and MICs\_ samples, it is possible to observe that samples showing bacterial adhesion to Ch MICs have higher intensity values than samples containing only microspheres (MICs\_), confirming bacterial adhesion at pH 2.6, 4.0, 6.0 and 7.5.

The fact that the samples showing bacterial adhesion (MICs\_ *B. cereus*) at pH 2.6, 4.0, 6.0 and 7.5, with higher values of fluorescence intensity in Ch02, had some intensity values close to the MICs\_ samples means that *B. cereus* adhesion did not occur to all Ch MICs in the different samples. Therefore, it is important to note that these samples show a large dispersion of results, related to the fact that within the same sample MICs\_ *B. cereus*, both Ch MICs with *B. cereus* adhesion to their surface and Ch MICs without bacterial adhesion were observed.

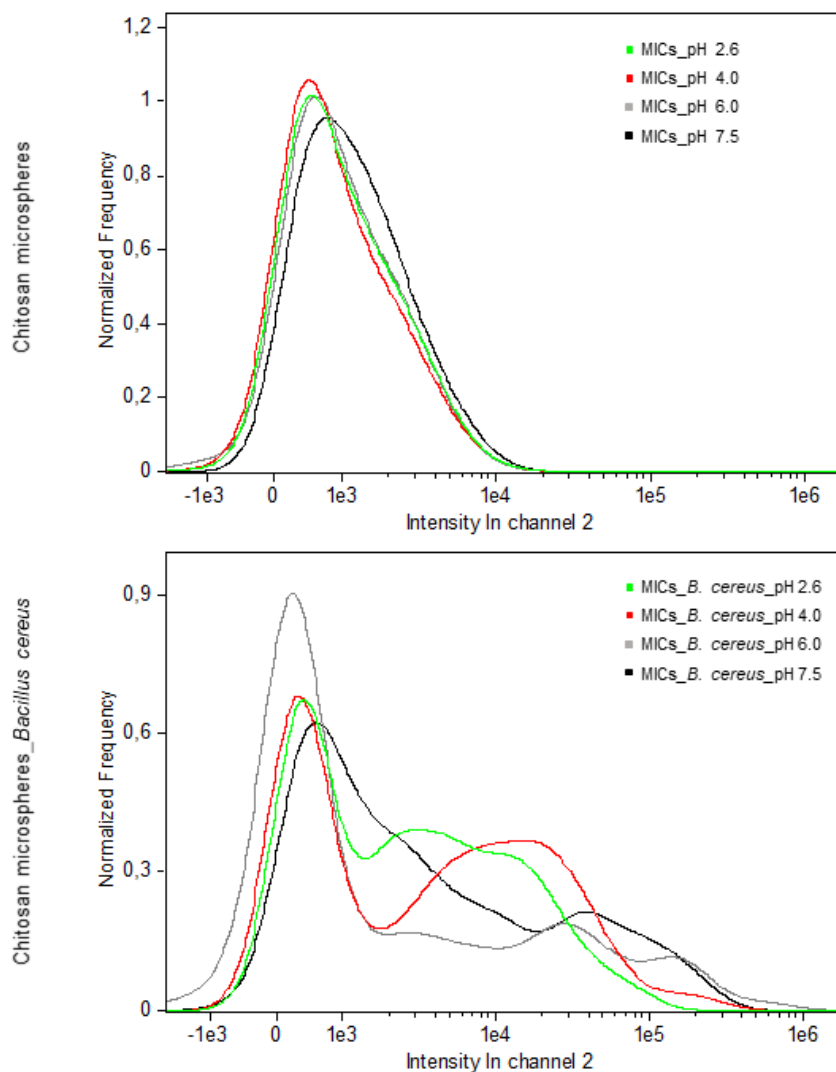


**Figure 4.24** - IDEAS® 6.2 histograms for the intensity on channel 2 for the samples MICs\_ *B. cereus* and MICs\_ at pH 2.6, 4.0, 6.0 and 7.5. For a better analyse of the obtained results, the histograms obtained has a maximum Histogram Smoothing.

According to the mean values obtained in SPSS for the intensity of fluorescence in Ch02 for MICs\_ *B. cereus* samples, in each experimental condition (citrate-phosphate buffer at pH 2.6, 4.0,

6.0, and 7.5), this bacterium appears to preferentially adhere to the Ch MICs at pH 6.0, with an average intensity value of about 21470, followed by pH 7.5, 4.0 and 2.6, with average intensity values of about 18772, 12925 and 7429, respectively (Table 4.8).

**Table 4.8** - Table with the mean and standard deviation values, of the fluorescence intensity in channel 2, obtained on SPSS for each of the samples containing chitosan microspheres and *Bacillus cereus* labelled with SYTO9. The average values presented are approximate to the unit.

pH		2.6	4.0	6.0	7.5
Intensity in channel 2 (Arbitrary units)	Mean	7429	12925	21470	18772
	Standard deviation	12985	28320	66119	39901

By the analysis of the results obtained after statistical analysis in the SPSS, based on the significant differences between the mean values for the MICs\_ *B. cereus* samples (Figure 4.25), there were statistically significant differences between some samples, with adhesion at pH 6.0 having the highest fluorescence intensity in Ch02, followed by pH 7.5, 4.0 and 2.6.

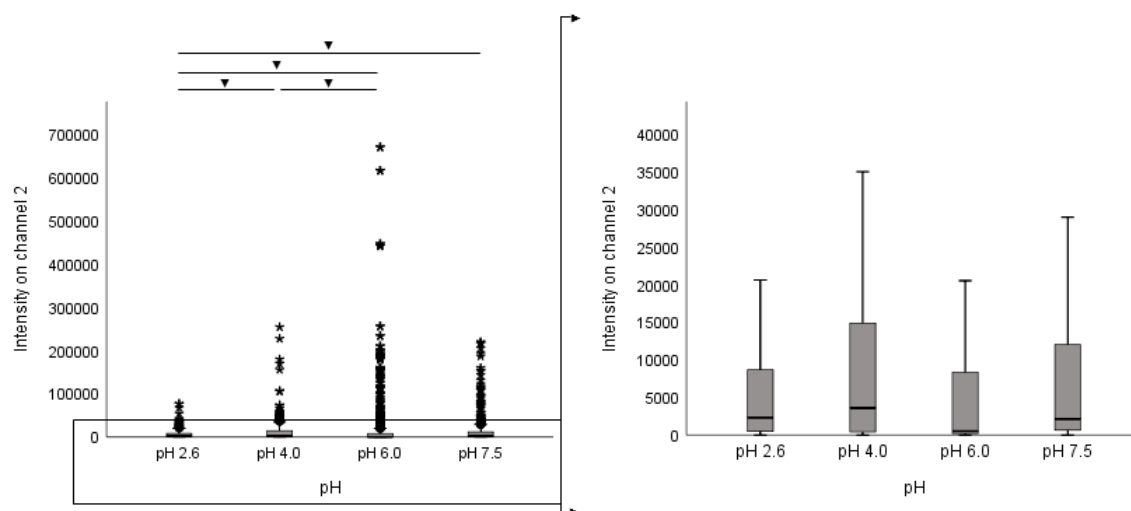


**Figure 4.25** - BoxPlot for the intensity on channel 2 for the samples MICs\_ *B. cereus*. Statistically significant differences between samples when  $p < 0.05$  ( $\blacktriangledown$ ). The graph on the right is a zoom-in excluding outliers ( $\bullet$ ) and extremes ( $\ast$ ), in order to better understand the behaviour between the different samples.

#### 4.4.1.7 - General discussion

- *Helicobacter pylori*

*H. pylori* is a bacilar/spiral shape Gram-negative microaerophilic pathogenic bacterium with 2.0-5.0  $\mu\text{m}$  of length, which preferentially colonizes the gastric mucosa of more than 50 % of the world's human population [51], [59]. This bacterium has a series of mechanisms and virulence

factors that facilitate the interaction and colonization of the host organism, allowing its survival in extreme conditions of acid pH and avoiding the defence mechanisms intrinsic to the host [51], [56].

Although the vast majority of individuals infected with *H. pylori* do not have clinical symptoms, chronic diseases caused as a result of *H. pylori* infections have been associated with an increased risk of gastric complications such as gastritis and peptic ulcers, sometimes related with the onset of gastric cancer and gastric mucosal lymphoma [72]–[75].

At pH 2.6 both *H. pylori* and Ch MICs are positively charged on its surface,  $24.5 \pm 1.7$  mV and  $3.5 \pm 2.5$  mV, respectively. On the other hand, at pH 6.0 both *H. pylori* and Ch MICs are negatively charged, with ZP values of  $-6.1 \pm 0.6$  mV and  $-7.2 \pm 1.1$  mV, in their respective order (Figure 4.26).

Thus, the Ch MICs adhesion to *H. pylori* can not be justify by the electrostatic interactions between the surface charge of *H. pylori* and the Ch MICs, otherwise a higher bacterial adhesion should not be observed at pH 6.0 (MICs\_ *H. pylori*\_pH6.0), as a result of the electric repulsion between surface charges. To this extent, there must be other factors responsible for the differential adhesion of the Ch MICs to *H. pylori* under different pH conditions.

According to the literature [14], [51], [56], [58]–[62], the vast majority of bacteria of this species are close to epithelial cells in the region of the gastric mucosa where the pH of gastric fluid presents values close to the neutral. This bacterium may still arise in the gut, but in very low amounts [14].

As previously described, this bacterium is a neutrophile microorganism with an optimal growth at neutral pH, although it may exhibit growth over a broad pH range of 5.5 to 8.0 and therefore compatible with the gastric mucosal region where this species is mostly found in the human stomach, presenting better conditions for its growth and development [14], [51], [56]. Thus, for samples with pH values close to the neutral, could be expected a higher *H. pylori* adhesion to Ch MICs.

- *Campilobacter jejuni*

*C. jejuni* is a slender spirally curved rod shape Gram-negative microaerophilic bacterium, with 0.5-5.0  $\mu\text{m}$  of length commonly commensal to animals, but pathogenic to humans, as a result of ingestion of poorly cooked meat, especially poultry [168], [169]. This is considered the leading cause of bacterial gastroenteritis in man, leading to ulcerative colitis [14] and to some cases of severe pathological condition after infection, such as the Guillain-Barré and Miller-Fisher Syndromes, characterized by the attack of the immune system to the peripheral nervous system. Its ability to invade a variety of animal models, associated with colonization and *in vitro* adhesion to human epithelial cells is thought to be in part related to the presence of flagella in the constitution of this bacterium [169]–[171].

One of the strategies described for the survival of *C. jejuni* against the environmental conditions verified, for example, in the human stomach is the ability to form biofilms, bound to biotic or abiotic surfaces and surrounded by a viscous matrix that protects them from the action of chemical agents and antibiotics [172].

At pH 2.6 both *C. jejuni* and Ch MICs are positively charged on its surface,  $1.7 \pm 0.3$  mV and  $3.5 \pm 2.5$  mV, respectively. On the other hand, at pH6.0 both *C. jejuni* and Ch MICs are negatively charged, with very similar ZP values of  $-5.6 \pm 0.5$  mV and  $-7.2 \pm 1.1$  mV, in their respective order (Figure 4.26).



Thus, the Ch MICs adhesion to *C. jejuni* can not be justify by the electrostatic interactions between the surface charge of *C. jejuni* and the Ch MICs, otherwise bacterial adhesion should not be observed at pH 6.0 (MICs\_ *C. jejuni*\_pH6.0), as a result of the electric repulsion between surface charges. To this extent, there must be other factors responsible for the differential adhesion of the Ch MICs to *C. jejuni* under different pH conditions.

This bacterium is a neutrophile microorganism with an optimal growth at pH between 6.5 and 7.5, compatible with the region of the gastric mucosa where this species is mostly found in the human stomach, as well as of the pH values found in the regions of the ilium and colon, regions of higher colonization by *C. jejuni* [14], [172], [173]. Thus, for samples with pH values close to the neutral, could be expected a higher Ch MICs adhesion to *C. jejuni*.

- *Escherichia coli*

*E. coli* is a rod-shaped Gram-negative facultative anaerobic bacterium with aproximatly 1.0-3.0  $\mu\text{m}$  of length [174], that inhabits mostly the gut of the GI tract, mainly in the mucus layer of caecum and colon regions of the large intestine ( $10^7$ - $10^9$  CFU/g of feces) and includes strains and serotypes with commensal characteristics, as well as with virulence factors [175]–[178]. Pathogenic strains can cause infections and, consequently, serious pathological conditions in man, being the more common cause of intestinal and extra-intestinal diseases, resulting in more than 2 million deaths per year [175], [176]. Commensal *E. coli* strains may also lead to disease situations in immunosuppressed individuals [176].

This bacterium is usually found in the mucus layer that delimits the human intestine, growing in a multi-species biofilm complex, in which it competes with other species to obtain a wide variety of nutrients [179]. This bacterial species has also pili and a secretory system of its own that help its interaction and adhesion with the GI epithelium.

The behaviour of *E. coli* commensal strains has been described in the literature as of extreme importance for the correct functioning of the human organism, contributing in large scale to the performance of functions, essential to the balance of the GI tract. Through the production of vitamins B12 and K necessary for man, as well as for example elimination by competition in their niches of pathogenic microorganisms. The secretion of immunoglobulin A in the intestine seems to facilitate the formation of *E. coli* biofilms in the intestinal mucosa [179], translating a symbiosis relation between this bacterium and the host.

On the other hand, the decrease in the natural colonization of new-borns by *E. coli* during child-birth (as a result of the increase of hygiene conditions in hospitals), has been associated with increased colonization of the GI tract by species such as *Staphylococcus aureus*, related to an increased risk of developing disorders such as diabetes, obesity, asthma, among others [179].

In citrate-phosphate buffer at pH 2.6 *E. coli* is slightly negatively charged, while Ch MICs are positively charged, with ZP values of  $-3.7 \pm 2.7$  mV and  $3.5 \pm 2.5$  mV, respectively. However, at this pH was not observed bacterial adhesion to Ch MICs. On the other hand, at pH 7.5 both *E. coli* and Ch MICs are negatively charged, with ZP values of  $-20.9 \pm 0.7$  mV and  $-14.2 \pm 1.7$  mV, in their respective order (Figure 4.26).

Thus, the Ch MICs adhesion to *E. coli* can not be justify by the electrostatic interactions between the surface charge of *E. coli* and the Ch MICs, otherwise a higher bacterial adhesion should not be observed at pH 7.5 (MICs\_ *E. coli*\_pH7.5), as a result of the electric repulsion between surface charges. To this extent, there must be other factors responsible for the differential adhesion of the Ch MICs to *E. coli* under different pH conditions.

This bacterium is a neutrophile microorganism with optimal growth at neutral pH and therefore compatible with the region of the intestinal mucosa where this species is mostly found in the human intestine [180]. Thus, for samples with pH values close to the neutral, could be expected a higher Ch MICs adhesion to *E. coli*.

The *E. coli* strain used in this study is a serotype O6, a very heterogeneous bacterial group that include commensal and pathogenic bacteria, the latter with a broad spectrum of virulence factors, being described as enterotoxigenic bacteria (associated with poor hygiene), which can cause GI diseases such as diarrhoea [176], [181].

In this research work, from the data provided, it is known that this strain is not a pathogenic bacteria, since this organism does not produce verotoxin and it is a common Clinical and Laboratory Standards Institute (CLSI) control strain for antimicrobial susceptibility testing.

- *Lactobacillus casei*

Species of the genus *Lactobacillus* are rod-shaped facultative anaerobic Gram-positive commensal bacteria with 2.0-4.0  $\mu\text{m}$  of length, capable of inhabiting the human GI tract ( $10^6$ - $10^8$  CFU/g of feces), especially the intestine, promoting a state of health in man, stimulating not only the metabolism in general and the production of essential vitamins and enzymes, but also mechanisms of immune response and fighting intestinal disorders associated with pathological situations [182]–[185].

The colonization of these bacteria in the GI tract, passes through the adhesion to the epithelial cells, with pH values between 5.0 and 7.5, approximately [14], [39]–[43], [186]–[188], thus resisting the passage of the contents resulting from digestion [14], [186]–[188].

These bacteria have been described as important for the establishment of beneficial symbiosis relations for the host organism, as well as for maintaining a state of equilibrium of the microbial populations that colonize the human GI tract.

*Lactobacillus spp.* demonstrated the ability to control intestinal microflora by reducing the colonization of pathogenic microorganisms from a series of mechanisms, in particular: 1) Adhesion to the intestinal wall; 2) Competition for available nutrients; 3) Production of substances with antimicrobial activity; 4) Reduction of the pH immediately surrounding the place where they are; 5) Production of peroxide hydrogen; and 6) Accelerating the repair process of epithelial cells, making them less vulnerable [186]–[188]. The ability of these bacteria to decrease the risk of developing colon cancer by tumour suppression through stimulation of the host immune system as well as by carcinogenic compounds detoxification and modulation of prokaryotic enzymes has also been described [188].

In citrate-phosphate buffer at pH 2.6 *L. casei* is slightly negatively charged, while Ch MICs are positively charged, with ZP values of  $-0.3 \pm 0.3$  mV and  $3.5 \pm 2.5$  mV, respectively. However, at this pH was not observed bacterial adhesion to Ch MICs. On the other hand, at pH 6.0 both *L. casei* and Ch MICs are negatively charged, with ZP values of  $-2.9 \pm 0.3$  mV and  $-7.2 \pm 1.1$  mV, in their respective order (Figure 4.26).

Thus, the Ch MICs adhesion to *L. casei* can not be justify by the electrostatic interactions between the surface charge of *L. casei* and the Ch MICs, otherwise a higher bacterial adhesion should not be observed at pH 6.0 (MICs\_ *L. casei*\_pH6.0), as a result of the electric repulsion between surface charges. To this extent, there must be other factors responsible for the differential adhesion of the Ch MICs to *L. casei* under different pH conditions.

*L. casei* is a mesophilic bacteria and the optimum pH growth for *Lactobacillus spp.* is about 5.4-6.4, which is within the pH limits observed in the regions most colonized by this bacterium

[189], [190]. Thus, for samples with pH values between 5.4-6.4, could be expected a higher Ch MICs adhesion to *L. casei*.

- *Enterococcus faecalis*

*Enterococcus spp.* are commonly commensal bacterial species of the human GI tract and clinically relevant opportunistic pathogenic microorganisms [191]–[194]. The most virulent species are the clinical isolates, whose pathogenicity is thought to be largely associated with the capacity of biofilm formation, with different characteristics of commensal isolates, associated with high colonization capacity of the GI tract (its natural habitat) and the capacity of adhere to a wide range of extracellular matrix proteins [191], [193].

The cells of a biofilm exhibit high levels of resistance to the host organism defense mechanisms and significantly reduce the susceptibility to the antibiotics applied, decreasing success rates in the combat and prevention of bacterial infections by the acquisition of resistance [191].

The species *E. faecalis* is a cocci facultative anaerobic Gram-positive bacterium with a high capacity to inhabit a wide variety of hosts and environments and that normally lives in large quantities in the human intestinal lumen ( $10^5$ - $10^8$  CFU/g of feces). Although it is one of the most common causes of nosocomial, including bacteremia in neutropenic patients and endocarditis, and urinary infections, among others, this microorganism normally don't causes damage to the host organism [191], [195], [196].

The great majority of the infections caused by this species are thought to be of the endogenous type, which occurs by the translocation of *E. faecalis* through the intestinal epithelial cells, causing infection via lymph nodes and allowing their arrival in several cells of the human body, even invade and colonize the host immune system in extreme cases [193].

In citrate-phosphate buffer at pH 2.6 *E. faecalis* is negatively charged, while Ch MICs are positively charged, with ZP values of  $-10.6 \pm 0.1$  mV and  $3.5 \pm 2.5$  mV, respectively. However, at this pH was observed a very small amount of bacterial adhered to Ch MICs, when compared to MICs\_ *E. faecalis* samples at pH 6.0 and 7.5. On the other hand, at pH 7.5 both *E. faecalis* and Ch MICs are negatively charged, with ZP values of  $-16.2 \pm 1.4$  mV and  $-14.6 \pm 1.7$  mV, in their respective order (Figure 4.26).

Thus, the Ch MICs adhesion to *E. faecalis* can not be justify by the electrostatic interactions between the surface charge of *E. faecalis* and the Ch MICs, otherwise a higher bacterial adhesion should not be observed at pH 7.5, as a result of the electric repulsion between surface charges. To this extent, there must be other factors responsible for the differential adhesion of the Ch MICs to *E. faecalis* under different pH conditions.

*E. faecalis* is a neutrophile bacterium with an optimum pH of about 7.5, which is within the pH limits observed in the most colonized regions by this bacterium [193]. Thus, for samples with pH values close to the neutral, could be expected a higher Ch MICs adhesion to *E. faecalis*.

- *Bacillus cereus*

*B. cereus* is a bacilar/rod shape Gram-positive aerobic-to-facultative bacterium widely distributed in the environment and which, despite being mostly found in soil as a saprophyte microorganism, has the ability to adapt and develop in the lower portions of the human GI tract [197]–[199]. The colonization of the human GI tract by this bacterium occurs as a result of the consumption of contaminated food and water with soil microflora [199], [200].

*B. cereus* species is composed of some strains that have been used as probiotics as well as opportunistic pathogenic strains capable of causing food poisoning, causing vomiting and diarrhea, or even local and systemic infections, which is thought to occur as a result of the adherence to intestinal epithelial cells [197]. Its pathogenicity is closely associated with the production of destructive tissue exoenzymes, which may lead to the onset of some diseases such as bacteremia, meningitis, pneumonia, among others [199].

The environmental conditions verified in the human stomach, in particular the conjugation of the low pH, the presence of digestive enzymes (such as pepsin) and the reduced amount of O<sub>2</sub> make it difficult to survive in this organ. However, spores of this bacterium and about 10% of the cells in the vegetative form can survive to these adverse conditions and reach more advantageous portions in the intestine, being able to reach about 10<sup>3</sup>-10<sup>8</sup> CFU/g of feces [197], [200].

In addition to the relative low digestion time in the stomach and the possible presence of some protective compounds associated with the foods with which this bacterium enters into the human GI tract, this microorganism has the ability to trigger a series of tolerance and survival responses at acidic pH, helping their adaptation in the intestine, as the pH increases along these organs [197].

In citrate-phosphate buffer at pH 2.6 *B. cereus* and Ch MICs are positively charged, with ZP values of 0.0 ± 0.4 mV and 3.5 ± 2.5 mV, respectively. At acidic pH was observed a small amount of bacterial adhered to Ch MICs, when compared to MICs\_ *B. cereus* samples at pH 6.0 and 7.5. At pH 6.0 both *B. cereus* and Ch MICs are negatively charged, with similar ZP values of -8.3 ± 0.3 mV and -7.2 ± 1.1 mV, in their respective order, which can not justify the high bacterial adhesion observed for the MICs\_ *B. cereus*\_pH6.0 sample (Figure 4.26).

Thus, the Ch MICs adhesion to *B. cereus* can not be justify by the electrostatic interactions between the surface charge of the Ch MICs and *B. cereus*, otherwise bacterial adhesion should not be observed at pH 6.0, as a result of the electric repulsion between surface charges.

*B. cereus* is a bacterium with an optimum pH range of 6.0 to 7.0, which is within the pH limits observed in the most colonized regions by this bacterium [193]. Thus, for samples with pH values close to the neutral, could be expected a higher Ch MICs adhesion to *B. cereus* [201].

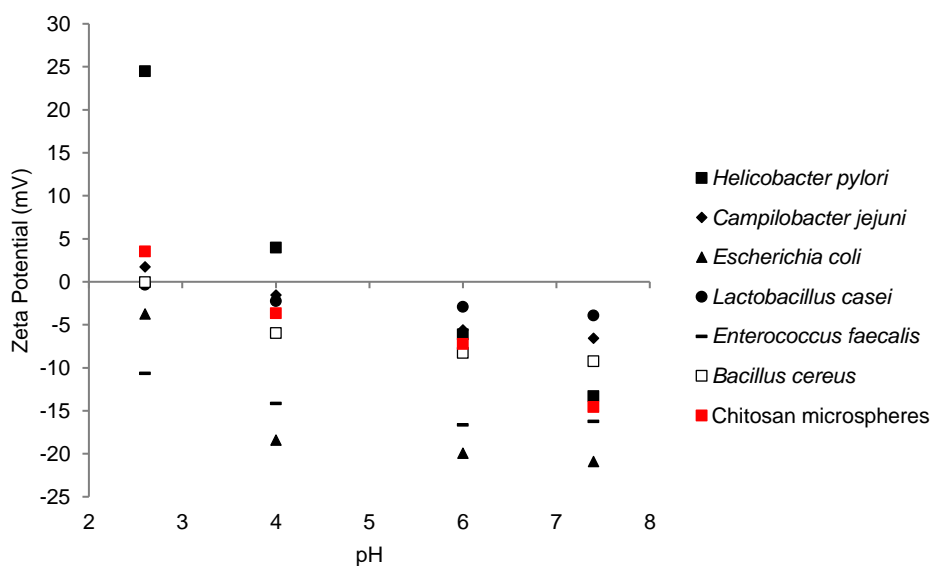


**Figure 4.26** - *Helicobacter pylori*, *Campilobacter jejuni*, *Escherichia coli*, *Lactobacillus casei*, *Enterococcus faecalis*, *Bacillus cereus* and chitosan microspheres zeta potential under citrate-phosphate buffer at pH 2.6, 4.0, 6.0 and 7.5, determined using Zetasizer Nano ZS (n = 3) and EKA (n = 6), respectively.

In this experimental project, a greater bacterial adhesion to Ch MICs was observed, in general, at pH 6.0 and 7.5 for all the bacterial species under analysis. *H. pylori*, *C. jejuni*, *L. casei* and *B. cereus* showed higher adhesion to Ch MICs at pH 6.0, while *E. coli* and *E. faecalis* have preferably adhered to Ch MICs at pH 7.5, which are within the pH limits verified for the regions where these species can be mainly found in the human GI tract. On the other hand, at more acidic pH, in particular at pH 2.6, a lower bacterial adhesion was observed for *E. faecalis* and *B. cereus* bacteria and no adhesion to *H. pylori*, *C. jejuni*, *E. coli* and *L. casei* bacteria in this same pH.

Bacteria of the human GI microbiota and thus capable of inhabiting this tract generally have a number of molecular mechanisms/strategies that allow them to tolerate and survive at acid pH when they reach the human stomach [202].

In general, Gram-negative neutrophile bacteria in stress situations, such as the reduction of the pH of the medium, can maintain their internal pH close to neutral (at pH 7.6 to 7.8), while Gram-positive bacteria, under the same conditions of pH, reduce its internal pH, in order to maintain a constant pH gradient, rather than maintaining a constant internal pH [202], [203].

The outer membrane of Gram-negative bacteria by standard does not constitute a physical barrier to the entrance of protons, as a result of the diameter of the porins, in this membrane, which allow the passage of these ions. In these type of bacteria, in acidic environments, a pH reduction of the periplasm occurs, with a pH similar to the external pH and the maintenance of an internal pH, beyond the cell's cytoplasmic membrane, at a constant approximately neutral pH. This maintenance of a constant pH occurs as a result of the mechanisms of buffering and ionic flow, relative impermeability to the passage of protons and the induction of responses to the acidic stress [202], [203].

In fact, in many bacteria, the modification of internal membrane phospholipids, from unsaturated fatty acids (UFAs) to cyclopropane fatty acids (CFAs), has been associated with the resistance of these microorganisms to acidic pH [202], [203].

In the case of Gram-positive bacteria, these also develop action mechanisms, in other to adapt and survive to the acidic pH, such as: 1) Protons removal; 2) Alkalinization of the external environment; 3) Changes in the composition of the cell membrane; 4) Expression of transcriptional regulators; 5) Changes in cell density; among others [204].

However, a severe reduction of the pH of the medium may cause some serious problems to the cells, especially if important components of defence and adaptation to acidic pH are damaged. Cell membrane damage, reduction of enzymatic activity, unfolding of proteins and DNA damage are some of the problems that can occur as a result of exposure of bacteria to low pH [167], [202], [204].

In this way, the acidic pH of the medium is a life threat for bacterial cells, leading to his death in a short time of exposure to these conditions [166], [167]. *Zhu H., et al.*, demonstrated that for pH values below 2.5, a severe death effect occurs in the analysed microorganisms, and in the case of *E. coli*, this bacteria was completely killed after 5min in this medium at pH 2.5 [166]. *Baatout S., et al.*, also demonstrated that at acidic pH the cell membrane integrity of bacteria appears to be compromised, with high damage observed at pH 2.0 [167].

Knowing that the adhesion of the bacteria to the Ch MICs should occur as a result of the interaction between the cell membrane and cell wall of the bacteria and the surface of these microparticles, the reduced or non-adhesion observed at pH 2.6 could be related not only to the changes in the cell membrane of the bacteria, which usually occur when exposed to acidic pH, but also as a result of possible damage, altering its ability to interact and adhere to Ch MICs. The

fact that the great majority of bacteria could die when exposed to pH 2.6 may, under these conditions, justify why they do not adhere at all to the Ch MICs.

On the other hand, if there is DNA damage of these microorganisms, the action of the fluorescent label SYTO9, which acts by the nucleic acid binding of the cells, can be drastically altered and does not allow the detection of the bacteria.

The higher adhesion observed at pHs closer to neutral (pH 6.0 and 7.5) may occur as a result of cells being in optimal growth conditions and not triggering defence mechanisms and actions to resist the environment, including structural changes in the cell membrane that may influence its adhesion to Ch MICs.

As with the bactericidal effect of Ch [141], adhesion of the bacteria to this polymer, in this case in particular with respect to Ch MICs, also seems to depend on factors such as pH variation of the medium, which are not intrinsic to this biomaterial, such as in case of its concentration, MW, hydrophilic/hydrophobic properties, ZP, among others.

In this case, as previously described, the surface charge (ZP) of bacteria and Ch MICs does not seem to justify at all the low bacterial adhesion observed for the samples at pH 2.6 and the higher adhesion observed in the samples at pH 6.0 and 7.5.

Assuming the oral application of Ch MICs in the human GI tract, especially the portions of the stomach and intestine, these microparticles, when passing through the stomach, with a transit time of approximately 4 h, would adhere to *H. pylori*, but also to *C. jejuni*, in the gastric mucosa regions and close to the epithelial cells, with pH values of approximately 7.4, in this region, and where colonization by these species is greatest (Figure 4.27) [39].

On the other hand, when reaching the small and large intestine, the Ch MICs would adhere to *C. jejuni*, *E. coli*, *L. casei*, *E. faecalis* and *B. cereus* species, associated with intestinal epithelial cells, free in the mucus layer or in the intestinal lumen. The pH range values of the human intestine are between 5.0 and 7.5, with a transit time between 3 to 4 h in the small intestine and about 2-4 days in the large intestine (Figure 4.27) [39]–[43].

As previously mentioned, *H. pylori* and *C. jejuni* are common pathogens of the human GI tract and the Ch MICs used in the project demonstrated the ability to adhere to these bacteria, with the prospect of eliminating it from the human GI tract, through feces. However, further studies will be needed to assess the amount of bacteria adhered and to understand if they are sufficient to substantially reduce disease situations caused by these pathogenic species.

*E. coli* and *L. casei* species used are considered commensal strains and the Ch MICs demonstrated a high adhesion capacity to these bacteria. These results do not seem very satisfactory considering the clinical applicability of these Ch MICs in the human GI tract for the control of bacterial infections since, in addition to adhering to pathogenic bacteria, they also adhere to commensal bacteria that contribute to the correct functioning of the human organism and, once again for the maintenance of a state of health in man, which may trigger the onset of certain pathologies.

Relatively to *E. faecalis* and *B. cereus* as opportunistic pathogens of the GI tract, the removal of these bacteria through the Ch MICs seems to be a good result, concerning the control and treatment of infections caused by infectious bacteria. On the other hand, these species in normal/healthy situations are commensal bacteria of the human GI tract and the occurrence of nefarious situations to the human organism are greatly reduced.

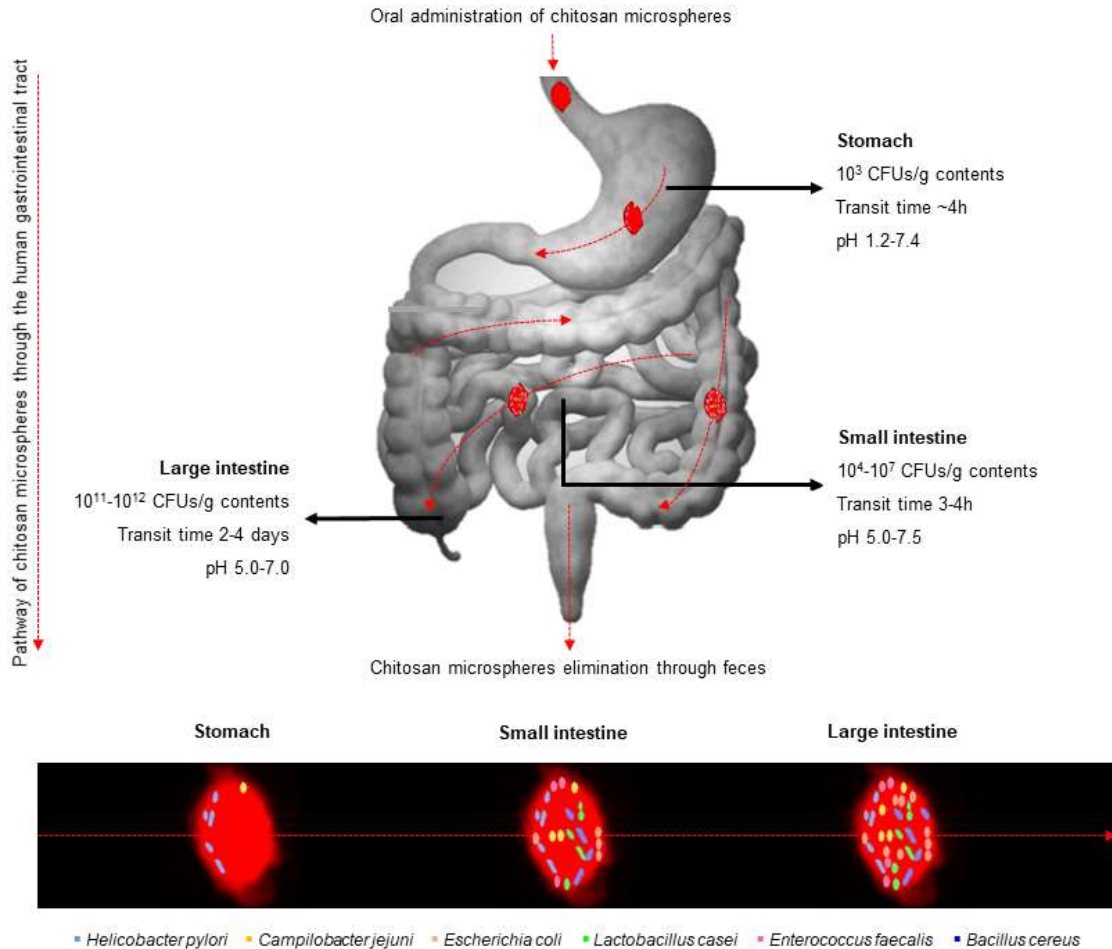


**Figure 4.27** - Scheme of the hypothetical adhesion of chitosan microspheres to the bacterial species *Helicobacter pylori*, *Campilobacter jejuni*, *Escherichia coli*, *Lactobacillus casei*, *Enterococcus faecalis* and *Bacillus cereus* along the lower portions of the human gastrointestinal tract, when applied orally (Adapted from [39]–[44]).

To that extent, further studies will be required to evaluate the amount of bacteria adhered and to understand if the Ch MICs cause a substantial reduction in the amount of commensal bacteria, as well as the dose of Ch MICs required, in order to cause harmful ecological changes in the level of homeostasis of the commensal GI microbiota and therefore associated with pathological situations.

Bacterial competition essay would be also interesting to perform, in order to understand if the initial adhesion of the Ch MICs in the stomach to certain bacterial species could or not be replaced by other species, when this biomaterial passes through the intestine, as well as perceive if the microsphere-bacterial binding force is different between different species.

## Chapter 5

# Conclusions and Future perspectives

### 5.1 - Conclusions

The exacerbated use of antibiotics in combating bacterial infections in the GI tract has led to an exponential increase in the resistance of pathogenic bacteria, causing nefarious ecological alterations to the number and diversity of the commensal bacteria that normally inhabit the human GI tract.

To this extent, the need arises to develop alternative therapies, such as Ch biomaterials, to the application of antibiotherapies in the fight against bacterial infections, without compromising the level of homeostasis established between the host organism, in healthy conditions, and the community of microorganism that inhabits it.

Thus, this research work aimed to evaluate the behaviour of Ch MICs, in terms of adhesion to bacteria of the human GI microbiota, including commensal and pathogenic bacteria, at different pHs that mimic the pH verified in the different portions of the lower GI tract. The evaluation of the adhesion of Ch MICs to bacteria from the human GI microbiota was evaluated in ImageStream<sup>x</sup> after incubation of the microparticles with the bacteria and staining of the bacteria with the fluorescent dye SYTO9, which labels both live as dead bacteria.

Regarding the characterization of the size and shape of the Ch MICs, under the same conditions of incubation and reading in the ImageStream<sup>x</sup> that were used in the bacterial adhesion tests, these presented very similar average values for the features under analysis, with an average size of about  $12 \pm 3 \mu\text{m}$  in diameter and  $18 \pm 8 \mu\text{m}$  in length and with a more round shape with values close to 1 of Aspect Ratio.

Ch MICs showed to be able to indifferently adhere to the different bacterial species under study, regardless of their pathogenicity. The species *H. pylori*, *C. jejuni*, *L. casei* and *B. cereus*, seem to adhere preferentially to Ch MICs at pH 6.0, while *E. coli* and *E. faecalis* showed higher adhesion values at pH 7.5. For *E. faecalis* and *B. cereus* species, bacterial adhesion at pH 2.6 was also observed, although in smaller quantity. The higher levels of bacterial adhesion to the Ch MICs are observed, in general, at pH 6.0 and 7.5, which are pH values observed at sites of higher colonization of the human GI tract by these microorganisms.



However, this cannot be justified by the surface charge of bacteria and microspheres, since both revealed to have negative zeta potential at these pHs. At pH 6.0 *H. pylori* has a ZP of  $-6.1 \pm 0.6$  mV, *C. jejuni* of  $-5.6 \pm 0.5$  mV, *L. casei* of  $-2.9 \pm 0.3$  mV and *B. cereus* of  $-8.3 \pm 0.3$  mV, whereas Ch MIC have a ZP of  $-7.2 \pm 1.1$  mV. At pH 7.5, *E. coli* has a ZP of  $-20.9 \pm 0.7$  mV, and *E. faecalis* of  $-16.2 \pm 1.4$  mV, whereas Ch MIC have a ZP of  $-14.6 \pm 1.7$  mV.

Although ImageStream<sup>X</sup> enabled a fast evaluation of a high number of events in a short time, analysis of the results using the IDEAS 6.2 image analysis software did not allow the quantification of the number of bacteria adhered in each experimental condition.

Still, this work enabled to qualitatively evaluate the adhesion of bacteria to the Ch MICs at pH 2.6, 4.0, 6.0 and 7.5 and demonstrated that these microspheres adhere indifferently to the pathogenic and commensal species analysed, revealing their potential to be exploited in the future for clinical applications and others to adhere and remove bacteria when necessary.

## 5.2 - Future perspectives

### Quantification of the number of bacteria adhered to chitosan microspheres

Quantification of bacterial adhesion to the Ch MICs in pH 2.6, 4.0, 6.0 and 7.5 buffer appears to be an important aspect for comparisons between bacteria adhered to the Ch MICs. This quantification would also be important to better understand whether the amount of bacteria adhered to the Ch MICs is or not sufficient to eliminate pathogenic bacteria from the human GI tract, reducing or completely treating diseases caused by them, without inducing ecological changes at the balance state of the community of commensal microorganisms of the human gut microbiota.

This bacterial quantification could be accomplished by labelling the bacteria with radioactive isotopes, for example with sulfur-35 radioisotope (<sup>35</sup>S), by culturing the bacteria in their culture medium, supplemented with [<sup>35</sup>S]L-methionine (methionine amino acid labelled with <sup>35</sup>S).

*Gonçalves .I.C., et al.*, used this method for the quantification of bacteria adhered to Ch MICs through a luminescence counter (Microbeta) and determined the number of bacteria adhered per microsphere [140].

### Evaluation of the adhesion of chitosan microspheres to bacteria of the human gut microbiota in simulated gastric and intestinal fluids

The evaluation of the adhesion of Ch MICs to bacteria of the human gut microbiota in simulated gastric and intestinal fluid seems to be interesting according as these fluids in the human GI tract, in addition to a given pH, are composed of substances and molecules, such as for example, proteins that may influence the adhesion of Ch MICs to bacteria.

*Nogueira F., et al.*, demonstrated that the presence of pepsin in the medium decreased *H. pylori* adhesion to Ch films, whereas urea had no influence on bacterial adhesion to these films [147]. On the other hand, *Gonçalves I.C., et al.*, verified that the presence of pepsin in the incubation buffer had no influence on the adhesion of different strains of *H. pylori* to the Ch MICs [140].

However, the fact that pepsin in *Gonçalves I.C., et al.*, did not influence *H. pylori* adhesion, does not mean that it does not influence the adhesion of other bacteria to the Ch MICs, so it would

be interesting to note the adhesive behaviour of bacteria from the human GI microbiota to Ch MICs in the presence of proteins present in human gastric and intestinal fluids [140].

### Bacterial competition assay

In the human GI tract the bacteria of the gut microbiota are in constant competition for nutrients and sites of adhesion to the gastric and intestinal epithelial cells, so a study of bacterial competition would be interesting to evaluate, in the presence of other bacteria, the behaviour of adhesion to Ch MICs. These studies could allow to evaluate when, for example, at the same concentrations, which bacteria prevail adhered to Ch MICs or whose adhesion forces to these particles are stronger.

These tests could be evaluated by incubating *in vitro* bacteria from the human GI microbiota with Ch MICs and by electrophoresis followed by Polymerase Chain Reaction (PCR) and genetic sequencing to identify the adhered species. The bacterial quantification could be done by labelling the bacteria with different radioactive isotopes that allowed to distinguish the different species under analysis.

### *In vivo* evaluation of the adhesion of the chitosan microspheres to bacteria of the human gut microbiota

*In vivo* evaluation in an animal model of the adhesion of Ch MICs to bacteria of the GI microbiota, since in a living organism that mimics the human GI tract may allow the evaluation, more accurately, of the adhesive behaviour of these particles to the bacteria.

Subsequent to the oral ingestion of the Ch MICs in the chosen animal model, these could be collected in the faeces and, by electrophoresis followed by PCR and genetic sequencing to identify the bacterial species adhered to the Ch MICs.



# Annex

## A.1 - Evaluation of the antibacterial effect of chitosan microspheres

In an attempt to evaluate the antibacterial activity of the Ch MICs in relation to the adhered bacteria, some preliminary tests were performed in order to determine if the bacteria adherent to the Ch MICs were live or dead. This was performed by labelling adherent bacteria with fluorescent dyes for live and dead bacteria followed by visualization using ImageStream<sup>×</sup> and Spectral Confocal Microscope (SCM), as well as by the incubating of the microspheres with adherent bacteria in liquid culture media and evaluating the colony-forming units (CFU).

### A.1.1 - Live/Dead fluorescent staining

To evaluate, in a single assay, both the ability of Ch MICs adhesion to bacteria from the human GI microbiota, and the antibacterial behaviour of these microparticles, were performed optimizations of bacteria labelling with different fluorescent dyes for Live/Dead studies.

The determination of the antibacterial behaviour of Ch MICs against bacteria in the GI tract with Live/Dead tests, would involve the use of two fluorescent dyes for conducting Live/Dead studies. This studies should allow not only to detect and differentiate live bacteria from dead bacteria (with some impairment of the integrity of the cell membrane), but also to distinguish bacteria from the Ch MICs themselves which have autofluorescence.

Since the Ch MICs under study emit autofluorescence over a wide range of wavelengths (about 450 nm to 650 nm), the fluorescent dyes chosen for conducting the Live/Dead tests should have an  $\lambda_{em}$  not superimposed with the maximum  $\lambda_{em}$  of the Ch MICs, for which the intensity of its autofluorescence is greater. When excited at a  $\lambda$  of 405 nm, these microparticles emit fluorescence in the red zone of the visible light spectrum, with maximums  $\lambda_{em}$  of 477 nm and 627 nm and, when excited at  $\lambda$  of 488 nm and 561 nm, the fluorescence behaviour of the Ch MICs is the same, but only with a peak emission of 627 nm [5].

For optimization of bacteria labelling with different fluorescent dyes in ImageStream<sup>×</sup> Mark II Imaging Flow Cytometer (ImageStream<sup>×</sup>, Merck), an *E. coli* inoculum was centrifuged (Eppendorf Centrifuge 5810R) for 10min at 816g and after discarding the supernatant the bacteria pellet was resuspended in 2 ml of citrate-phosphate buffer at pH 6.0. From this bacterial inoculum 1 ml was withdrawn for two falcons of 50 ml each, for the preparation of live and dead bacteria. To the falcon corresponding to the preparation of live bacteria was added 20 ml of buffer

at pH 6.0, while to the falcon corresponding to the dead bacteria were added 20 ml of 70 % isopropyl alcohol (VWR, Germany). Both falcons were incubated in their solutions for 1h with rotation every 15 min at RT.

After 1h incubation, both falcons were centrifuged two times for 10 min at 816 g and, after the last centrifugation the bacteria pellet was resuspended in 10 ml of buffer at pH 6.0 and its OD<sub>600</sub> measured on a spectrophotometer (PerkinElmer Lambda 35 UV/VIS Spectrometer) at a dilution of 1:10. The bacterial inoculum was then adjusted in buffer at pH 6.0 to an OD<sub>600</sub> of 0.0017, which corresponds to a concentration of approximately  $1.0 \times 10^7$  CFU/ml.

For this adhesion assay in ImageStream<sup>X</sup>, 50  $\mu$ l of Ch MICs (about 2000 Ch MICs) in citrate-phosphate buffer at pH 6.0 were incubated with 25  $\mu$ l of live *E. coli* and 25  $\mu$ l of dead *E. coli* in the same buffer at a final concentration of approximately  $0.5 \times 10^7$  CFU/ml for 2 h at 37 °C and 120 rpm of stirring on an orbital shaker (IKA® KS 4000 ic control). After incubation, the samples were rinsed three times in 100  $\mu$ l buffer at pH 6.0 for 6 min and 1792 g at RT and fluorescently labelled.

SYTO9, a fluorescent dye with high affinity for cell nucleic acid binding, is one of the fluorescent labels present in the LIVE/DEAD™ Backlight™ Bacterial Viability Kit, with a maximum excitation wavelength ( $\lambda_{ex}$ ) of about 485 nm and of 498 nm of emission for DNA. This fluorescent dye is permeable to the cell membrane, generally marking all bacteria in a population, both those with intact membranes and those with damaged membranes. When excited with the ImageStream<sup>X</sup> 488 nm laser, it should emit fluorescence in the green region of the visible light spectrum, identifying in Ch02 the bacteria it labelled [163].

For identification of dead bacteria, the dye present in the LIVE/DEAD™ Backlight™ Bacterial Viability Kit is Propidium Iodide (PI). The fluorescent label PI was not tested on the ImageStream<sup>X</sup> because with the 488 nm laser the PI emission wavelength (with a maximum  $\lambda_{em}$  of 617 nm) is more intense in Ch05, the higher intensity region of the Ch MICs, which would not allow distinguishing the dead bacteria of the own autofluorescence of these microparticles. As such another dye was used.

The label DRAQ7 is a fluorescent dye with high binding affinity to the cells DNA and impermeable to the cell membrane of living cells, which allows the identification of dead cells whose cell membrane integrity has been compromised. It has a maximum  $\lambda_{ex}$  of 599/644 nm and a  $\lambda_{em}$  of 694 nm, allowing the identification of dead bacteria in the red or far-red region of the visible light spectrum. DRAQ7 can still be excited between 488-647 nm for detection in Flow Cytometry, emitting fluorescence in the far-red region of the visible light spectrum, identifying on channel 6 (Ch06) of ImageStream<sup>X</sup> the bacteria it labelled [205].

Since it was intended to determine the adhesion and antibacterial activity of Ch MICs against bacteria of the human GI microbiota in the ImageStream<sup>X</sup> Flow Cytometer, with a single excitation laser of 488 nm, SYTO9 and DRAQ7 fluorescent dyes appeared to be promising candidates. Despite SYTO9 both label live and dead cells, according to the bull of the LIVE/DEAD™ Backlight™ Bacterial Viability Kit, this marker in the presence of a specific dye for dead cells ends up replacing its binding in dead cells by the latter one.

The bacteria were then labelled with the fluorescent dye SYTO9 (LIVE/DEAD™ Backlight™ Bacterial Viability Kit L13152, Invitrogen by Thermo Scientific) at a concentration of 0.015  $\mu$ M and with DRAQ7 (BioLegend) at a concentration of 0.3 $\mu$ M and, after 15min of staining the samples were run in ImageStream<sup>X</sup> with 10.0 laser power in PBS (0.01 M, pH 7.4; Sigma- Aldrich), using the only excitation laser available, the 488nm, which should allow the observation of both MICs, due to their autofluorescence, and bacteria, since they were labelled with SYTO9 (with a maximum  $\lambda_{em}$  of 498 nm) and DRAQ7 (with a maximum  $\lambda_{em}$  of 678/694 nm). As previously

explained, before reading the samples on ImageStream<sup>X</sup>, samples were filtered through a Falcon<sup>TM</sup> Cell Strainer with a mesh size of 70  $\mu\text{m}$  (Fisher Scientific).

The same protocol was used to observe the samples in the first test in Spectral Confocal Microscope TCS-SP5 AOBS (SCM; Leica Microsystems, Germany), this time with the fluorescent dyes propidium iodide (PI, LIVE/DEAD<sup>TM</sup> Backlight<sup>TM</sup> Bacterial Viability Kit L13152, Invitrogen by Thermo Scientific) and DRAQ7 on a concentration of 0.075  $\mu\text{M}$  and 1.5  $\mu\text{M}$ , respectively, to verify if with other type of lasers, other than 488 nm of the ImageStream<sup>X</sup>, it was possible to visualize dead bacteria adherent to Ch MICs. In this case the samples were observed using the 561 nm and 405 nm lasers, at a laser power of 2 % and of 8 %, respectively.

PI is a fluorescent dye impermeable to the cell membrane of living cells, such as DRAQ7, that binds to nucleic acids, allowing the identification of dead cells with cell membrane damaged. This label has a maximum  $\lambda_{\text{ex}}$  of 535 nm and a  $\lambda_{\text{em}}$  of 617 nm, allowing the identification of dead bacteria in the red region of the visible light spectrum.

SCM was used to visualize adhesion of the Ch MICs to bacteria of the human GI microbiota in the optimization tests for bacteria labelling with different fluorescent dyes for Live/Dead studies. For this, a first step of image acquisition was performed in LAS AF software and then a step of analysing the obtained images in LAS X software. LAS X software was only used to scale the images obtained in SCM. The samples were prepared in slides with mounting medium and then covered with a coverslip and sealed with varnish. After this the samples can be stored at 4 °C protected from light, until observation in SCM.

In this case the lasers 561 and 405 nm were used to try to understand if in this instrument it would be possible to distinguish the Ch MICs autofluorescence from dead bacteria labelled with the fluorescence dyes PI or DRAQ7. The SCM used was the Leica TCS SP5 inverted confocal microscope, which provides a full range of scan speeds at the highest resolution. This microscope allows the acquisition of bright, noise-free images with minimal photo damage at high speed, as a result of the operation with three detectors with the AOBS (Acousto Optical Beam Splitter) mode.

Spectral confocal microscopy has as main advantages: 1) The ability to collect serial thin optical sections (sequentially acquired) through specimens that emit fluorescence, with a thickness up to 50 $\mu\text{m}$ ; 2) High definition and contrast, improved by the reduction or elimination of the background fluorescence information away from the focal plane, which contribute to damage the image; 3) High signal-noise relation; 4) Artifacts elimination by the optical sectioning; 5) Observation in a wide range of different conditions and with great precision of both live and fixed specimens, due to the non-invasive optical sectioning; and also 6) The restriction of the image information to a well-defined plane, instead of coming from signals with different locations in the specimen [206].

Compared to ImageStream<sup>X</sup>, SCM allows the visualization of 3D images with high contrast and resolution, in addition to having a greater number of excitation lasers. On the other hand, the amount of images obtained for the same time of analysis that in the case of ImageStream<sup>X</sup> is much smaller.

As for the principles of operation of the SCM, the excitation source of the laser, referred to as the laser system, emits light that passes through a pinhole, located in the confocal plane with a scanning point in the specimen and then the light passes through a second pinhole located in front of the photomultiplier tube, the detector.

The light produced by the excitation source, after passing the first pinhole is reflected by a dichromatic mirror and will scan the specimen in defined focal planes. This light upon contact with

the specimen will produce secondary fluorescence in the same focal plane as the incident light. This secondary fluorescent emitted from the specimen, along the lateral confocal plane, is able to cross the dichromatic mirror and is focused on the second pinhole as a confocal point. The fluorescence emitted at points not coming from the confocal plane are not focused on the second pinhole and as such are not detected by the photomultiplier and therefore do not contribute to the formation of the final image.

The image of a given specimen is obtained from the scanning, with a defined scanning pattern, of the focused beam along a defined region, by the high-speed movement of two mirrors, one on the x-axis (lateral movement) and another on the y-axis (vertical movement). This process is called the flyback in which after a single scan on the x-axis, the beam quickly passes to the starting point and begins to scan the y-axis.

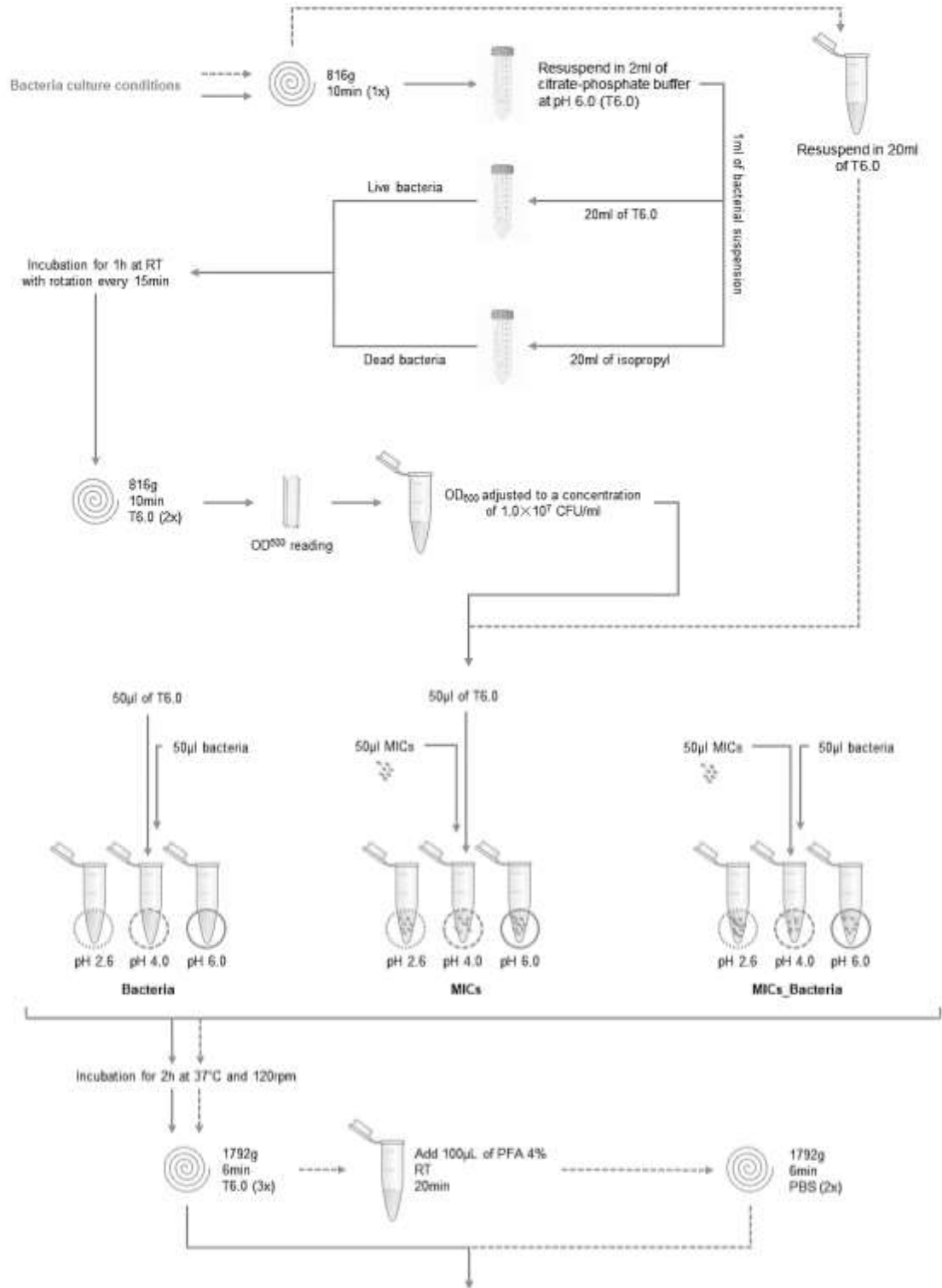
The fluorescence emitted from the specimen and which is confocal with the plane of the second pinhole passes through this hole and is converted by the photomultiplier into an electric analog signal, with a variable continuous voltage.

For the second assay in SCM, the bacterial inoculum after centrifugation at 816g for 10min, was resuspended in 20 ml of citrate-phosphate buffer at pH 6.0 and, in order to use a high amount of *E. coli*, the bacterial concentration was not adjusted. The samples preparation and incubation protocol for this assay were the same used in the previous tests. After incubation, the samples were rinsed three times in 100 $\mu$ l buffer at pH 6.0 for 6 min and 1792 g at RT. After the last centrifugation, the supernatant was discarded and the pellet resuspended in 100 $\mu$ l of paraformaldehyde 4 % (PFA, Sigma-Aldrich) during 20 min at RT, to kill the bacteria only after incubation with the Ch MICs. Then the samples were rinsed two times in PBS (0.01 M, pH 7.4; Sigma-Aldrich).

The bacteria were then labelled with the fluorescent dyes PI and DRAQ7 on a concentration of 0.075  $\mu$ M and 1.5  $\mu$ M, respectively, and the samples were observed using the 561 nm and 405nm lasers at a laser power of 19 % and of 8 %, respectively.

In the case of the ImageStream<sup>X</sup> the samples were directly visualized, whereas in the case of the SCM the samples were prepared on a microscope slide. The images obtained in ImageStream<sup>X</sup> were acquired in INSPIRE<sup>®</sup> software (INSPIRE) and analysed in IDEAS<sup>®</sup> 6.2 software (Image Data Exploration and Analysis Software, IDEAS 6.2) and the images from SCM were acquired using Leica Application Suite Advanced Fluorescence (LAS AF) software and then analyzed with the Leica Application Suite X (LAS X) software.

Figure A.1 shows the protocol scheme for the adhesion tests of Ch MICs to *E. coli* in ImageStream<sup>X</sup> and SCM for the optimization of bacteria labelling with different fluorescent dyes for Live/Dead studies.





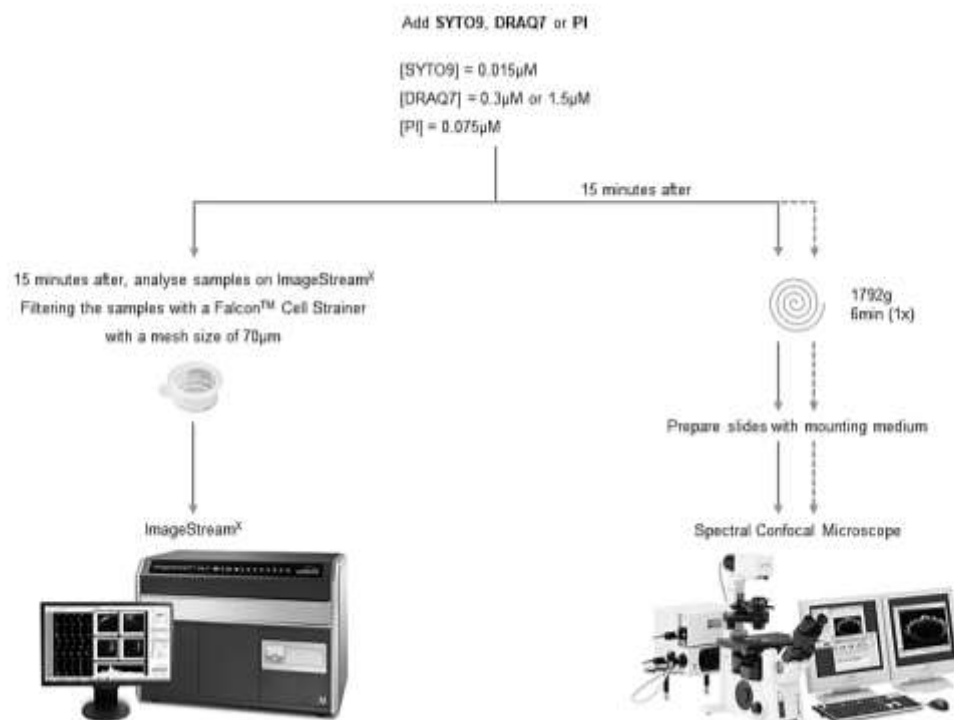


**Figure A.1** - Protocol for the adhesion tests of chitosan microspheres to *Escherichia coli* in ImageStream<sup>X</sup> and Spectral Confocal Microscope for the optimization of bacteria labelling with different fluorescent dyes for Live/Dead studies. Filled arrows indicate the pathways performed for the adhesion assay in ImageStream<sup>X</sup> and in the Spectral Confocal Microscope, with live and dead bacteria. In the case of dashed arrows correspond to the pathways performed for the adhesion assay in Spectral Confocal Microscope, with killing bacteria afterwards to the incubation.

Regarding the results obtained in the experiment performed in ImageStream<sup>X</sup>, the images are shown in Figure A.2. In the sample containing MICs\_ *E. coli*\_SYTO9\_DRAQ7 it was possible to observe in Ch02 bacteria adhered to the Ch MICs and to distinguish them from the Ch MICs autofluorescent in all channels of the ImageStream<sup>X</sup>. On the other hand, without the application of compensation in Ch06 (NoComp\_Ch06), that is, without the contribution of the Ch MICs autofluorescence in this channel, it was observed that this also appears very visible in this channel, which could difficult the detection of the bacteria labelled with DRAQ7. Compensation was then applied to Ch06 to withdraw the contribution of the fluorescence intensity of the microparticles in this channel. However, bacteria marked with DRAQ7 and therefore dead were not observed in channels 5 and 6.

As the highest fluorescence intensity for this label is expected in Ch05, after the application of the compensation matrix in Ch06, the contribution of the bacterium in Ch05 to Ch06 may be withdrawn. However, since the Ch MICs have fluorescence in Ch06, even if the bacteria were present, the most likely was not to be distinguished from the Ch MICs.

The fact that no bacteria labelled with DRAQ7 were observed could have occurred as a result of 1) The low concentration of DRAQ7 used and, therefore such a low pipetted amount that it is not known whether any dye was actually transferred to the samples with DRAQ7; 2) Non-detection of DRAQ7 in Ch06, which may be appearing in Ch05 the region of greatest intensity of the Ch MICs); or 3) As a result of dead bacteria not adhering to these microparticles. For the sample containing only *E. coli* labelled with DRAQ7 no bacteria were observed, which may have occurred, again, due to the low concentration of DRAQ7 used.

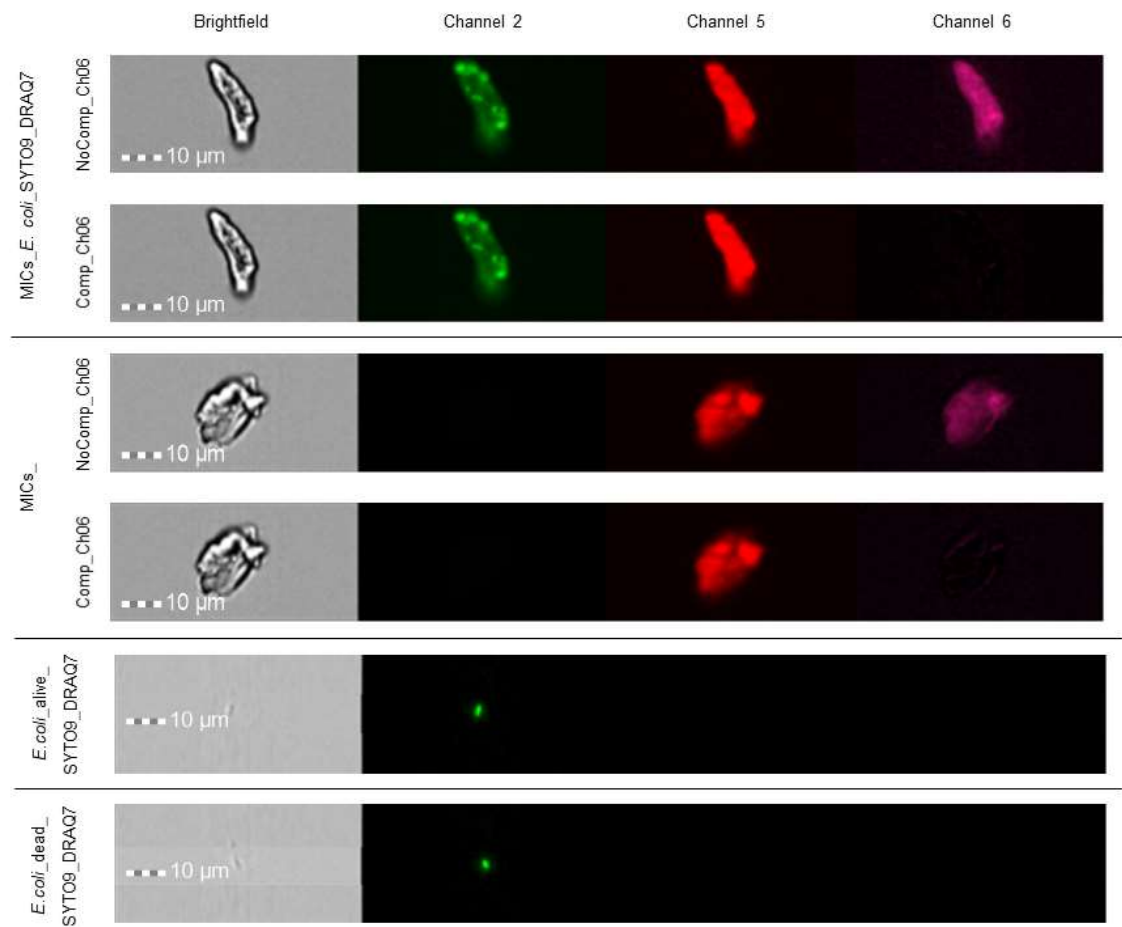


**Figure A.2** - ImageStream®X images of *Escherichia coli* Live/Dead assay with chitosan microspheres. All samples were labelled with 0.015 µM of SYTO9 and 0.3 µM of DRAQ7. Scale bar corresponds to 10 µm.

According to Pan Y. and Kaatz L., *E. coli* labelled with 1.5 µM of DRAQ7, using ImageStream<sup>X</sup> 488nm laser at a minimum power of 10.0 mW were observed in Ch05 [207]. In the case of the Ch MICs, the fact that the Ch MICs are generally visualized with greater intensity in Ch05, even though the bacteria dead cells had been labelled with DRAQ7 it might not be possible to distinguish these bacteria from the Ch MICs themselves.

In order to test with other lasers other than 488 nm whether or not it is possible to distinguish dead bacteria marked with PI or DRAQ7, it was decided to visualize the adhesion of dead bacteria to Ch MICs in the SCM. Regarding the results obtained in this assay in SCM, the images are shown in Figure A.3, and the HCX PL 40.0x1.30 OIL UV objective was used for images visualization.

Both for the MICs\_*E.coli\_dead\_PI* and for the MICs\_*E. coli\_dead\_DRAQ7* samples, no bacteria adhered to the Ch MICs were observed, as well as in the respective controls, containing only PI and DRAQ7 labelled bacteria, respectively.

These results suggest that even if the dead bacteria labelled with these fluorescent dyes can be distinguished from the autofluorescence of the Ch MICs, they could be in such low concentration that they were not detected. Bacterial labelling does not appear to be effective, since both with PI and with DRAQ7 no bacteria were detected, even in controls containing only bacteria.

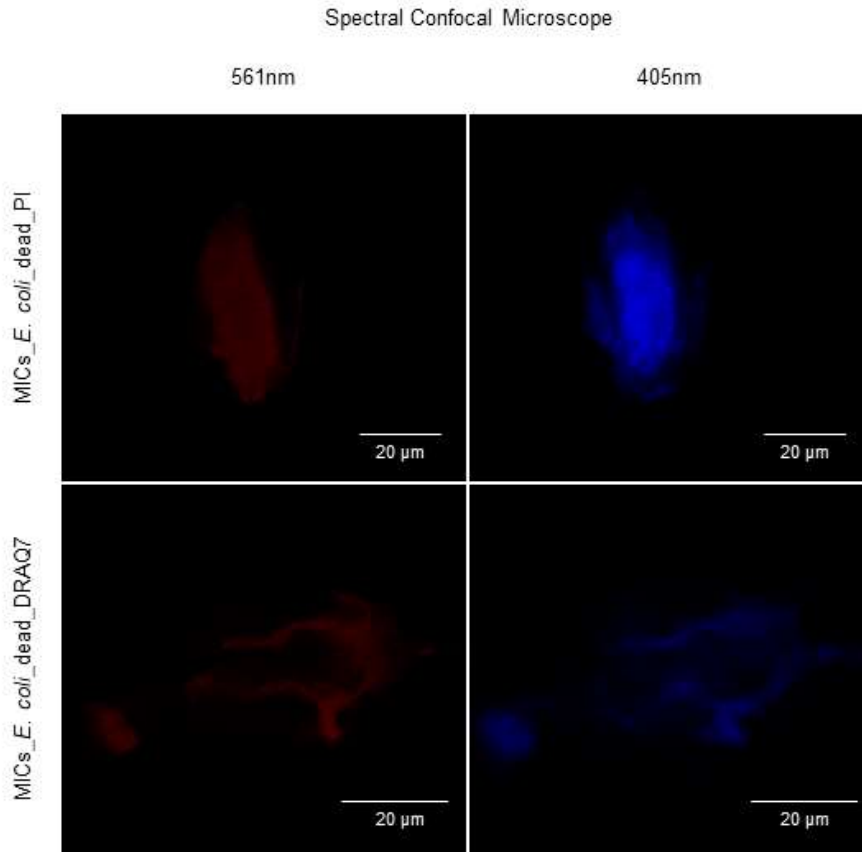


**Figure A.3** - Spectral Confocal Microscope images of dead *Escherichia coli* adhesion assay to chitosan microspheres with an HCX PL 40.0x1.30 OIL UV objective and a laser power of 2 % for 561 nm laser and 8 % for 405 nm laser. The samples were labelled with 0.075  $\mu\text{M}$  of PI and 1.5  $\mu\text{M}$  of DRAQ7, respectively. Scale bar corresponds to 20  $\mu\text{m}$ .

In order to realize if indeed in the presence of bacteria, if it is possible to distinguish them from the Ch MICs, a new assay was carried out under the same experimental conditions as the previous assay, but this time with a very high concentration of bacteria, to ensure its visualization in the samples and fixed only after incubation. The images obtained in the SCM for the 561 nm and 405 nm lasers are shown in Figure A.4, and the HCX PL 40.0x1.30 OIL UV objective was used for images visualization.

In the MICs\_E. coli\_fixed\_PI sample, only when it was increased the power of the 561 nm laser to 19% it was possible to observe bacteria in the mounting medium surrounding the Ch MICs. However, at this laser power the fluorescence intensity of the Ch MICs was so high that it did not allow the distinction of adhered bacteria to the surface of these microparticles.

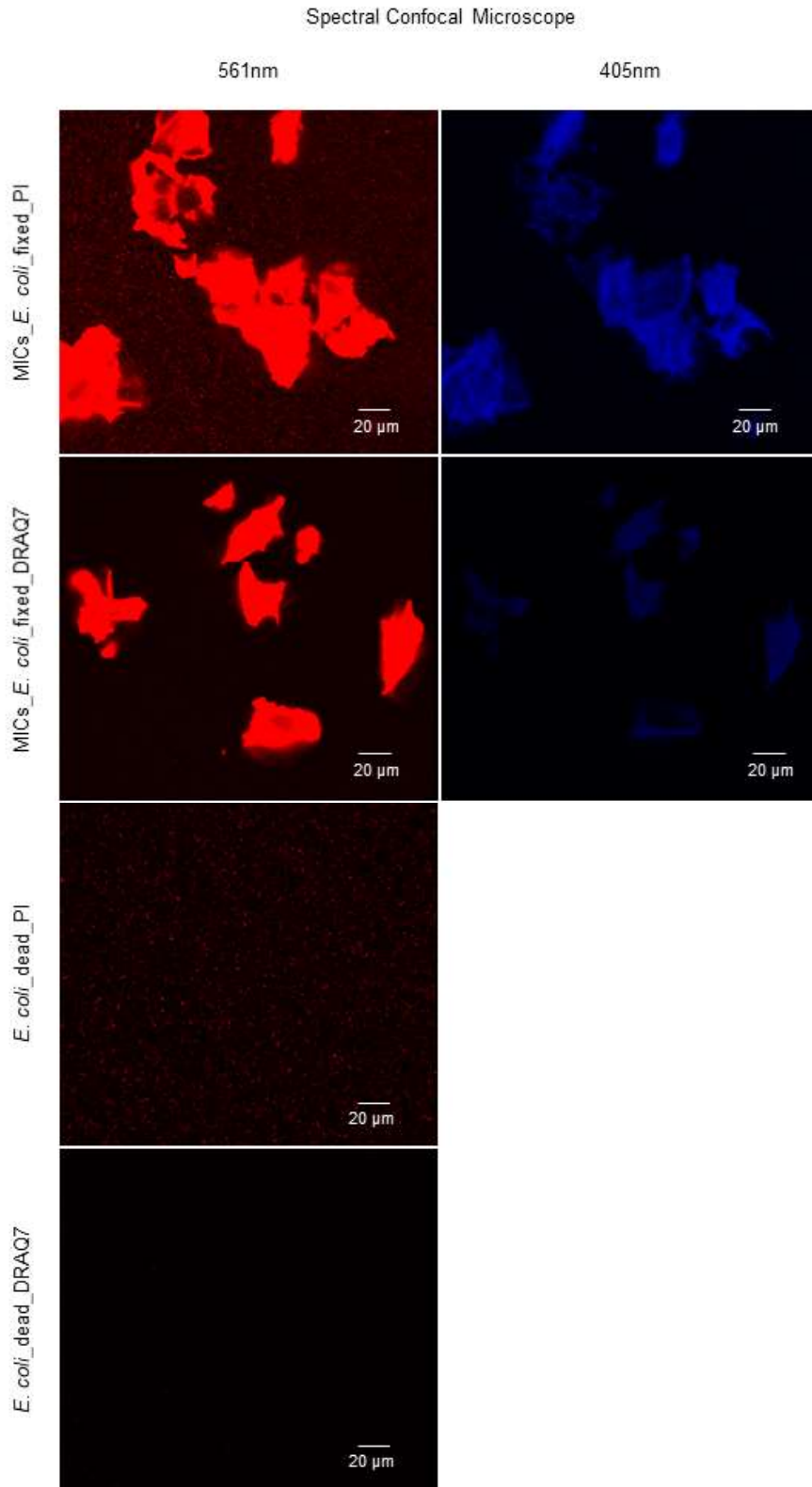


**Figure A.4** - Spectral Confocal Microscope images of fixed *Escherichia coli* adhesion assay to chitosan microspheres with an HCX PL 40.0x1.30 OIL UV objective and a laser power of 19 % for 561 nm laser and 8 % for 405 nm laser. The samples were labelled with 0.075  $\mu\text{M}$  of PI and 1.5  $\mu\text{M}$  of DRAQ7, respectively. Scale bar corresponds to 20  $\mu\text{m}$ .

In relation to the MICs *E. coli*\_fixed\_DRAQ7 sample, even at a laser power of 19% for 561 nm laser it was not possible to observe bacteria, at least at a fluorescence intensity as in the case of PI. However, in the sample containing only bacteria labelled with DRAQ7 the presence of bacteria through the brightfield was observed, meaning that it was the labelling that was no efficient.

In conclusion, PI appear to have an  $\lambda_{em}$  overlaid to the  $\lambda_{em}$  of the Ch MICs so, visually through ImageStream<sup>X</sup> and the SCM it does not appear to be possible to distinguish dead bacteria labelled with this fluorescent dye from these microparticles autofluorescence. Regarding the fluorescent label DRAQ7, there must be some problem in the labelling of the bacteria, since it was never possible to visualize them marked with this fluorescent dye.

### A.1.2 - Colony-forming units counting

Since the optimization of bacterial labelling with fluorescent dyes for Live/Dead studies did not work, antibacterial activity of Ch MICs was tested by counting CFU.

The behaviour of Ch MICs in relation to bacteria of the human GI microbiota were evaluated in order to understand if the Ch MICs, besides their capacity of adhesion to bacteria such as *H. pylori*, have a bactericidal or bacteriostatic effect on these microorganisms.

If antibacterial activity cannot be quantified using fluorescent dyes for Live/Dead studies, MICs with adherent bacteria would be incubated in fresh bacteria culture medium to allow bacteria growth and afterwards plated in solid culture medium for quantification of CFU/ml (CFU counting).

Tests for the evaluation of antibacterial effect of Ch MICs were performed only with the bacteria *E. coli* and *L. casei* with two types of Ch MICs one prepared using Ch with a DA of 6 % (XSMICs) and the other one with a diameter of ~170  $\mu\text{m}$  prepared using Ch with a DA of 16 % (XLMICs), respectively, only under the experimental conditions at pH 2.6, 4.0 and 6.0.

For the evaluation of the antibacterial effect of the Ch MICs and after culture conditions for the different bacterial species under analysis, the protocol previously established for the adhesion test described in 3.6.1 was used, although in this case it was only tested in citrate-phosphate buffer at pH 2.6, 4.0 and 6.0.

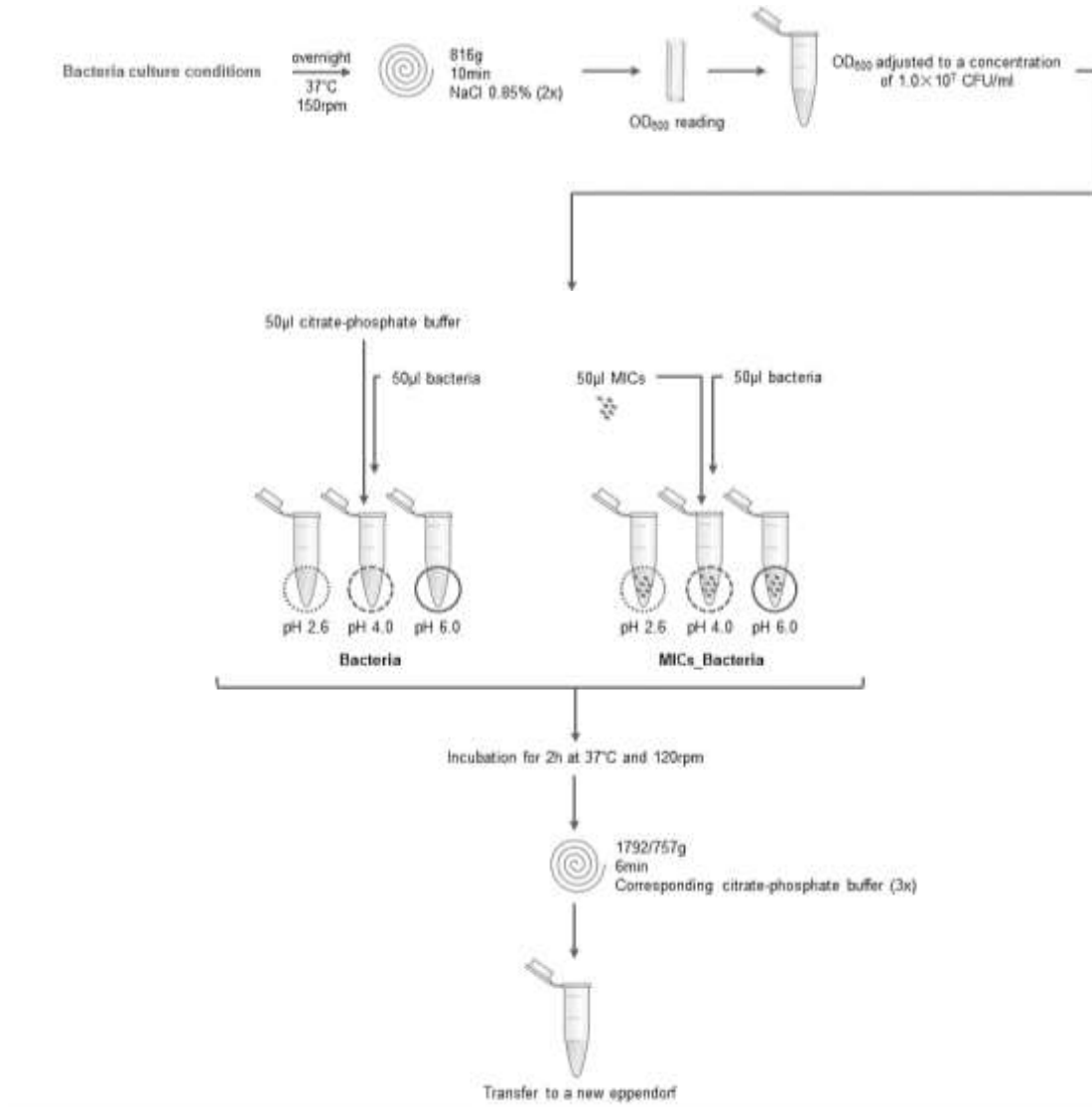
After incubation and in order to eliminate unbound bacteria, each sample was centrifuged three times in 100  $\mu\text{l}$  of citrate-phosphate buffer at the corresponding pH for 6 min and 1792 g for XSMICs and 757 g for XLMICs at RT.

The contents of the resuspended eppendorf are then transferred in the appropriate buffer to a new eppendorf in order to discard the bacteria that may be adhered to the walls of the initial eppendorf and centrifuged once again for 6 min, at 1792 g for XSMICs and 757 g for XLMICs at RT. After this last centrifugation supernatant was discard, bacterial pellet resuspended in 300  $\mu\text{l}$  of liquid culture medium (TSB for *E. coli* and MRS broth for *L. casei*) and the contents centrifuged again for 6 min and 1792 g for XSMICs and 757 g for XLMICs at RT.

After that, the supernatant was plated 2h after MICs incubation with bacteria (T2 time-point) with the following dilutions, nondiluted (ND),  $10^{-1}$ ,  $10^{-2}$  and  $10^{-3}$  in solid medium (TSA for *E. coli* and MRS agar for *L. casei*) for CFUs/ml counts, during the corresponding and proper culture time of each bacterium (24 h for *E. coli* and 48 h for *L. casei*). After this, CFU/ml were counted. This step has as main objective to eliminate all bacteria not adhered to the Ch MICs and thus guarantee the evaluation of the antibacterial activity of these microparticles to the adhered bacteria.

The material remaining in the eppendorfs of the different experimental conditions was incubated in the liquid medium in which it was present during 24 h for *E. coli* and 48 h for *L. casei*.

After this time the supernatant was plated at the time-point T2+24 for *E. coli* and T2+48 for *L. casei* with the following dilutions, ND,  $10^{-2}$ ,  $10^{-4}$  and  $10^{-6}$ , in solid medium (TSA for *E. coli* and MRS agar for *L. casei*) for counting CFU/ml during the corresponding and proper culture time of each bacterium mentioned above and after centrifugation for 6 min at 1792 g. After the culture time conditions, CFU/ml were counted. The schematic of the assay for the evaluation of the antibacterial effect of the Ch MICs is shown in the Figure A.5.



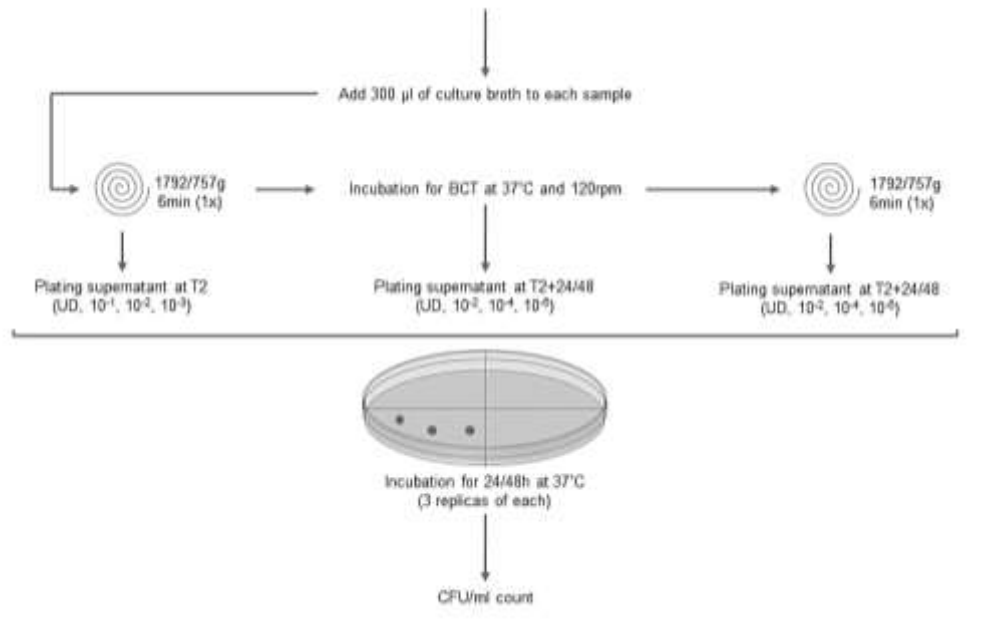


**Figure A.5** - Protocol for the evaluation of antibacterial activity of chitosan microspheres.

The first assay was carried out for the *E. coli* bacterium with smaller Ch MICs with prepared using Ch with a DA of 6 % at pH 2.6, 4.0 and 6.0 and the results obtained for time points T2, T2+24 without centrifugation (T2+24\_noCent) and T2+24 with centrifugation (T2+24\_Cent) are also shown in the graphs of the Figure A.6.

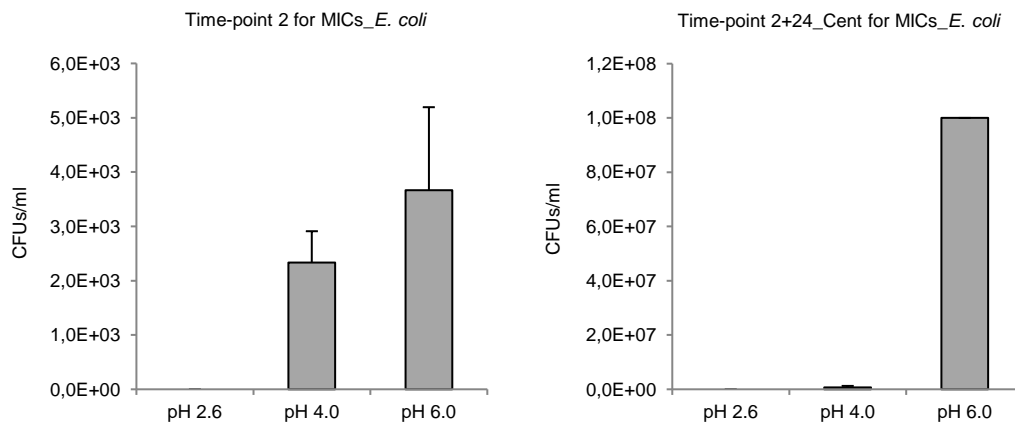


**Figure A.6** - Effect of chitosan microparticles on the growth of *Escherichia coli* at pH 2.6, 4.0 and 6.0, at different time-points (T2 and T2+24\_Cent).

The sample at pH 2.6, for all the time-points, namely T2, T2+24\_noCent and T2+24\_Cent, did not observe any bacterial growth at this pH. On the other hand, the samples at pH 4.0 and 6.0 presented bacterial growth in all time points evaluated. However, for the T2+24\_noCent time-point, the amount of bacteria was so high for the dilutions performed (up to  $10^{-3}$  dilution), that it was not possible to count CFU/ml.

In the time-point T2 bacterial growth should not be observed for any sample, since the objective of the centrifugations after the 2h incubation of the Ch MICs with the bacteria is to eliminate all the bacteria that did not adhere to the Ch MICs. Only the antibacterial activity of Ch

MICs relative to *E. coli* could be concluded, in this specific case, if no bacterial growth was observed in any of the samples in T2.

These results are indicative that the centrifugations performed after the 2 h incubation of the chitosan microspheres with the bacteria were not sufficient to eliminate all bacteria that did not adhere to the Ch MICs.

As in the protocols for the preparation of bacteria, centrifugation cycles of 816 g for 10 min were used, the number of revolutions per minute would have to be reduced below these values, so that the chitosan microspheres deposit, but the bacteria that did not adhered to these microparticles would be eliminated with the washes.

Since below 816 g, for 10 min was not sufficient to deposit these chitosan microspheres, the same assay was tested for microspheres of about 170  $\mu\text{m}$  in length, this time for the bacterium *L. casei* and with 757 g centrifugations for 6 min. The results obtained for time-points T2, T2+48 without centrifugation (T2+48\_noCent) and T2+24 with centrifugation (T2+48\_Cent) are represented in the graphs of the Figure A.7.

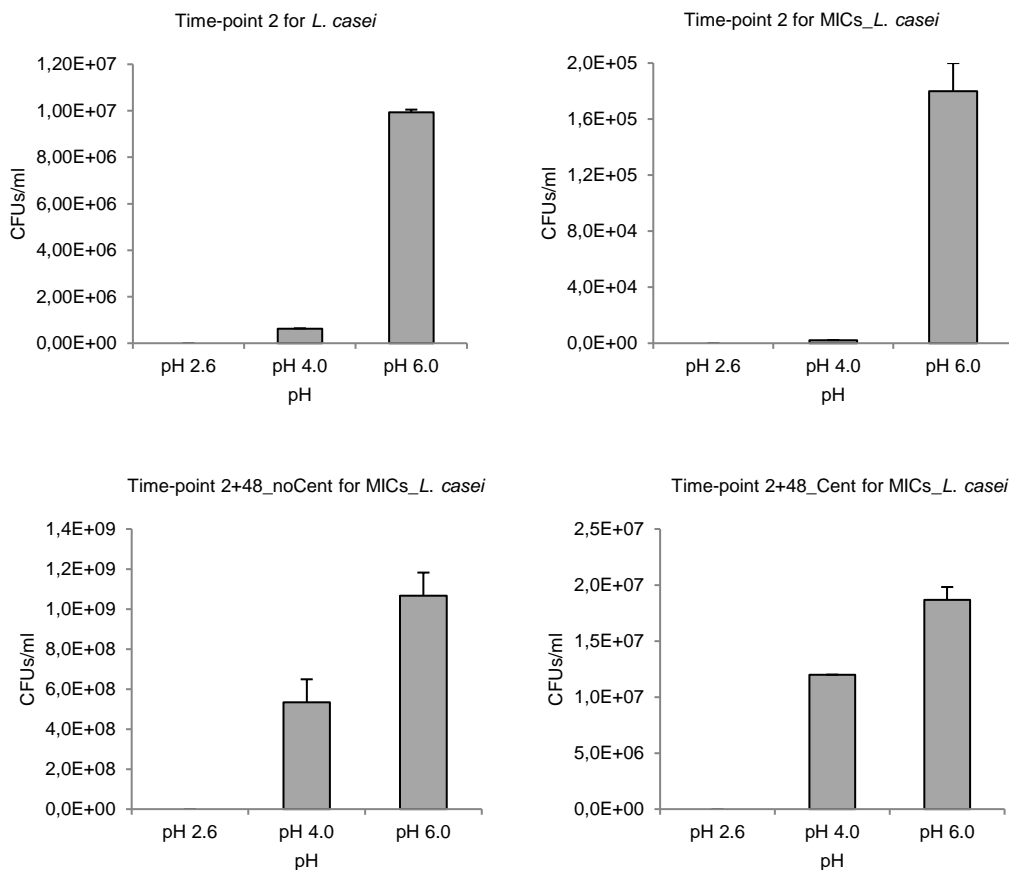


**Figure A.7** - Effect of chitosan microparticles on the growth of *Lactobacillus casei* at pH 2.6, 4.0 and 6.0, at different time-points (T2 T2+48\_noCent and T2+48\_Cent) and the control for bacterial growth without chitosan microspheres at the time-point T2.

By observing the graph of time-point T2 for the sample containing only *L. casei*, it is clear that this bacterium does not grow at pH 2.6, which means that it does not survive at such a low pH, so no bacterial growth is observed in any of the time-points at pH 2.6 analysed in this assay. On



the other hand, at time-point T2 for the sample containing Ch MICs and *L. casei* bacterial growth occurred at pH 4.0 and 6.0.

Although bacterial growth was observed for the sample containing microspheres and *L. casei* at the different time-points, the speed and time of the centrifugations, although reduced to 757 g for 6 min, was not enough to eliminate all the bacteria in suspension that did not adhere to the Ch MICs.

Thus, for the Ch MICs tested, it was not possible by the counting method of CFU/ml to evaluate the antibacterial behaviour of these same ones. Although all of the work focused on the behaviour of microspheres produced by aerodynamically driven system prepared using Ch with a DA of 6 %, these tests were also tested for Ch MICs with a diameter of ~170µm prepared using Ch with a DA of 16 %, since larger microspheres deposit better with lower centrifugation than smaller microspheres and therefore would be easier to separate the non-adhered bacteria.

## References

- [1] T. Patel, P. Bhattacharya, and S. Das, "Gut microbiota: an Indicator to Gastrointestinal Tract Diseases," *J. Gastrointest. Cancer*, vol. 47, no. 3, pp. 232–238, 2016.
- [2] S. Bellmann *et al.*, "Mammalian gastrointestinal tract parameters modulating the integrity, surface properties, and absorption of food-relevant nanomaterials," *Wiley Interdiscip. Rev. Nanomedicine Nanobiotechnology*, vol. 7, no. 5, pp. 609–622, 2015.
- [3] S. Standing, *Gray's Anatomy E-Book: The Anatomical Basis of Clinical Practice*, 41st ed. Elsevier Health Sciences, 2016.
- [4] W. Boron and E. Boulpaep, *Medical Physiology*, 3rd ed. Elsevier, 2016.
- [5] P. A. C. Henriques, "Chitosan microspheres to remove *Helicobacter pylori* adhesion in human gastric mucosa," Dissertação de Mestrado, Departamento de Bioengenharia, Faculdade de Engenharia, Universidade do Porto, Porto, 2014.
- [6] M. H. Ross and P. Wojciech, *Histology: A Text and Atlas*, 6th ed. Lippincott Williams & Wilkins, 2013.
- [7] J. Regan, C. VanPutte, and A. Russo, *Seeley's Essentials of Anatomy & Physiology*, 9th ed. New York: McGraw-Hill Education, 2016.
- [8] N. Kamada, G. Y. Chen, N. Inohara, and G. Núñez, "Control of pathogens and pathobionts by the gut microbiota," *Nat. Immunol.*, vol. 14, no. 7, pp. 685–690, 2013.
- [9] P. J. Turnbaugh, R. E. Ley, M. Hamady, C. M. Fraser-Liggett, R. Knight, and J. I. Gordon, "The Human Microbiome Project," *Nature*, vol. 449, no. 7164, pp. 804–810, 2007.
- [10] L. K. Ursell, J. L. Metcalf, L. W. Parfrey, and R. Knight, "Defining the human microbiome," *Nutr. Rev.*, vol. 70, no. suppl\_1, pp. S38–S44, 2012.
- [11] J. Qin *et al.*, "A human gut microbial gene catalog established by metagenomic sequencing," *Nature*, vol. 464, no. 7285, pp. 59–65, 2010.
- [12] C. J. Walsh, C. M. Guinane, P. W. O'Toole, and P. D. Cotter, "Beneficial modulation of the gut microbiota," *FEBS Lett.*, vol. 588, no. 22, pp. 4120–4130, 2014.
- [13] M. Rajilić-Stojanović, H. Smidt, and W. M. De Vos, "Diversity of the human gastrointestinal tract microbiota revisited," *Environ. Microbiol.*, vol. 9, no. 9, pp. 2125–2136, 2007.
- [14] M. Rajilić-Stojanović and W. M. de Vos, "The first 1000 cultured species of the human gastrointestinal microbiota," *FEMS Microbiol. Rev.*, vol. 38, no. 5, pp. 996–1047, 2014.
- [15] E. M. Bik *et al.*, "Molecular analysis of the bacterial microbiota in the human stomach.," *Proc. Natl. Acad. Sci. U. S. A.*, vol. 103, no. 3, pp. 732–7, 2006.
- [16] H. E. Jakobsson, C. Jernberg, A. F. Andersson, M. Sjölund-Karlsson, J. K. Jansson, and L. Engstrand, "Short-term antibiotic treatment has differing long-term impacts on the

- human throat and gut microbiome," *PLoS One*, vol. 5, no. 3, pp. e9836–e9836, 2010.
- [17] L. Engstrand and M. Lindberg, "*Helicobacter pylori* and the gastric microbiota," *Best Pract. Res. Clin. Gastroenterol.*, vol. 27, no. 1, pp. 39–45, 2013.
- [18] Andersson, A.F., Lindberg, M., Jakobsson, H., Backhed, F., Nyrén, P., Engstrand L., "Comparative analysis of human gut microbiota by barcoded pyrosequencing," *PLoS One*, vol. 3, no. 7, pp. e2836–e2836, 2008.
- [19] P. B. Eckburg *et al.*, "Diversity of the Human Intestinal Microbial Flora," *Science*, vol. 308, no. 5728, pp. 1635–1638, 2005.
- [20] A. Bühling, D. Radun, W. A. Müller, and P. Malfertheiner, "Influence of anti-*Helicobacter* triple-therapy with metronidazole, omeprazole and clarithromycin on intestinal microflora," *Aliment. Pharmacol. Ther.*, vol. 15, no. 9, pp. 1445–1452, 2001.
- [21] E. Myllyluoma, T. Ahlroos, L. Veijola, H. Rautelin, S. Tynkkynen, and R. Korpela, "Effects of anti-*Helicobacter pylori* treatment and probiotic supplementation on intestinal microbiota," *Int. J. Antimicrob. Agents*, vol. 29, no. 1, pp. 66–72, 2007.
- [22] V. M. Cardoso, "O microbioma humano," Dissertação de Mestrado, Departamento de Ciências Farmacêuticas, Faculdade de Ciências da Saúde, Universidade Fernando Pessoa, 2015.
- [23] M. A. P. Gonçalves, "Microbiota – implicações na imunidade e no metabolismo," Dissertação de Mestrado, Departamento de Ciências Farmacêuticas, Faculdade de Ciências da Saúde, Universidade Fernando Pessoa, 2014.
- [24] M. G. Dominguez-Bello, M. J. Blaser, R. E. Ley, and R. Knight, "Development of the human gastrointestinal microbiota and insights from high-throughput sequencing," *Gastroenterology*, vol. 140, no. 6, pp. 1713–1719, 2011.
- [25] J. Z. H. von Martels *et al.*, "The role of gut microbiota in health and disease: *In vitro* modeling of host-microbe interactions at the aerobe-anaerobe interphase of the human gut," *Anaerobe*, vol. 44, pp. 3–12, 2017.
- [26] C. Schulz, N. Koch, K. Schütte, D. H. Pieper, and P. Malfertheiner, "*H. pylori* and its modulation of gastrointestinal microbiota," *J. Dig. Dis.*, vol. 16, no. 3, pp. 109–117, 2015.
- [27] T. Patel, P. Bhattacharya, and S. Das, "Gut microbiota: an Indicator to Gastrointestinal Tract Diseases," *J. Gastrointest. Cancer*, vol. 47, no. 3, pp. 232–238, 2016.
- [28] E. Russo, A. Taddei, M. N. Ringressi, F. Ricci, and A. Amedei, "The interplay between the microbiome and the adaptive immune response in cancer development," *Therap. Adv. Gastroenterol.*, vol. 9, no. 4, pp. 594–605, 2016.
- [29] S. D. Syer *et al.*, "NSAID enteropathy and bacteria: a complicated relationship," *J. Gastroenterol.*, vol. 50, no. 4, pp. 387–393, 2015.
- [30] C. M. Galdeano and G. Perdigo, "The Probiotic Bacterium *Lactobacillus casei* Induces Activation of the Gut Mucosal Immune System through Innate Immunity," *Society*, vol. 13, no. 2, pp. 219–226, 2006.
- [31] R. D'Arienzo *et al.*, "Immunomodulatory effects of *Lactobacillus casei* administration in a mouse model of gliadin-sensitive enteropathy," *Scand. J. Immunol.*, vol. 74, no. 4, pp. 335–341, 2011.
- [32] K. M. Tuohy, M. Pinart-Gilberga, M. Jones, L. Hoyles, A. L. McCartney, and G. R. Gibson, "Survivability of a probiotic *Lactobacillus casei* in the gastrointestinal tract of healthy human volunteers and its impact on the faecal microflora," *J. Appl. Microbiol.*, vol. 102, no. 4, pp. 1026–1032, 2007.
- [33] A. V. Hartstra, M. Nieuwdorp, and H. Herrema, "Interplay between gut microbiota, its

- metabolites and human metabolism: Dissecting cause from consequence,” *Trends Food Sci. Technol.*, vol. 57, pp. 233–243, 2016.
- [34] A. A. Althani *et al.*, “Human Microbiome and its Association With Health and Diseases,” *J. Cell. Physiol.*, vol. 231, no. 8, pp. 1688–1694, 2016.
- [35] L. R. Lopetuso, F. Scaldaferri, F. Franceschi, and A. Gasbarrini, “The gastrointestinal microbiome - Functional interference between stomach and intestine,” *Best Pract. Res. Clin. Gastroenterol.*, vol. 28, no. 6, pp. 995–1002, 2014.
- [36] J. Lloyd-Price, G. Abu-Ali, and C. Huttenhower, “The healthy human microbiome,” *Genome Med.*, vol. 8, no. 1, pp. 1–11, 2016.
- [37] A. F. Andersson, M. Lindberg, H. Jakobsson, F. Bäckhed, P. Nyrén, and L. Engstrand, “Comparative analysis of human gut microbiota by barcoded pyrosequencing,” *PLoS One*, vol. 3, no. 7, pp. e2836–e2836, 2008.
- [38] A. J. Bäumlér and V. Sperandio, “Interactions between the microbiota and pathogenic bacteria in the gut,” *Nature*, vol. 535, no. 7610, pp. 85–93, 2016.
- [39] I. C. Gonçalves, P. C. Henriques, C. L. Seabra, and M. C. L. Martins, “The potential utility of chitosan micro/nanoparticles in the treatment of gastric infection,” *Expert Rev. Anti. Infect. Ther.*, vol. 12, no. 8, pp. 981–992, 2014.
- [40] E. L. McConnell, H. M. Fadda, and A. W. Basit, “Gut instincts: explorations in intestinal physiology and drug delivery,” *Int J Pharm*, vol. 364, no. 2, pp. 213–226, 2008.
- [41] S. M. Jandhyala, R. Talukdar, C. Subramanyam, H. Vuyyuru, M. Sasikala, and D. N. Reddy, “Role of the normal gut microbiota,” *World J. Gastroenterol.*, vol. 21, no. 29, pp. 8836–8847, 2015.
- [42] I. Sekirov, S. Russell, and L. Antunes, “Gut microbiota in health and disease,” *Physiol. Rev.*, vol. 90, no. 3, pp. 859–904, 2010.
- [43] R. B. Sartor, “Microbial Influences in Inflammatory Bowel Diseases,” *Gastroenterology*, vol. 134, no. 2, pp. 577–594, 2008.
- [44] J. M. DeSesso and C. F. Jacobson, “Anatomical and physiological parameters affecting gastrointestinal absorption in humans and rats,” *Food Chem. Toxicol.*, vol. 39, pp. 209–228, 2001.
- [45] A. Shafquat, R. Joice, S. L. Simmons, and C. Huttenhower, “Functional and phylogenetic assembly of microbial communities in the human microbiome,” *Trends Microbiol.*, vol. 22, no. 5, pp. 261–266, 2014.
- [46] S. Magnúsdóttir *et al.*, “Generation of genome-scale metabolic reconstructions for 773 members of the human gut microbiota,” *Nat. Biotechnol.*, vol. 35, no. 1, pp. 81–89, 2017.
- [47] C. Petersen and J. L. Round, “Defining dysbiosis and its influence on host immunity and disease,” *Cell. Microbiol.*, vol. 16, no. 7, pp. 1024–1033, 2014.
- [48] C. Kampmann, J. Dicksved, L. Engstrand, and H. Rautelin, “Composition of human faecal microbiota in resistance to *Campylobacter* infection,” *Clin. Microbiol. Infect.*, vol. 22, no. 1, pp. 61.e1-61.e8, 2016.
- [49] A. S. Rolig, C. Cech, E. Ahler, J. E. Carter, and K. M. Ottemann, “The degree of *Helicobacter pylori*-triggered inflammation is manipulated by preinfection host microbiota,” *Infect. Immun.*, vol. 81, no. 5, pp. 1382–1389, 2013.
- [50] Y. Khosravi, Y. Dieye, M. F. Loke, K. L. Goh, and J. Vadivelu, “*Streptococcus mitis* induces conversion of *Helicobacter pylori* to coccoid cells during co-culture *in vitro*,” *PLoS One*, vol. 9, no. 11, pp. 1–11, 2014.
- [51] X. Wang, “*Helicobacter pylori* infection in a mouse model: Development, optimization and

- inhibitory effects of antioxidants,” Ph.D. dissertation, Dept. of Med. Microbiol., Dermatol. & Infect., Faculty of Medicine, Lund University, Lund, 2001.
- [52] J. G. Kusters, M. M. Gerrits, J. A. G. Van Strijp, and C. M. J. E. Vandenbroucke-Grauls, “Cocoid forms of *Helicobacter pylori* are the morphologic manifestation of cell death,” *Infect. Immun.*, vol. 65, no. 9, pp. 3672–3679, 1997.
- [53] L. P. Andersen and T. Wadström, “Basic bacteriology and culture,” in *Helicobacter pylori: Physiology and Genetics*, S. L. Mobley, H.L.T., Mendz, G.L., Hazell, Ed. Washington (DC): ASM Press, 2001, p. 36.
- [54] W. Levinson, *Microbiologia médica e imunologia*, 13<sup>a</sup> ed. Porto Alegre: McGraw Hill Education, 2016.
- [55] G. Bukholm *et al.*, “Colony variation of *Helicobacter pylori*: pathogenic potential is correlated to cell wall lipid composition,” *Scand. J. Gastroenterol.*, vol. 32, no. 5, pp. 445–454, 1997.
- [56] J. F. Tomb *et al.*, “The complete genome sequence of the gastric pathogen *Helicobacter pylori*,” *Nature*, vol. 388, no. 6642, pp. 539–547, 1997.
- [57] J. G. Kusters, A. H. M. van Vliet, and E. J. Kuipers, “Pathogenesis of *Helicobacter pylori* Infection,” *Clin. Microbiol. Rev.*, vol. 19, no. 3, pp. 449–490, 2006.
- [58] C. Dunne, B. Dolan, and M. Clyne, “Factors that mediate colonization of the human stomach by *Helicobacter pylori*,” *World J. Gastroenterol.*, vol. 20, no. 19, pp. 5610–5624, 2014.
- [59] L. E. Wroblewski, R. M. Peek, and K. T. Wilson, “*Helicobacter pylori* and gastric cancer: Factors that modulate disease risk,” *Clin. Microbiol. Rev.*, vol. 23, no. 4, pp. 713–739, 2010.
- [60] J. Seyler R.W., J. W. Olson, and R. J. Maier, “Superoxide dismutase-deficient mutants of *Helicobacter pylori* are hypersensitive to oxidative stress and defective in host colonization,” *Infect. Immun.*, vol. 69, no. 6, pp. 4034–4040, 2001.
- [61] K. Stingl, K. Altendorf, and E. P. Bakker, “Acid survival of *Helicobacter pylori*: How does urease activity trigger cytoplasmic pH homeostasis?,” *Trends Microbiol.*, vol. 10, no. 2, pp. 70–74, 2002.
- [62] S. Arora, G. Bisen, and R. Budhiraja, “Mucoadhesive and muco-penetrating delivery systems for eradication of *Helicobacter pylori*,” *Asian J. Pharm.*, vol. 6, no. 1, pp. 18–30, 2012.
- [63] A. G. Harris, F. E. Hinds, A. G. Beckhouse, T. Kolesnikow, and S. L. Hazell, “Resistance to hydrogen peroxide in *Helicobacter pylori*: Role of catalase (KatA) and Fur, and functional analysis of a novel gene product designated ‘KatA-associated protein’, KapA (HP0874),” *Microbiology*, vol. 148, no. 12, pp. 3813–3825, 2002.
- [64] A. A. Olczak, R. W. Seyler, W. Jonathan, R. J. Maier, and J. W. Olson, “Association of *Helicobacter pylori* Antioxidant Activities with Host Colonization Proficiency,” *Infect. Immun.*, vol. 71, no. 1, pp. 580–583, 2003.
- [65] S. Schreiber *et al.*, “The spatial orientation of *Helicobacter pylori* in the gastric mucus,” *Proc. Natl. Acad. Sci. U. S. A.*, vol. 101, no. 14, pp. 5024–5029, 2004.
- [66] S. Backert, M. Clyne, and N. Tegtmeyer, “Molecular mechanisms of gastric epithelial cell adhesion and injection of CagA by *Helicobacter pylori*,” *Cell Commun. Signal.*, vol. 9, p. 28, 2011.
- [67] J. Yu *et al.*, “Relationship between *Helicobacter pylori* babA2 status with gastric epithelial cell turnover and premalignant gastric lesions,” *Gut*, vol. 51, no. 4, pp. 480–484, 2002.

- [68] M. Gerhard *et al.*, "Clinical relevance of the *Helicobacter pylori* gene for blood-group antigen-binding adhesin," *Proc. Natl. Acad. Sci.*, vol. 96, no. 22, pp. 12778–12783, 1999.
- [69] R. Rad *et al.*, "The *Helicobacter pylori* Blood Group Antigen-Binding Adhesin Facilitates Bacterial Colonization and Augments a Nonspecific Immune Response," *J. Immunol.*, vol. 168, no. 6, pp. 3033–3041, 2002.
- [70] H. Enroth, W. Kraaz, L. Engstrand, O. Nyrén, and T. Rohan, "Helicobacter pylori strain types and risk of gastric cancer: a case-control study.," *Cancer Epidemiol. Biomarkers Prev.*, vol. 9, no. 9, pp. 981–985, 2000.
- [71] M. Azevedo *et al.*, "Infection by *Helicobacter pylori* expressing the BabA adhesin is influenced by the secretor phenotype," *J. Pathol.*, vol. 215, no. 3, pp. 308–316, 2008.
- [72] P. Correa and J. M. Houghton, "Carcinogenesis of *Helicobacter pylori*," *Gastroenterology*, vol. 133, no. 2, pp. 659–672, 2007.
- [73] P. R. M. Polk D Brent, "*Helicobacter pylori*: gastric cancer and beyond," *Nat Rev Cancer*, vol. 10, no. 6, pp. 403–414, 2010.
- [74] D. Y. Graham and E. M. El-Omar, "*Helicobacter pylori*," *Nat. Rev. Gastroenterol. Hepatol.*, p. 1, 2013.
- [75] M. Fock Kwong Ming, Graham David Y, "*Helicobacter pylori* research: historical insights and future directions," *Nat Rev Gastroenterol Hepatol.*, vol. 10, no. 8, pp. 495–500, 2013.
- [76] N. Kim *et al.*, "Genes of *Helicobacter pylori* Regulated by Attachment to AGS Cells," *Infect. Immun.*, vol. 72, no. 4, pp. 2358–2368, 2004.
- [77] *IARC Monographs on the Evaluation of Carcinogenic Risks to Humans*. Lyon, France: International Agency for Research on Cancer, 1994.
- [78] D. Basso *et al.*, "Clinical Relevance of *Helicobacter pylori* cagA and vacA Gene Polymorphisms," *Gastroenterology*, vol. 135, no. 1, pp. 91–99, 2008.
- [79] S. Suerbaum and C. Josenhans, "*Helicobacter pylori* evolution and phenotypic diversification in a changing host," *Nat. Rev. Microbiol.*, vol. 5, no. 6, pp. 441–452, 2007.
- [80] R. P. H. Logan and M. M. Walker, "ABC of the upper gastrointestinal tract: Epidemiology and diagnosis of *Helicobacter pylori* infection.," *Bmj*, vol. 323, no. 7318, pp. 920–922, 2001.
- [81] M. Kobayashi, H. Lee, J. Nakayama, and M. Fukuda, "Carbohydrate-dependent defense mechanisms against *Helicobacter pylori* infection," *Curr. Drug Metab.*, vol. 10, no. 1, pp. 29–40, 2009.
- [82] J. Mahdavi *et al.*, "*Helicobacter pylori* SabA adhesin in persistent infection and chronic inflammation.," *Science.*, vol. 297, no. 5581, pp. 573–578, 2008.
- [83] D. Ilver *et al.*, "*Helicobacter pylori* Adhesin Binding Fucosylated Histo-Blood Group Antigens Revealed by Retagging," *Science.*, vol. 279, no. 5349, pp. 373–377, 1998.
- [84] I. C. Gonçalves *et al.*, "Bacteria-targeted biomaterials: Glycan-coated microspheres to bind *Helicobacter pylori*," *Acta Biomater.*, vol. 33, pp. 40–50, 2016.
- [85] M. Aspholm *et al.*, "SabA is the *H. pylori* hemagglutinin and is polymorphic in binding to sialylated glycans," *PLoS Pathog.*, vol. 2, no. 10, pp. 0989-1001, 2006.
- [86] P. Parreira, A. Magalhães, C. A. Reis, T. Borén, D. Leckband, and M. C. L. Martins, "Bioengineered surfaces promote specific protein–glycan mediated binding of the gastric pathogen *Helicobacter pylori*," *Acta Biomater.*, vol. 9, no. 11, pp. 8885–8893, 2013.
- [87] J. Benktander, J. Ångström, M. E. Breimer, and S. Teneberg, "Redefinition of the carbohydrate binding specificity of *Helicobacter pylori* BabA adhesin," *J. Biol. Chem.*, vol. 287, no. 38, pp. 31712–31724, 2012.

- [88] C. M. Styer *et al.*, "Expression of the BabA adhesin during experimental infection with *Helicobacter pylori*," *Infect. Immun.*, vol. 78, no. 4, pp. 1593–1600, 2010.
- [89] K. Pütsep, C. I. Brändén, H. G. Boman, and S. Normark, "Antibacterial peptide from *H. pylori*," *Nature*, vol. 398, no. 6729, pp. 671–2, 1999.
- [90] A. Muotiala, I. M. Helander, L. Pyhala, T. U. Kosunen, and A. P. Morant, "Low Biological Activity of *Helicobacter pylori* Lipopolysaccharide," *Microbiology*, vol. 60, no. 4, pp. 1714–1716, 1992.
- [91] B. J. Appelmelk, R. Negrini, A. P. Moran, and E. J. Kuipers, "Molecular mimicry between *Helicobacter pylori* and the host," *Trends Microbiol.*, vol. 5, no. 2, pp. 70–73, 1997.
- [92] B. Ma, J. L. Simala-Grant, and D. E. Taylor, "Fucosylation in prokaryotes and eukaryotes," *Glycobiology*, vol. 16, no. 12, p. 158R–184R, 2006.
- [93] P. M. Lepper, M. Triantafilou, C. Schumann, E. M. Schneider, and K. Triantafilou, "Lipopolysaccharides from *Helicobacter pylori* can act as antagonists for Toll-like receptor 4," *Cell. Microbiol.*, vol. 7, no. 4, pp. 519–528, 2005.
- [94] J. C. Atherton, "The Pathogenesis of *Helicobacter pylori* - Induced Gastrointestinal Diseases," *Annu. Rev. Pathol. Mech. Dis.*, vol. 1, no. 1, pp. 63–96, 2006.
- [95] R. M. L. Pontes, "A erradicação do *Helicobacter pylori* na actualidade e o problema da resistência," Dissertação de Mestrado, Departamento de Medicina, Instituto de Ciências Biomédicas Abel Salazar, Universidade do Porto, Porto, 2014.
- [96] E. M. Malfertheiner, P., Megraud, F., O'Morain, C.A., Gisbert, J.P., Kuipers, E.J., Axon, A.T., Bazzoli, F., Gasbarrini, A., Atherton, J., Graham, D.Y., Hunt, R., Moayyedi, P., Rokkas, T., Rugge, M., Selgrad, M., Suerbaum, S., Sugano, K., El-Omar, "Management of *Helicobacter pylori* infection-the Maastricht V/Florence consensus report," *Gut*, vol. 0, pp. 1–25, 2016.
- [97] H. K. Parsons, M. J. Carter, D. S. Sanders, T. Winstanley, and a J. Lobo, "*Helicobacter pylori* antimicrobial resistance in the United Kingdom: the effect of age, sex and socio-economic status.," *Aliment. Pharmacol. Ther.*, vol. 15, no. 9, pp. 1473–8, 2001.
- [98] P. Malfertheiner *et al.*, "Management of *Helicobacter pylori* infection - The Maastricht IV/ Florence consensus report," *Gut*, vol. 61, no. 5, pp. 646–664, 2012.
- [99] R. Hejazi and M. Amiji, "Stomach-specific anti- *H. pylori* therapy Part III : Effect of chitosan microspheres crosslinking on the gastric residence and local tetracycline concentrations in fasted gerbils," vol. 272, no. 1-2, pp. 99–108, 2004.
- [100] Y. Niv and R. Hazazi, "*Helicobacter pylori* Recurrence in Developed and Developing Countries: Meta-Analysis of 13 C-Urea Breath Test Follow-Up after Eradication," *Helicobacter*, vol. 13, no. 1, pp. 56–61, 2008.
- [101] J. C. Thijs, A. A. Van Zwet, W. Moolenaar, M. Wolfhagen, and J. ten Bokkel Huinink, "Triple therapy vs. amoxicillin plus omeprazole for treatment of *Helicobacter pylori* infection: a multicenter, prospective, randomized, controlled study of efficacy and side effects," *Am. J. Gastroenterol.*, vol. 91, pp. 93–97, 1996.
- [102] R. Hejazi and M. Amiji, "Stomach-specific anti-*H. pylori* therapy. I: Preparation and characterization of tetracycline-loaded chitosan microspheres," *Int. J. Pharm.*, vol. 235, no. 1-2, pp. 87–94, 2002.
- [103] G. Fontana, M. Licciardi, S. Mansueto, D. Schillaci, and G. Giammona, "Amoxicillin-loaded polyethylcyanoacrylate nanoparticles: Influence of PEG coating on the particle size, drug release rate and phagocytic uptake," *Biomaterials*, vol. 22, no. 21, pp. 2857–2865, 2001.
- [104] "Cancro do Estômago," 2017. [Online]. Available: <https://www.saudecuf.pt/oncologia/o->

- cancro/cancro-do-estomago. [Accessed: 01-Nov-2017].
- [105] N. Petrovsky and J. C. Aguilar, "Vaccine adjuvants : Current state and future trends," *Immunol. Cell Biol.*, vol. 82, no. 5, pp. 488–496, 2004.
- [106] G. Ayala, W. I. Escobedo-Hinojosa, C. F. de La Cruz-Herrera, and I. Romero, "Exploring alternative treatments for *Helicobacter pylori* infection," *World J. Gastroenterol.*, vol. 20, no. 6, pp. 1450–1469, 2014.
- [107] C.-F. Flach, N. Svensson, M. Blomquist, A. Ekman, S. Raghavan, and J. Holmgren, "A truncated form of HpaA is a promising antigen for use in a vaccine against *Helicobacter pylori*," *Vaccine*, vol. 29, no. 6, pp. 1235–1241, 2011.
- [108] P. Malfertheiner *et al.*, "Safety and Immunogenicity of an Intramuscular *Helicobacter pylori* Vaccine in Noninfected Volunteers: A Phase I Study," *Gastroenterology*, vol. 135, no. 3, pp. 787–795, 2008.
- [109] C. Romero, E. Medina, J. Vargas, M. Brenes, and A. De Castro, "In vitro activity of olive oil polyphenols against *Helicobacter pylori*," *J. Agric. Food Chem.*, vol. 55, no. 3, pp. 680–686, 2007.
- [110] C. L. Seabra *et al.*, "Docosahexaenoic acid loaded lipid nanoparticles with bactericidal activity against *Helicobacter pylori*," *Int. J. Pharm.*, vol. 519, no. 1–2, pp. 128–137, 2017.
- [111] H. Cetin-Karaca, "Evaluation of Natural Antimicrobial Phenolic Compounds Against Foodborne Pathogens," Master dissertation, College of Agriculture, University of Kentucky, Kentucky, 2011.
- [112] J. K. Y. Hooi *et al.*, "Global Prevalence of *Helicobacter pylori* Infection: Systematic Review and Meta-Analysis," *Gastroenterology*, vol. 153, no. 2, pp. 420–429, 2017.
- [113] M. Correia *et al.*, "Docosahexaenoic Acid Inhibits *Helicobacter pylori* Growth In Vitro and Mice Gastric Mucosa Colonization," *PLoS One*, vol. 7, no. 4, pp. e35072–e35072, 2012.
- [114] A. P. Desbois and V. J. Smith, "Antibacterial free fatty acids: activities, mechanisms of action and biotechnological potential.," *Appl. Microbiol. Biotechnol.*, vol. 85, no. 6, pp. 1629–1642, 2010.
- [115] P. Gao, X. Nie, M. Zou, Y. Shi, and G. Cheng, "Recent advances in materials for extended-release antibiotic delivery system," *J. Antibiot. (Tokyo)*, vol. 64, no. 9, pp. 625–634, 2011.
- [116] S. Shah, R. Qaqish, V. Patel, and M. Amiji, "Evaluation of the Factors Influencing Stomach-specific Delivery of Antibacterial Agents for *Helicobacter pylori* Infection," *J. Pharm. Pharmacol.*, vol. 51, no. 1, pp. 667–672, 1999.
- [117] N. Nagahara, Y. Akiyama, M. Nakao, M. Tada, M. Kitano, and Y. Ogawa, "Mucoadhesive microspheres containing amoxicillin for clearance of *Helicobacter pylori*," *Antimicrob. Agents Chemother.*, vol. 42, no. 10, pp. 2492–2494, 1998.
- [118] M. P. Cooreman, P. Krausgrill, and K. J. Hengels, "Local gastric and serum amoxicillin concentrations after different oral application forms," *Antimicrob. Agents Chemother.*, vol. 37, no. 7, pp. 1506–1509, 1993.
- [119] S. Zhao, Y. Lv, J.-B. Zhang, B. Wang, G.-J. Lv, and X.-J. Ma, "Gastroretentive drug delivery systems for the treatment of *Helicobacter pylori*," *World J. Gastroenterol.*, vol. 20, no. 28, pp. 9321–9329, 2014.
- [120] G. Rajput, F. Majmudar, J. Patel, R. Thakor, and N. Rajgor, "Stomach-Specific Mucoadhesive Microsphere as a Controlled Drug Delivery System," *Syst. Rev. Pharm.*, vol. 1, no. 1, pp. 70–78, 2010.
- [121] N. A. Peppas and J. J. Sahlin, "Hydrogels as mucoadhesive and bioadhesive materials: A review," *Biomaterials*, vol. 17, no. 16, pp. 1553–1561, 1996.



- [122] S. Dhawan, A. K. Singla, and V. R. Sinha, "Evaluation of Mucoadhesive Properties of Chitosan Microspheres Prepared by Different Methods," *AAPS PharmSciTech*, vol. 5, no. 4, pp. 122–128, 2004.
- [123] D. Sendil, I. Gursel, and D. L. Wise, "Antibiotic release from biodegradable PHBV microparticles," vol. 59, no. 2, pp. 207–217, 1999.
- [124] R. Saini, J. Bajpai, and A. K. Bajpai, "Synthesis of Poly (2-Hydroxyethyl Methacrylate) (PHEMA) Based Nanoparticles for Biomedical and Pharmaceutical Applications," *Nanoparticles Biol. Med.*, vol. 95, no. 4, pp. 1921–9, 2012.
- [125] R. Hejazi and M. Amiji, "Chitosan-based gastrointestinal delivery systems," *J. Control. Release*, vol. 89, no. 2, pp. 151–165, 2003.
- [126] F. Croisier and C. Jérôme, "Chitosan-based biomaterials for tissue engineering," *Eur. Polym. J.*, vol. 49, no. 4, pp. 780–792, 2013.
- [127] S. Mao, W. Sun, and T. Kissel, "Chitosan-based formulations for delivery of DNA and siRNA," *Adv. Drug Deliv. Rev.*, vol. 62, no. 1, pp. 12–27, 2010.
- [128] F. L. Mi, H. W. Sung, and S. S. Shyu, "Synthesis and characterization of a novel chitosan-based network prepared using naturally occurring crosslinker," *J. Polym. Sci. Part A Polym. Chem.*, vol. 38, no. 15, pp. 2804–2814, 2000.
- [129] D. Luo *et al.*, "Preparation and Evaluation of Anti-*Helicobacter pylori* Efficacy of Chitosan Nanoparticles in Vitro and in Vivo," *J. Biomater. Sci.*, vol. 20, no. 11, pp. 1587–1596, 2009.
- [130] C. A. Martínez-Huitile, N. S. Fernandes, M. Cerro-Lopez, M.A. Quiroz, and M. A. Quiroz, "Determination of Trace Metals by Differential Pulse Voltammetry at Chitosan Modified Electrodes," *Port. Electrochim. Acta*, vol. 28, no. 1, pp. 39–49, 2010.
- [131] M. Dash, F. Chiellini, R. M. Ottenbrite, and E. Chiellini, "Chitosan - A versatile semi-synthetic polymer in biomedical applications," *Prog. Polym. Sci.*, vol. 36, no. 8, pp. 981–1014, 2011.
- [132] T. Jiang, M. Deng, R. James, L. S. Nair, and C. T. Laurencin, "Micro- and nanofabrication of chitosan structures for regenerative engineering," *Acta Biomater.*, vol. 10, no. 4, pp. 1632–1645, 2014.
- [133] F. Mi, H. Sung, S. Shyu, C. Su, and C. Peng, "Synthesis and characterization of biodegradable TPP/genipin co-crosslinked chitosan gel beads," *Polymer (Guildf)*, vol. 44, no. 21, pp. 6521–6530, 2003.
- [134] M. Hosseinejad and S. M. Jafari, "Evaluation of different factors affecting antimicrobial properties of chitosan," *Int. J. Biol. Macromol.*, vol. 85, pp. 467–475, 2016.
- [135] H. Q. Mao *et al.*, "Chitosan-DNA nanoparticles as gene carriers: Synthesis, characterization and transfection efficiency," *J. Control. Release*, vol. 70, no. 3, pp. 399–421, 2001.
- [136] F. Mi, H. Sung, S. Shyu, C. Su, and C. Peng, "Synthesis and characterization of biodegradable TPP/genipin co-crosslinked chitosan gel beads," vol. 44, no. 21, pp. 6521–6530, 2003.
- [137] M. P. Patel, R. R. Patel, and J. K. Patel, "Chitosan mediated targeted drug delivery system: a review," *J. Pharm. Pharm. Sci.*, vol. 13, no. 4, pp. 536–557, 2010.
- [138] A. M. S. Costa, "Chitosan microspheres for *Helicobacter pylori* infection treatment: a study using gastric mucosa models," Dissertação de Mestrado, Departamento de Bioengenharia, Faculdade de Engenharia, Universidade do Porto, Porto, 2013.
- [139] S. Rodrigues, M. Dionísio, C. R. López, and A. Grenha, "Biocompatibility of Chitosan Carriers with Application in Drug Delivery," *J. Funct. Biomater.*, vol. 3, no. 4, pp. 615–641,

- 2012.
- [140] I. C. Gonçalves, A. Magalhães, M. Fernandes, I. V. Rodrigues, C. A. Reis, and M. C. L. Martins, "Bacterial-binding chitosan microspheres for gastric infection treatment and prevention," *Acta Biomater.*, vol. 9, no. 12, pp. 9370–9378, 2013.
- [141] M. Kong, X. G. Chen, K. Xing, and H. J. Park, "Antimicrobial properties of chitosan and mode of action: A state of the art review," *Int. J. Food Microbiol.*, vol. 144, no. 1, pp. 51–63, 2010.
- [142] P. He, S. S. Davis, and L. Illum, "In vitro evaluation of the mucoadhesive properties of chitosan microspheres," *Int. J. Pharm.*, vol. 166, no. 1, pp. 75–88, 1998.
- [143] J. Woodley, "Bioadhesion: new possibilities for drug administration?," *Clin. Pharmacokinet.*, vol. 40, no. 2, pp. 77–84, 2001.
- [144] Y. Akiyama *et al.*, "Evaluation of oral mucoadhesive microspheres in man on the basis of the pharmacokinetics of furosemide and riboflavin, compounds with limited gastrointestinal absorption sites," *J. Pharm. Pharmacol.*, vol. 50, no. 2, pp. 159–166, 1998.
- [145] J. Yang *et al.*, "Development of chitosan-sodium phytate nanoparticles as a potent antibacterial agent," *Carbohydr. Polym.*, vol. 178, pp. 311–321, 2017.
- [146] M. Fernandes, I. C. Gonçalves, S. Nardecchia, I. F. Amaral, M. A. Barbosa, and M. C. L. Martins, "Modulation of stability and mucoadhesive properties of chitosan microspheres for therapeutic gastric application," *Int. J. Pharm.*, vol. 454, no. 1, pp. 116–124, 2013.
- [147] F. Nogueira, I. C. Gonçalves, and M. C. L. Martins, "Effect of gastric environment on *Helicobacter pylori* adhesion to a mucoadhesive polymer," *Acta Biomater.*, vol. 9, no. 2, pp. 5208–5215, 2013.
- [148] M. Arkoun, F. Daigle, M. C. Heuzey, and A. Ajji, "Mechanism of Action of Electrospun Chitosan-Based Nanofibers Against Meat Spoilage and Pathogenic Bacteria," *Molecules*, vol. 22, no. 4, p. 585, 2017.
- [149] H. Liu, Y. Du, X. Wang, and L. Sun, "Chitosan kills bacteria through cell membrane damage," *Int. J. Food Microbiol.*, vol. 95, no. 2, pp. 147–155, 2004.
- [150] Y. Chung *et al.*, "Relationship between antibacterial activity of chitosan and surface characteristics of cell wall.," *Acta Pharmacol. Sin.*, vol. 25, no. 7, pp. 932–936, 2004.
- [151] T. Takahashi, M. Imai, I. Suzuki, and J. Sawai, "Growth inhibitory effect on bacteria of chitosan membranes regulated with deacetylation degree," *Biochem. Eng. J.*, vol. 40, no. 3, pp. 485–491, 2008.
- [152] L. M. R. Costa, "*In vivo* mouse model to evaluate glycan-coated microparticles as *H. pylori* treatment," Dissertação de Mestrado, Departamento de Bioengenharia, Faculdade de Engenharia, Universidade do Porto, Porto, 2015.
- [153] A. Z. Wilczewska, K. Niemirowicz, K. H. Markiewicz, and H. Car, "Nanoparticles as drug delivery systems," *Pharmacol. Reports*, vol. 64, no. 5, pp. 1020–1037, 2012.
- [154] D. Lopes, C. Nunes, M. C. L. Martins, B. Sarmiento, and S. Reis, "Eradication of *Helicobacter pylori*: Past, present and future," *J. Control. Release*, vol. 189, pp. 169–186, 2014.
- [155] A. Mitra and B. Dey, "Chitosan microspheres in novel drug delivery systems," *Indian J. Pharm. Sci.*, vol. 73, no. 4, pp. 355–366, 2011.
- [156] G. Crini and P.-M. Badot, "Application of chitosan, a natural aminopolysaccharide, for dye removal from aqueous solutions by adsorption processes using batch studies: a review of recent literature," *Prog. Polym. Sci.*, vol. 33, no. 4, pp. 399–447, 2008.
- [157] J. Ko, H. Park, S. Hwang, J. Park, and J. Lee, "Preparation and characterization of

- chitosan microparticles intended for controlled drug delivery," *Int. J. Pharm.*, vol. 249, no. 1–2, pp. 165–174, 2002.
- [158] Y. Dong, W. K. Ng, S. Shen, S. Kim, and R. B. H. Tan, "Scalable ionic gelation synthesis of chitosan nanoparticles for drug delivery in static mixers," *Carbohydr. Polym.*, vol. 94, no. 2, pp. 940–945, 2013.
- [159] F. Mi, S. Shyu, S. Lee, and T. Wong, "Kinetic Study of Chitosan-Tripolyphosphate Complex Reaction and Acid-Resistive Properties of the Chitosan-Tripolyphosphate Gel Beads Prepared by in-Liquid Curing Method," *J. Polym. Sci. B: Polym Phys.*, vol. 37, no. 14, pp. 1551–1564, 1999.
- [160] C. H. Yao, B. S. Liu, C. J. Chang, S. H. Hsu, and Y. S. Chen, "Preparation of networks of gelatin and genipin as degradable biomaterials," *Mater. Chem. Phys.*, vol. 83, no. 2–3, pp. 204–208, 2004.
- [161] F. Mi, H. Sung, and S. Shyu, "Release of Indomethacin from a Novel Chitosan Microsphere Prepared by a Naturally Occurring Crosslinker : Examination of Crosslinking and Polycation – Anionic Drug Interaction," *J. Appl. Polymer Sci.*, vol. 81, no. 7, pp. 1700–1711, 2001.
- [162] L. Boulos, M. Prevost, B. Barbeau, J. Coallier, and R. Desjardins, "LIVE/DEAD BacLight : Application of a new rapid Staining Method for Direct Enumeration of viable and total Bacteria in drinking Water," *J. Microbiol. Methods*, vol. 37, no. 1, pp. 77–86, 1999.
- [163] "LIVE/DEAD® BacLight™ Bacterial Viability Kits," *Thermo Fisher Scientific*, 2004. [Online]. Available: <https://www.thermofisher.com/order/catalog/product/L7007>. [Accessed: 15-Sep-2017].
- [164] W. Wang, X. Ding, Q. Xu, J. Wang, L. Wang, and X. Lou, "Zeta-potential data reliability of gold nanoparticle biomolecular conjugates and its application in sensitive quantification of surface absorbed protein," *Colloids Surfaces B Biointerfaces*, vol. 148, pp. 541–548, 2016.
- [165] I. C. Henriques, P.C., Costa, L.M., Seabra, C.L., Antunes, B., Silva-Carvalho, R., Junqueira-Neto, S., Maia, A.F., Oliveira, P., Magalhães, A., Reis, C.A., Gartner, F., Touati, E., Gomes, J., Costa, P., Martins, M.C.L., Gonçalves, "Biocompatible and mucoadhesive chitosan microspheres inhibit *Helicobacter pylori* gastric colonization in mice," *Biomaterials*, 2018 (Submitted).
- [166] H. Zhu, C. A. Hart, D. Sales, and N. B. Roberts, "Bacterial killing in gastric juice - Effect of pH and pepsin on Escherichia coli and *Helicobacter pylori*," *J. Med. Microbiol.*, vol. 55, no. 9, pp. 1265–1270, 2006.
- [167] S. Baatout, N. Leys, L. Hendrickx, A. Dams, and M. Mergeay, "Physiological changes induced in bacteria following pH stress as a model for space research," *Acta Astronaut.*, vol. 60, no. 4–7, pp. 451–459, 2007.
- [168] R. D. Haigh and J. M. Ketley, "Growth of *Campylobacter* using a microplate reader equipped with ACU," *BMG LABTECH*, 2011. [Online]. Available: <https://www.bmglabtech.com/pt/growth-of-campylobacter-using-a-microplate-reader-equipped-with-acu/>. [Accessed: 01-Aug-2018].
- [169] J. Silva, D. Leite, M. Fernandes, C. Mena, P. A. Gibbs, and P. Teixeira, "*Campylobacter* spp. as a foodborne pathogen: a review," *Front. Microbiol.*, vol. 2, p. 200, 2011.
- [170] J. A. Wright *et al.*, "Metabolite and transcriptome analysis of *Campylobacter jejuni* *in vitro* growth reveals a stationary-phase physiological switch," *Microbiology*, vol. 155, no. 1, pp. 80–94, 2009.
- [171] F. Hilbert, M. Scherwitzel, P. Paulsen, and M. P. Szostak, "Survival of *Campylobacter*

- jejuni* under conditions of atmospheric oxygen tension with the support of *Pseudomonas* spp,” *Appl. Environ. Microbiol.*, vol. 76, no. 17, pp. 5911–5917, 2010.
- [172] R. T. Melo *et al.*, “Intrinsic and extrinsic aspects on *Campylobacter jejuni* Biofilms,” *Front. Microbiol.*, vol. 8, p. 1332, 2017.
- [173] C. Murphy, C. Carroll, and K. N. Jordan, “Environmental survival mechanisms of the foodborne pathogen *Campylobacter jejuni*,” *J. Appl. Microbiol.*, vol. 100, no. 4, pp. 623–632, 2006.
- [174] G. Reshes, S. Vanounou, I. Fishov, and M. Feingold, “Cell shape dynamics in *Escherichia coli*,” *Biophys. J.*, vol. 94, no. 1, pp. 251–264, 2008.
- [175] J. Jang, H. G. Hur, M. J. Sadowsky, M. N. Byappanahalli, T. Yan, and S. Ishii, “Environmental *Escherichia coli*: ecology and public health implications—a review,” *J. Appl. Microbiol.*, vol. 123, no. 3, pp. 570–581, 2017.
- [176] L. Grozdanov *et al.*, “Analysis of the Genome Structure of the Nonpathogenic Probiotic *Escherichia coli* Strain Nissle 1917,” *J. Bacteriol.*, vol. 186, no. 16, pp. 5432–41, 2004.
- [177] O. Tenailon, D. Skurnik, B. Picard, and E. Denamur, “The population genetics of commensal *Escherichia coli*,” *Nat. Rev. Microbiol.*, vol. 8, no. 3, pp. 207–217, 2010.
- [178] N. Nanninga, “Morphogenesis of *Escherichia coli*,” *Microbiol Mol Biol Rev.*, *Microbiol. Mol. Biol. Rev.*, vol. 62, no. 1, pp. 110–125, 1998.
- [179] Z. D. Blount, “The unexhausted potential of *E. coli*,” *Elife*, vol. 4, p. e05826, 2015.
- [180] D. a N. Zilberstein, V. Agmon, and E. Padan, “*Escherichia coli* Intracellular pH, Membrane Potential, and Cell Growth,” vol. 158, no. 1, pp. 246–252, 1984.
- [181] J. W. Sahl *et al.*, “Examination of the Enterotoxigenic *Escherichia coli* Population Structure during Human Infection,” vol. 6, no. 3, pp. 1–6, 2015.
- [182] E. Stefanovic, A. Casey, P. Cotter, D. Cavanagh, G. Fitzgerald, and O. McAuliffe, “Draft Genome Sequence of *Lactobacillus casei* DPC6800, an Isolate with the Potential to Diversify Flavor in Cheese,” *Genome Announc.*, vol. 4, no. 2, pp. e00063-16, 2016.
- [183] E. J. C. Goldstein, K. L. Tyrrell, and D. M. Citron, “*Lactobacillus* species: Taxonomic complexity and controversial susceptibilities,” *Clin. Infect. Dis.*, vol. 60, no. S2, pp. S98–S107, 2015.
- [184] A. Lahtinen, S., Ouwehand, A.C., Salminen, S., von Wright, *Lactic Acid Bacteria: Microbiological and Functional Aspects*, 4th ed. CRC Press, 2011.
- [185] H. G. H. J. Heilig, E. G. Zoetendal, E. E. Vaughan, P. Marteau, A. D. L. Akkermans, and W. M. de Vos, “Molecular Diversity of *Lactobacillus* spp. and Other Lactic Acid Bacteria in the Human Intestine as Determined by Specific Amplification of 16S Ribosomal DNA,” *Appl. Environ. Microbiol.*, vol. 68, no. 1, pp. 114–123, 2002.
- [186] B. Aktas, T. J. De Wolfe, N. Safdar, B. J. Darien, and J. L. Steele, “The impact of *Lactobacillus casei* on the composition of the cecal microbiota and innate immune system is strain specific,” *PLoS One*, vol. 11, no. 5, pp. 1–15, 2016.
- [187] H. Licandro-Seraut, H. Scornec, T. Pedron, J.-F. Cavin, and P. J. Sansonetti, “Functional genomics of *Lactobacillus casei* establishment in the gut,” *Proc. Natl. Acad. Sci.*, vol. 111, no. 30, pp. E3101–E3109, 2014.
- [188] S. A. Denev, “Role of Lactobacilli in Gastrointestinal Ecosystem,” *Bulg. J. Agric. Sci.*, vol. 12, pp. 63–114, 2006.
- [189] K. Adamberg, S. Kask, T. M. Laht, and T. Paalme, “The effect of temperature and pH on the growth of lactic acid bacteria: A pH-auxostat study,” *Int. J. Food Microbiol.*, vol. 85, no. 1–2, pp. 171–183, 2003.

- [190] A. Alexandra *et al.*, "The Influence of PH on The Growth of Some *Lactobacillus* Strains with Different Origins," *Bull. UASVM Vet. Med.*, vol. 71, no. 1, pp. 270–271, 2014.
- [191] W. Meissner, T. A. Jarzembowski, H. Rzycka, C. Botelho, and A. Pałubicka, "Low metabolic activity of biofilm formed by *Enterococcus faecalis* isolated from healthy humans and wild mallards (*Anas platyrhynchos*)," *Ann. Microbiol.*, vol. 63, no. 4, pp. 1477–1482, 2013.
- [192] A. M. T. Barnes *et al.*, "*Enterococcus faecalis* readily colonizes the entire gastrointestinal tract and forms biofilms in a germ-free mouse model," *Virulence*, vol. 8, no. 3, pp. 282–296, 2017.
- [193] K. Fisher and C. Phillips, "The ecology, epidemiology and virulence of *Enterococcus*," *Microbiology*, vol. 155, no. 6, pp. 1749–1757, 2009.
- [194] M. N. Byappanahalli, M. B. Nevers, A. Korajkic, Z. R. Staley, and V. J. Harwood, "Enterococci in the Environment," *Microbiol. Mol. Biol. Rev.*, vol. 76, no. 4, pp. 685–706, 2012.
- [195] C. H. Stuart, S. A. Schwartz, T. J. Beeson, and C. B. Owatz, "*Enterococcus faecalis*: Its role in root canal treatment failure and current concepts in retreatment," *J. Endod.*, vol. 32, no. 2, pp. 93–98, 2006.
- [196] C. A. Linte, J. J. Camp, M. E. Rettmann, D. R. H. Iii, and A. Richard, "Influence of isolate origin and presence of various genes on biofilm formation by *Enterococcus faecium*," vol. 353, no. 2, pp. 1–13, 2015.
- [197] A. Berthold-Pluta, A. Pluta, and M. Garbowska, "The effect of selected factors on the survival of *Bacillus cereus* in the human gastrointestinal tract," *Microb. Pathog.*, vol. 82, pp. 7–14, 2015.
- [198] L. M. Wijnands, J. B. Dufrenne, and F. M. Van Leusden, "*Bacillus cereus*: characteristics, behaviour in the gastro-intestinal tract, and interaction with Caco-2 cells," RIVM report 250912003, Bilthoven, pp. 86, 2005.
- [199] E. J. Bottone, "*Bacillus cereus*, a volatile human pathogen," *Clin. Microbiol. Rev.*, vol. 23, no. 2, pp. 382–398, 2010.
- [200] F. M. F. Elshaghabee, N. Rokana, R. D. Gulhane, C. Sharma, and H. Panwar, "*Bacillus* as potential probiotics: Status, concerns, and future perspectives," *Front. Microbiol.*, vol. 8, p. 1490, 2017.
- [201] Autoridade de Segurança Alimentar e Económica, "*Bacillus cereus*." [Online]. Available: <https://www.asae.gov.pt/seguranca-alimentar/riscos-biologicos/bacillus-cereus.aspx>. [Accessed: 01-Aug-2018].
- [202] P. Lund, A. Tramonti, and D. De Biase, "Coping with low pH: Molecular strategies in neutralophilic bacteria," *FEMS Microbiol. Rev.*, vol. 38, no. 6, pp. 1091–1125, 2014.
- [203] A. Alvarez-Ordóñez, V. Broussolle, P. Colin, C. Nguyen-The, and M. Prieto, "The adaptive response of bacterial food-borne pathogens in the environment, host and food: Implications for food safety," *Int. J. Food Microbiol.*, vol. 213, pp. 99–109, 2015.
- [204] P. D. Cotter and C. Hill, "Surviving the Acid Test: Responses of Gram-Positive Bacteria to Low pH Surviving the Acid Test: Responses of Gram-Positive Bacteria to Low pH," *Microbiol. Mol. Biol. Rev.*, vol. 67, no. 3, pp. 429–453, 2003.
- [205] "DRAQ7™," *Biolegend*, 2017. [Online]. Available: <https://www.biolegend.com/en-us/products/draq7-9628>. [Accessed: 15-Sep-2017].
- [206] N. S. Claxton, T. J. Fellers, and M. W. Davidson, "Laser scanning confocal microscopy." p. 37, 2006.

- [207] Y. Pan and L. Kaatz, "Use of image-based flow cytometry in bacterial viability analysis using fluorescent probes," *Curr. Protoc. Microbiol.*, vol. 27, no. 1, p. 2C.5.1-2C.5.11, 2012.